The Department of Civil and Structural Engineering

The University of Sheffield

Dynamic Performance of High Frequency Floors

by

Christopher James Middleton

A thesis submitted for the Degree of Doctor of Philosophy in Engineering

June 2009

Abstract

This thesis presents an investigation into the dynamic performance of high frequency floors (HFFs) due to walking excitation. The rationale behind the research is the lack of knowledge of the dynamic characteristics of the HFFs and the poor guidance available in estimating the vibration response due to walking excitation. The most recent design guides published for the evaluation of HFF are by the Concrete Centre and the Steel Construction Institute. The design of HFF is based on similar principles used in the design of low frequency floors (LFFs). However, the dynamic characteristics of each floor type are very different, which leads to inaccurate response estimations.

The thesis is split into three main sections: the classic source, path, receiver layout. The source, within the scope of this work, is excitation due to walking. HFFs are defined at which resonance will not occur from walking, and are designed for environments that require low levels of vibration. Traditionally, a floor's response to walking was analysed using the harmonic amplitudes of the footfall force. As resonance does not occur, this approach is no longer valid, and a number of different methods were developed, namely the 'kf mehtod', Arup's 'effective impulse', and a polynomial method presented in a European Commission (EC) report. It was shown that each method has a number of flaws and characteristics for a new, improved, footfall model are defined.

A new footfall model is created based on a cubic spline fit of 'key points' of the footfall force. The new model included intra-subject variability (i.e. natural variation between each pace rate). The new model was shown to be more accurate than current models recommended in the relevant guidance. Due to the inclusion of variation in the model, the spline force was also valid for LFFs and is therefore the first accurate universal force model.

Assessment of the path consisted evaluating current deign methods for HFFs. It was found that for a transient response of floor (i.e. not resonant) a large number of modes contribute to the response. As such, the only simplified guidance suitable for analysis was the guide published by the Concrete Centre. The Concrete Centre guide was then compared with finite element analysis (FEA) and was found to give inaccurate response estimates due to poor estimates of modal mass and mode shapes.

HFFs are often large structures containing many floor bays. These multi-bay structures have interesting characteristics, unique to this style of floor. A large parametric study considering the effects of the number of bays within the structure, the size of the floor bay and the stiffness of columns had on the characteristics of the floor. It was found that mode groupings of closely spaced modes exist due to the large number of bays. It was also found the column stiffness affects the modal mass of the floor.

Due to the complexities of the large multi-bay floors, a number of methods were investigated to make the analysis process more efficient. A method of modal participation was developed to assess the

importance of the large number of modes. The degree of modelling detail that was required in the model was investigated, and it was found that away from areas of interest the structure could be modelled very crudely. Wave propagation analysis was conducted on the floors using the spectral element method (SEM) applied to a grillage model of the floor. It was shown that the SEM had advantages over conventional FEA, including more efficient analysis and the use of semi-infinite elements.

Assessment of the receiver consisted of an evaluation of the current generic vibration criteria for sensitive occupancies. The vibration criteria were assessed under a number of different types of responses. It was shown that if a criteria for a sensitive machine was developed using one type of excitation (e.g. pure-tone sine) it could not be compared with the response of another type of excitation (e.g. broadband random).

Overall, it was shown that all aspects regarding response estimation of HFFs require further research. The work presented in this thesis adds to the current knowledge surrounding HFFs.

Acknowledgements

The author would like to acknowledge the support of his supervisor, Professor James M. W. Brownjohn, for his continual support during the work. Without his guidance, support and patience this thesis would not have been possible.

The author would also like to thank the other members of the Vibration Engineering Section at the University of Sheffield, notably Professor Aleksandar Pavic and Dr Paul Reynolds who's sharing of knowledge considerably aided the progression of this work.

Thanks are also expressed to Mrs Eunice Lawton whose administrative support in the later stages of the work helped relive a great deal of stress.

Finally, thanks must also be expressed to all my many friends for their support through the difficult times. These include Nicky Ward, Dr Peter Carden, Dr Stana Zivanovic, Vito Racic, Donald Nyawako, Chris Jones, Spiros Siouris, among many others.

Memorandum

This thesis is submitted for the degree of Doctor of Philosophy in the Department of Ci Structural Engineering at the University of Sheffield. The thesis is based on independent work out by the Author between the dates of October 2005 and June 2009 under the supervi Professor James M. W. Brownjohn. All the work and ideas written are original except referenced in the text. The work contained in the thesis has not previously been submitted other degree, diploma, or other such qualification.

Christopher James Middleton
June 2009

Contents

List of Figures

List of Tables

Nomenclature

$[\ ]$	=	Matrix
$\{\ \}$	=	Column vector
$[\ ]^T$	=	Transpose
$[\ ]^*$	=	Complex conjugate
$[T]$	=	Transformation matrix
$[I]$	=	Identity matrix
α_n	=	Fourier co-efficient
Δ	=	Static deflection
ϕ	=	Phase angle, mode shape
Φ	=	Dynamic amplification factor
γ	=	Mass per unit area
λ	=	Value depending on ratio of length and width of a plate
ρ	=	Resonance reduction factor, density
ω	=	Angular natural frequency
ϖ	=	Damped angular natural frequency
ζ	=	Damping ration
ψ	=	Continuous displacement
a	=	Acceleration / Length of plate
A_m	=	Amplification factor
B	=	Ratio between forcing and natural frequency / Joist Spacing
C_i	=	Empirical constant
C_s	=	Empirical constant
C_w	=	Empirical constant
E	=	Young's Modulus
f_0	=	Fundamental natural frequency
f_n	=	Natural frequency
f_t	=	Pace rate / Forcing frequency
f_p	=	Pace rate
$f(t)$	=	Time variable force
$F(t)$	=	Forcing function
g	=	Acceleration due to gravity
h	=	Thickness of plate, impulse response function

H	=	Mobility FRF
I	=	Impulse / Second moment of area
k	=	Stiffness, wave number
K	=	Constant depending on floor construction type, stiffness matrix
(KE)	=	Kinetic energy
L	=	Effective length, length
m	=	Mass, modal mass, number of modes
$\tilde{m}$	=	Distributed mass
M	=	Modal mass / Mass matrix
n	=	nth harmonic, nth mode, number of bays
N	=	Reduction factor based on floor span and stride length, total number of degrees of freedom
P	=	Weight of a person, modal force
(PE)	=	Potential energy
Q	=	Gain factor, modal participation
r	=	Current mode number
s	=	Laplace variable
S	=	Effective width
S_{ff}	=	Auto spectral Density
t	=	Time
t_0	=	Rise time
u	=	Modal amplitude, displacement, translational degree of freedom
v	=	translational degree of freedom
w	=	translational degree of freedom
W	=	Width of floor / Effective width
(WD)	=	Work done
x	=	Deflection, distance, co-ordinate
y	=	Deflection, distance, co-ordinate
z	=	Deflection, distance, co-ordinate

Abbreviations

AISC	=	American Institute of Steel Construction
BBN	=	Bolt, Beranek and Newman
CSA	=	Canadian Standards Association
DOF	=	Degree Of Freedom
EC	=	European Commission
FE	=	Finite Element
FEA	=	Finite Element Analysis
FEM	=	Finite Element Method
FRF	=	Frequency Response Function
HF	=	High Frequency
HFF	=	High Frequency Floor
IRF	=	Impulse Response Function
LF	=	Low Frequency
LFF	=	Low Frequency Floor
MDOF	=	Multi-Degree Of Freedom
PSD	=	Power Spectral Density
RRF	=	Resonant Response Floor
SCI	=	Steel Construction Institute
SDOF	=	Single Degree Of Freedom
SEM	=	Spectral Element Method
SLS	=	Serviceability Limit State
TRF	=	Transient Response Floor
ULS	=	Ultimate Limit State
VC	=	Vibration Criteria

1 Introduction

A floor is an integral part of any building and has many different uses and occupancy. In terms of vibration performance, the relevant design criteria are serviceability, rather the ultimate, limits for design. That is, if the serviceability criteria are exceeded structural damage will not occur to the building, but the building will be unsuitable for the intended occupier. Many floors, such as those in offices and residential buildings, will be designed exclusively with human users in mind. Others will be designed for an industrial process, such as a warehouse, storage centre or some sort of manufacturing plant. In these cases, the floor will be designed for the specific use, and usually the vibration criteria will be more stringent the designing for humans alone; as such, people working in these areas rarely complain of excessive vibrations.

There are many types of industrial process which a floor could accommodate. Over the last century, there has been a rapid increase in technological advancement, which is now commonplace in many industrial processes. The technical advancements have involved miniaturisation of components and processes to micro-levels of precision, also requiring micro-levels of vibration tolerance. The tolerance is reduced further in research establishments, which require precision finer than that used in industry. Examples of these vibration sensitive facilities can be:

- Laboratories
    - High precession measurements (metrology) and processes
- Hospitals and other medical institutions
    - Instruments, such as microscopes in operating theatres, MRI scanners, etc.
- Industrial manufacturing
    - Photolithography used in microchip manufacturing facilities (FABs), micro hard disk drives, etc.

In the past, such low levels of tolerance were rare, but as the miniature high-technology products become more common place, such facilities with stringent vibration criteria have become more common. Not only are low vibration levels required, but due to a competitive market, cost, including construction cost, is an important factor. To keep costs at a minimum efficient building designs are essential. An important feature of this type of floor is that strength is not the governing factor in design. Due to the low levels of vibration required, the structural members are much larger than required for a conventional static design, resulting in the design purely governed by a serviceability limit state.

1.1 The Research Problem

As it is the invention of advanced technology that has driven a need for low vibration environments, it is a relatively new problem. However, vibrations of structures with human occupancy have been a research topic for much longer. The criteria, when designing for human occupancy is much less stringent, with the lowest level of vibration required at the threshold of human perception. The tolerance required for sensitive machinery is below what any person can perceive.

Historically, human perception of vibration was the only vibration problem and much of the research and design methods were based on this. Originally, much research was focused on excessive vibrations of pedestrian footbridges. These long span, flexible structures, often had low fundamental natural frequencies. If the frequency of a mode of vibration matched the pace rate excessive vibrations due to walking could easily be achieved. As such, the first design requirement for such bridges was to attempt to have the fundamental natural frequency above the maximum pace rate that was likely to be achieved while walking [1]. However, higher harmonics contained within the walking force could also significantly excite the structures.

The design process evolved into considering a simplification of a walking force, and applying it to a simplification of a structure (in this case the approach for a footbridge or a floor is the same). If a footfall force is considered in the frequency domain, it is noticeable there are a number of harmonics at multiples of the pace rate. The amplitude of the harmonic at the same frequency of the pace rate is much larger than the other harmonics. As such, the rationale behind design was to construct a floor that had a fundamental natural frequency that avoided the first harmonic of walking. It was then considered that an excessive floor response was unlikely [2, 3]. This method worked well until a recent trend in buildings to use more slender elements, resulting in less mass participating in the modes of vibration, and therefore easier to excite, requiring a more rigorous approach [2, 4].

Walking models including more than just the first harmonic were developed [1]. The amplitude of the harmonics of the footfall force were averaged for sample of the population, it was then possible to conduct a harmonic analysis if the modal properties of the floor were known. The largest response to a footfall force will occur if the fundamental mode matches the first harmonic of the walking force. Between the first and second harmonic there is a large drop in force, and this trends continues into the higher harmonics. As such, a small change in floor frequency can change which harmonic will excite it, which can cause a large change in the force and floor response. As such, frequency is the governing factor of design in this case. The lowest natural frequency of the floor (i.e. the fundamental mode) will be excited by the lowest possible harmonic. As the lower harmonic contains more force, often the response will be higher. As such, the fundamental mode dominates the response and other modes are not required to be analysed.

The fundamental modal frequency was generally obtained from the floors static deflection. The modal mass was generally obtained assuming the floor as a simply supported, but with empirically modified

lengths and widths. This approach was conservative, but due to the lack of computer power it was considered sufficient. This is highlighted by a quote in a design guide published by the SCI in 1989 [3]: "precise calculations are neither justified, nor required, for floor vibrations". Although modal analysis using FE software was available, simplified methods were considered sufficient.

As floors with vibration levels below the limit of human perception were required, a change in design methods was required. Initially, designing a floor that had a fundamental natural frequency above the highest harmonic of footfall was considered sufficient for vibration sensitive occupancies. This boundary is the fourth harmonic at approximately 10 Hz (i.e. the 4 times the fastest reasonable pace rate of 2.5 Hz). However, as these environments became more sensitive it was soon realised that an even more rigorous approach was required.

Above 10 Hz there are no distinctive harmonics within the footfall force. However, there are still force components, although with a very low magnitude, that cause a response in a floor above 10 Hz. Due to the harmonic method of analysis requiring harmonic amplitudes, it was not possible to accurately model the response above 10 Hz. Due to this, different methods of analysis were used depending on the frequency of the floor, the most recent and accurate being Arup's effective impulse. When harmonic analysis was used the floor was termed a low frequency floor (LFF) and when the effective impulse, or similar methods, is used the floor was termed a high frequency floor (HFF).

The analysis of HFFs is based on many years of research into LFFs, but as the floors characteristics will be shown to be very different, it is inaccurate to assume that LFF analysis techniques can be applied to HFFs. This causes issues in three main areas:

1. The excitation of the floor.
2. Characteristics and estimation of the floor's dynamic properties.
3. Valid vibration criteria for sensitive machinery.

These three points are discussed in detail in Chapter 2 but will briefly be described here.

1.1.1 Floor Excitation

When a floor is designed for human occupancy, the governing source of excitation is usually from humans (usually walking). However, other sources of excitation may have magnitudes that cause perceptible levels of vibration. However, in the case of human occupancy it is often possible to mitigate the source of vibration (e.g. balancing of rotating machinery, positioning machinery away from offices etc.) In the case of sensitive machinery, due to the low tolerance of vibration, many more sources of excitation should be considered, for example:

- Ground borne (external traffic, transmission from other building, etc.)

- Internal machinery (pumps, generators, etc.)
- Human induced (walking, running, etc.)

Due to the large range of excitation sources, this thesis will only consider walking forces.

As already mentioned, analysis of HFFs requires a different forcing function then a LFF. A number of models have been proposed for this, with various levels of accuracy. However, they all share on fundamental problem: if the footfall force is required to be modelled differently in different situations then none of the force models accurately represent the real force. Further to this, the boundary between high and low frequency floors is disputed, with questions on how many harmonics are likely to contribute to the response. The solution is to produce a force model that accurately represents the real force in all situations, therefore removing the need to classify the floor.

1.1.2 Characteristics and Dynamic Properties of High Frequency Floors

Analysts in industry require simplified guidance. Often the project they are working on does not allow for a rigorous analysis of a structure, and a quick, simple and accurate method of analysis is required. Each current design guide in the UK [5, 6] offers a simplified guidance, based on obtaining modal properties of a structure and performing modal superposition.

The design guides regarding HFFs, are again, developed on the analysis techniques used for LFFs. Considering LFFs using harmonic analysis, by the very nature of harmonic analysis, it is clear that one mode will govern the response. In addition, there are large jumps in the magnitude of the force between the harmonics. As the fundamental frequency of the floor will govern which harmonic is required for analysis, frequency becomes the governing factor in response estimation. As the response of the floor is resonant, damping also has a large influence in the magnitude of response. As such, much of the research has been concerned with accurately obtaining modal frequencies and damping, modal mass was somewhat neglected. This is echoed in the simplified guidance, frequency estimates, based on static deflection, are usually quite accurate, and there are tables describing damping levels appropriate for certain structures. However, mass is often inaccurate, based on estimates from simply supported plates with empirically adjusted lengths and widths.

With HFFs, the characteristics of the response are much different. Due to the transient nature, the decay is not governed so much by damping, but by the geometrical spread of energy, this effect is greater as the floor becomes larger. In addition, changing the frequency of the floor has less effect on the magnitude of the floor's response, with the effect reduces as the frequency of the floor increases. As the frequency has less effect on the force, and there is not a resonant build up, mass becomes much more important in the response estimate. In addition, as the response is not resonant, there is no single mode that governs the response, and multiple modes are required for an accurate prediction

of response. As such, the current guidance is poorly suited for HFFs, with only the Concrete Centre guidance [5] providing as simplified method to estimate modal properties of higher modes of vibration.

1.1.3 Vibration Criteria for Sensitive Machinery

The generic vibration criteria most commonly used for vibration evaluation of sensitive facilities was developed by *Bolt, Beranek and Newman* (BBN) and is known as the 'VC curves' [7, 8]. Once again, the criteria are developed on the basis of analysis techniques involving humans. The basic approach was to extend the generic criteria for human perception (which for a large frequency range lies on a line of constant velocity) to a number of more sensitive levels, below the threshold of human perception. BBN then stated what machines fit into which band retrospectively, and did not create the curves on a study of machine-specific criteria.

The rationale for generic criteria for humans is based upon many people will use a certain floor; it could be measured in many thousands of people. It would not be sensible to obtain the 'criteria' for an individual, and design such a floor to suit just them. This leaves two important questions regarding vibration criteria for sensitive machinery. Firstly, can the same rationale be applied? Often, a floor that supports sensitive machinery will solely support that piece of machinery for a long period of time. It will not, as it is for humans, support hundreds of different types of machine. Secondly, does the assumption of constant velocity sensitivity over a wide frequency range hold true? This assumes that a machine has the same sense to vibration as a human.

1.2 Solution and Scope of Work

The scope of work is fixed to HFFs with regular bays subject to walking excitation. Due to the difficulty in obtaining access to these types of floors, a larger part of the work will be analytical. The analytical studies are backed up with experimental work when available. Each of the problems identified earlier will be investigated.

1.2.1 Thesis Layout

Chapter 1 (the current chapter) introduces the research problem, proposes work and its scope and has a short summary of the findings.

Chapter 2 contains an in-depth literature survey of the research topic, identifying gaps in the current knowledge.

Chapter 3 and Chapter 4 consider modelling of a footfall force. Chapter 3 is a critical review of current methods and discusses characteristics required for a universal footfall model. Chapter 4, using the characteristics outlines in Chapter 3 proposes a new footfall model using a cubic spline.

Chapter 5 and Chapter 6 consider modelling of the floor. Chapter 5 examines the current simplified methods and compares the results with FEA. A number of parametric studies are conducted to ascertain the dynamic characteristics of multi-bay floors. Chapter 6 considers floors as wave propagation problems using the SEM. The method is derived an implemented in software written by the author. A number of floors are assessed using 3D grillage analysis, including the use of semi-infinite elements to model large structures.

Chapter 7 assess vibration criteria. The VC curves are compared to Ahlin's response spectrum method with the use of hypothetical tools analysed with base excitation of SDOF oscillators. A discussion is presented on the relevance on generic vibration criteria versus machine specific criteria.

Chapter 8 concludes the main points of the thesis, and offers discussion of the results. Recommendations for future work are also presented.

2 Literature Review

Construction methods for floors and their uses have changed over the last 100 years. Floors were traditionally designed to an Ultimate Limit State (ULS), where design for strength governed the size of the floor components. The concept of serviceability Limit State (SLS) was to limit the maximum deflection of the floor and the SLS limit was not set to avoid damage of structural components, but to avoid cracking of finishes.

Now instead of deflection, vibration serviceability has become a major concern for several reasons:

1. Construction techniques have changed, allowing for longer span floors with much lighter construction.
2. Occupancy of 'normal' floors has changed. Historically office spaces were cellular, filled with filing cabinets and bookcases. With moves towards open plan, paperless offices and increasing use of computer equipment, the mass of non-structural components supported has in general been reduced.
3. Huge technological advances have been made in medical, scientific and micro-manufacturing and as these disciplines move towards greater dimensional precision, the type of equipment used becomes extremely sensitive to vibration.

As a result, in order to ensure adequate performance and avoid vibration serviceability problems there has in the last decade been a significant increase in the volume of research on floor vibrations and vibration criteria.

The original problem was limited to perception by humans, a problem not specific to floors and more commonly experienced (or at least made public) in footbridges. In this respect, reviews of human perception to vibration for floors and footbridges are given respectively by Pavic *et al.* [9] and Zivanovic *et al. [1]*, with the relevant standards for human perceptibility of vibration being BS6472 [10] and ISO2631 [11].

These guidelines for human perception are not suitable as criteria for sensitive machinery and these have developed independently. During the 70's, prompted by lack of guidance by machine manufacturers, Bolt Beranek & Newman Inc. (BBN) attempted to create a generic set of criteria specific to sensitive machinery [12]. These criteria are known as the VC curves and are now widely used.

Having a well defined set of criteria is an excellent step, leaving the major problem of predicting floor response before construction. There are then four steps even before an analysis is done and a judgement is made:

1. The design force for the floor needs to be defined.

2. The floor stiffness distribution needs to be evaluated with adequate accuracy.
3. The floor mass distribution needs to be evaluated with adequate accuracy.
4. An appropriate level of damping needs to be associated with the floor.

For the first step, research into human walking forces has predated vibration serviceability problems, due to interest in the health sector [13] and for intruder detection [14]. As with acceptance criteria, the research on walking forces for floors has to some extent tracked research for bridges [1, 9], and it is now commonly agreed that for most applications a footfall force is best represented in the frequency domain. It can be shown that a footfall contains most of its energy below 10 Hz, and in this region can be assumed to be best represented by harmonic forcing functions. However, there is still energy present above 10 Hz and this is assumed to be best represented via an impulsive forcing function.

This notional boundary at 10 Hz was the origin of the term 'high frequency floor' (HFF) [15] since a HFF by definition does not exhibit a resonance response due to walking, but appears to respond as if to a sequence of impulses.

Given the forcing function, for steps 2 to 4, the technique of modal superposition is commonly used (and advocated in design codes) to predict the response. Stiffness and mass are linked via modal frequency, and design guides from the Steel Construction Institute (SCI) [3, 16-18], American Institute of Steel Construction (AISC) [19], Canadian Standards Association (CSA) [20], the Concrete Society [21] and the Concrete Centre [5] all offer methods of predicting natural frequency and 'participating mass'. These methods have superficial differences but are based on similar theory.

Prediction of natural frequency is either by assuming the floor to act like a beam or a plate, and usually only the fundamental frequency is estimated, while the participating (or modal) mass estimation is based on a crude estimation of the mode shape. Such methods, designed to simplify management of floor vibration serviceability, become inaccurate when applied to complex floor arrangements. Given the inaccuracies due to simplifications and access to powerful computer software and hardware, detailed finite element (FE) analysis is now often preferred and if applied correctly should be capable to estimate more accurately the modal frequencies and masses of a floor, not limited to the fundamental mode. On the other hand damping ratios cannot be derived analytically and are usually selected from experience, or through suggested values in the design guides.

2.1 Types of High Frequency Floors

The type of construction of a HFF depends on the sensitivity of its occupancy. Two main construction types exist: slab on grade, which is built directly on the ground, and suspended slabs supported by columns. Slab on grade floors perform very well in response to internal vibrations, however they can only perform as well as the ambient conditions of the ground supporting them. When considering a

suspended slab for a sensitive occupancy the design criteria shift from an ultimate limit state (ULS) to serviceability limit state (SLS) (i.e. design for vibration performance governs over strength).

For sensitive floors such as hospitals, this extra performance can be met with a standard office style floor[12, 16], but with larger member sizes. The SCI have recently been involved in the construction of many new hospital buildings using their SlimDek floors [22] shown in Figure 1. There has been a public debate arguing whether steel-composite floors are suitable for sensitive occupancy due to their lightweight construction [16, 23-26]. Floors with sensitive occupancy were traditionally constructed using reinforced concrete, providing a large mass but still enough stiffness for the fundamental frequency to be above 10 Hz. There was concern that due to the reduction in mass of the steel composite floor, even if the floor high frequency would perform poorly. Independent studies and measurements [16, 24, 27] have shown that these floors can meet the hospital's stringent vibration criteria.

For sensitive laboratories and microelectronic fabrication plants (fabs) the vibration criteria are more stringent than hospitals. Here the office style of design does not perform adequately and a concrete waffle slab, shown in Figure 2, is the typical design style and is more economical then a flat slab [12]. Waffle slabs are often more than a metre deep and are very stiff and massive [12]. In the case of a fab the production machinery, also known as a tool, will then be supported upon a pedestal on the slab.

The design of columns plays an important part of the floor response. If the columns are not stiff enough they can drastically decrease the overall stiffness of the floor [12, 28]. It can be shown that with the massive waffle slabs, columns can act as springs and deform axially [12, 28] reducing the vibration performance.

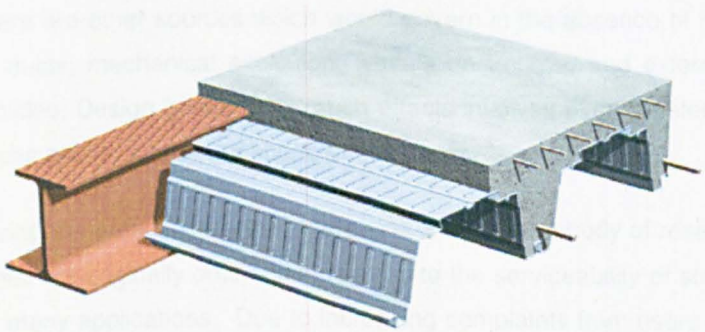

Figure 1 - SCI's SlimDek

Figure 2 - A typical waffle slab

If a floor or its columns are supported directly by the ground, the floor's performance is somewhat related to the ambient conditions at the site. Isolation techniques are an important research topic in achieving 'better then ambient' conditions. Some isolation techniques in use and being research include low frequency pneumatic springs, low frequency folded pendulums [29] and active vibration isolation.

2.2 Excitation Sources

The most severe source of excitation for floors is usually due to people walking on the floor [30]. There are other sources which would govern in the absence of human traffic, including: turbulence in air ducts, mechanical excitation, wheels on trolleys, and external vibration from micro-tremors and vehicles. Design governed by such effects involves even greater uncertainties than design for footfall forces and is outside the scope of this paper.

During the early 20th century there was a significant body of research focused on forces from walking. While not originally obtained in relation to the serviceability of structures, the data collected are useful for many applications. Due to increasing complaints from users of office floors from human excitation there has been renewed interest in effects of footfall forces on large structures.

As floor resonance from walking has the potential to cause large response, floors for microelectronic fabrication plants (fabs), were designed to be stiff enough to achieve fundamental frequencies over 10Hz. These HFFs avoided resonance by vibrations to the footfalls dissipating before the successive footfall could contribute to the response. Simplistic procedures have until recently been used to

predict the response of these HFFs, but guidance recently introduced in the UK uses a first-principles approach for prediction based on equivalent impulse values [31].

This section discusses the development of models to predict footfall forces and how these have been implemented into design guides.

2.2.1.1 Pedestrian Excitation

The vertical force generated by a typical pedestrian footfall can be by characterised as having a saddle shape as shown in Figure 3. It can be shown that the shape of the footfall force is similar for different people, however, certain characteristics, such as the peak force, are dependent on the walker [13, 14, 31-37].

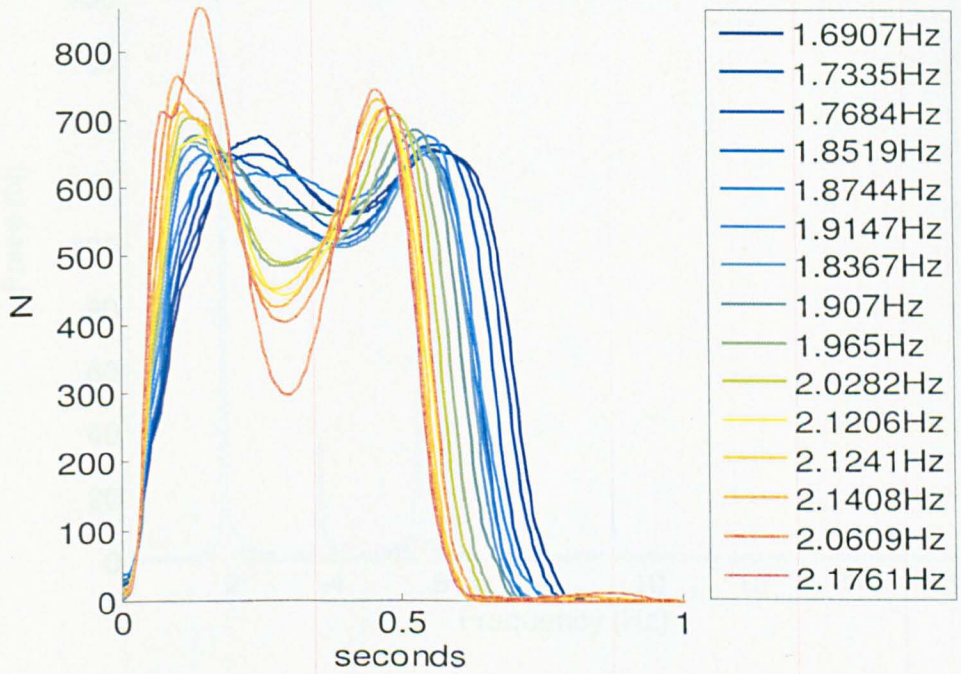

Figure 3 – Footfall time histories for walking recorded on an instrumented treadmill for different pace rates; separate colours represent different pace rates.

Many of the investigations into vibration serviceability were conducted on footbridges [38, 39] due to problems arising from their low frequency, long span construction. As the force measurements were generally carried out on a stiff platform or structure they are probably more relevant for floors.

If the walking force is presented in the frequency domain a number of peaks are evident at multiples of the pacing frequency. Figure 4 shows the frequency spectrum of a measured force containing multiple paces. Average amplitude values for these harmonics (or Fourier components) have been

presented by different authorities, and are summarised by Zivanovic *et al.* [1]. The force can be represented using:

$$F(t) = P\left(1 + \sum_{n=1}^{N} \alpha_n sin(n2\pi f_p + \phi_n)\right) \quad \text{Equation 1}$$

where $F(t)$ is the force at time t, P is the static weight (often taken as 700 N for simplicity, the mean is 746 N [30, 40]), n is the order of the harmonic, α is Fourier component of the n^{th} harmonic, f_p is the pace rate and ϕ_n is the phase angle of the n^{th} harmonic.

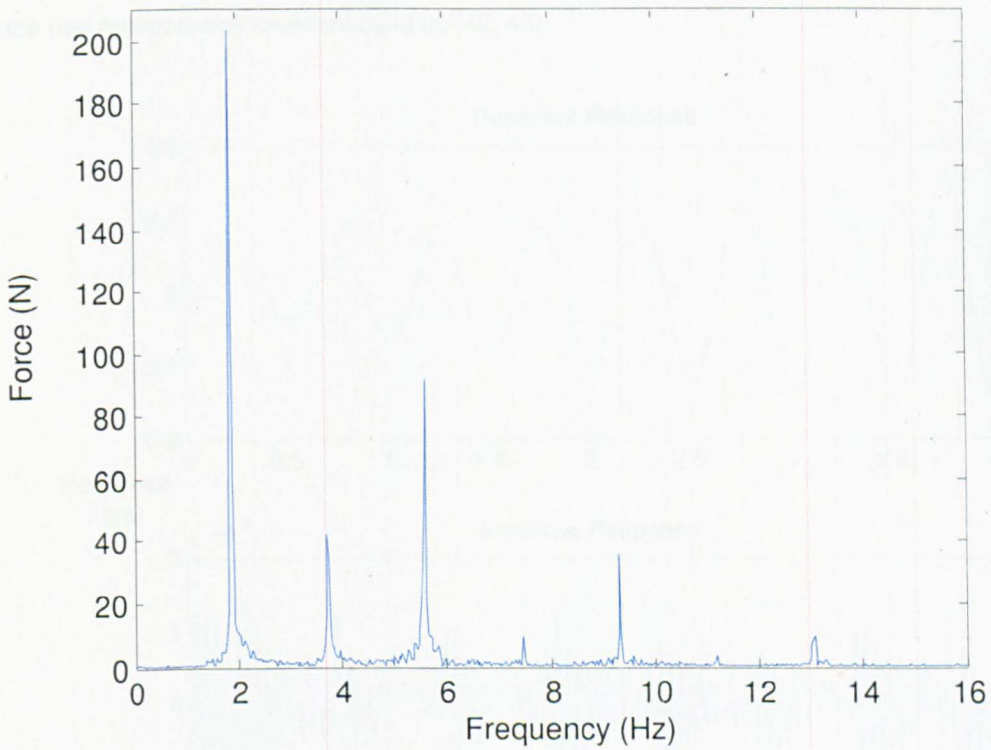

Figure 4 - A typical footfall represented in the frequency domain with a pace rate slightly less than 2 Hz, each harmonic clearly shown with a spike at multiples of the pace rate

Rainer *et al.* [36] conducted one of the early studies used to derive harmonic amplitudes by measuring forces indirectly on a stiff truss. Because the natural frequency of the truss was just over 10 Hz, it was possible only to identify harmonic components of the force for frequencies up to 10 Hz. The authors argued the case for a 10 Hz limit by showing that most of the energy is contained in the first three or four harmonics, although this is not a universally held view [41]. Kerr [42] conducted an extensive study into the harmonics of footfalls and found it necessary to normalise the force to the subjects' weight, height (and therefore stride length) and pace rate in order to reduce scatter among harmonic amplitudes. His data were obtained from single footfalls on a force plate, reconstructing walking force

time series by superposing the same footfall delayed by the footfall interval. By reconstructing the walking force from the Fourier components and their corresponding phase angles he showed that with 5 harmonics the force was very similar to the original, and with 10 harmonics it was practically indistinguishable by eye.

Due to there being less force at higher frequencies Wyatt and Dier in 1989 [15, 42] suggested that resonance will not occur above a certain frequency and a floor will act impulsively with response from each footstep dissipating before the next. This distinction between high and low frequency floors was the basis of the SCI design guide [3, 42] in which response of low frequency floors is governed by a resonant build up from the first three or four harmonics of walking while high frequency floors display transient response as if to a sequence of impulses, with the response dissipated before the next footfall. These different characteristics are shown in Figure 5. This distinction assumes either that the higher harmonics do not have sufficient energy to cause resonance or that the natural variation in pace rate prevents any resonant build up [42, 43].

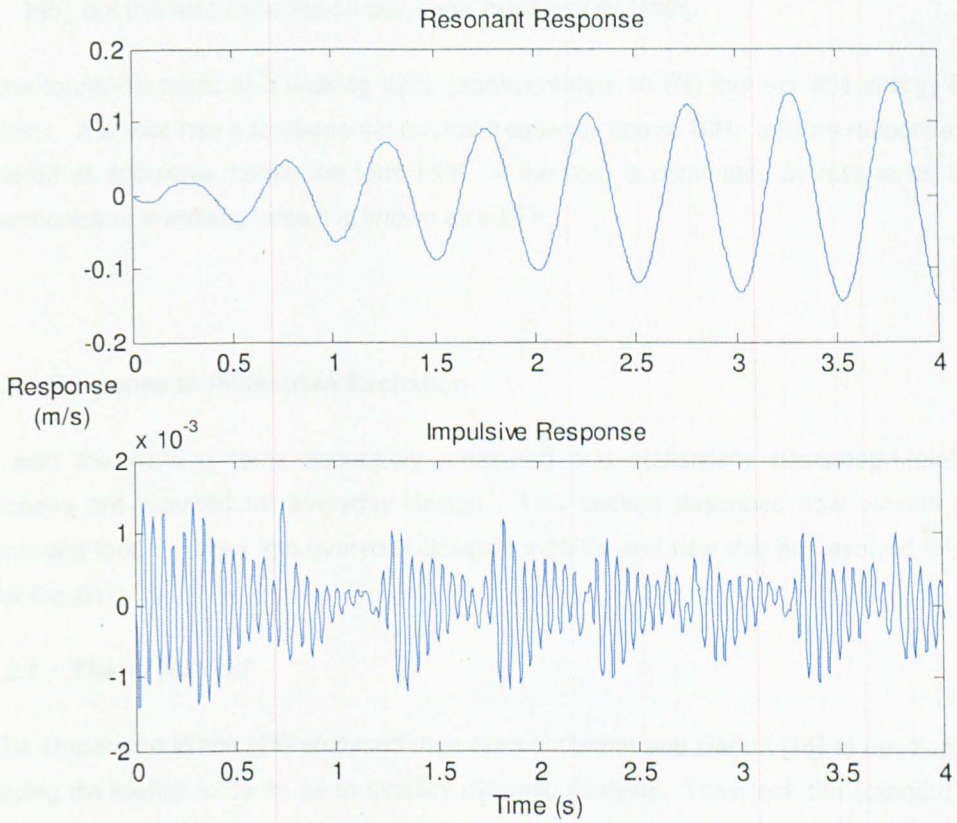

Figure 5 - Comparison of the response of high and low frequency floors

Since this distinction was made there have been varying opinions on the LF/HF boundary, originally set at 8 Hz, but 10 Hz is currently the value used in the latest design criteria [5, 30, 40]. However, there is evidence that resonant response can occur above this value [44], and low frequency floors have high frequency modes which are impulsively driven that can dominate local responses.

A recent attempt to represent footfall forces for design [45] used a high-order polynomial fitted to the walking time histories, with polynomial coefficients dependent on pacing rate, and with the Fourier components derived from the polynomials. With this approach the Fourier components are likely to be less accurate and appear to be too high. However, the method does have potential for creating a force time history.

Some conclusions from the various investigations into walking forces are:

- The general shape of a footfall force is similar, and is independent of the individual who is walking, their weight, pace rate and stride length.
- The maximum force increases if the weight, stride length or pace rate of the person increases.
- A normalised force can be obtained by normalising to both weight, pace rate and stride length. For higher harmonics pace rate and stride length have little influence so only normalisation with weight is necessary.
- The average pacing rate of a person is 2 Hz with an average velocity of slightly over 1 m/s [35], but this also depends on sex, race, build and situation.

After the fourth harmonic of a walking force (approximately 10 Hz) there is little energy in the higher harmonics. If a floor has a fundamental natural frequency above 10Hz a floors response can now be considered as impulsive, hence the term HFF. If the floor is dominated by resonance from the first four harmonics of a walking force it is known as a LFF.

2.2.1.2 Response to Pedestrian Excitation

Even with the walking force accurately measured and statistically described, relatively simple descriptions are required for everyday design. This section describes how various guides have implemented footfall forces into everyday design for HFFs and how this has evolved into the current state of the art.

2.2.1.2.1 The 'kf Method'

In 1979, Ungar and White [46] analysed data from Galbraith and Barton [14] to develop a method of simplifying the footfall force so as to simplify dynamic analysis. They took the standard footfall trace and disregarded the plateau (Figure 6), believing this approximation will only produce minor errors for intermediate walking speeds.

For a SDOF oscillator, the dynamic deflection, x_{max}, due to this force is derived as being equal to the static deflection, x_{static}, multiplied by an amplification factor, A_m, where:

Equation 2

$$A_m = \frac{\sqrt{2(1+\cos(2\pi f_n t_o))}}{1-(2f_n t_o)^2}$$

t_o is the rise time and f_n is the natural frequency of the floor. It can be seen that the maximum amplification factor is 2 as the footfall rise time and the natural frequency approach 0 (so that the rise time is very short compared to the floor fundamental period). For larger values of $f_n t_o$ (as floor period becomes short compared to rise time) it is possible to approximate A_m as:

Equation 3

$$A_m \approx \frac{1}{2(f_n t_0)^2}$$

The authors showed that a faster pace rate increases the gradient of the rise (reduces rise time) and therefore increases the amplification factor. With a rapid pace rate and a floor frequency of at least 5 Hz:

$$f_n t_0 > 0.5$$ **Equation 4**

as

$$x_{static} = F_{peak}/k$$ **Equation 5**

and

Equation 6

$$f_n = \frac{1}{2\pi}\sqrt{\frac{k}{M}},$$

x_{max} can be expressed as:

Equation 7

$$x_{max} \approx F_{peak}/2k(f_n t_0)^2 \approx 2\pi^2 F_{peak} M/t_0^2 k^2,$$

where F_{peak} is the peak force, k is the static stiffness for mid-span load and M is the 'participating mass'. For harmonic response at first mode frequency (neglecting damping and a few other considerations), velocity is:

Equation 8

$$v_{max} \approx \left(\frac{\pi}{t_0^2}\right) F_{peak}/k f_n$$

This method was the basis of a method proposed by Amick *et al.* [12] where they presented the response of a floor as:

$$v_{max} \approx C_w / k f_n$$ **Equation 9**

where C_w is an empirical constant which must be based on Equation 8. This method will now be referred to as the kf method and is currently used by Bolt Beranek & Newman Inc. (BBN) and recommended by the American Institute of Steel Construction (AISC) [19].

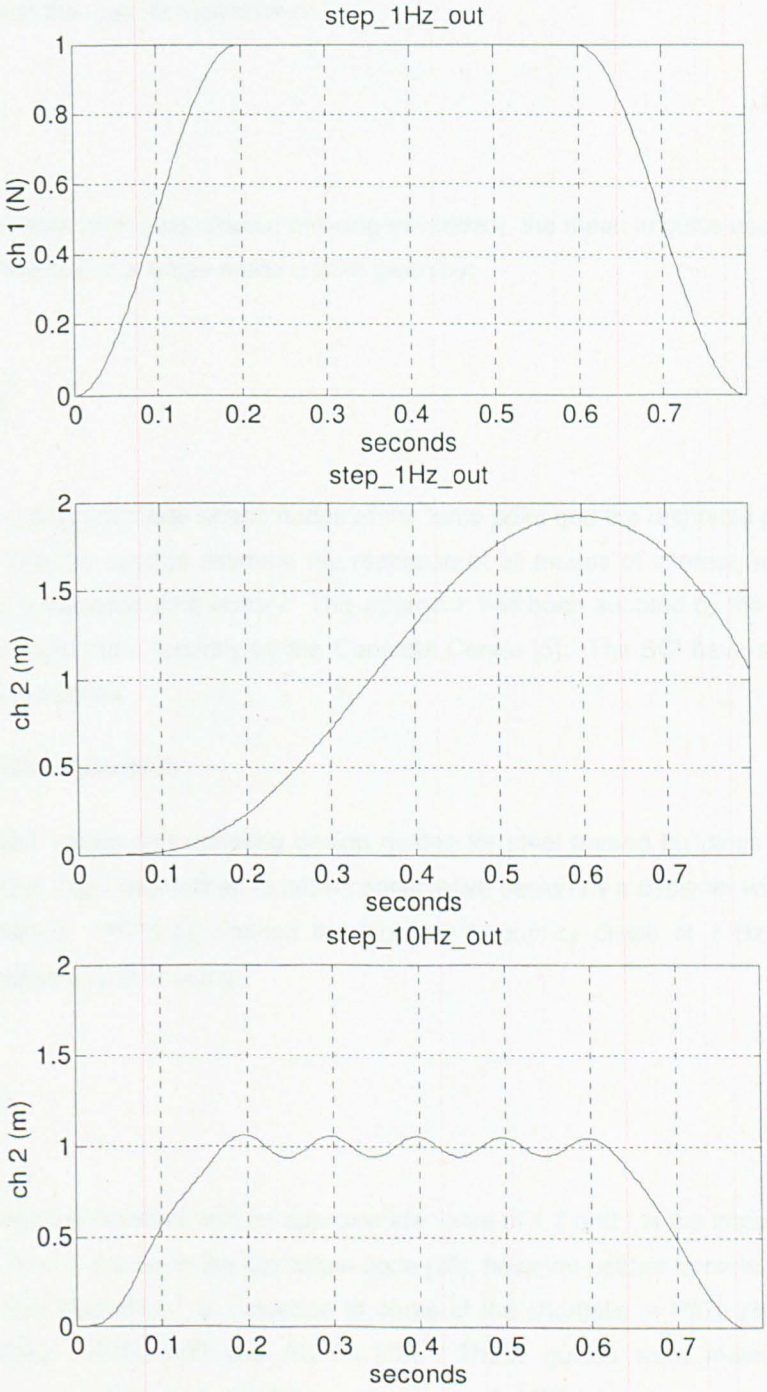

Figure 6 – (top to bottom) a) Idealised footfall force using the kf method, b) response of a 1 Hz, 1 N/m oscillator, c) response of a 10 Hz 1 N/m oscillator

2.2.1.2.2 *Arup's 'effective impulse'*

Based on Kerr's walking force data [42], Arup developed a method for predicting response of HFFs based on an 'effective impulse' [5, 31, 43, 47]. The high / low frequency threshold is set at the upper limit for the fourth harmonic of pacing rates, approximately 10 Hz. The formula for the effective impulse was derived by feeding Kerr's footfall forces into SDOF oscillators with unit mass and a range of frequencies. Taking the resulting peak velocity as the impulse for that floor/pacing rate frequency combination leads to the best-fit relationship:

$$I_{eff} = 54 f_p^{1.43} / f_n^{1.3}$$ **Equation 10**

This is the 75%ile value (with 25% chance of being exceeded); the mean impulse uses 42 as the scale factor. The peak velocity of a single mode is then given by:

$$v_{\max\,(i,j)} = \mu_i \mu_j \frac{I_{eff}}{M_r}$$ **Equation 11**

where subscripts *i* and *j* are mode shape nodes of the force point and the response point respectively. Equation 11 can then be used to estimate the response of all modes of interest, which can then be summed to obtain a response time history. This approach has been adopted by the Concrete Society in Appendix G [40] and more recently by the Concrete Centre [5]. The SCI have slightly altered the method as presented below.

2.2.1.2.3 *The SCI's Approach*

The SCI have been writing and updating design guides for steel framed buildings since the 1980's. Publication 076 [3] in 1989 was written to allow conservative design by a designer with little knowledge of structural dynamics. P076 [3] defined the high-low frequency divide at 7 Hz and predicts the acceleration response of a HFF using:

$$a_{max} = \frac{I}{mWL} 2\pi C_i$$ **Equation 12**

where C_i is an empirical constant with an approximate value of 1.7 and I is the impulse from a person, given at 3-4 Ns. This is similar to the Canadian code [20], however neither formula shows any benefit from increasing floor frequency. In response to some of the shortfalls of P076 [3] the SCI released two guidance notes, AD253 [17] and AD254 [18]. These guides were mainly concerned with estimating modal properties and predicting response of LFFs, however they did mention the

importance of response prediction rather than just trying to exceed a minimum value for natural frequency.

In 2004 a new guide was released, The Design Guide on the Vibration of Floors in Hospitals (P331) [16] was published to address the misconception of the inadequacy of steel frames in hospitals, as it was becoming a common belief that steel floors would not work well as HFFs due to low mass and damping. In this guide, the high-low divide was increased to 10 Hz, and the acceleration response given by:

Equation 13

$$a_{aax} = 2\pi f_n \frac{I_{eff}}{m_n},$$

where

Equation 14

$$I_{eff} = \frac{190}{f_n^{1.3}},$$

which is based on Arup's effective impulse [31, 43, 47].

The natural frequency of the floor is now included in the equation, but there is no allowance for different walking speeds and the formula generally over-estimates Arup's impulse.

The most recent publication from the SCI, P354 [30] supersedes P331 [16] and P076 [3] and offers two approaches, one generalised and one simplified. The general assessment uses modal properties obtained from finite element analysis. For HFFs acceleration is estimated by:

Equation 15

$$a_{peak} = 2\pi f_0 \sqrt{1-\zeta} u_i u_j \frac{I_{eff}}{M_n} W,$$

where

Equation 16

$$I_{eff} = 60 \frac{f_p^{1.43}}{f_m^{1.3}} \left(\frac{P}{700}\right).$$

Equation 16 is similar to the Arup impulse [31, 43, 47], but increased in accordance with BS EN 1990 annex C [48]. Response should be calculated by summing contributions from modes up to twice the fundamental natural frequency.

For the simplified assessment, modal properties are obtained by hand calculations and for the first mode only. A different set of formulae are used to describe the forces.

For LFFs:

$$a_{rms} = u_i u_j \frac{0.1P}{2\sqrt{2M\zeta}} W\rho \,, \qquad \textbf{Equation 17}$$

where P is the weight of a person and ρ is a resonance reduction factor due to the length of the walking path.

For HFFs:

$$a_{rms} = 2\pi f_0 u_i u_j \frac{185}{M_n f_0^{1.3}} \frac{P}{700} \frac{1}{\sqrt{2}} W \,, \qquad \textbf{Equation 18}$$

which oversimplifies Arup's impulse.

Apparently a steady state harmonic response is assumed in order to calculate the RMS value without accounting for the effect and variation of damping. Clearly, the forces used for the two assessments are very different, possibly to compensate for using a single mode in the simplified method. P354 [30] has a range of HFF – LFF boundaries, depending on the type of the floor, as shown in Table 1.

Floor Type	High – Low Cut off frequency
General floors, open plan offices etc.	10 Hz
Enclosed spaces, e.g. operating theatres, residential	8 Hz
Staircases	12 Hz
Floors subject to rhythmic activities	24 Hz

Table 1 - High - Low cut off frequencies from SCI's P354 [39]

2.2.1.2.4 *Other Methods*

Ohlsson [49, 50] presented a method of predicting response for floor modes with frequencies higher than 8 Hz by a frequency domain method using a power spectral density (PSD) description of walking forces. He approximates the walking force PSD as:

Equation 19

$$S_{ff}(f) = \frac{30000}{f^2},$$

where f is frequency. Via the frequency response function (FRF), PSDs of displacement, velocity or acceleration are obtained, from which RMS values can be derived:

Equation 20

$$v_{rms} = \sqrt{\int_a^b |H(f)|^2 S_{ff}(f) df},$$

where $H(f)$ is the mobility FRF, and a and b are the lower and upper bounds of the frequency window respectively.

Ellis [41] believed that resonance from the higher harmonics can cause significant excitation and produced a method using the first eight harmonics of walking. This corresponds to a floor frequency of approximately 16-20 Hz. Even if there is enough energy in the higher harmonics a person's natural variation in pace rate would probably not allow a resonant response.

2.2.1.2.5 *Comparison of Methods*

In 2006 Brownjohn compared the kf method, Arup's method and simulations with real (continuous) footfall force time histories [41, 51]. Figure 7 shows how the response of a SDOF oscillator varies with stiffness and frequency for a single pacing rate in each method, the black contours are lines of equal mass, with constant mass increments between contours, converging for increasing mass to the bottom right of each plot. Compared to Figure 7c, Figure 7a apparently shows that lower mass results in lower response, which contradicts the laws of physics. On the other hand Figure 7c demonstrate that the Arup formula reflects a real footfall.

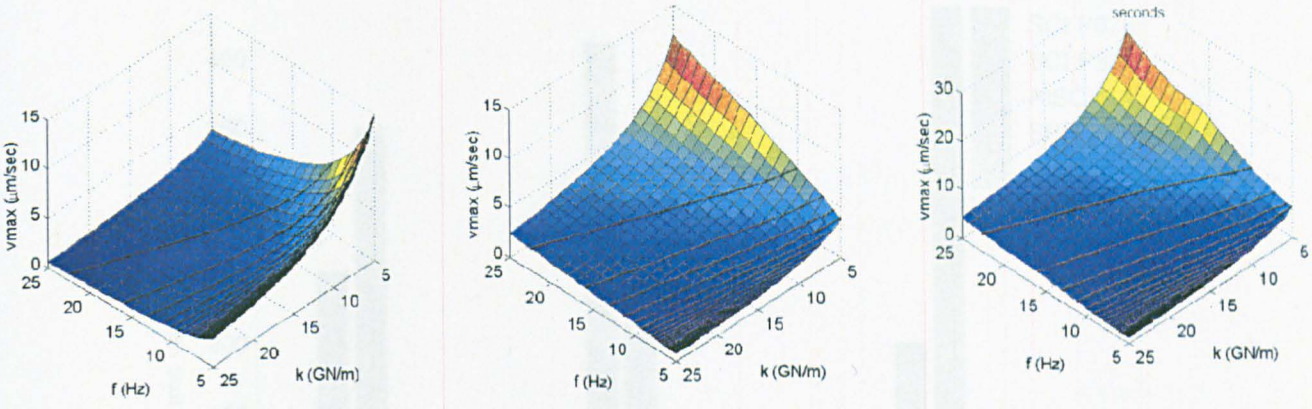

a) kf method b) Arup's impulse c) Real footfall

Figure 7 – Brownjohn's comparison of footfall force methods [51]

In 2005 Pavic *et al.* investigated [52] Arup's impulse [31, 43, 47], along with the Ellis harmonic method [41] and Ohlsson's frequency domain method [49, 50] using a FE model, and compared predictions with measured results from dynamic testing of the real structure. They found that Arup's effective impulse gave the closest values to the measured response, but still overestimated the response. Ohlsson's frequency domain method gave results twice as large as Arup's impulse, and the Ellis method overestimated the response by a factor of 10. The investigation suggests that Arup's method is the most accurate method to date.

Arup recently published their own comparison study [31], in a two part publication, the second of which is concerned with HFFs. The various methodologies are introduced and compared with Arup's effective impulsive method. It must be made clear that Arup's effective impulse was the only method applied to modal properties obtained from an FE model, not from simplified hand calculations; as such the result may be biased. However, even if modal properties obtained using the FE model were used with the other methodologies, they would only use the first mode. The comparison shown in

Figure 8 demonstrates that Arup's method produces the closest results to measured data.

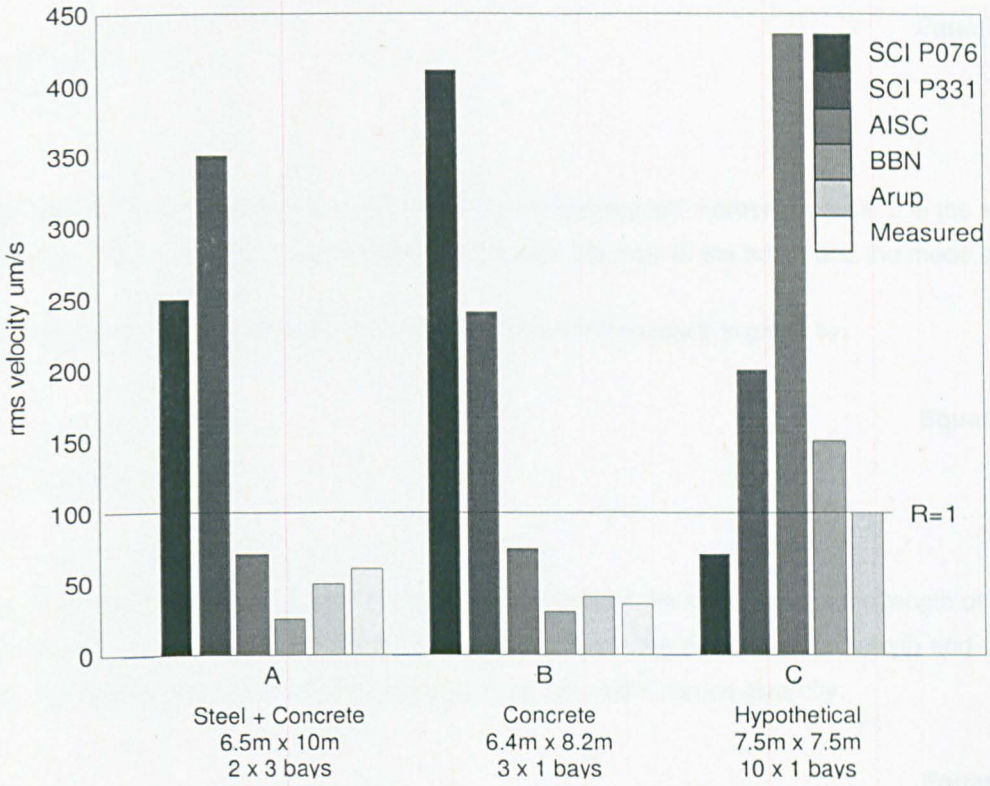

Figure 8 - Comparison of velocity responses using various methodologies after Willford *et el.* [31]

2.3 Transmission Path

An accurate prediction of a floors performance requires a good estimation of the modal parameters, i.e. natural frequencies, modal masses and damping ratios. This section is concerned with accurate estimation of these parameters using simplified hand calculations or detailed FE analysis.

2.3.1 Natural Frequency

If a floor is regarded as a system of beams and plates, standard formulae can be used for estimating natural frequency, described in detail in [53]. The fundamental frequency of a beam can be calculated using:

Equation 21

$$f_0 = \frac{K}{2\pi}\sqrt{\frac{EI}{mL^4}},$$

where E is the Young's modulus of the material, I is the second moment of area, L is the span and m is mass per metre. K is a constant which depends on the fixity of the beam and the mode of vibration.

For an isotropic, simply supported plate the fundamental frequency is given by:

Equation 22

$$f_0 = \frac{\lambda^2}{2\pi a^2}\sqrt{\frac{Eh^3}{12\gamma(1-v)^2}},$$

where h is the depth of the plate, v is the Poisson's ratio of the material, a is the length of the plate, γ is the mass per unit area and λ is a value depending on the ratio between length and width of the plate. For a plate the second moment of area for a unit width can be given by:

Equation 23

$$I = \frac{h^3}{12},$$

so that:

Equation 24

$$f_0 = \frac{\lambda^2}{2\pi a^2}\sqrt{\frac{EI}{\gamma(1-v^2)}}.$$

If the equivalent stiffness and mass k and m can be found, the natural frequencies can be estimated using a spring model:

Equation 25

$$f_0 = \frac{1}{2\pi}\sqrt{\frac{k}{m}}$$

The natural frequency of a vibrating system relates potential energy to kinetic energy. The deflection of a spring to a mass due to gravity is given by:

Equation 26

$$\Delta = \frac{mg}{k},$$

where Δ is the total deflection, m is the total mass and g is acceleration due to gravity. This can be substituted into Equation 25 to give:

$$f_0 = \frac{1}{2\pi}\sqrt{\frac{g}{\Delta}} \approx \frac{18}{\sqrt{\Delta}}.$$ **Equation 27**

This is the basis of many design guides [3, 5, 18, 19, 30] and shows that the fundamental natural frequency can be estimated from the total static deflection of the floor system, a standard result from design checks.

The accuracy of this approximation depends on the similarity between the statically deformed shape and the mode shape. It is exact for a simple SDOF spring mass system [53], but underestimates response in more complex systems, approximately 11% for a beam and 22% for a plate [53]. The accuracy of the approximation depends on how well the static deformation matches the mode shape. Zaman and Boswell [54] addressed this by updating finite element models with data from real structures, and produced a modified deflection equation:

$$f = \frac{K}{\sqrt{\Delta}},$$ **Equation 28**

where K depends on the type of floor and is given by Table 2. This method increases the frequency for double T and flat slab style floors, suggesting that their mode shape is different to their static deflected shape.

Floor Type	Beam and Slab	Double T	Flat Slab
K	17.0	17.7	18.7

Table 2 - K for Zaman and Boswell's deflection formula [54]

Another common method relies on Dunkerley's formula [55] which approximates fundamental frequency as:

$$\frac{1}{f_0^2} \approx \frac{1}{f_1^2} + \frac{1}{f_2^2} + \cdots + \frac{1}{f_n^2}$$ **Equation 29**

where f_n are the fundamental frequencies of the component parts of the system i.e. beams in different directions, slab etc.. This formula always underestimates the exact frequency [53] which in the case of pedestrian excited floor vibration, typically gives conservative results.

The SCI's original P076 document [3] recognises the difficulties and importance in predicting natural frequencies of floors and provides four methods of frequency prediction, given in order of increasing accuracy:

- From a global estimate of self weight deflection, using $f_0 \approx \frac{18}{\sqrt{\Delta}}$.
- From component frequencies from the different parts of the floor then estimating the fundamental frequency using Dunkerly's formula.
- By an iterative Rayleigh-Ritz method; using static analysis software.
- Using dynamic analysis software such as FE analysis.

Subsequent SCI guides [16, 18] recommend the deflection method (Equation 27) and offer more equations to provide an accurate estimate of the deflection.

The AISC design guide [19] recommends either Dunkerly's formula, or the deflection method. They offer alterations for:

- Composite action (by increasing the Young's modulus to 1.35 times that of concrete).
- Alternative beam loadings.
- Continuous spans with non uniform spacing.
- Deflection due to shear in beams and trusses.
- Reduced stiffness in open web joists and girders.

Although estimation of natural frequency using the AISC guide is complicated, with many correction factors, it clear that calculating the natural frequency is not a simple matter.

So far, all the methods shown have been equivalent beam models and none have looked at the floor as a plate; as such, these models are often inaccurate. Bainbridge and Mettem [56] when investigating natural frequencies of timber floors suggested increasing the frequency by 1.5 times the values from equation 23 to allow for the actual floor being stiffer. Ljunggen's [57] used:

Equation 30

$$f_0 = \frac{\pi}{2}\sqrt{\frac{EI}{mL^4}}\sqrt{a + \left[1 + \left(\frac{L}{W}\right)^2 - \left(\frac{L}{W}\right)^4 \frac{EI_y}{EI_x}\right]},$$

where W is the width of the floor and the subscripts x and y represent the main and transverse span of the floor respectively. This is basically the original equivalent beam equation given by Equation 21 modified depending on the size and stiffness of the slab, and 'smears' joist stiffness into the slab

stiffness. However. Chada and Allen [58] noted that estimating the natural frequency as a plate was inaccurate due to the smearing, with the inaccuracy increasing as the joist spacing increased.

Whilst the new Concrete Centre guide [5] uses the deflection method for simple checks, it also presents an advanced beam and plate representation having additional factors including the number of floor bays. In their worked examples they accurately predict many modes of vibration of a floor with this hand calculation.

The main problem with predicting frequency is estimating the stiffness of a floor. The task is simplified if the floor has a uniform bay spacing, but partitions and other non-structural elements, along with unknown joint stiffnesses render the predictions less accurate. Parametric studies using FE analysis [59] can improve the standard equations for predicting frequencies, but these new methodologies can only be used for the same type of floors used in the studies.

Predicting natural frequencies of floors is difficult and prediction accuracy will decrease as the floor becomes more complicated, with ribbed slabs, orthotropic properties and multiple bays. The difficulty is compounded with non-uniform bay spacing and variable boundary conditions. Hand calculations are useful for a quick first estimation of the fundamental frequency of a floor, but for a more accurate estimation, it is clear that FE analysis should be used.

2.3.2 Modal Mass

To model a mode of vibration as a SDOF system, the mass of the floor that is participating in each mode must be known. This is called the modal mass and is a key factor in determining response of a HFF.

Modal mass is obtained by summing physical mass contributions to total mass, scaled by the mode shape values. For mode shape and mass defined as a function of position:

Equation 31

$$M_n = \iint \phi^T(x,y)M(x,y)\phi(x,y)dxdy\,.$$

For a FE model representation: $M_n = \phi^T M \phi$, where M is the mass matrix and ϕ is a vector representing the mode shape.

For example, for a simply supported beam with a uniform mass distribution, sine and half-sine shape, unit normalised mode shape, the resulting modal mass is always 0.5M and likewise for a simply supported plate it is 0.25M, a value used in the new Concrete Centre guide [5].

In most design guides the modal mass is usually assumed by simplifying the mode shape to form effective widths and lengths to estimate the 'participating mass' via e.g.

$$M = mSL$$ **Equation 32**

where m is mass per square metre and S and L are the effective widths and lengths, with various implementation in the guides outlined in Table 3. The origin of these formulae is not clear but they mostly appear to be empirical (from parametric finite element analysis) rather than via first principles and they lack consistency across the various forms.

	Effective width		Effective length	
SCI P076 [3]	$S = 4.5\left(\frac{EI_t}{mf_0^2}\right)^{1/4}$		$L = 3.8\left(\frac{EI_b}{mbf_0^2}\right)^{1/4}$	
SCI P331[60]	$S = C\left(\frac{EI_t}{mf_0^2}\right)^{1/4} \le W$		$L_{eff} = n_y L_y$	
SCI P354 [6]	Shallow Decking	Deep Decking	Shallow Decking	Deep Decking
	$S = C_s(1.15)^{n-1}\left(\frac{EI_s}{mf_0^2}\right)^{1/4}$ But not more than W	$S = 2.25\left(\frac{EI_s}{mf_0^2}\right)^{1/4}$ But not more than W	$L = 1.09(1.10)^{n-1}\left(\frac{EI_b}{mbf_0^2}\right)^{1/4}$ but not more then n_yL_y	$L = 1.09\left(\frac{EI_b}{mL_x f_0^2}\right)^{1/4}$ but not more then n_yL_y
Canadian guide [20]	$SL = \left(\frac{f}{f_1}\right)^2 B_1L_1 + \left(\frac{f}{f_2}\right)^2 B_2L_2$			
AISC [19]	$S_j = C_j(D_s/D_j)^{1/4} L_j$		L_j	

Table 3 - Effective lengths and widths of various guides

As the fundamental frequency becomes sufficiently high (approximately 20 Hz) [61] modal mass becomes more important than damping or frequency for predicting performance of these floors so using simplifications for modal mass can introduce the greatest inaccuracy.

For a multi-bay floor each bay contributes to the modal mass of each mode to some degree so there is a significant concern about single-panel single-mode representations overestimating the response.

Willford *et al.* [62] investigated the response of a floor with increasing number of bays using various prediction methodologies, the results are shown in Figure 9. In this study FE model simulations show that as the number of bays increases the response decreases asymptotically a value above zero [47]. It can also be seen that the AISC [19] guide gives no benefit to increasing the number of bays, and the SCI's P331 [16] asymptotes to zero; both are intuitively incorrect.

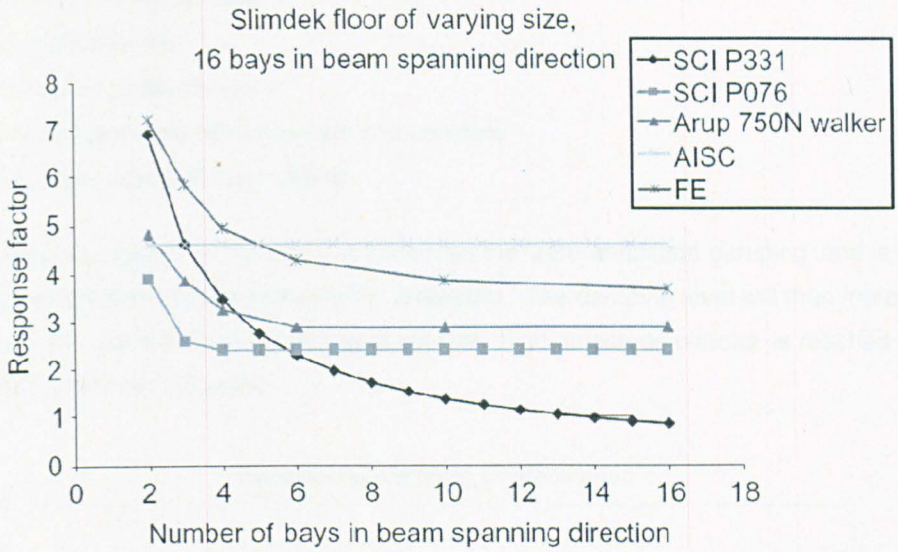

Figure 9 - Reduction of response due to number of bays, after Willford et el. [62]

2.3.3 Damping

Damping is a measure of how much energy is dissipated from a structure and occurs in three main forms: Viscous, Coulomb (dry frictional) and hysteretic (material) damping. However, there is another form of damping known as radiation damping where energy is transferred to another system, e.g. through columns into the ground. Generally a structure is considered to behave as if it conforms to the viscous model due to a mathematical convenience and for low amplitudes of oscillation the free decay seems to fit the viscous model. Although mathematically convenient, it is not evident how viscous damping is characterised in structures, as a mechanism for this type of damping is not evident. Wyatt [63] offered a solution to this problem and proposed that damping mechanisms in structures are frictional in nature, but there are many of them, the sum of which is similar to viscous damping. The frictional mechanisms only engage after certain amplitude is reached, so the summation of the engaged mechanisms provide the appearance of viscous damping which allows for an 'equivalent viscous damping' value.

Wyatt's model [63] suggest that damping will be non-linear and will increase as the amplitude increases. Jeary [64] has investigated non-linear damping in relation to Wyatt's model in depth and has developed a generalised damping characteristic for structures shown in Figure 10. It is clear that the damping value is amplitude dependent but is constant at high and low amplitudes. It is argued that the damping is provided by 'imperfections' in the structure with the largest imperfections mobilised with the smallest forces. Examples of imperfections can be some of the following (largest to smallest):

- Furniture

- Cabling and other services
- Construction joints
- Connections in the structure
- Interaction between reinforcement and concrete
- Microscopic cracks in the material

The 'low amplitude plateau' in Figure 10 is known as the 'zero amplitude damping' and is a product of all the large imperfections being permanently mobilised. The damping level will then increase with the amplitude as more mechanisms are engaged until the 'high amplitude plateau' is reached when all the smaller imperfections are engaged.

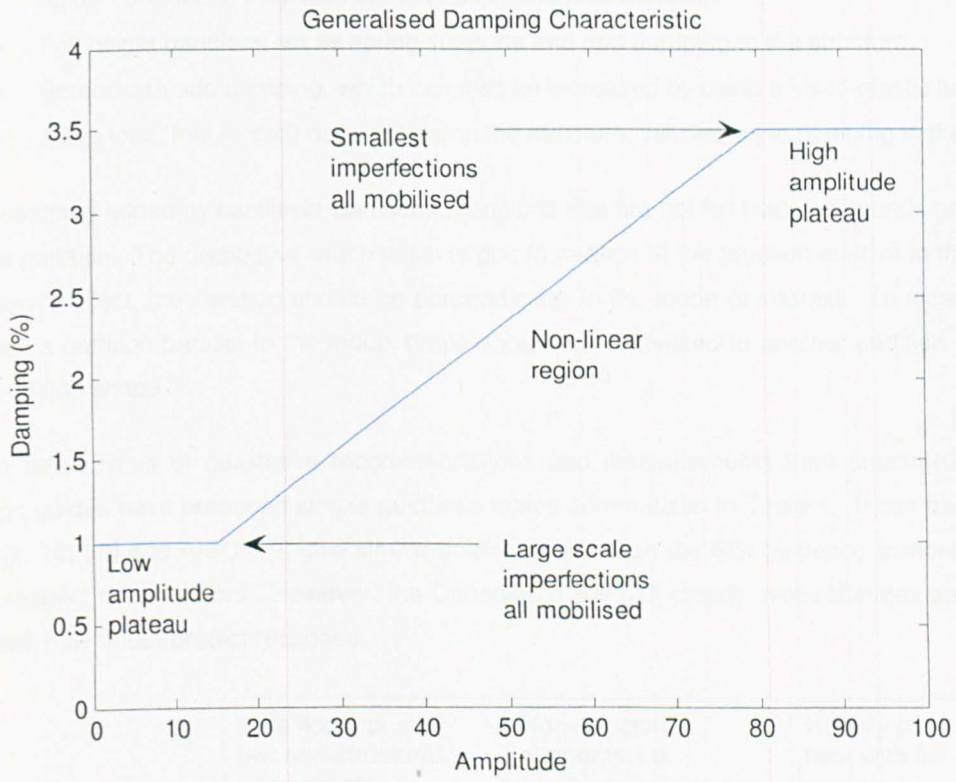

Figure 10 - Generalised damping characteristics after Jeary [64]

Although some structures seem to conform to Jeary's [64] generalised damping characteristic it is difficult, if not impossible to quantify accurately damping values. Whereas stiffness and mass properties can be predicted from physical principles, damping properties cannot. Some attempts have been made to describe damping of material properties via a dissipative Young's modulus and Poisson's ratio [65, 66], but such methods are not practical for design use. Methods have also been developed to obtain mass, stiffness and damping matrices from FRF measurements [67] but these will be case specific, i.e. the values will not have any physical meaning and will just fit with the measurements for that arrangement of the FE model. The damping due to micro cracking of materials has been investigated [66, 68] but is considered to be negligible compared to damping provided by

connections and non-structural elements [69]. Damping due to micro cracks is also highly dependant on the type of material, fatigue and many other factors which make if very difficult to predict.

For predicting damping ratios it is generally assumed using viscous damping will not introduce significant errors [55, 70], and a constant damping value can be used for the small amplitude of oscillation of floors. Bare structures do not provide a great deal of damping, generally less then 3%, with most of the damping provided by non-structural elements. Semi-permanent non-structural elements such as partitions and false floors have been the main focus of research in this area and the following conclusions can be made [71]:

- False floors will only contribute to damping if they are not rigidly connected to the structure. If rigidly connected, they will not increase stiffness or damping.
- Full height partitions act as spring supports and add damping to the structure.
- Screed can add damping, which can also be increased by using a visco-elastic admixture.
- A live load, that in itself does not damp the structure, will decrease damping in the floor.

The damping added by cantilever partitions (partitions that are not full height) depends on the direction of the partition. The dissipative mechanism is due to rotation of the partition relative to the floor, so for maximum effect, the partition should be perpendicular to the mode of interest. To increase damping further, a partition parallel to the mode shape should be connected to another partition perpendicular to the mode shape.

From these types of qualitative recommendations and measurements from structures the relevant design guides have produced simple guidance tables summarised in Table 4. It can be seen that the SCI [3, 16, 30] and AISC [19] give similar guidance, although the SCI guidance is more conservative with respect to bare floors. However, the Canadian guide [20] clearly over-estimates damping and as a result may under predict response.

	Bare floors or very few non-structural components	Non-structural elements, i.e. furniture, fixtures and fittings and cantilever partitions	Heavily partitioned floor with full height partitions
SCI P076 [3]	1.5%	3%	4.5%
SCI P331 [16]	1.1%	3%	4.5%
AISC [19]	2%	3%	5%
Canadian [20]	3%	6%	12%

Table 4 - Damping guidelines

The new Concrete Centre guide [5] has a slightly more detailed table for damping and includes bridges, but the range of damping is similar to that in Table 4.

The European report [45] has the most detailed table for damping shown in Table 5. The table gives damping for components of the construction. The total damping is the sum of the individual components.

Type	Damping (% of critical damping)
Structural damping	
Wood	6%
Concrete	2%
Steel	1%
Steel-Composite	1%
Damping due to furniture	
Traditional office for 1 to 3 persons with separation walls	2%
Paperless office	0%
Open plan office	0.5%
Library	1%
Houses	1%
Schools	0%
Gymnastic	0%
Damping due to finishes	
Ceiling under the floor	0.5%
Free floating floor	0%

Table 5 - Damping values from the European report [35]

For design purposes it is recommended that either these values are used or ones from measurements or experience [3, 5, 11, 30, 69, 72].

For the response of a HFF, damping is not so important due to the fact that a resonant response will not occur. However, it will play a part in reducing the RMS values of velocity due to decay in the averaging period.

2.3.4 Finite Element Analysis (FEA)

Finite element analysis has become an increasingly used tool in structural analysis due to the reduction in cost of computing power. FEA offers a more accurate and flexible solutions [54] in estimating dynamic responses, especially when the structural geometry is complex. Even so, a dynamic analysis can take a significant amount of time to run, requiring simplifications of the structure with minimal loss of accuracy by skilled analysts. A good general overview of the FEA process is provided by NAFEMS [73].

2.3.4.1 Modelling of floors

A HFF has many similarities with a LFF, floors are often constructed in a similar way using the same materials. This section considers a generic floor typical of all cases, and specific details in modelling of HFFs. It is a common misconception that modelling a structure in more detail, with a greater number of elements, will yield more accurate results. This is not the case, in fact a dynamic analysis may require less detail then a static analysis. Accurate modelling is a skill built up from knowledge and experience, and is essential for efficient modelling of any structure. Guidance for the modelling of floors is not widely available, although the latest design guides offer a little advice [5, 30]. There are two main points of excessive detail in FE models:

- Node density. The node density does however influence the maximum frequency of the model; therefore a HFF requires a greater node density then a LFF.
- Too much of the structure. If we are concerned with the response of one floor, then it is probably unnecessary to model the whole structure. Usually the floor and the columns above and below will suffice.

Another point to be made is that the stresses involved in dynamic analysis are much lower then for a static analysis. This has two consequences: the dynamic Young's modulus of concrete will be higher than that used for a static analysis, and pinned connections may act as if they are fully fixed. A number of modelling recommendations can be made for certain modelling scenarios:

The floor area: HFFs are often constructed with a typical slab and beam construction, this can be effectively modelled using beam and shell elements [5, 30], but care must be taken to compensate for the offset of the beam from the neutral axis. If additional stiffness is required the slab is often 'ribbed'. In analysis this extra stiffness can be smeared across the slab with a good degree of accuracy when compared with 3D block elements so long as the rib spacing is not to high [74]. Smearing can also be applied to a steel composite construction. This method can use as little as 1% of the computing time of the 3D block element. There are many options for waffle slab, which can be modelled as 3D block elements, or shell elements and a grillage of beam elements [75].

A common feature of HFFs is a large number of bays, which can number over 100. Analysing a waffle type structure with 3D elements with this number of bays often takes many days and can generate huge results files, creating problems even with powerful computers. This emphasises the need for efficient modelling.

Columns: Columns were traditionally modelled as pinned or fixed supports on the floor, however it has been shown that when the floor stiffness (in this case point stiffness at the floor centre) approaches half the column stiffness the error of this assumption became significant [12]. HFFs tend to be massive, causing a dynamic deflection of the columns indicating that the modelling of the columns is essential. The addition of columns would not add a significant amount of computing time.

Non-structural elements: It is generally agreed that non-structural elements can have an effect on the dynamic properties of a structure although how much they alter the dynamic properties and how to effectively model them is still being researched [71, 76]. Non-structural elements such as furniture can add mass and damping to a structure, but this is mainly concerned with a residential or office space, typically the domain of LFFs. The type of common non-structural elements found in HFFs are:

Partitions: Many studies have been conducted on the effects of partitions; probably the most in depth study is by Falati [71]. He found that partitions can add stiffness and damping, the degree of which depends on how the partition is oriented with the mode shape. Guidance on how to model them in an FEA is sparse but generally they are modelled as shell elements [5], although the material properties are unknown.

False floors: Services can be hidden below these and they are effectively another dynamic system between a footfall force and the floor structure. The most in depth study into false floors was by Reynolds [76]. He found that adding the false floor had little or no effect on natural frequencies, which suggest that the increase in mass is cancelled by an increase in stiffness of the floor. The affects on damping seemed to be random

Large mass objects: Objects such as machinery may add mass to a structure, but may be able to be considered not to act dynamically with the floor (excluding any force exerted by the object). These can simply be treated as extra mass.

Non-structural screed: Falati [71] also investigated the effect of non-structural screed and found that it added both mass and stiffness.

It is clear that non-structural elements change the dynamic properties of the structure but more research is required into how to model them accurately.

2.3.4.2 Solution Methods

As discussed previously there are three types of forcing methods commonly used in floor vibration analysis: A harmonic approach using Fourier co-effecients, Arup's effective impulse and a real force time history. Which form of forcing method is chosen can influence the solution method used. The methods described here are modal analysis, harmonic or spectral analysis, and transient analysis.

	Fourier Co-eff's	Arup's Effective Impulse	Real Time History
Spectral/Harmonic	X		
Modal Superposition	X	X	X
Full integration	X		X

Table 6 - Solution methods for various forcing methods

2.3.4.2.1 Modal Analysis

Modal analysis in the context of a FE analysis is the estimation of modal frequencies, masses and shapes for the FE model by solving the Eigen problem:

$$([K] - \omega^2[M])u = 0$$ **Equation 33**

where $[M]$ and $[K]$ are the mass and stiffness matrices respectively and u is a vector of displacement. This knowledge of modal properties is essential, as initial design is based on avoiding a minimum frequency. There are many methods of solving the Eigen problem, depending on which FE code is used (e.g. ANSYS, LUSAS, Nastran etc.).

The results from the modal analysis are required for spectral analysis and modal superposition. FE modal analysis is also a recommended step before an experimental modal analysis (EMA) [77] since estimates of mode shapes and frequencies can be used to design an efficient testing procedure.

2.3.4.2.2 Harmonic and Spectral Analysis

A steady state response can be obtained from a harmonic or spectral analysis. This method of analysis is useful when a force can be clearly described in the frequency domain, such as a walking force for a LFF, or for machinery with harmonic force output. The problems with this method are that the waking path may not allow a steady state response and non-lineararties are not supported.

2.3.4.2.3 Transient Analysis

There are three common methods of transient analysis, each with their advantages and disadvantages:

Modal Superposition

Modal superposition works on the principle that a vibratory system can be split into a number of vibration modes, the maximum possible number of modes is equal to N, the number of DOFs in the system. If the response is known for each of the individual modes the total response can be obtained by summing n modes:

$$v = \sum_{n=1}^{N} \phi_n v_n$$ **Equation 34**

where v is velocity and ϕ is mode shape of the nth mode. The main points of modal superposition are:

- n is much less then N, usually less than 100 modes for many thousands of DOF
- Less computer time then the other two methods
- Modal damping and a constant damping ratio can be used
- Non-linearities and non-proportional damping are not supported

Direct Integration using Matrix Reduction

Matrix reduction works by reducing the size of the system matrices using methods such as 'Guyan reduction' [78]. The user will choose master DOFs which will then be used to solve the problem. the results can then be expanded to the rest of the nodes in the model. The main points of matrix reduction are:

- Less computer time then full integration
- Loads must be applied only at master DOFs (although loads applied elsewhere can be interpolated onto the master DOFs)
- Non-linearities are not supported

Direct Integration with full matrices

Full integration uses the complete system matrices and will obtain the most accurate analytical solution. The main points of full integration are:

- Most simple as mode shapes and master DOFs do not need to be considered
- Allows non-linearities
- Very expensive in terms of computer time, and memory.

If the master DOFs are correctly selected or the correct number of modes is chosen all methods can give similar results. As modal superposition is least expensive, and for floor vibrations non- linearities are not of a concern, this is the best compromise between ease and expense, hence this is the method adopted by the latest design guides [5, 30, 40].

2.3.4.2.4 Mode Participation

The difficulty with modal superposition is deciding how many modes to include in the summation. NAFEMS [44, 73] suggest a method similar to the mode participation factor used in seismic analysis, but adapted for a more generalised loading. The method has not been published in a peer reviewed journal and is poorly described. The participation is split into two parts, a spatially varying part A, and a time varying part B where:

Equation 35

$$A = \sum_{r=1}^{m} P_r P_r$$

where m is the number of modes and P_r is a modal force of mode r defined by $P_r = \phi_r^T F$ where ϕ_r is the mode shape vector of mode r and F is a force vector.

Equation 36

$$B = max \left| \int_0^t \frac{\sin(\bar{\omega}_r t)\, e^{\omega_r \xi_r t}(t-\tau)a(\tau)}{m_r \bar{\omega}_r} d\tau \right|$$

which is derived using the Duhamel integral. Subscript r represents the current mode, $\bar{\omega}_r$ is the damped natural frequency, $\bar{\omega}_r$ is the un-damped natural frequency, m_r is the modal mass and a is a force time history.

If the mode shapes are mass-normalised, part A can be shown to tend towards $\{F\}^T[M]^{-1}\{F\}$ as more modes are used, where $\{F\}$ is a global force vector and $[M]$ is the mass matrix. It can be considered that enough modes have been used when part A reaches a certain percentage of $\{F\}^T[M]^{-1}\{F\}$.

The time varying part B simply makes a frequency spectrum of response in terms of displacement with respect to the force time history. This allows the user to observe when the response of the spectrum will reduce to a negligible level (i.e. the point at which there is little response at higher frequencies), this frequency can be the upper limit cut-off. Part B can easily be differentiated to obtain velocity or acceleration.

This method is poorly described in the original publication, however, in Chapter 5.5 the method has been reversed engineered and is described in detail.

2.4 Receiver

Traditionally, vibration serviceability assessments for floors have been based on human sensitivity as the vibration criteria, but sensitive equipment requires vibration levels one or two orders of magnitude less than humans will tolerate. This section briefly describes how the vibration criteria for humans were created and how they evolved into the current criteria for sensitive machinery.

2.4.1 Humans

The history of perception of vibrations for humans has been covered in detail by Pavic *et el.* [9] and Zivanovic *et al.* [1] and will only briefly be presented here.

One of the earliest works, and probably the most frequently cited, was by Reiher and Meister in 1931 [79] who studied the reaction of people in different postures to harmonic excitation. They developed perception curves that have been constantly updated as more data have become available. Goldman [80] derived new perception curves using data available from other authors in terms of perception, discomfort and maximum tolerance and was the first to specify different tolerance levels. The curves developed so far were developed in laboratory conditions which did not account for the activity or situation of the occupants [81], but the activity and situation played an important aspect of vibration sensitivity [10, 11]. For example, pedestrians walking were more tolerant then those standing [38, 39], certain postures made pedestrians more sensitive, and if pedestrians 'expects' vibrations they are likely to be more tolerant. Irwin [82] used data from laboratory work and tests on real structures to create perception curves for different types of structures and different types of vibrations. He proposed a baseline curve for the limit of perceptibility, this curve could then be multiplied by factor depending on the situation, e.g. for storm conditions he suggested a multiplication factor of 6. This is the basis behind the modern perception criteria [10, 11, 83] where a perception limit is given depending on a person's posture, and a multiplication factor depending on the activity. As the perception curves have developed, there has been debate on which unit to present them as, displacement [80], velocity [84] or acceleration [85]. If the response is considered to be a function of harmonic frequencies then by integration or differentiation it is easy to switch between metric, however it is noted that human tolerance seems to be a constant when expressed as velocity [84] (true when above 8 Hz [10, 11]).

2.4.2 Machines

In the past, vibration criteria for sensitive machinery were poorly specified by the tool manufacturers. Generalised criteria have been developed to categorise the performance of a floor, and to allow tools of a common sensitivity to be grouped. This section deals with the most common of the criteria used today.

2.4.2.1 Bolt Beranek and Newman's (BBN) Vibration Criteria

During the 1970's BBN started working on the problem of excessive vibrations of floors for sensitive machinery after Intel reported problems arising from vibrations [86]. Many manufacturers were

offering poor, if any, vibration acceptance criteria with their products [87, 88]. It was not clear whether to use RMS or peak values of vibration, whether to represent response in the time or the frequency domain, and if the frequency domain was chosen, how to define the criteria in terms of frequency range or bandwidth. BBN created sensitivity curves (known as the VC curves) from criteria of individual items of sensitive equipment and from data from facilities before and after vibration problems were solved. Figure 11 shows the VC curves ranging from the least stringent, VC-A, to the most stringent, VC-E, represent as proportional bandwidth, RMS velocity spectrum.

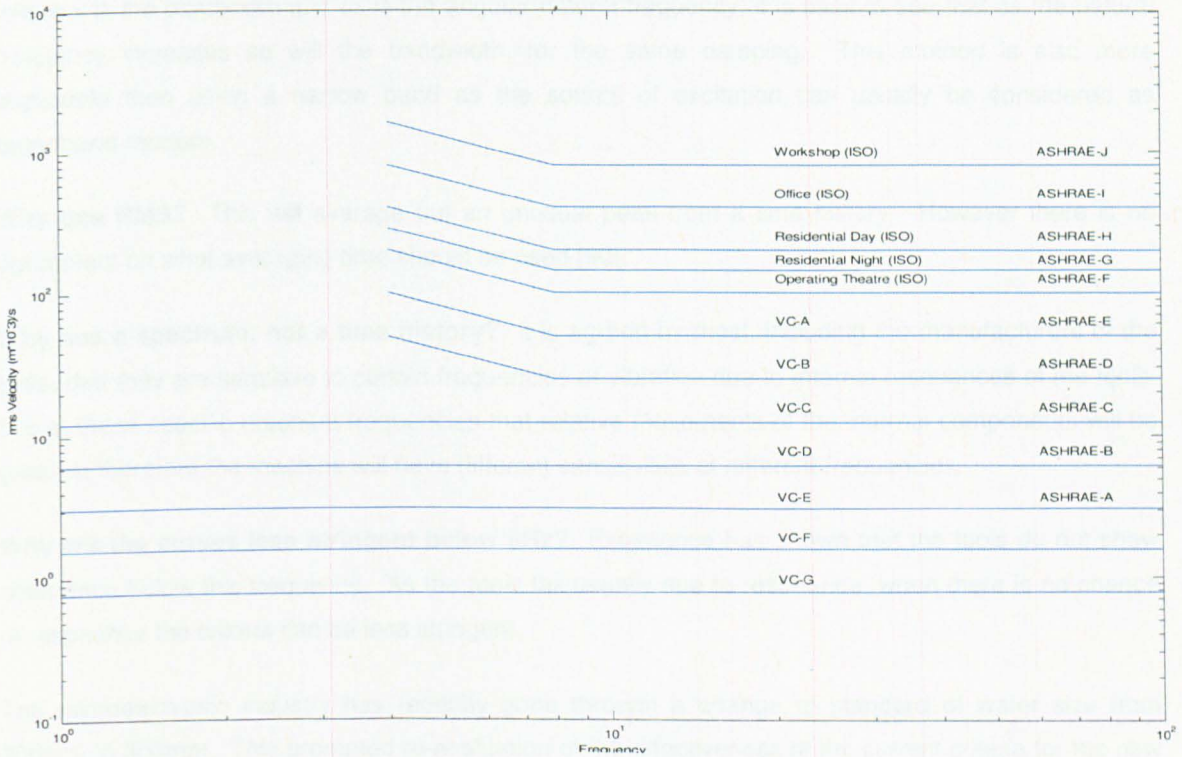

Figure 11 - Generic vibration criteria (VC) curves for sensitive machinery, including ISO and ASHRAE guidelines

Although BBN's justification of the VC curves, they seem to be an extension of the ISO2631 and BS6472 [10] velocity limits for humans using the technology that was available (FFT analysers were rare and expensive, 3rd octave analysers were the norm). The main criticisms of the VC curves, with explanations, can be summarised [86, 89]:

Why velocity? Many of the processes in vibration sensitive areas are photographic in nature (i.e. using photosensitive sensors) [86]. Such processes can tolerate limited blurring, which is defined as the distance travelled during the exposure, i.e. velocity. The velocity criteria appear constant within a class of machine with respect to frequency. Also, using the frequency domain a conversion can be made between displacement, velocity and acceleration, with velocity only one integration or differentiation step from the other metrics.

Why proportional bandwidth? It allows for a conservative view of the internal damping of the tool. Increased damping widens a resonant peak, allowing it to be excited more by a range of frequencies around its natural frequency. As the relationship of damping and the width of the peak can be given by:

$$\zeta = \frac{x}{2\omega_r}, \qquad \textbf{Equation 37}$$

where x is the bandwidth and ω_r is the angular natural frequency, it is easy to see that as the natural frequency increases so will the bandwidth, for the same damping. This method is also more applicable then using a narrow band as the source of excitation can usually be considered as broadband random.

Why use RMS? This will average out an unusual peak from a time history. However there is no agreement on what averaging time should be used [90].

Why use a spectrum, not a time history? It is agreed by most, including the manufacturers of the tools, that they are sensitive to certain frequencies of vibration due to internal resonances of the tools. It is at these specific resonant frequencies that relative movements of the internal components will be greatest therefore the machine will have different sensitivities at different frequencies.

Why are the curves less stringent below 8Hz? Experience has shown that the tools do not show resonance below this frequency. As the tools fail usually due to resonance, when there is no chance of resonance the criteria can be less stringent.

The microelectronic industry has recently gone through a change of standard of wafer size from 200mm to 300mm. This prompted re-evaluation of the effectiveness of the current criteria for the new standard. Bayat and Gordon [87] discussed the VC curves and noted that although the feature sizes are getting smaller, manufacturers are paying more attention to the vibration design of their tools. The current criteria are still valid but a modern tool of a certain feature size can now operate in a noisier environment than before. VC-E should be the highest standard for a long time to come as this curve is almost at ambient vibration levels which are always present in the earth. As manufacturers are developing their tools in light industrial areas, using a slab on grade floor with traffic present, they cannot expect better operating environments than VC-E without specialist vibration mitigation [86] such as low frequency air springs and folded pendulums [29]. Some new tools are being developed with pneumatic supports for vibration isolation, making the tool susceptible to low frequency vibration, so it has been suggested that the curves below 8Hz also stay constant for tools with pneumatic supports [86]. Leung and Papadimos [88] studied criteria of metrology equipment and found that these can be more sensitive at lower frequencies and suggested that the curves are made more stringent below 8 Hz.

The VC curves have been by far the most generic and useful criteria available to date, however, they do have some problems. Using RMS velocity to average out peaks can cause problems as signals with large crest factors and unusual peak factors are hidden, and the result can be disruption of tool operation due to large but short transients.

The VC curves have been updated to try to address some of these issues. The curves from VC-C and below are now flat, so the tolerance does not increase in the lower frequencies, and there have also been two more classes added, VC-F and VC-G [91]. These new classes are not intended for design, but to address a call from scientists to classify their ultra quiet spaces.

2.4.2.1.1 Evaluation of Floor Areas

Colin Gordon and Associates have published methods of determining the response of a floor [91] containing two floor states: 'as built state' and 'after as built'. The as built state is defined as: "the building's structure is complete and its mechanical equipment is operating". The after as built state is defined as: "with these tools installed but not operating". This suggests the as built state is the floor with all the support equipment installed but no tools and after as built is when the tools are installed but not operating.

If it is a small space it is reasonable to characterise the vibration of the floor at the tools location. However, if it is a large space that needs characterising they suggest measuring a "statistically significant number of randomly selected locations" and to characterise the space using a log mean average plus the standard deviation:

$$\log(A_{mean+sig}) = \log(A_{mean}) + \log(A_{sig}) \qquad \textbf{Equation 38}$$

where A_{mean} and A_{sig} are the log average and log standard deviation of a set of measurements respectively.

2.4.2.2 Ahlin's Equivalent Peak Velocity Spectrum

Ahlin [92] developed a machine specific method published by the ISO in ISO TS 10811-1 [93] so that the method can be tested for its validity. Each filter corresponds to the Q normalized pseudo velocity response of a single-degree-of-freedom system with a defined resonance frequency and Q value, where Q is a gain factor of a SDOF oscillator. The method gives the amplitude of a sine wave having the same maximum relative displacement response as the studied vibration. The spectrum obtained can then be compared with vibration criteria based on sinusoidal testing of equipment.

The filter is shown in Figure 12 and defined by:

$$H_a(s,w_0,Q)=\frac{-\omega_0}{Q}\Big/\left(s^2+\frac{\omega_0 s}{Q}+\omega_0^2\right)$$ **Equation 39**

where Q is the gain factor, ω_o is the natural frequency of the oscillator and s is the laplace variable. The derivation of the filter is based on a SDOF transfer function and is described in [93]. The filter should be applied to the signal at all frequencies up to 100 Hz.

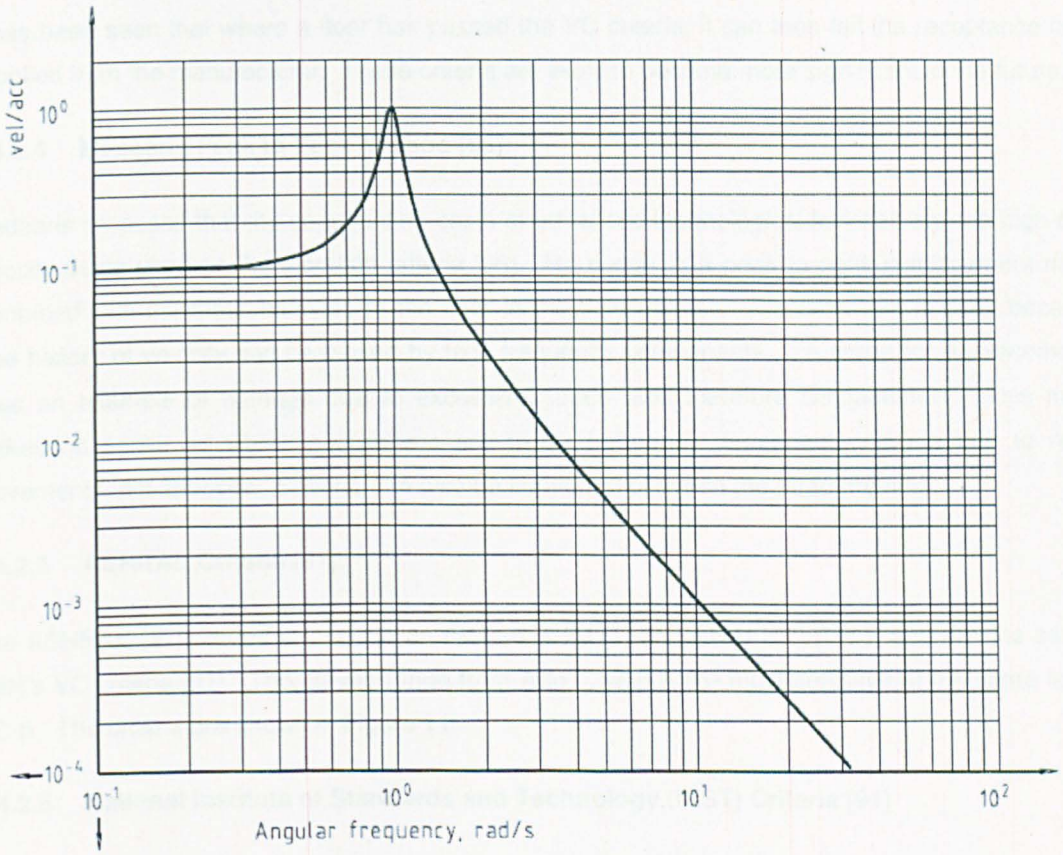

Figure 12 - Filter function for SDOF system (Q=10 Fn=1)

In his paper, Ahlin [92] used a CD player and a lorry as an example. He attached the CD player to a shaking table to produce a spectrum of when the CD player would skip using pure tone sinusoids. This spectrum was used to generate the filter that was applied to the response time history of the lorry. It was demonstrated that if the equivalent spectrum from the truck is below the CD player's spectrum then the CD player will not skip. It is an interesting point that this method does not require RMS averaging.

2.4.2.3 Receptance Criteria:

Traditionally, photolithography tools were know as 'steppers', i.e. the tool stopped and was at rest during the exposure. The newest tools are known as 'scanners', i.e. they do the exposure on the fly, increasing production, but not allowing the tool to be at rest before the exposure. The floor must be stiff enough to resist the force of the scanner as it is moving; as such, some tool manufacturers specify receptance criteria [94, 95] (i.e. how much the floor will displace with respect to force).

It has been seen that where a floor has passed the VC criteria, it can then fail the receptance criteria supplied from the manufacturer. These criteria are likely to become more significant in the future.

2.4.2.4 Medearis Peak to Peak Method [96]:

Medearis proposes that the construction costs of advanced technological facilities are too high due to velocity being used as the vibration criteria [96]. He suggests a peak to peak displacement method combined with the static stiffness of the floor in the time domain. Displacement is used because a time history of velocity can be biased by high frequency components. To argue for displacement he uses an example of damage due to excessive stress, and therefore displacement. This method makes no sense as vibration problems are highly frequency dependent and are due to relative movements, not stresses. Spectra can also be converted between the three metrics.

2.4.2.5 ASHRAE Criteria [97]:

The ASHRAE [97] criteria are based on ISO 2631-2 [11] and ANSI S3.29 [83] and are the same as BBN's VC criteria [91]. The curves range from A to J, with A the most sensitive at the same level as VC-E. The criteria are shown in Figure 11.

2.4.2.6 National Institute of Standards and Technology (NIST) Criteria [91]

The NIST criteria were developed for metrology equipment at NIST's Advanced Measurements Laboratory. There are two NIST criteria, NIST-A and NIST-A1. NIST-A is more stringent then VC-E below 20 Hz and the NIST-A1 criterion is generally "better then ambient" and requires vibration isolation. These criteria are very stringent and are not widely used.

2.5 Conclusion and Discussion

This review has discussed the response of high frequency floors (HFFs) to a footfall which is commonly assumed to be the most severe excitation of the floor. Simplifying a footfall force time history for use in design has been the subject of research for many years, with the current state of the art using Fourier harmonics of the force for low frequency floors (LFFs) and an 'effective impulse' for

HFF's. The different approaches are due to the consensus of little energy in a footfall above the fourth harmonic (approximately 10 Hz) so resonance is unlikely to occur. The latest method produces reasonable predictions of floor response, however there are three main issues worth addressing:

- Floor resonance can be shown to appear above the 10 Hz boundary
- The effective impulse is only suitable for modal superposition
- Arup's effective impulse was developed using peak responses, not RMS values, which are used in the relevant criteria.

The latest SCI design guide [30] addresses the first point by changing the high/low boundary depending on activity, increasing the frequency for rhythmic activities. This does not help with the rare occasions when resonance has occurred due to walking above 10 Hz. What is required to address each point is a universal footfall force that can be used in all cases without alteration. Presently the most accurate simulation of floor response is to use real recorded footfall time histories, but these are not widely available.

Estimation of floor dynamic properties has traditionally been carried out with LFFs in mind, which is with resonance as the worst case. With this approach the response is sensitive to the accuracy of the fundamental mode, damping values and Fourier co-efficients. The guidelines have been focused on estimating these properties for simple uniform structures. This simplified guidance is not suitable for estimating higher modes of vibration, modal mass and for non-uniform structures, which are all essential for response estimation of HFFs and many LFFs. As a result, it is highly recommended that a dynamic analysis is carried out using FEA. With modern inexpensive computing power and the fact an FE model is usually created for the static analysis, this method should become the norm, with the simplified method used for preliminary design only. Unfortunately, there is very little guidance given about modelling floors for dynamic analysis. There is also a question about how much of a structure needs to be modelled. A large fab can have over 100 bays, and it has been shown that after a point, increasing the number of bays in a structure does not mitigate the response. It therefore seems logical that after modelling a certain amount of the whole structure, the model would produce response representative of the complete structure.

Modal superposition has become the method of choice due to the efficiency of the method and due to the nature of the forcing methods. The issue with this method is the number of modes to include. With LFFs it is relatively straight forward, with the choice limited to the modes that may achieve resonance, however with HFFs this is not the case. The design guides [5, 30, 40] state that modes up to twice the fundamental natural frequency should be used. This guidance is suitable if the first mode of vibration is below approximately 20 Hz, as the magnitude of the force spectrum of a footfall drops sharply with respect to frequency at this point. However, the force drop is not linear and hence is much less at higher frequencies, so that doubling the frequency will not achieve a substantial force drop. As a result the mitigation from increasing the frequency is negligible when compared with other factors. Usually it is the modal mass which is the mitigating factor [61] and the 'twice the fundamental

natural frequency' is no longer accurate. Inclusion of all modes up to 100 Hz (the same as the criteria) seems like a possible solution, but for a large fab this could include many hundreds of closely spaced modes which is somewhat reducing the efficiency of the modal superposition method. A neat method of including only relevant modes is required.

The most widely used vibration criteria for HFFs is BBN's third octave band criteria [86]. This method is an extension of ISO guidance for human tolerance of vibration [11] extended beyond the perception range of humans, with grouping in third octave bands. The method has had publications issued by the creators of the method justifying its application, but there have not been many independent attempts at verifying the criteria. The problem with validating the method is that testing opportunities of relevant tools and machinery are rare, but machine specific criteria could be important for two reasons:

1. From the 1st author's experience, the sensitivity of a machine does not sit on a constant velocity line and seems somewhat random.
2. Generic criteria for humans are used due to many different people using the same floor, the design is not for a specific human, it is for an average human. Although individuals will have individual tolerances, having criteria which are suitable for most people is deemed most appropriate. For floors supporting machines or tools, their will only be a small number of different tolerances, designing for a generic criteria instead of tool specific criteria could be inefficient. For example, if a floor is to be fitted with a tool that under current guidance requires a VC-D floor, the floor would have to be designed to this standard. However, if the tool only needed VC-D in a small range of frequencies, and was VC-C elsewhere the floor could be designed more efficiently.

A new ISO publication [93] suggests a tool specific criteria based on a shock response spectrum, which may hold promise. Generic criteria are a very good for a general categorisation a floor, and would allow for change in the floor's usage (a VC-D floor would support any VC-D tool). However, it may be more economic to have a detailed knowledge of the dynamic performance for an individual tool and floor.

A new problem has recently been identified; the latest tools complete their sensitive operation while parts of the tool are in motion requiring the floor to be stiff enough to resist these movements. A receptance criterion is being developed [94] to address this, which is effectively a minimum dynamic stiffness the floor must also meet.

The review has shown that the design of a high frequency floor possesses many unknowns which make the response prediction from walking difficult. Experimental verification is the only way to know the dynamic properties of the floor. Experimental modal analysis can be conducted to provide estimation of modal properties, including damping, and actual response measurements can be obtained to estimate the response to a walking force. This can then be compared to the criteria of the actual machine that will be placed upon the floor. This is the only method available to determine for sure if the floor will pass.

3 Evaluation of Footfall Forcing Models

This chapter investigates the current state of the art in footfall forcing models. The models investigated are the models often used in current design guides: the 'kf method' [46] used in the AISC design guide [19], Arup's effective impulse [31, 98] used in all current guidance [5, 6, 21] in the UK and the European Commission (EC) polynomial method presented in an EC funded research project [45]. All the models listed are either for high frequency floors (HFFs), or are presumed to be acceptable for all floor types. For low frequency floors (LFFs) different force models are used. The rationale for different models is due to the response of the floors. HFFs are assumed not to resonate, responding transiently, whereas LFFs are assumed to resonate, with the resonant response dominating the response. A resonant response can be accurately determined by harmonic analysis so long as the harmonics within the footfall force are accurately determined. The accuracy of the harmonic method, which is used in all current design guides for LFF response, is dependent on the published harmonics. This chapter is not concerned with the published magnitude of the forces but with the method behind the model; as such an analysis of the LFF harmonic method is out of the scope of this evaluation.

This chapter begins by investigating the validity of the boundary between high and low frequency floors. The boundary is defined as the transition from a floor responding with resonance to a floor that has a transient response, and is discussed in detail in Chapter 2. In the most current guidance, the boundary is fuzzy, suggesting a resonant response could occur above 10 Hz, and the effective impulse is valid from 4 Hz [5]. The key factor in determining the magnitude of a resonant response is the force amplitude of the harmonic at the systems resonant frequency. The maximum significant harmonic of walking shall be experimentally determined by examining variations in pace rate. The maximum frequency at which resonance is likely to occur can then be determined and compared to the current boundary in the guidance.

The chapter then continues to analyse the various force models. This analysis will be different to past analyses measured where the validations of the models have been somewhat incomplete. For example, when the kf method was originally presented, no response comparisons were conducted, and the rationale for the simplified pulse was: "This approximation may be expected generally to produce only minor errors in any corresponding structural response estimates" [46], with no proof of that statement. When Arup's effective impulse was presented, their rationale was much more detailed. Arup discussed why existing models performed poorly and what their model would try to address. Response comparisons were then conducted on three floors to validate the method. Some independent evaluations have also been conducted, such as by Pavic *et al.* [99]. In their study they compared the accuracy of a number of models by comparing with measured results. However, the study was on a single floor so it is not conclusive. A more scientific method by Brownjohn was used comparing the effective impulse and kf method with measured forces using an SDOF oscillator [51]. Brownjohn's method allowed for a large number of stiffness and mass combinations, not achievable using floor responses for comparisons. Each model, when presented, has had its rationale described,

with the validation consisting of comparing simulated response (usually from finite element analysis) to measured responses from walking. There are two problems with this approach:

1. The accuracy of the FE model can significantly affect the response.

2. The force applied to the real structure during the response measurements is not the same force that was used to create the simulated force function.

As such, the response may have the same order of magnitude and have a similar looking time history, but there is no indication of where inaccuracies lie. Another problem is that a footfall force model may be accurate under specific circumstances (e.g. for a certain frequency range or number of paces). As such, for the specific floor used in a comparison the model may perform well, although the model may be poor. For another floor, with different dynamic properties or different participants, the performance may be very different. The analysis presented here shall investigate the method used to create the footfall model and then compare response spectra and time histories accurately determining where the inaccuracies and the limitations of each model.

Based on the analysis, the chapter then concludes by presenting clear characteristics that a new footfall model should have, leading towards a universal force model suitable for all floor types.

This chapter uses measured walking forces of the author. The collection of these forces is briefly described in Appendix A, but has not been included in the main text for clarity.

3.1 Evaluation of the High Frequency and Low Frequency Floor Boundary

Currently the classification of the type of floor dictates the method of analysis to be used in estimating the floor's performance, therefore the accuracy of this distinction is an important factor. The boundary has not been static, varying from 8 Hz to 12 Hz for walking and between 16 Hz to 22 Hz for rhythmic activities. The value of the boundary is still under discussion in the research community, primarily due to the number of significant harmonics generated by an individual walking not being well defined.

Applying the discrete Fourier transform to a transient signal will produce discrete frequency points in the corresponding spectrum. If the transient is not random, and is a simple signal, there are often smaller subsets of the Fourier amplitudes that govern the signal, and this is the case for a footfall force. If this type of transient is repeated periodically, then clear maxima of the Fourier amplitudes are shown in the spectrum which correspond to harmonics in the signal. In the case of a footfall, these harmonics are at multiples of the pace rate. When considering a walking time history, containing many paces, the signal is usually assumed as periodic. However, in reality, the pace rate is a random variable with measurable statistical properties. As such, the walking force, even if using the same

single footfall force, is a random signal. In the case of walking, the degree of variation of the pace rate, and therefore the degree which the force is a periodic, affects the harmonics of the force. This, in turn, affects how many significant harmonics are likely to be contained within the force and which are likely to have caused resonance of the floor.

An experiment was designed to measure variation in pace rate with participants attempting to walk at a fixed pace rate aided with a metronome (i.e. prompted). A single pace was then used to create two walking force time histories: one with no variation of the pace rate and the other using the measured variation. The Fourier amplitude spectra of the two constructed walking time histories were compared to determine how the amplitudes of the harmonics have varied. Finally, using the results from the analysis, the validity of the high frequency and low frequency boundary is discussed.

3.1.1 Experimental Method

The acceleration response of eleven individuals were measured walking along an 11m long, simply supported slab strip (described in more detail in the following chapter). To achieve the best statistical sample the group had six nationalities, a mixture of male and female (although it was slightly biased towards male), and age range from early 20's to approximately 50 and with a variety of body type and height. Each individual walked along the slab strip twice (i.e. 2x11m) at a range of frequencies prompted by a metronome. The frequencies varied from the uncomfortably slow, at 1.5 Hz, to uncomfortably fast, at 2.5 Hz, with 0.1 Hz intervals. Eleven accelerometers were evenly spaced along the slab strip to measure the response. Figure 13 shows two photographs of the experiment in progress, Figure 14 shows the accelerometer positions and describes the procedure.

Figure 13 – Pace rate variation walking experiment

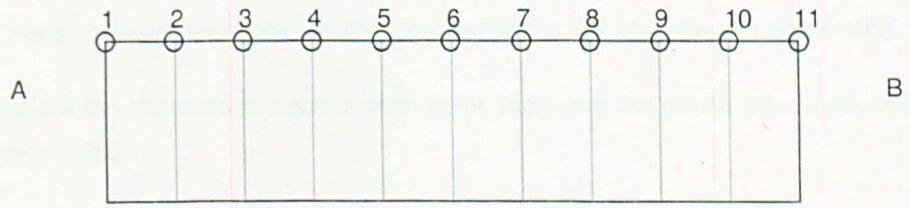

O Accelerometer points

Procedure:

Start on platform at B on 1st pace rate.
Walk to platform at A, turn around on the platform.
Walk to platform at B.
Change pace rate, repeat.

Figure 14 – Accelerometer placement and experimental procedure

3.1.2 Analysis of Results

The first two modes of vibration are 4.5 Hz and 16.2 Hz respectively with damping below 1% (refer to the following chapter for more detail). For both of these modes, even though the second mode would fit the HFF category, the response does not decay enough to distinguish successive footfalls (shown in Figure 15(top)). As such, it is not possible to identify individual paces to determine pace rate variations. Two possible solutions were developed to identify the impact of a footfall:

1. Band-pass filter around a higher vibration mode
    - A higher mode would allow more oscillations before the next footfall, this would allow the response to decay to a lower response level before the successive footfall, making it easier to determine.
2. Band-pass filter between the first two natural frequencies using a rectangular FFT filter
    - As there is no mode in the frequency range the response would exhibit a quasi static response that quickly decays, making each footfall easy to determine.

Each method was investigated and method 2 was chosen. The reason for this choice was that both methods worsen the signal to noise ratio, but due to there being more energy in the footfall force between the first two vibration modes than at a higher vibration mode, the filtered response was much cleaner. The complete procedure for filtering these data was:

1. Choose measurement points with large responses (i.e. low signal to noise ratio).
2. Square the response of each chosen point, then sum the values (also improves the signal to noise ratio).
3. Apply FFT band-pass filter between 5-16 Hz

Figure 15(bottom) shows the filtered response with each individual footfall is now very clear and its temporal properties identifiable. The period between each footfall is determined by a series of peak picking. The inverse of the period represents the pace rate in Hz, these data are collected and probability density functions are to the data for each pace rate.

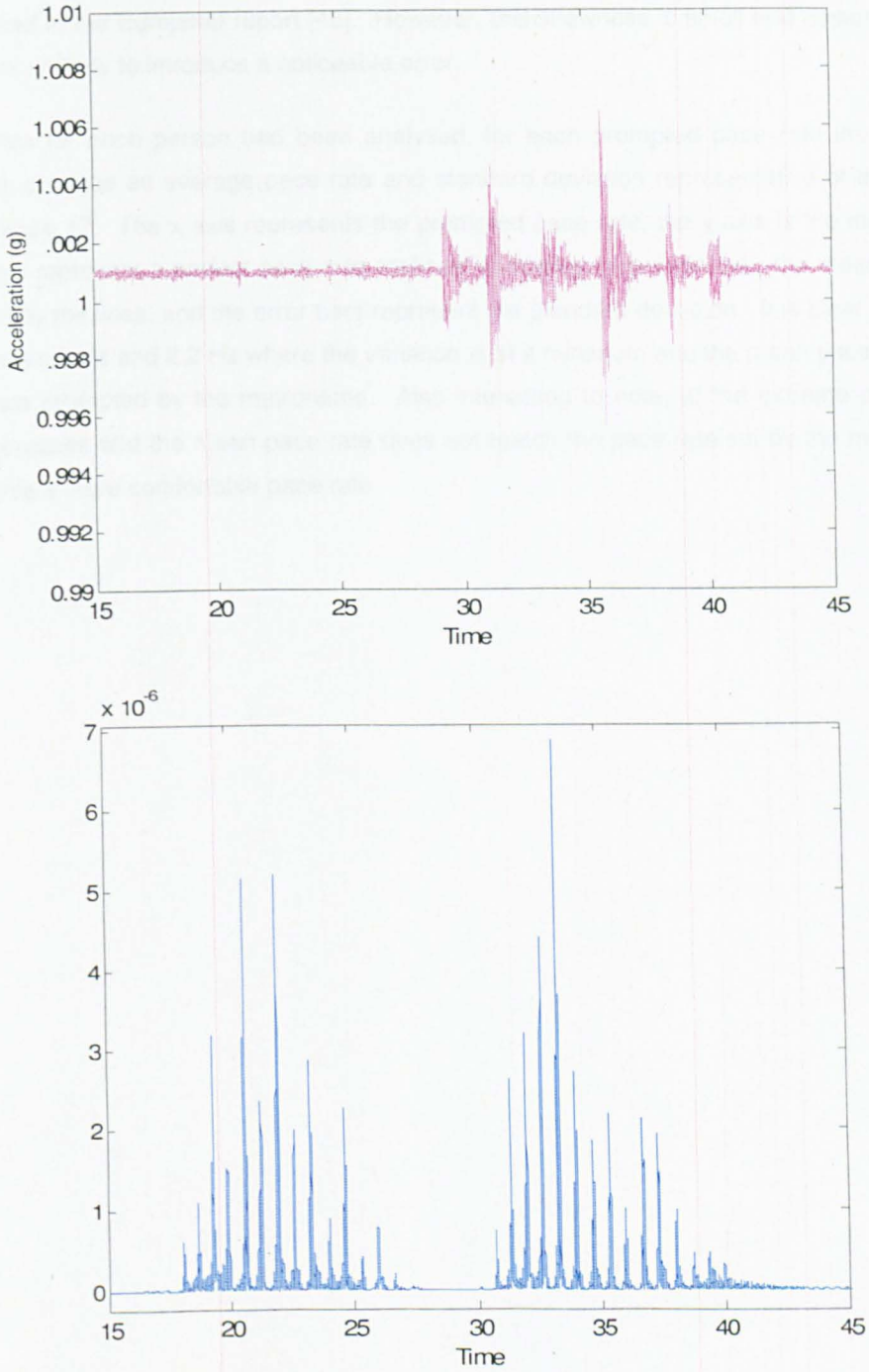

Figure 15 ***(from top to bottom)*** **– Unfiltered acceleration time history response; filtered acceleration time history response; due to the filtering applied, the units of the bottom plot no longer have real meaning**

Figure 16(top) shows a normal distribution check for 2.1 Hz pace rate and it seems to fit well. However, on close inspection it is evident that at the extreme ends of the pace rate range the data is biased towards a comfortable pace rate. For instance, at 1.5 Hz pace rate, more pace rates are above 1.5 Hz, at 2.0 Hz, which is comfortable, the distribution is normal with a relatively even distribution, and for a 2.5 Hz pace rate there are more paces below 2.5 Hz). This tendency skews the

distribution as shown in Figure 16(bottom). This similar type of distribution of walking data has also been identified in the European report [45]. However, this skewness is small and assuming a normal distribution is unlikely to introduce a noticeable error.

After the data for each person had been analysed, for each prompted pace rate the results were combined to produce an average pace rate and standard deviation representative of the 11 people, shown in Figure 17. The x axis represents the prompted pace rate, the y axis is the measured pace rate, the dots represent a perfect pace rate (defined as having zero variation), the mean pace rate is represented by the lines, and the error bars represent the standard deviation. It is clear that there is a region between 2 Hz and 2.2 Hz where the variation is at a minimum and the mean pace rate matches the pace rate prompted by the metronome. Also interesting to note, at the extreme pace rates the variation increases and the mean pace rate does not match the pace rate set by the metronome, but tends towards a more comfortable pace rate.

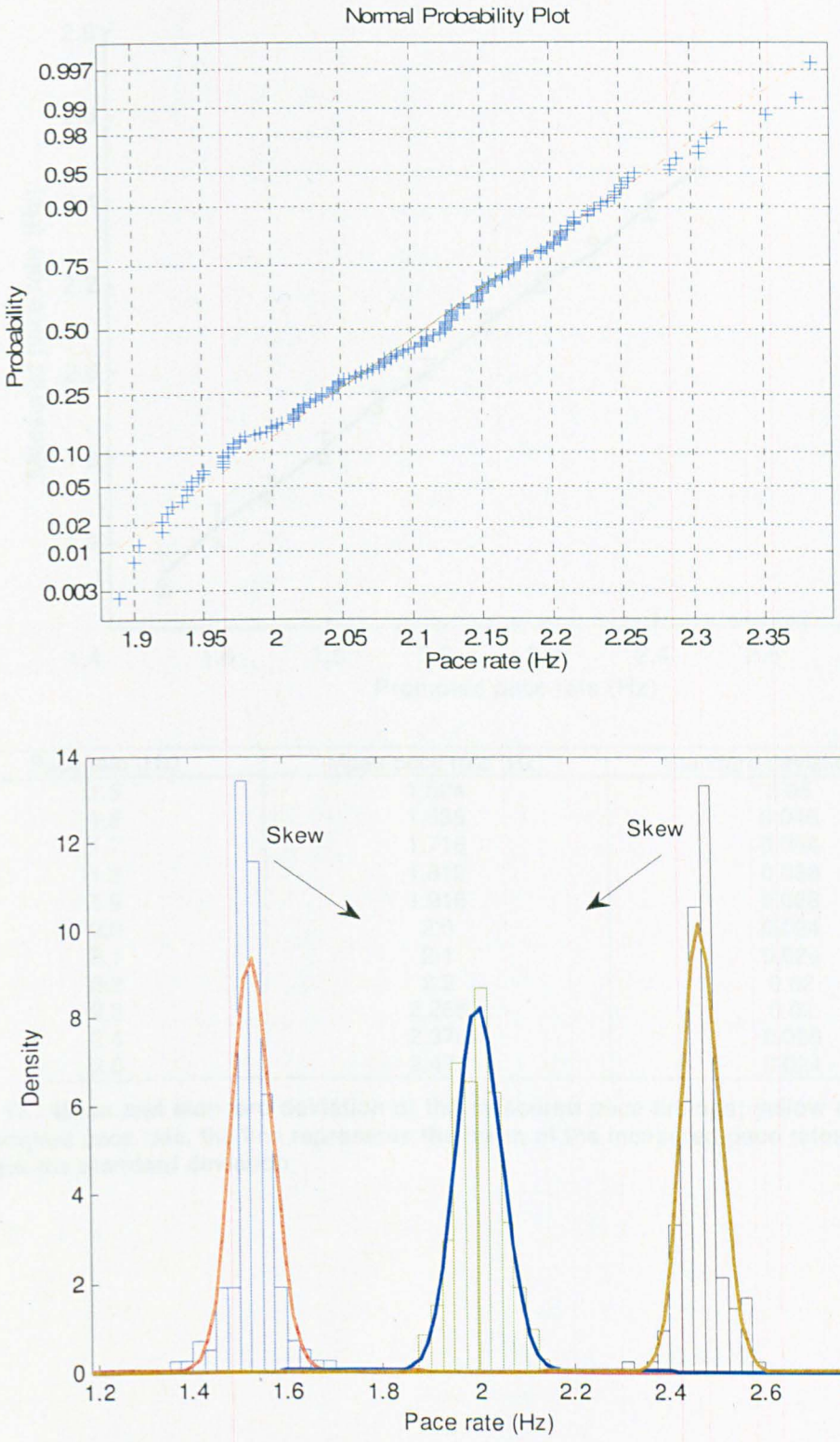

Figure 16 *(from top to bottom)* **– Normal distribution check for a 2.1 Hz pacing rate, for all subjects; Probability distribution plots for 1.5, 2.0 and 2.5 Hz pacing rates**

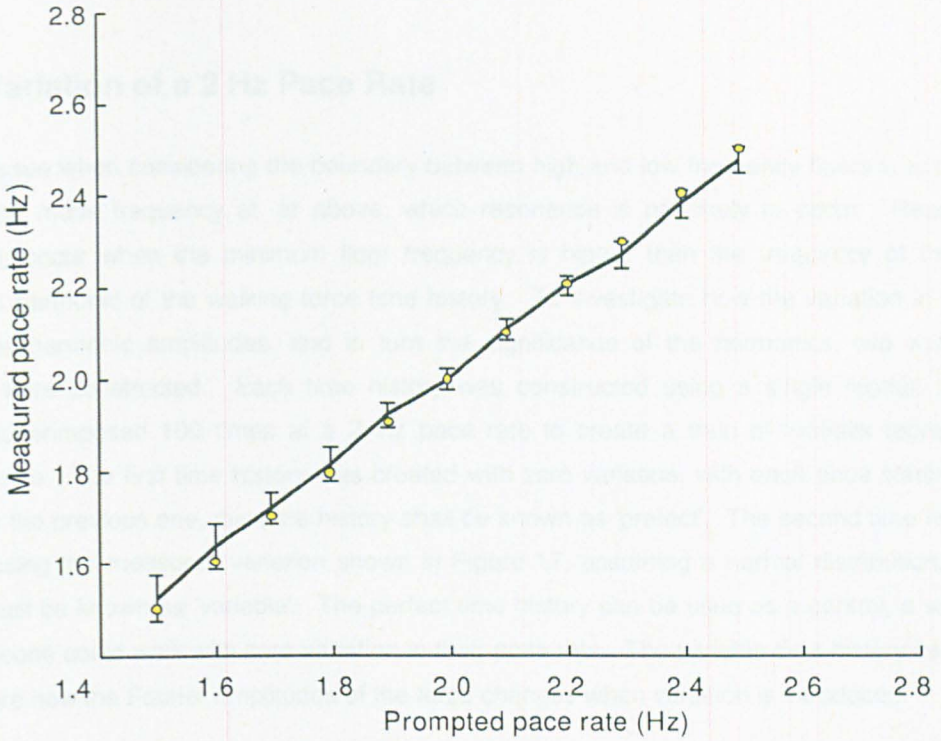

Pace rate (Hz)	Mean pace rate (Hz)	Standard deviation (Hz)
1.5	1.524	0.05
1.6	1.636	0.048
1.7	1.716	0.034
1.8	1.812	0.038
1.9	1.916	0.028
2.0	2.0	0.024
2.1	2.1	0.024
2.2	2.2	0.02
2.3	2.268	0.03
2.4	2.376	0.026
2.5	2.472	0.024

Figure 17 - Mean and standard deviation of the measured pace timings; yellow dots represent the prompted pace rate, the line represents the mean of the measured pace rates, and the bars represent the standard deviation

3.1.3 Variation of a 2 Hz Pace Rate

The key issue when considering the boundary between high and low frequency floors is to determine what is the mode frequency at, or above, which resonance is not likely to occur. Resonance is unlikely to occur when the minimum floor frequency is higher than the frequency of the highest significant harmonic of the walking force time history. To investigate how the variation in pace rate affects the harmonic amplitudes, and in turn the significance of the harmonics, two walking time histories were constructed. Each time history was constructed using a single footfall force time history, superimposed 100 times at a 2 Hz pace rate to create a train of footfalls representing a walking force. The first time history was created with zero variation, with each pace starting exactly 0.5s after the previous one, this time history shall be known as 'prefect'. The second time history was created using the measured variation shown in Figure 17, assuming a normal distribution, this time history shall be known as 'variable'. The perfect time history can be used as a control, a worst case, as if someone could walk with zero variation in their pace rate. The variable time history can be used to compare how the Fourier amplitudes of the force changes when variation is introduced.

Figure 18(top) shows the unity normalised spectrum of the perfect time history, it is clear that there are spikes at the pace rate and at harmonics corresponding to multiples of the pace rate. The harmonics continue to 40 Hz and beyond, characteristic of a periodic function. This suggests that if someone could walk with no variation, resonance could occur at very high frequencies. Figure 18(bottom) shows the normalised spectrum for the variable time history. It is again clear that there are spikes at the pace rate and at harmonics corresponding to multiples of the pace rate. However, the harmonics are no longer clean spikes with the amplitudes decreasing much quicker when compared to the perfect spectrum. They also have a wider base, due to the variation of the pace rate. Most of the energy is contained at the mean pace rate and its harmonics. However, some of the energy is shared to the surrounding frequencies (i.e. leaks). A simplified explanation can be given: if the pace rate is set at 2 Hz ± 0.1 Hz then the second harmonic would be at 4 Hz ± 0.2 Hz, i.e. if the pace rate is at f_p Hz ± σ Hz then for the *nth* harmonic would be nf_p Hz ± $n\sigma$ Hz. As a result, as the frequency becomes sufficiently large the variation will spread harmonic energy over a large frequency range which will eventually appear to be a constant value. The spread of energy results in an asymptotic reduction in peak harmonic force as the harmonic frequency increases. The number of harmonics that can be considered to contribute to floor resonance can be defined on the graph by the frequency at which the harmonics within spectra can no longer visually be identified. In this case, there are four visible peaks which suggests only four harmonics need to be considered.

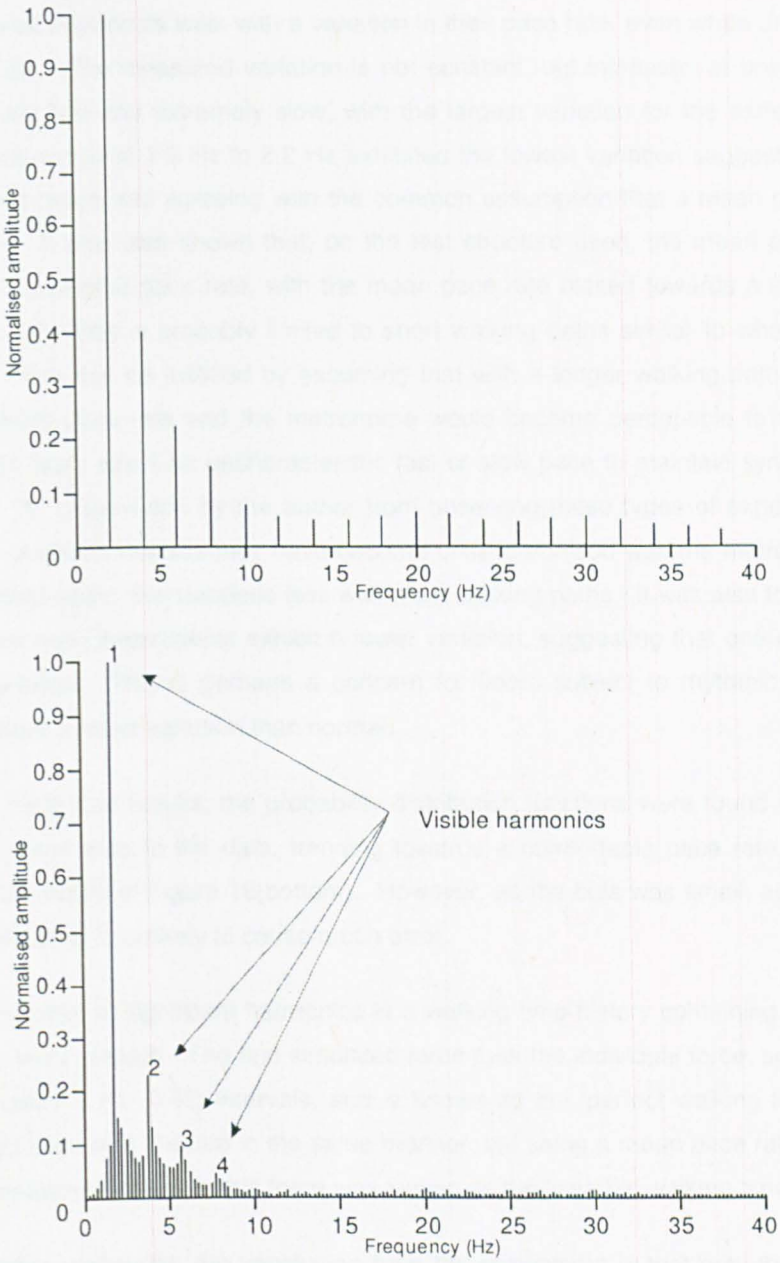

Figure 18 ***(from top to bottom)*** **– Normalised spectrum, of a perfect walking time history at 2 Hz; normalised spectrum of a variable walking time history at 2 Hz with the four visible harmonics identified; some spectral lines have been removed for clarity**

3.1.4 Summary

The experiment presented measures the variation in pace rate while a person attempted to walk at a prompted, fixed pace rate. The variation was used to determine the properties of the harmonics in a walking force spectrum containing many paces. With the properties of the spectra for different pace rates, it is then possible to estimate at what frequency floor resonance is unlikely to occur.

It was shown that all individuals walk with a variation in their pace rate, even when attempting to walk at a fixed pace rate. The measured variation is not constant, but increases at uncomfortable pace rates, i.e. extremely fast and extremely slow, with the largest variation for the extremely slow pace rates. A frequency range of 1.9 Hz to 2.2 Hz exhibited the lowest variation suggesting that this is a comfortable pacing range and agreeing with the common assumption that a mean pace rate can be assumed at 2 Hz. It was also shown that, on the test structure used, the mean pace rate did not always match the prompted pace rate, with the mean pace rate biased towards a more comfortable pace rate. This difference is probably limited to short walking paths similar to what would occur in most structures. This can be justified by assuming that with a longer walking path the discrepancy between the walkers pace rate and the metronome would become perceptible to the walker. The walker would then likely adopt an uncharacteristic fast or slow pace to maintain synchronisation with the metronome. An observation by the author from observing these types of experiments is useful here: often when a walker realises they have become unsynchronised with the metronome they often stop and ask to start again, this happens less with short walking paths. It was also found that walkers who often perform such experiments exhibit a lower variation, suggesting that one can be trained to have a lower variation. This is perhaps a concern for floors subject to rhythmic activities, where participants will have a lower variation than normal.

In analysing the pace rate results, the probability distribution functions were found not to be normal. There was a common bias to the data, trending towards a comfortable pace rate, producing a log normal distribution shown in Figure 16(bottom). However, as the bias was small, assuming a normal distribution for simplicity is unlikely to cause much error.

To analyse the number of significant harmonics in a walking time history containing many paces, two simulated forces were created. The first simulated force took the individual force, superimposed it for 100 paces at exactly 2 Hz (0.5s) intervals, and is known as the 'perfect walking time history'. The second simulated force was created in the same manner, but using a mean pace rate of 2 Hz and the corresponding measured variation, this force was known as the 'variable walking time history'.

Using the variations measured, the conclusion from the experiment is that only the fourth harmonic needs to be included in the response estimation. If a maximum possible pace rate of 2.5 Hz is considered, the high frequency/low frequency boundary would be at 4x 2.5 Hz = 10 Hz. However, in reality it is not as simple as this. For a start, 2.5 Hz is an unnaturally fast pace rate and is rarely going to be achieved. Also, the fourth harmonic maximum was obtained using a 2 Hz pace rate, which has the minimum variation, at this pace rate the fourth harmonic was still very small. For a 2.5 Hz pace rate the variation would increase and it is likely that the fourth harmonic would not cause any significant resonance. Two comments must also be made on the validity of the experiment:

1. How often do people walk, prompted, at a fixed pace rate?

2. Approximately half the people in the experiment are 'trained' at walking experiments, which could reduce the variation if compared with a larger sample.

Due to the long-standing debate on how many harmonics may cause a resonant response, the experiment needs to be repeated with a larger sample of the population, including measurements without pace rate prompting. In addition, the effects of the 'training' of an individual to keep in time with prompts needs to assessed.

Unfortunately, no definite conclusions can be made, which echoes the complex nature of walking forces. The frequency at which resonance would no longer occur was shown to depend on walking path length, the individual walking, the type of activity and whether there is any prompting to synchronise the walking. This leads to two main conclusions:

1. It is desirable to have a walking force model that includes variation of pace rate and can produce individual, unique, variable forces for each pace contained within the force. This would render classification of the floor for analysis obsolete.

2. As the frequency at which the response of a floor changes from resonant to transient depends on a number of factors, the frequency can vary. As such, the terms high and low frequency floors are not descriptive of the floor. A better terminology would be resonant and transient response floors (RRFs and TRFs respectively). This terminology is descriptive of the floor's response, and is not bound by frequency but the nature of the response. This terminology shall be used from now on in this thesis

3.2 Evaluation of Current Force Models

None of the investigations into the accuracy of the various footfall force models directly examine the validity of the method used in the creating the force model [31, 45, 46]. Validation of force models in the literature have their rationale described, with the validation consisting of comparing simulated response (usually from finite element analysis) to measured responses from walking. The problem with this approach is that the force applied to the real structure during the response measurements is not the same force that was used to create the simulated force function. There was no example in the literature which examines the validity of the method used creating the force model by first applying the method to measured forces to create a unique model force (when referring to a unique force, it is the method behind a model applied to an individual pace), and then comparing the unique model force against forces used to create the model.

The examples in the literature allow for an identification of which force models are inaccurate. However, as the situation response scenarios are different (i.e. different floors), the inaccuracies and their magnitudes cannot be determined.

This section examines the procedures and methods used in creating the various footfall force models. Each method is examined by indentifying key assumptions used in the model when simplifying the

footfall force. The key assumptions are then examined to see what inaccuracies they introduce into the model. A unique model is created by applying the procedures to measured footfall forces (see Appendix A for a description of measuring the walking forces). Finally, each model is used to create response spectra for various pace rates and compared with response spectra from the forces used to create the unique models. The spectra are compared and frequency ranges that are inaccurate can clearly be seen.

Using the method proposed here, the accuracy of each footfall model can be determined, locating precisely where their inaccuracies lie. This will give knowledge of circumstances where certain models can be used to obtain accurate responses and reveal why certain models can sometimes produce an accurate response, and at other times produce unreliable predictions. This knowledge can also be used to define desirable characteristics for a new footfall model.

In design, two footfall models that are most commonly used in transient response floor (TRF) design: the kf method and the effective impulse; both these methods shall be examined. The polynomial model, published in the EC report, shall also be examined due to it being the only one that produces a force in the time domain that resembles to a measured footfall force in time domain.

In each section, each measured footfall will be replaced by its unique counterpart, and will be known as such, i.e. for the kf method, each new individual pace well be known as an unique pulse, for the effective impulse a unique impulse, etc..

3.2.1 The kf Method [46]

The kf method is presented in detail in Chapter 2.2.1.2.1, and the method behind the model and the terminology will not be repeated here. There are two key assumptions in defining this method:

- Disregarding the minimum force between the two maxima and assuming a constant force will only produce a minor error.
- A footfall force can be approximated by a so-called 'versed step pulse', which is shown in Figure 19.

Each of these assumptions shall be considered separately.

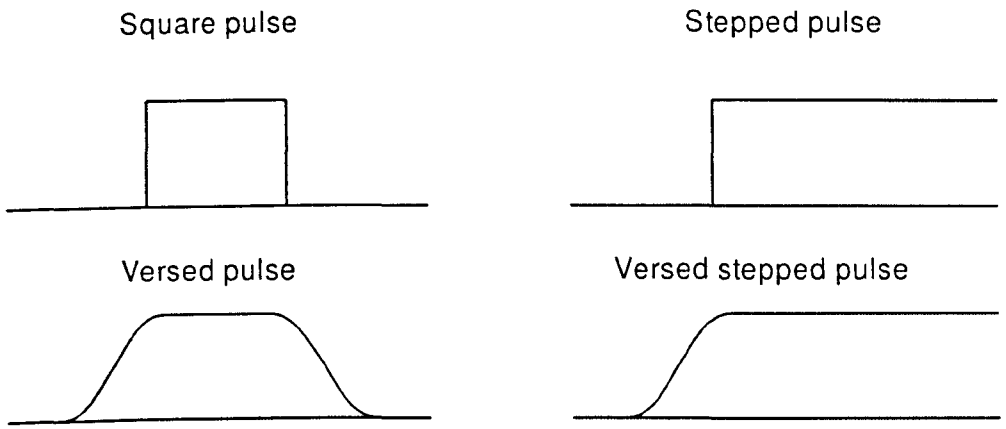

Figure 19 - Square pulses and versed pulses

3.2.1.1 Assumption 1: Disregarding the Plateau

When creating the model it is assumed that approximating the footfall force as a pulse will only produce minor errors, an example of such a pulse is shown in Figure 20(top). This type of pulse is known as a versed pulse, the characteristics of which are that the ramps of the slope are made up by half sine waves. The justification of the assumption is that a force obtained by measuring walking at a low pace rate is visually similar to the versed pulse. Figure 20(bottom) shows many individual footfall force time histories overlaid, starting from a fast, 2.5 Hz pace rate (the lightest shade of grey), and ending at a slow, (the darkest shade of grey) 1.5 Hz pace rate. It is clear that the fast pace rates have two maxima and a minimum between them, characteristic of a footfall force. As the pace rate decreases the magnitudes of the maxima decrease, whilst the magnitude of the minimum increases, and the force becomes more pulse-like. However, even at 1.5 Hz, which is an unnaturally slow walking rate, there are clear differences between the measured force and the versed pulse. When considering natural walking pace rates this difference is considerable. This brings into question whether assuming a pulse does only produce minor errors.

As an initial investigation, the frequency content of the footfall force was examined and compared while the pace rate was varied. As for slower pace rates the force appears more pulse-like, which is what the force model assumes, comparing the changes in the frequency domain as the pace rate increases (from pulse like to non-pulse like) will allow an indication to how the frequency content of the force changes as it becomes more pulse-like. Figure 21 shows a smoothed, normalised plot of the force in the frequency domain, light grey represents a fast pace rate (2.5 Hz) and dark grey represents a slow pace rate (1.5 Hz). The forces were normalised so that each force has an equal impulse. Some trends are clear:

- Below 5 Hz, there is little difference between pace rates.

- Between 5-10 Hz, there is more energy contained within the slower pace rates.
- Between 10-25 Hz, there is more energy contained within faster pace rates.
- Above 25 Hz, there is little change with pace rate variation.

This suggests that significant errors will be introduced due to this assumption.

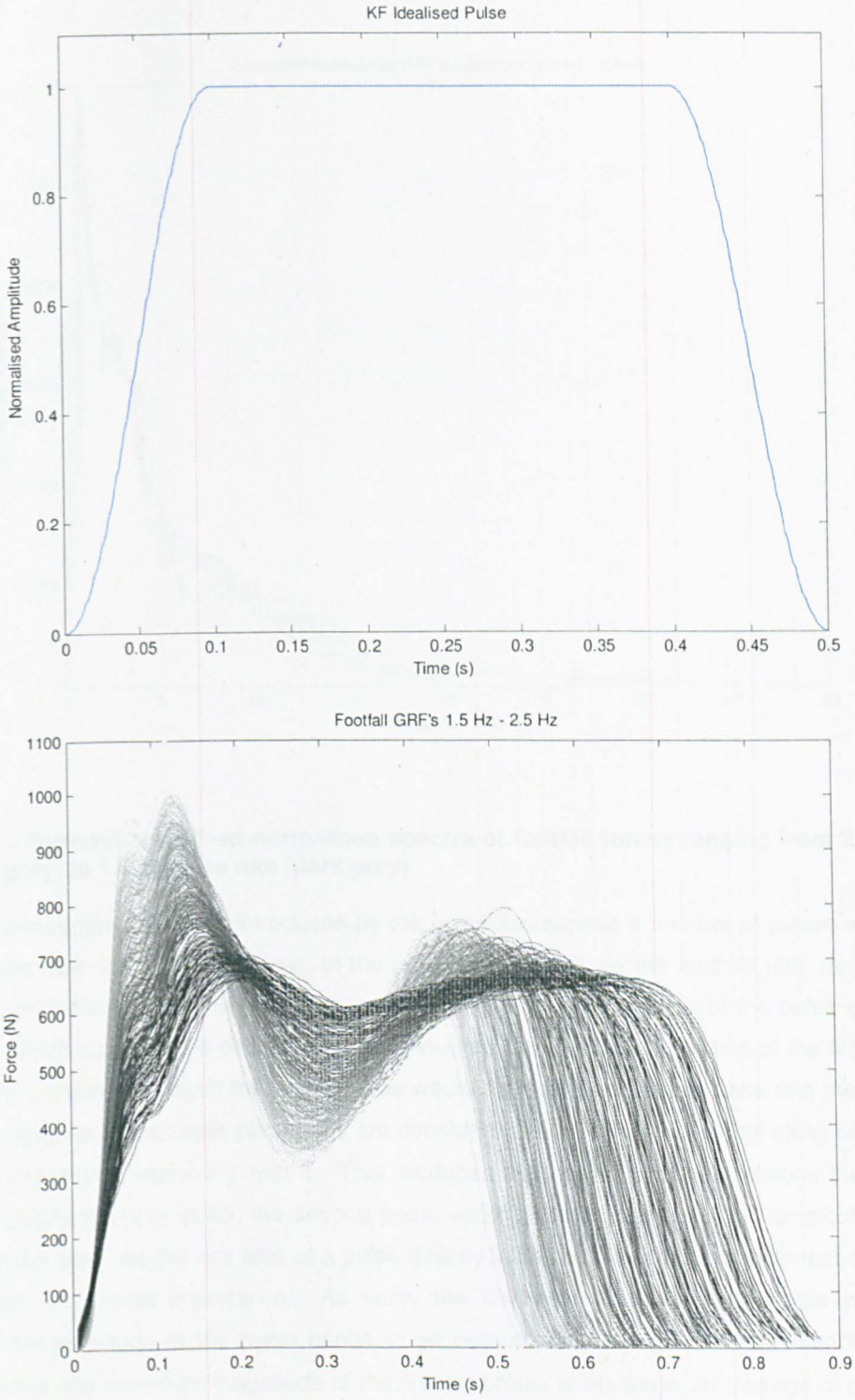

Figure 20 ***(from top to bottom)*** **- Idealised versed pulse; overlaid footfall force from 2.5 Hz pace rate (light grey) to 1.5 Hz pace rate (dark grey)**

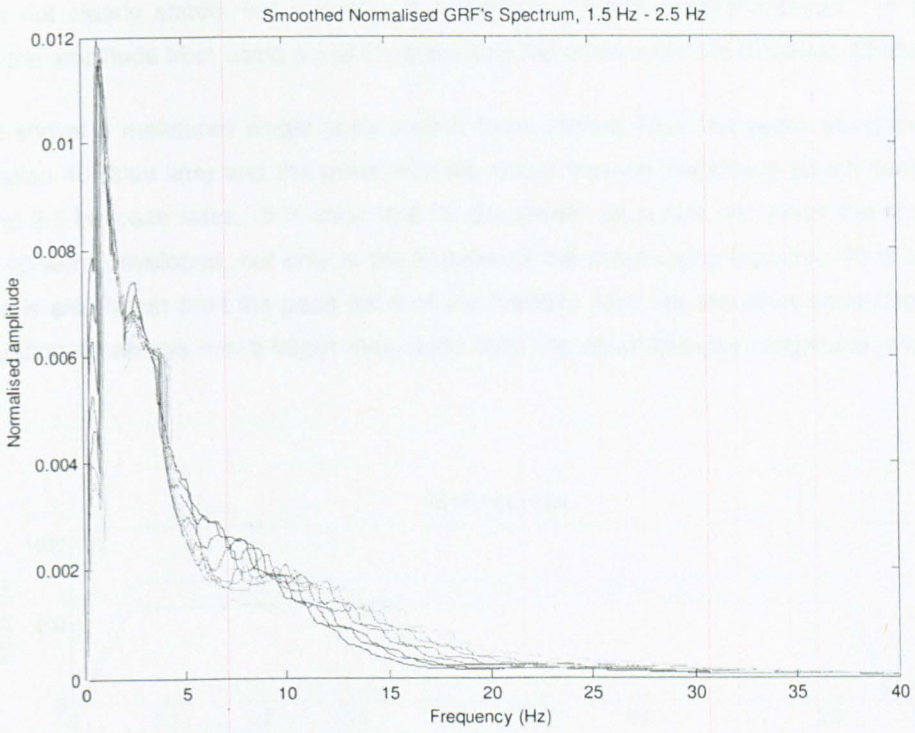

Figure 21 – Overlaid smoothed normalised spectra of footfall forces ranging from 2.5 Hz pace rate (light grey) to 1.5 Hz pace rate (dark grey)

To further investigate the errors introduced by the pulse assumption a number of pulses was fitted to footfall forces from various pace rates. In the publication describing the method [46], descriptions to obtain the characteristics of the pulse are not given. Firstly, the rise time of the pulse needs to be quantified, which can be more difficult than first thought. If the temporal position of the first maximum of the force is chosen to obtain the rise time, as would be logical, for a slow pace rate the task would be trivial. However, if the faster pace rates are considered, the characteristic heel strike occurs closer to the first maximum, interfering with it. This produces two peaks: does one choose the first peak, which is actually the heel strike, the second peak, which generally has a larger amplitude, or some average of the two? As the rise time of a pulse directly influences the frequency content of the pulse, the gradient is of most importance. As such, the first zero gradient of the force was chosen. Secondly, the amplitude of the pulse needs to be determined. Again, there are number of logical options for this: the maximum magnitude of the first maximum of the force, an average of both maxima of the force or a value so that the impulse of the real force matches the impulse of the idealised pulse. To the author, equal impulses seemed most logical, as this would ensure the total force applied to the structure would be equal. However, a recent publication [100] gives a formula for the pulse magnitude:

$$F_{Pulse} = P_{walker}(4 \times 10^{-5} f_{walker}^2 - 0.0052 f_{walker} + 1.2778) \qquad \textbf{Equation 40}$$

where P_{walker} is the weight of the walker and f_{walker} is the pace rate in Hz. The derivation of the formula is not clearly stated, but it seems it is derived through experimentation. In all following examples the amplitude from using equal impulses and the amplitude from Equation 40 shall be used.

Figure 22 shows a measured single pace footfall force (dotted line), the pulse using the amplitude from Equation 40 (blue line) and the pulse with the equal impulse magnitude (black line) for 1.5 Hz, 2.0 Hz and 2.5 Hz pace rates. It is clear that for the slower pace rate, for which the kf method and Equation 40 were developed, not only is the impulse of the pulse using Equation 40 is too high, the magnitude is also larger than the peak force of the footfall. Also, for the other pace rates, the pulse using Equation 40 always has a larger magnitude than the equal impulse magnitude, overestimating the force.

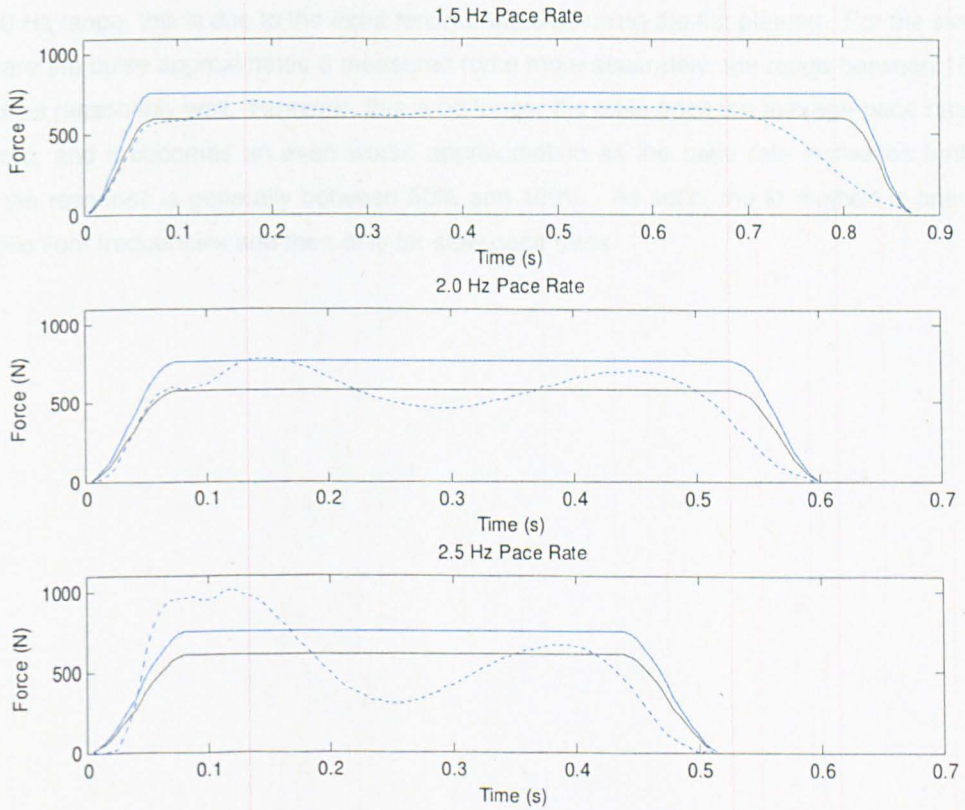

Figure 22 – Measured walking force tie histories (dotted line) overlaid with the equal impulse pulse (black line) and the pulse generated using Equation 40 (blue line) for 1.5 Hz, 2.0 Hz and 2.5 Hz pace rates

The Analysis:

All three force time histories, for each pace rate, were applied to a SDOF oscillator with a fixed mass and varying frequency. The response was filtered around the oscillator frequency to eliminate any pseudo static components in the response. Obtaining the peak and RMS response values, response spectra were created. The response spectra of the two pulse forces were divided by the response spectrum from the real measured force, the result can then be shown as a percentage difference, shown in Figure 23. The black line represents the equal impulse pulse and the blue line represents the pulse created with Equation 40. As the measured force was used in creating the pulses, when the percent difference is large it shows when the simplification is not accurate.

It is clear from all plots that there is a large difference between the idealised pulse and measured force. However there is not much difference between the two pulses. The largest difference is in the 0 Hz - 10 Hz range, this is due to the extra force created by using the flat plateau. For the slower pace rate, where the pulse approximates a measured force more accurately, the range between 10 Hz – 20 Hz matches reasonably well. However, this is no longer the case once the average pace rate, 2 Hz, is considered, and it becomes an even worse approximation as the pace rate increases further. The error in the response is generally between 50% and 100%. As such, the kf method is only accurate for specific floor frequencies and then only for slow pace rates.

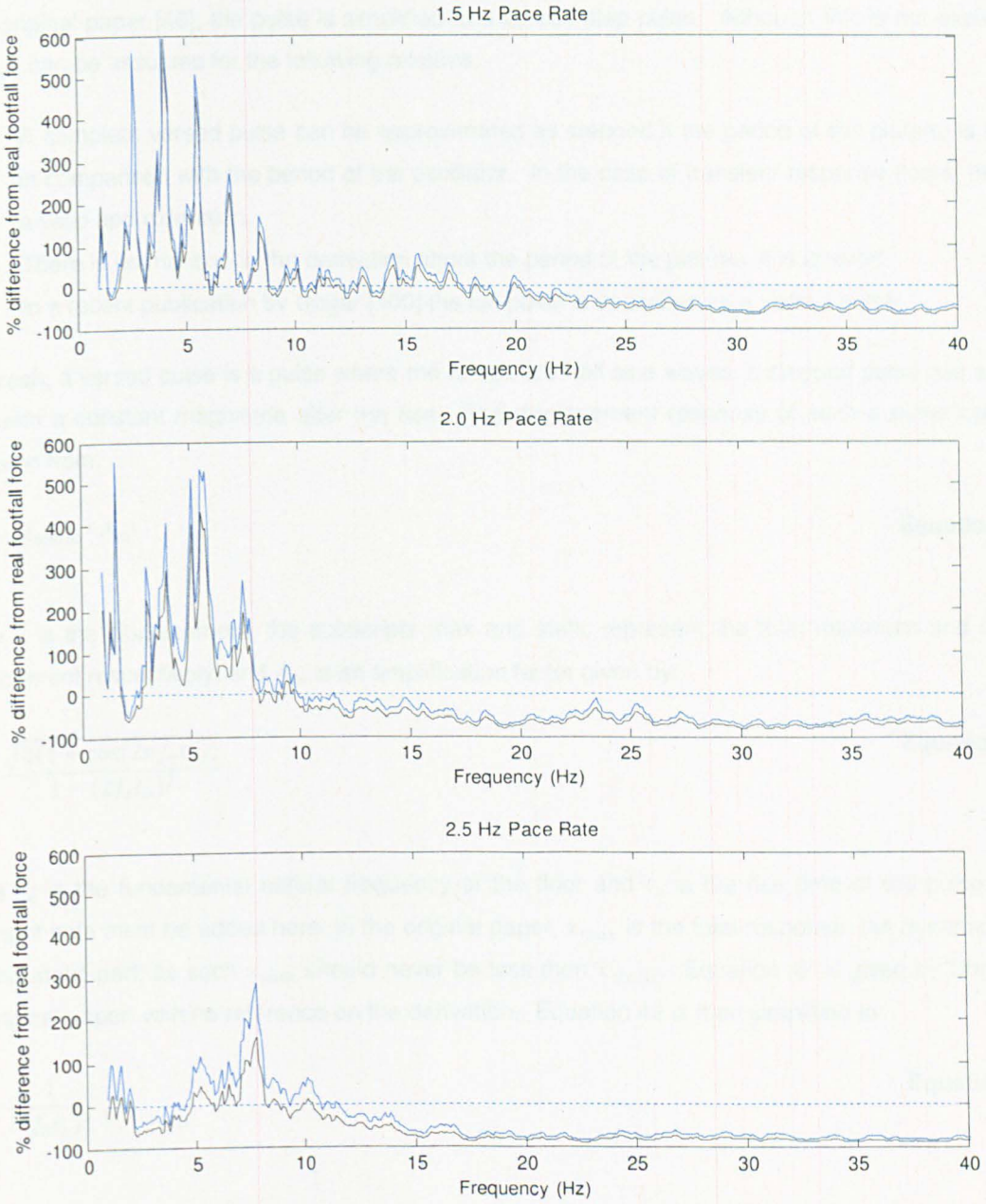

Figure 23 ***(From top to bottom)*** **– Percentage difference velocity spectra for the kf method at 1.5 Hz, 2.0 Hz and 2.5 Hz pace rates; the blue line represents the pulse magnitude from Equation 40, the black line is the equal impulse amplitude, the dotted line represents the measured force**

3.2.1.2 Assumption 2: The Simplified Versed Pulse

In the original paper [46], the pulse is simplified to a versed step pulse. Although this is not explicitly stated, it can be assumed for the following reasons:

- A complete versed pulse can be approximated as stepped if the period of the plateau is long in comparison with the period of the oscillator. In the case of transient response floors, this is a valid approximation.
- There is no mention in the derivation about the period of the plateau, it is ignored.
- In a recent publication by Ungar [100] the full pulse is describes as a versed pulse.

To refresh, a versed pulse is a pulse where the ramps are half sine waves, a stepped pulse has a rise ramp with a constant magnitude after the rise. The displacement response of such a pulse can be estimated from:

$$x_{max} = x_{static} \cdot A_m \qquad \textbf{Equation 41}$$

where x is the displacement, the subscripts max and static represent the total maximum and static displacement respectively, and A_m is an amplification factor given by:

$$A_m = \frac{\sqrt{2(1+\cos(2\pi f_n t_o))}}{1-(2f_n t_o)^2} \qquad \textbf{Equation 42}$$

where f_n is the fundamental natural frequency of the floor and t_o is the rise time of the pulse. An important note must be added here: in the original paper, x_{max} is the total response, the dynamic part and the static part; as such x_{max} should never be less then x_{static}. Equation 42 is given by Ungar in the original paper with no reference on the derivation. Equation 42 is then simplified to:

$$A_m = \frac{1}{2(f_n t_o)^2} \qquad \textbf{Equation 43}$$

Figure 24 shows a plot of the amplification factor with increasing $f_n t_o$, and the simplification. The strange feature of this plot is that the amplification factor goes below 1, effectively giving a less than static response for a forcing function with a period much larger than the response frequency, which is intuitively wrong. For a pulse with rise time 0.15s on a floor of 10 Hz, $f_n t_o$ = 1.5, therefore the response would be 0, which is nonsense. The simplification becomes accurate when $f_n t_o$ is approximately 1, i.e. a rise time of 0.1s and floor frequency of 10 Hz which is typical for a TRF.

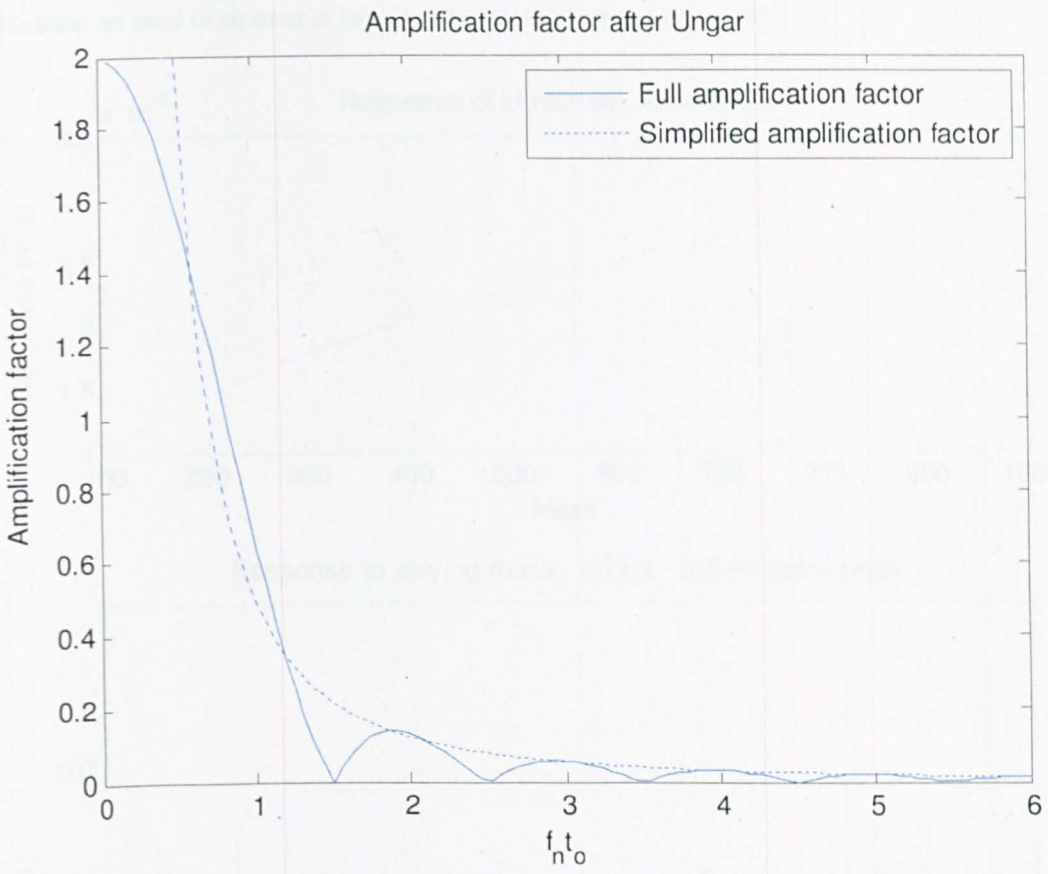

Figure 24 – Amplification factors, after Ungar [46]; full amplification factor from Equation 42, simplified amplification factor from Equation 43

The simplified amplification factor is then transformed into a peak velocity response as shown in Chapter 2.2.1.2.1, given by:

$$v_{max} \approx \left(\frac{\pi}{t_o^2}\right)\frac{F_{pulse}}{k f_n} \qquad \textbf{Equation 44}$$

where k and f_n are the point stiffness and the fundamental natural frequency of the floor respectively and F_{pulse} is the peak force of the pulse. As can be seen from the formula, if the floor frequency is varied and the stiffness is constant (i.e. the mass is varied), decreasing the mass decreases the response, shown in Figure 25(top). This strange relationship was discussed in Chapter 2.2.1.2.1, if the frequency was increased while fixing the stiffness, i.e. decreasing the mass, the response decreased. As it is an impulsive type of excitation where the response is inversely proportional to the mass, this must be incorrect. Figure 25(bottom) shows the response to the generalised pulse time history for an oscillator with a fixed frequency and varying mass for varying pace rates, darker represented a slower pace rate. It is clear that the response is as expected, with increasing the mass

reducing the response. As the response of the pulse time history does not match the response of the simplification an error must exist in the simplified derivation by Ungar [46].

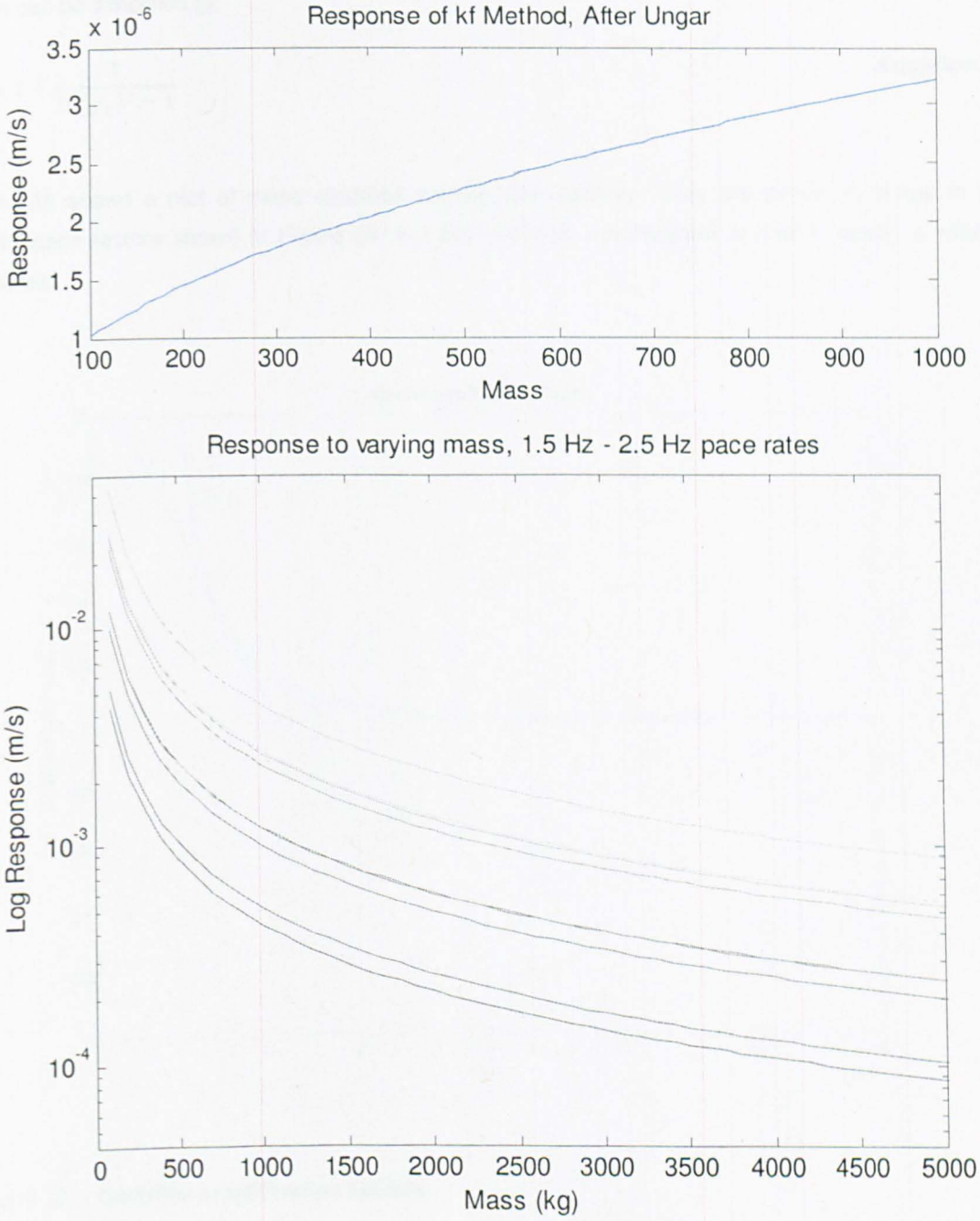

Figure 25 ***(from top to bottom)*** **– Peak velocity response with respect to fixed frequency and increasing mass, kf method; response with respect to fixed stiffness and increasing mass, analytical method using time domain pulses**

According to a different source [101], amplification factor for a versed pulse is:

$$A_m = 1 + cos\frac{\pi f_n t_o}{2(f_n t_o)^2 - 1}$$ **Equation 45**

which can be simplified to:

$$A_m = 1 + \frac{1}{2(f_n t_o)^2 - 1}$$ **Equation 46**

Figure 26 shows a plot of these modified amplification factors. They are similar in shape to the amplification factors shown in Figure 24, but the minimum amplification is now 1, which is what is expected.

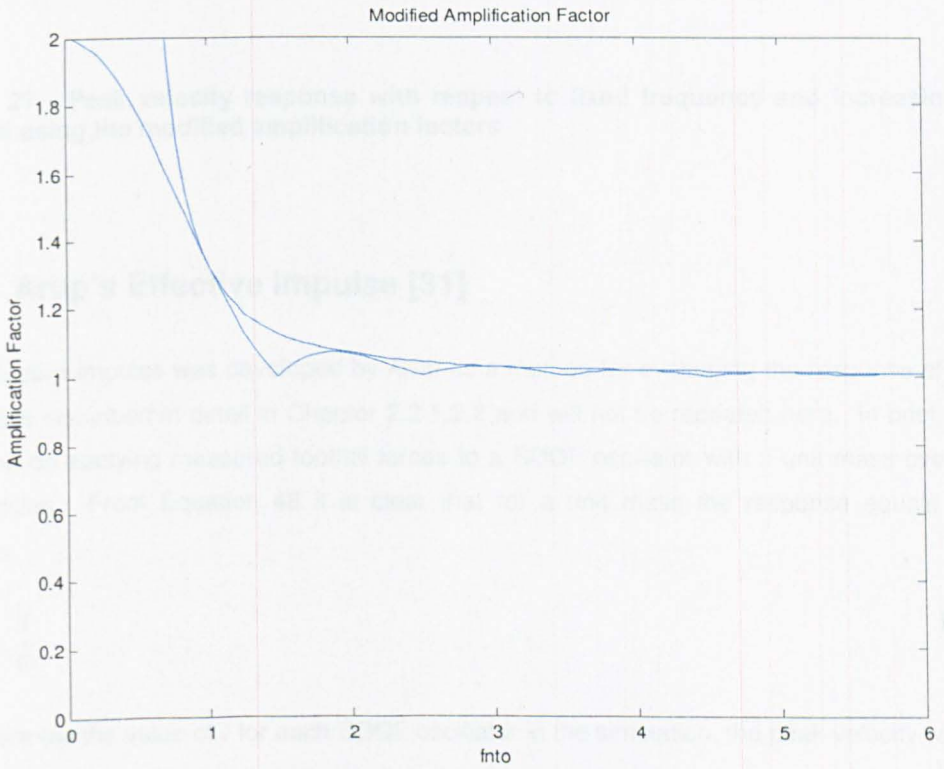

Figure 26 – Modified amplification factors

The simplified modified amplification factor can now be converted in the same manner as before to get an expression for peak velocity, this is given by:

$$v_{max} \approx \left(\frac{2\pi f_n}{k}\right) + \frac{2\pi F_{pulse}}{f_n(2kt_o^2 - 1)}$$ **Equation 47**

The response of varying mass with fixed frequency can be obtained with this modified velocity and is shown in Figure 27. As the mass is increased the response decreases, as expected.

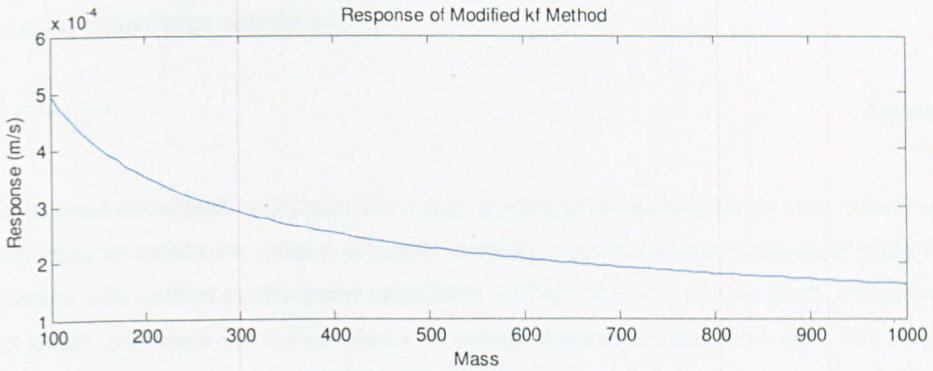

Figure 27 - Peak velocity response with respect to fixed frequency and increasing mass, kf method using the modified amplification factors

3.2.2 Arup's Effective Impulse [31]

The effective impulse was developed by Arup as a method for evaluating the response of TRFs. The method is described in detail in Chapter 2.2.1.2.2 and will not be repeated here. In brief, the method is based on applying measured footfall forces to a SDOF oscillator with a unit mass over a range of frequencies. From Equation 48 it is clear that for a unit mass the response equals the applied impulse:

$$v_{max} = \frac{I}{m}$$ **Equation 48**

To determine the value of I for each SDOF oscillator in the simulation, the peak velocity was recorded. There is a number of key assumptions when developing this method:

- The response of an instantaneous impulse is comparable to the response of the transient footfall force.
- When the calculated effective impulses are curve fitted to give the published expression, no significant error is introduced.

Each of these assumptions shall be evaluated using unique impulses created using measured footfall forces and comparing properties of the forces to the impulses. Each assumption shall be considered separately.

3.2.2.1 Assumption 1: the Response of the Effective Impulse is Comparable with the Response from a Measured Force

As stated in Chapter 2.2.1.2.2, the effective impulse is based on the relationship of peak velocity of an object to an impulsive force defined by:

$$I_{eff} = 54 f_p^{1.43} / f_n^{1.3} \qquad \textbf{Equation 49}$$

Using the method described in Chapter 2.2.1.2.2, a measured walking force time history with multiple paces was used to determine unique effective impulse created for each individual pace it contained. This procedure was carried out for pace rates from 1.5 Hz - 2.5 Hz. At this point, the unique impulses were kept exact, and were not curve fitted in a similar manner as Equation 49. The measured force was then compared to the chain of effective impulses by comparing the response of a 15 Hz oscillator for each excitation. Figure 28 shows the time history and RMS response for the two force types for a single pace, the blue line represents the measured excitation and the black line represents the effective impulse. Examining the figure it can be seen that due to the nature of a footfall force it takes a few cycles to reach the maximum response amplitude, whereas the effective impulse reaches peak response instantly. Damping has a small effect in reducing the response to a real footfall compared to the instantaneous maximum of the ideal impulse. The effective impulse overestimated the response for the initial phase, with a bigger effect on the RMS. The magnitude of this error is proportional to the amount of damping present; in this example, a value of 1% was used. Another consequence of the impulse causing an instant velocity is that the two responses are out of phase. During the response decay, the response from the excitation is approximately equal.

Each footfall in the time histories was replaced by a unique impulse (a number of time histories had to be created for each pace rate as the impulse is only correct for an exact frequency). The train of unique impulses for the range of pace rates was applied to an SDOF oscillator with a fixed mass of 100 kg and varying frequency of range 0-50 Hz, where the peak velocity response was used to form response spectra. The response spectra from the effective impulses were then compared with response spectra obtained from the measured forces used in creating the effective impulses. Figure 29 shows the percentage difference for 1.5 Hz, 2.0 Hz and 2.5 Hz pace rates. A few observations can be made from these plots: The slowest pace rate has the highest error. Oscillator frequencies below 10 Hz have the highest error, with the error increasing again after 25 Hz. Between 10 Hz and 25 Hz the error is relatively small. It seems strange that the error is so high considering the effective impulse is created for the corresponding footfall, but it is now evident that including damping and changing the frequency of the oscillator introduces these errors.

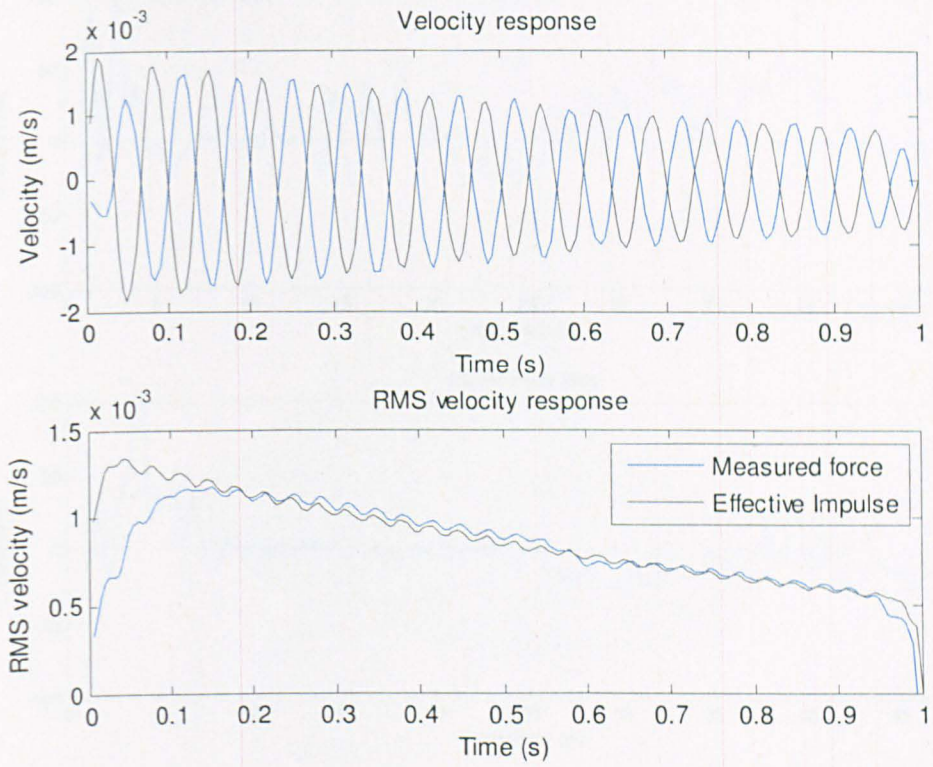

Figure 28 (*from top to bottom*) - Velocity, and RMS velocity response of measured force (blue) and its unique effective impulse (black)

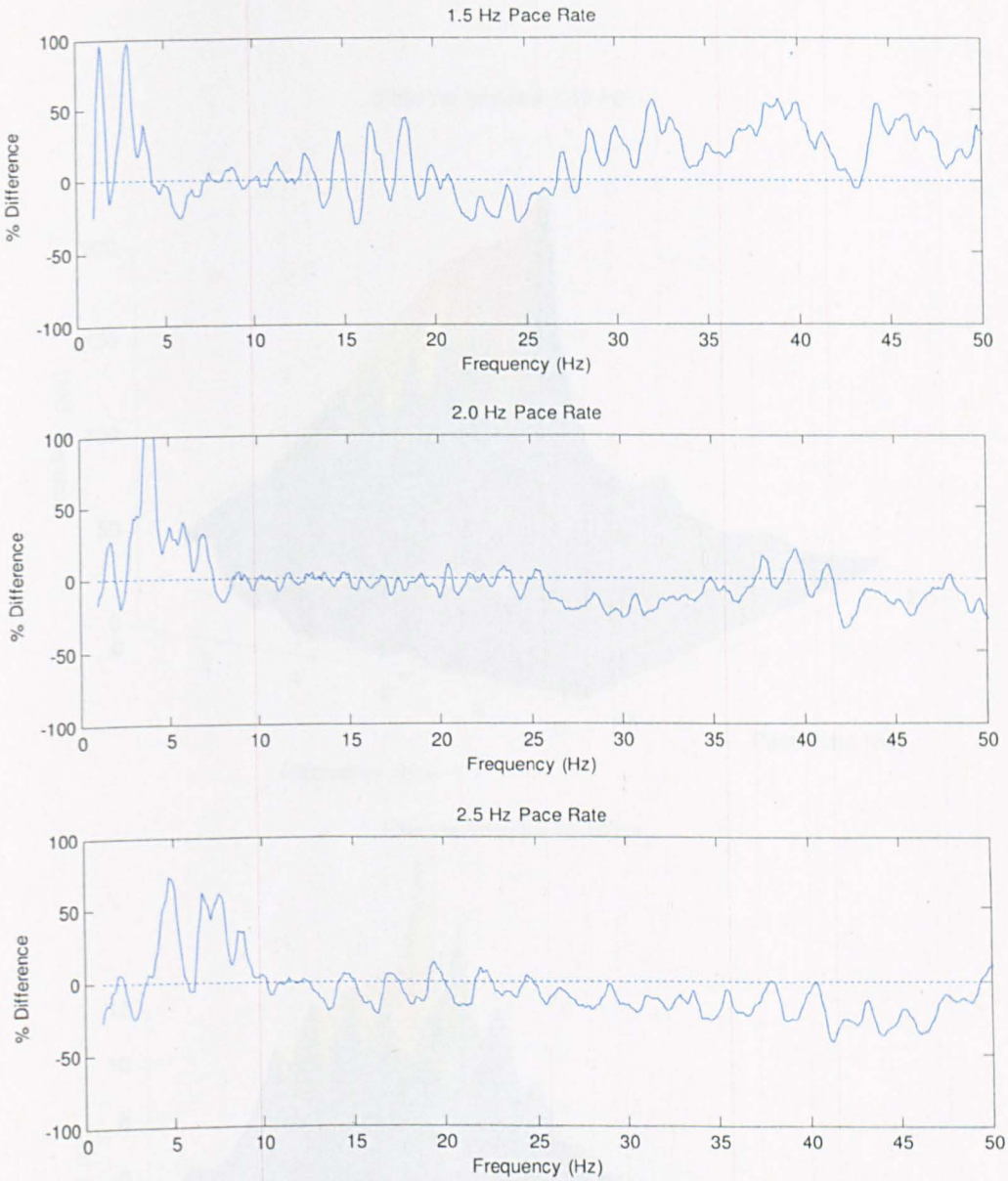

Figure 29 *(From top to bottom)* - Percentage difference velocity spectra for the modified effective impulse method at 1.5 Hz, 2.0 Hz and 2.5 Hz pace rates, the dotted line represents the measured force

3.2.2.2 Assumption 2: Curve Fitting the Effective Impulse Values Retains Accuracy

In the creation of the published effective impulse the unique values were curve fitted (Equation 50) to give a value of impulse which is a function of floor frequency and pace rate. It is assumed that during the curve fitting stage that the unique impulses fit the equation well and little error is introduced, but this error has never been investigated. Figure 30 shows the unique modified effective impulse obtained from the measured forces.

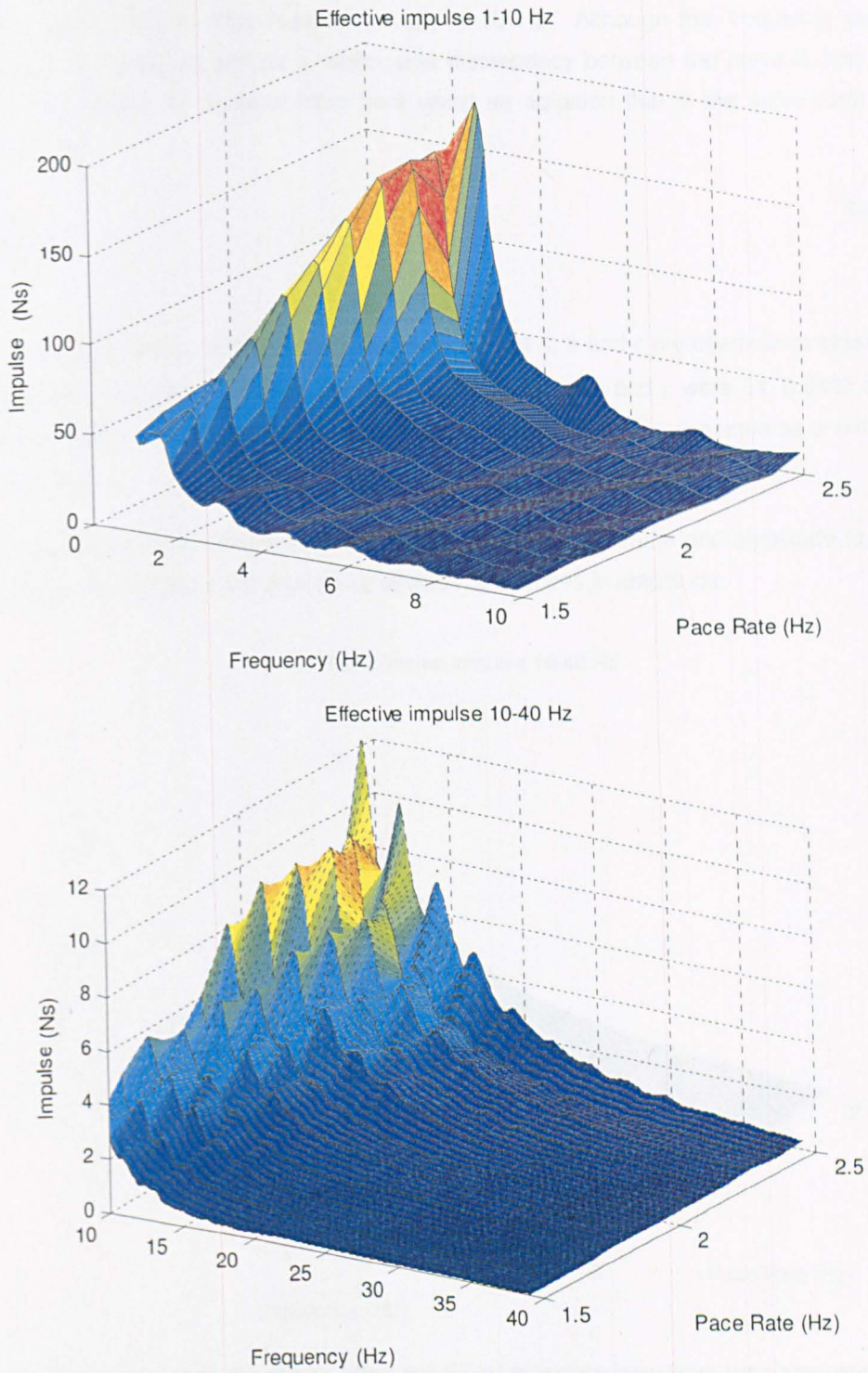

Figure 30 ***(From top to bottom)*** **- Surface plot of the modified effective impulses for pace rates of 1.5 - 2.5 Hz and oscillator frequencies of 0 - 10 Hz (top) and 10 - 40 Hz (bottom)**

It is clear for the frequency range below 10 Hz there are large values at the pace rate and the corresponding harmonics, with troughs between them. Due to this oscillatory feature, this frequency

range is not suitable for curve fitting. Above 10 Hz the effects of the harmonics are still apparent, but less so, making for a smoother curve. The published effective impulse is for TRF method and curve fits a similar set of data for floor frequencies above 10 Hz. Although this frequency range has a smoother data set, there will still be a reasonable discrepancy between the curve fit and measured data. The data above 10 Hz were fitted here using an equation that is the same form as Arup's effective impulse:

$$I_{eff} = A\frac{f_p^b}{f_n^c}$$ **Equation 50**

where f_p is the pace rate, f_n is the oscillator frequency, and A, b and c are coefficients obtained during the curve fitting. The values obtained during curve fitting for A, b and c were 54, 3.8483 and 2.4363 respectively. These differ to the values published by Arup, but this is expected as a different force dataset was used.

Figure 31 shows the curve fitted effective impulse, it is similar to shape and amplitude to the explicit values in Figure 30, but there are also some obvious differences in amplitude.

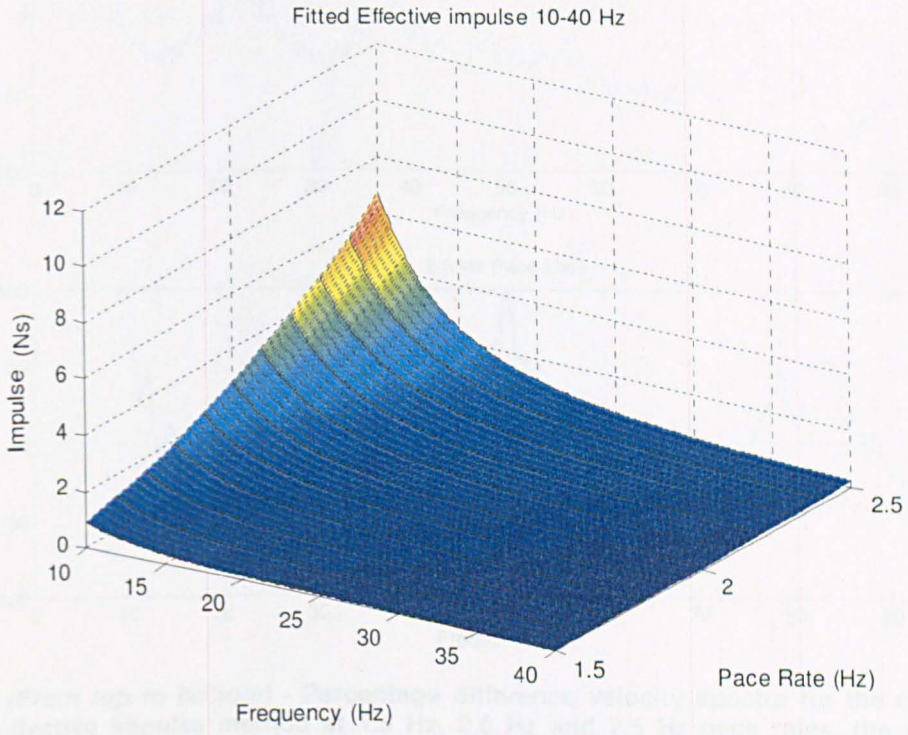

Figure 31 - Surface plot of the curve fitted modified effective impulses for pace rates of 1.5 - 2.5 Hz and oscillator frequencies of 10 - 40 Hz

Figure 32 shows, using the response spectrum method, the percentage difference in oscillator response between the curve fitted modified effective impulses and measured forces used. The plots show many of the characteristics of the explicit impulse values before curve fitting (Figure 29), but are

now considerably less accurate. The largest error is below 10 Hz, the most accurate part of the response being between 10 Hz - 25 Hz. The maximum error in the 10 Hz – 25 Hz range is approximately 40%

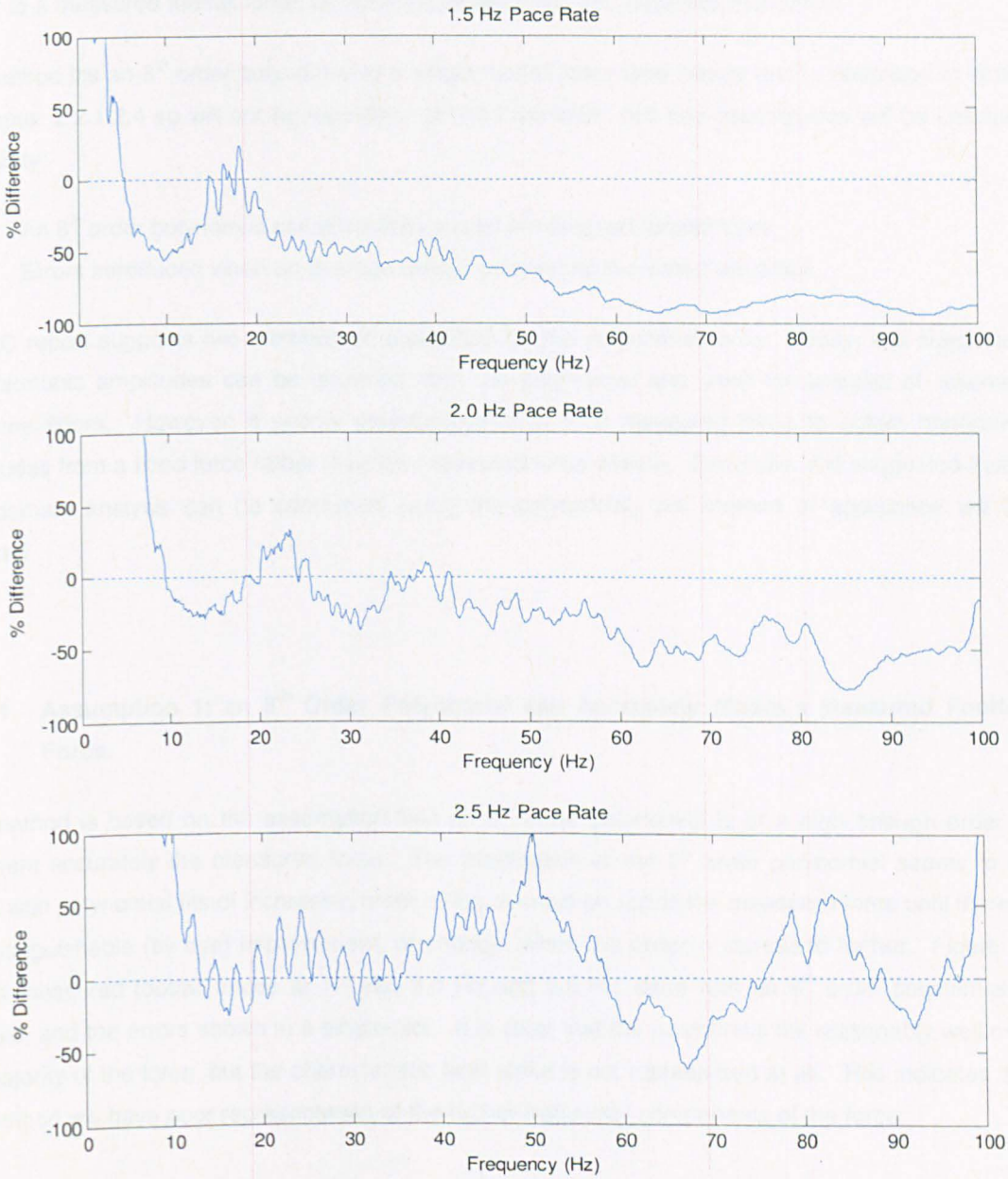

Figure 32 ***(From top to bottom)*** **- Percentage difference velocity spectra for the curve fitted modified effective impulse method at 1.5 Hz, 2.0 Hz and 2.5 Hz pace rates, the dotted line represents the measured force**

3.2.3 EC Polynomial Method [45]

The polynomial method was published in a report funded by the European Commission. It has not been introduced into any design guides, but it is the only method that produces a force that is visually similar to a measured footfall force, as such it is rather novel and deserves evaluation.

The method fits an 8^{th} order polynomial to a single footfall force time history and is described in detail in Chapter 2.2.1.2.4 so will not be repeated. In the evaluation, two key assumptions will be checked for validity:

1. An 8^{th} order polynomial can accurately model a measured footfall force.
2. Errors introduced when an average design polynomial is created are small.

The EC report suggests two methods of application for the polynomial force. Firstly, it is suggested that harmonic amplitudes can be obtained from the polynomial and used for analysis of resonant response floors. However, it seems counterintuitive to fit a measured force to obtain harmonics amplitudes from a fitted force rather than the measured force directly. Secondly, it is suggested that a time domain analysis can be conducted using the polynomial; this method of application will be explored

3.2.3.1 Assumption 1: an 8^{th} Order Polynomial can Accurately Model a Measured Footfall Force.

The method is based on the assumption that an 8^{th} order polynomial is of a high enough order to represent accurately the measured force. The justification of the 8^{th} order polynomial seems to be visual with polynomial fits of increasing order being overlaid on top of the measured force until there is no distinguishable (by eye) improvement, or change, when the order is increased further. Figure 33 shows measured footfall forces at 1.5 Hz, 2.0 Hz and 2.5 Hz, each with an 8^{th} order polynomial fit overlaid, and the errors shown in a single plot. It is clear that the polynomial fits reasonably well over the majority of the force, but the characteristic heel strike is not represented at all. This indicates that the method will have poor representation of the higher frequency components of the force.

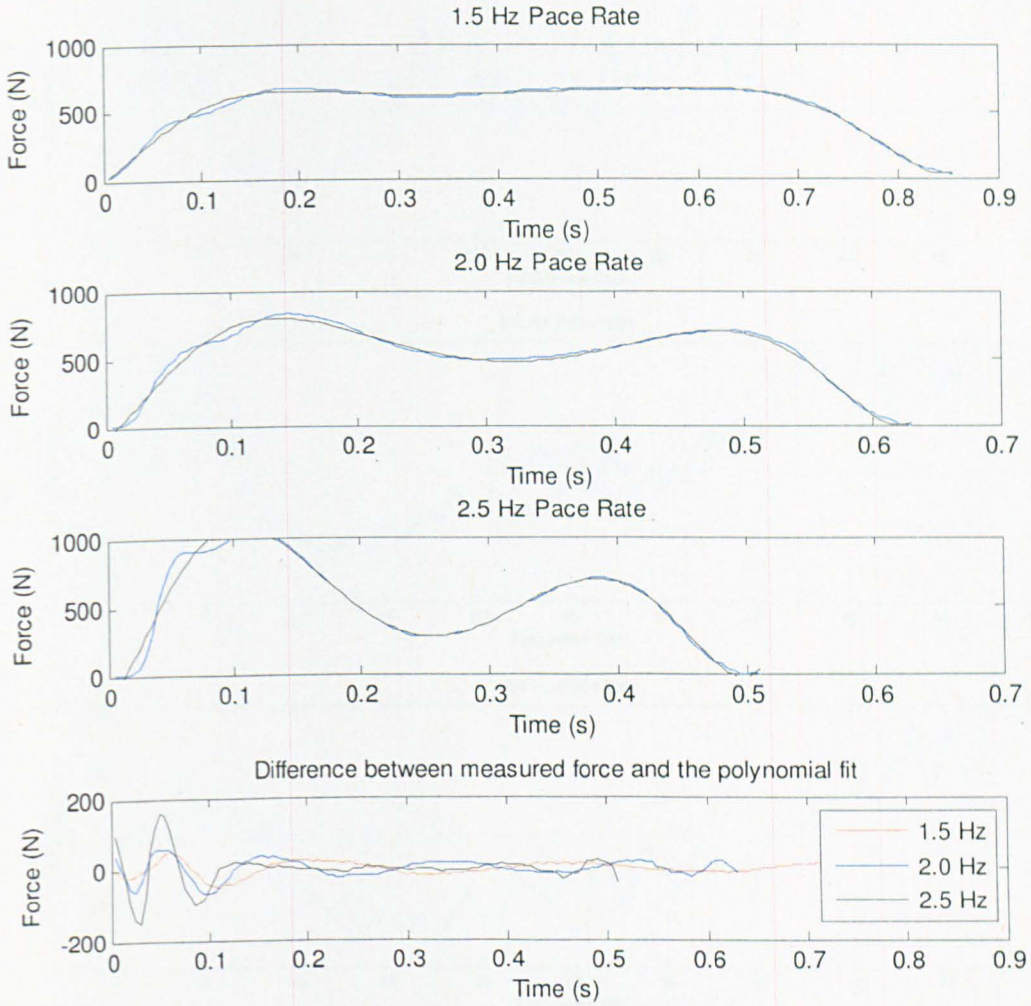

Figure 33 - Top three plots show measured footfall forces at 1.5 Hz, 2.0 Hz and 2.5 Hz respectively with their corresponding polynomial fits; the bottom plot shows the difference between the measured force and the fit, clearly showing the maximum error at the heel strike spike

Each footfall from a force time history containing many paces has unique polynomial fits created for a range of pace rates. Each unique polynomial fit was then used to recreate the walking force time histories with the exact same pace timings. Each force was then applied to an SDOF oscillator of varying frequency and fixed mass where the peak response was found to create response spectra. Figure 34 shows the percentage difference between the two response spectra, with the dotted line showing no difference. Each plot shows a general over estimation of response between 5-10 Hz. After this frequency range there is a sudden drop with a large underestimate in response, until the response difference increases and overestimates the response. Each plot is similar, but the frequencies at which the characteristic errors occur change, due to the pace rate. The percent difference over the frequency range is approximately +- 100%.

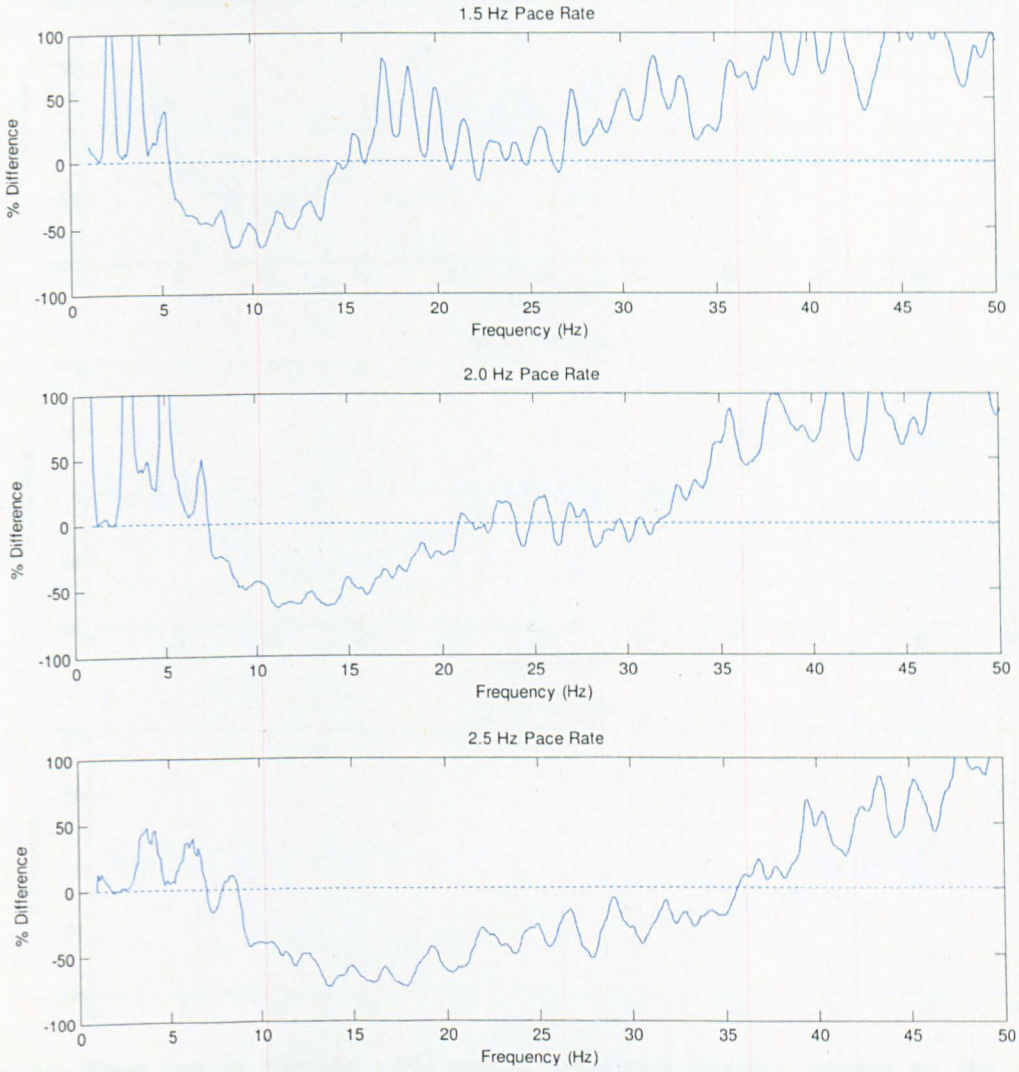

Figure 34 ***(From top to bottom)*** **- Percentage difference velocity spectra for the modified unique polynomial fits at 1.5 Hz, 2.0 Hz and 2.5 Hz pace rates, the dotted line represents the measured force**

3.2.3.2 Assumption 2: an Average Design Polynomial does not Introduce Significant Errors.

To create a design force, the EC report averages the co-efficients to produce an average design polynomial. The same procedure was applied here to produce a single fitted force at each pace rate. Again, an equivalent walking time history containing many paces was created with the polynomial force, using the exact pace timings. Figure 35 shows the percent difference between the corresponding response spectra. The unexpected result here is that the design polynomial, which is essentially a simplification with a loss of accuracy, has a lower error. The low frequency, resonance response difference has reduced noticeably, with the peak differences occurring between the harmonics. For the spectrum as a whole, the percent difference is approximately +- 80%.

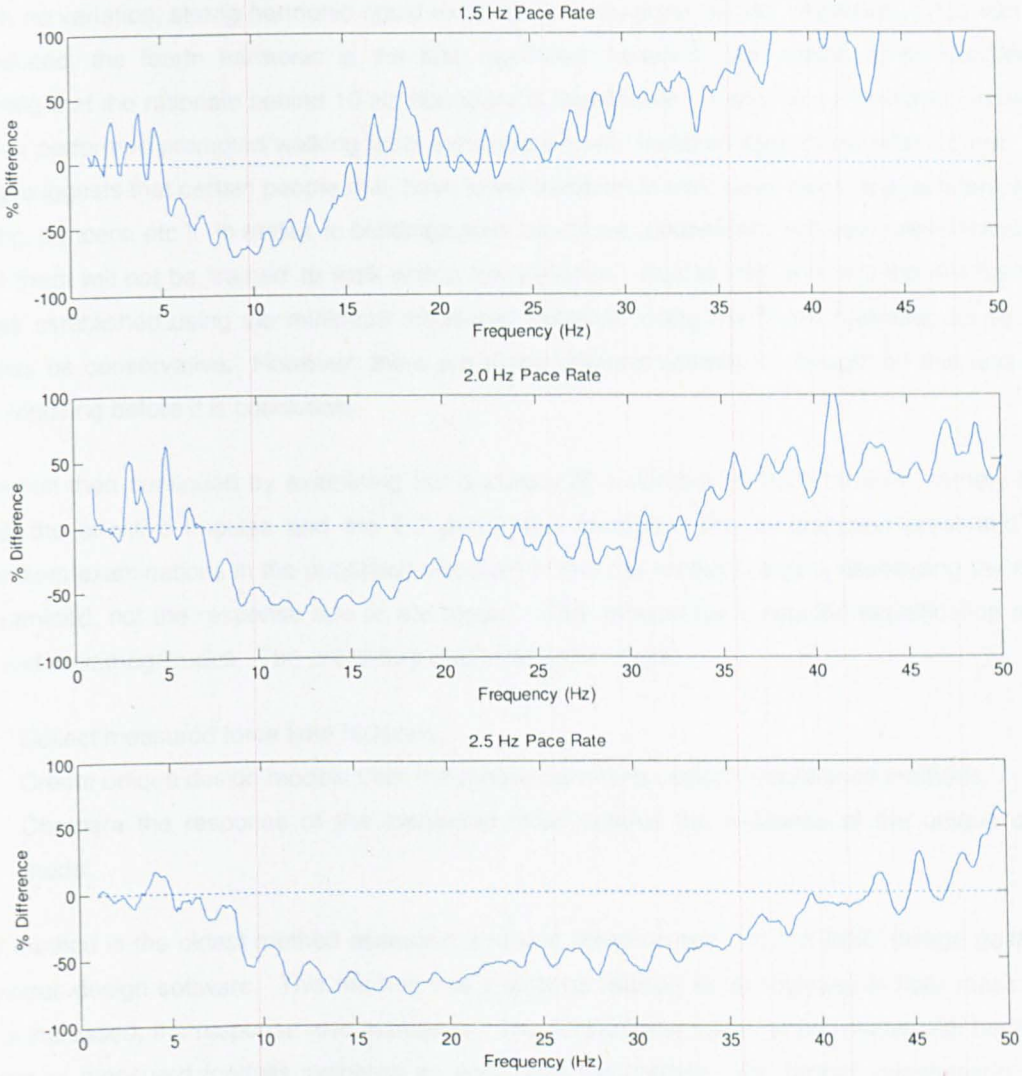

Figure 35 ***(From top to bottom)*** **- Percentage difference velocity spectra for the design polynomial fits at 1.5 Hz, 2.0 Hz and 2.5 Hz pace rates, the dotted line represents the measured force**

3.3 Discussion and Conclusion

The chapter began by examining the variation in pace rate for someone attempting to walk at a fixed pace rate to determine how many significant harmonics are likely to be present in a walking force time history. When the number of significant harmonics is ascertained it will then be possible to estimate the cut-off frequency above which a resonant response from the force is unlikely to occur.

There was a clear variation in the pace rate, with the variation higher at pace rate extremes (i.e. very fast or very slow). Within the pacing range of 1.9-2.2 Hz, the variation was at a minimum. Using the measured variation, a walking time history was constructed from individual paces and compared with a constructed walking time history, using the same individual paces, with no variation. It was shown,

that with no variation, strong harmonic could exist up to, and above, 40 Hz. However, once variation is introduced, the fourth harmonic is the last significant harmonic that needs to be considered, suggesting that the rationale behind 10 Hz boundary is reasonable. It was also noted that individuals that often performed prompted walking tests exhibited a lower variation then those who did not. This 'training' suggests that certain people may have lower variation in their pace rates (e.g. soilders due to marching, dancers, etc.). In reality, in buildings such as offices, pedestrians will walk unprompted, and most of them will not be 'trained' to walk with a low variation. Due to this, and that the 4th harmonic limit was established using the minimum measured variation, using the fourth harmonic for all pace rates may be conservative. However, there are many different schools of thought on this and more data is requiring before it is conclusive.

The section then continued by examining the accuracy of a number of force models, namely the kf method, the effective impulse and the EC polynomial method. The examination presented here differed from examinations in the published literature in that the method used in developing the model was examined, not the response due to the model. This allowed for a detailed identification of any errors and their magnitudes. The procedure had three main steps:

1. Collect measured force time histories.
2. Create unique design models from the measured forces using the published methods.
3. Compare the response of the measured force against the response of the unique design model.

The kf method is the oldest method assessed and it is implemented into the AISC design guide [19] and various design software. This method has a strange relation to an increase in floor mass: if the mass is increased, the response also increases. The relationship does not correlated with floor mass response to measured footfalls indicated an error with the method. On further investigation it was shown that there is an error with an amplification factor used in the original 1979 publication [46] which can cause no response for some floors. Correcting the amplification then remedies the relationship between the response and floor mass, with it now having a similar relationship as measured forces (i.e. increasing floor mass decreases response). However, even with the error fixed, the method is very inaccurate except for unnaturally slow pace rates. Due to the poor performace, and the error identified, it is worrying that the kf method is the basis of the AISC design guide and that it is implemented into some analysis software. It is recommended that the kf method not be used for analysis.

Arup's effective impulse [31] is currently the most common method used in the UK to assess floor response when resonance does not occur. It is a sound method, and gives a reasonably accurate representation of the force. However, some inaccuracies remain, with the largest error introduced during curve fitting. The method also limits the response type to modal superposition, which is on the most part acceptable, but there may be some cases where another analysis method would be desired. However, the effective impulse is the most accurate simplified method to date for a transient response floor.

The EC polynomial method [45] was generally inaccurate, at all frequencies. However, it better predicts a resonant response than both the kf method and the effective impulse, and would estimate a transient response better than using harmonics. As such, this method can be considered to be the best all round performer (i.e. the best universal force). The EC polynomial method is also the only method the produces a force that visually looks like a real force.

This section has shown that the latest guidance, using harmonics for resonant response floors, and the effective impulse for transient response floors, represents the current state of the art. The boundary between the two floor types will generally be valid. However, this boundary should be used with some engineering judgement and should be decided on a case by case basis. Even though the most accurate methods are being used in the current guidance, there are still large areas for improvement. Each footfall force model seems to have over simplified a footfall force time history. None of the models include variation of the pace rate or force, assuming that a footfall force in consistent and periodic. The next chapter will show that the pace rate, and the small variations of it, greatly change the nature of the force, not just the number of harmonics but also with the force spectral amplitudes. As the forces, and the people creating the forces, are so variable it would make sense to move away from a design philosophy concerned with absolute values of response, and towards statistical chances of response.

This section shall conclude with suggestions, which all new force models should use:

1. Use a time domain method
    - The simulated force, and response, in the time domain will look like their real measured counterparts.
    - Will allow for a universal force, for all floor types.
    - Will allow for any analysis type.
2. Equal impulses
    - The impulse of the simulated force should equal the impulse of the design force. It seems obvious, but this is generally not done.
3. Variation
    - Variation in pace rate will allow for modelling of the harmonics.
    - Variations in force will allow more accurate simulation of the force.
    - Variation of the person will allow an accurate simulation of the population.

A walking force time history is a complex, random force and should be treated as such. If a method can be developed to incorporate all the above points then a statistical based response analysis method can be developed. The next chapter will introduce a method that includes all of the above suggestions and it is shown that it is a universal method.

4 A Universal Footfall Force Model

The previous chapter examined the current state of the art footfall force models in detail. All the current methods can be considered to produce an uncharacteristic force for a number of reasons. The forces the models produce do not resemble a footfall force in that they do not contain the key characteristics. Also, all the models presume that the force is constant at a fixed pace race, with no variability in pace rate or amplitudes in the force. The closest any method has come to achieving a characteristic force is the method outlined in the European report [45]. However, due to not modelling the high frequency content of the characteristic heel strike and the lack of variation it is still not representative of a measured force.

The key problem with the existing methods is that floors are split into two categories: high and low frequency, and each category has a different force model. Chapter 3 argued that the boundary would vary, depending on how much variation there was in an individual pace rate. The variation is likely to be dependent on many factors: number of paces, pace rate, walking path length (and how straight it is), the individual, etc.. As such, the value of the high/low boundary could change depending on circumstances, i.e. the frequency at which resonance will likely not occur is case specific. Due to this, the previous chapter suggested that the terminology be changed to resonant response floors (RRFs) and transient response floors (TRFs) as this is more descriptive of the response. The classification of the floor should be case specific and governed by the nature of the measured or estimated response. Currently, due to the ambiguous nature of the boundary, there is a current overlap in frequency of when the two methods could be applied (the Concrete Centre [5] guide say the effective impulse is valid above 4 Hz and harmonics could govern the response up to 15 Hz). Also, there is no current model available that can accurately estimate response when the floor natural frequencies fall between the harmonics of the footfall force. Although this would not govern the response, an accurate force model should be able to achieve this.

Due to the current methods not being characteristic of a measured force and the different force models being used for different floor types, Chapter 3 suggested some criteria that a new force model should satisfy:

- A time domain representation
    - Ideally the force should resemble a measured force for a number of reasons. Firstly, applying a simulated force that visually appears to be a real force will result in less confusion for an analyst. Secondly, if the force is accurately modelled in the time domain, it is reasonable to assume that the model would inherit the characteristics of a measured force.
- Randomness and variation represented

- A real measured walking time history has variation in pace rate, which can be considered to be normally distributed. The randomness of the variation was shown in Chapter 3 to influence directly the number of significant harmonics in the force, their amplitudes and the energy between the harmonics. Also, the variation in the magnitude of the force will also vary the harmonic amplitudes of the harmonic component.

- Impulses Match Reality

  - Many of the existing force models have a higher impulse than the force they were created from. Essentially, this increases the magnitude of force applied by the model when compared to a measured force. A new force model should have the same impulse as the force it was based on.

If all the suggested criteria can be satisfied, the resulting model should be a universal footfall that is suitable for all floor types and more accurate then all current models. This chapter will outline a method, based on a cubic spline, which satisfies these characteristics. The spline force is verified as described in Chapter 3. The verification is taken further, with the simulated force applied to a resonant response floor and a transient response floor using measured mode shapes, and compared with experimental data.

The chapter begins by describing the key characteristics that need to be modelled in a footfall force to give accurate response estimations. From these characteristics, points are chosen to fit the quadratic spline and analyses are conducted to demonstrate the accuracy of the fit. Once the points are defined, statistical properties (i.e. their mean and variation) of time and force data point pairs are obtained. The cubic spline is then be fitted to points generated from their known statistical properties to obtain a unique random force. To create a walking force with multiple paces the procedure is repeated for each pace, and the timing for each pace is established from the experiment in Chapter 3.

The chapter then continues by validating the 'spline force', three situations are studied:

1. Response of an SDOF oscillator with fixed mass and varying frequency.
2. Resonant response of a simply supported concrete slab using measured modal properties.
3. Transient response for a very stiff and massive floor using measured modal properties.

Two comparisons will be conducted for each method: a time domain comparison and a frequency domain comparison.

4.1 Key Characteristics Required for a Footfall Model

From the analysis of footfall methods in Chapter 3 a number of characteristics can be identified that a footfall model will have to contain. It was shown that the EC method was the best universal method due to its visual likeness to a measured force. However, there were inaccuracies at both low and high frequencies, which require improvements. The low frequency inaccuracies were due to variation not being considered. The largest error was in the high frequency range due to the missing heel strike, which contains most of the footfalls high frequency energy. Therefore, if the main shape of the force can be modelled, with variation included, it is likely that the low frequency content of the force will be modelled well. Likewise, if the heel strike can be modelled it is likely that the high frequency content will also be modelled well. In this chapter, all measured forces are from the author and were collected as described in Appendix A.

Figure 36a shows many footfall force paces overlaid at a prompted pacing rate of 2 Hz. The shape is quite simple and relatively constant with each pace. However, there is clear variation in the contact time and the amplitude between each pace. Figure 36b shows an individual pace with a number of key points included:

1. Initial heel strike.
2. Maximum force from the heel.
3. Minimum force between the heel strike and the push-off.
4. Maximum force from the toe during push-off.
5. The contact time of the force.

The amplitudes and temporal position need to be modelled accurately for each one of these points, including the gradient of the force. From knowing the key points, the force can be reconstructed using a cubic spline.

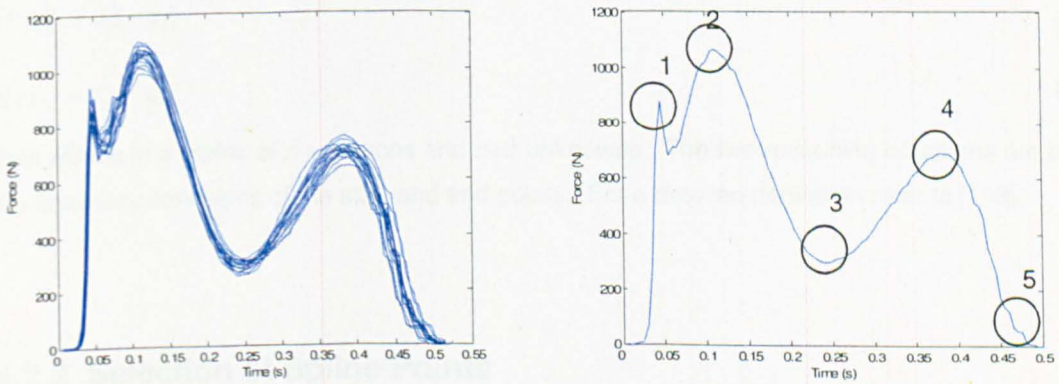

Figure 36a - Overlaid forces for a constant pace rate **b – Key characteristics of a force**

4.2 Cubic Spline Fit of a Footfall Force

The spline function is used to fit a smooth curve through the explicit data points using piecewise polynomial. It has advantages over fitting a curve through all of the points using one equation, i.e. a high order polynomial. With a large number of points, fitting a polynomial would produce a high order equation, and could suffer from Runge's phenomenon [102], which is an oscillation type distortion. A spline is much simpler and preserves the shape of the signal more accurately, and the values used in its calculation represent real world values.

4.2.1 Spline Theory

For a cubic spline over n intervals that involves fitting n equations over n+1 data points, the cubic polynomial fit for each segment can be defined by:

$$y = a_i(x - x_i)^3 + b_i(x - x_i)^2 + c_i(x - x_i) + d_i \qquad \textbf{Equation 51}$$

where the spacing in time between each data point is:

$$h_i = x_{i+1} - x_i \qquad \textbf{Equation 52}$$

with x and y being the x and y (i.e. time and force respectively) values of the data points and, a, b, c and d the constants that make up the piecewise polynomial.

The cubic spline constrains the functions, defined by Equation 51, and their 1st and 2nd derivatives to be equal at node points for all adjoining segments allowing for the smooth transition between each piecewise polynomial:

$$f_i''(x_i) = f_{i+1}''(x_i) \qquad \textbf{Equation 53}$$

$$f_i'(x_i) = f_{i+1}'(x_i) \qquad \textbf{Equation 54}$$

This results in a matrix of n equations and n+2 unknowns. The two remaining equations are based on the boundary conditions of the start and end points. For a detailed derivation refer to [103].

4.2.2 Selection of Spline Points

Initially, the minimum number of points required to estimate a footfall was determined by eye. To represent accurately the measured force, points are required at maximum changes in gradients, i.e. at the two maxima and the minimum, with additional points either side to define the curve (refer to Figure

36). Between two maximum changes in gradient, e.g. between the minimum and the second maximum, a further point is required to define the relatively straight line. One additional point is also required to include the heel strike.

Once the number of points had been defined for a particular footfall sequence (Figure 36a), a least squares optimisation algorithm was applied to define their location. The algorithm worked by fixing the points at the two maxima and the minimum and normalising so the peak force is 1, all other points were defined by ratios of the force at these points. An initial guess of the ratios was chosen and a spline force was created. The spline force was then compared to the measured force by the difference in total impulse to obtain an error. The points were then adjusted until the error was at a minimum. The error was minimised over a range of pacing rates, with the final point locations then used for all pace rates. This achieves an overall minimised error, however, for an individual pace rate it is possible to reduce the error further.

Figure 37 shows the selection of the spline points after the least squares optimisation, the figure can be used to clarify some points made above. If one considers the number of spline points to construct the force, point 9 is the location of the minimum and point 8 and point 10 are required to represent accurately the curve through point 9. Between the maximum gradient of point 9 and point 13, point 11 is required to represent accurately the relatively straight line between the two. Point 3 is added to represent the heel strike, which, due to the nature of a qubic curve it represents the heel strike quite well. The table shows how the other points are represented. Points 1-4 are a proportion of the peak force of point 5, points 6-8 are a proportion of the force at point 5 minus the force at point 9, and so on.

Now that the point locations have been defined, the general procedure to locate the points on any footfall force is as follows:

1. Normalise the force so that the peak force is 1.
2. Determine the magnitude and time of the maxima and minimum (points 5,9 and 13)
3. As the magnitudes for all other points are proportions of the maxima and minimum, these are all ready known.
4. From the known magnitudes of the other points, locate their position in time.

This method creates a force that resembles a footfall force, and models the key characteristics described in the previous section.

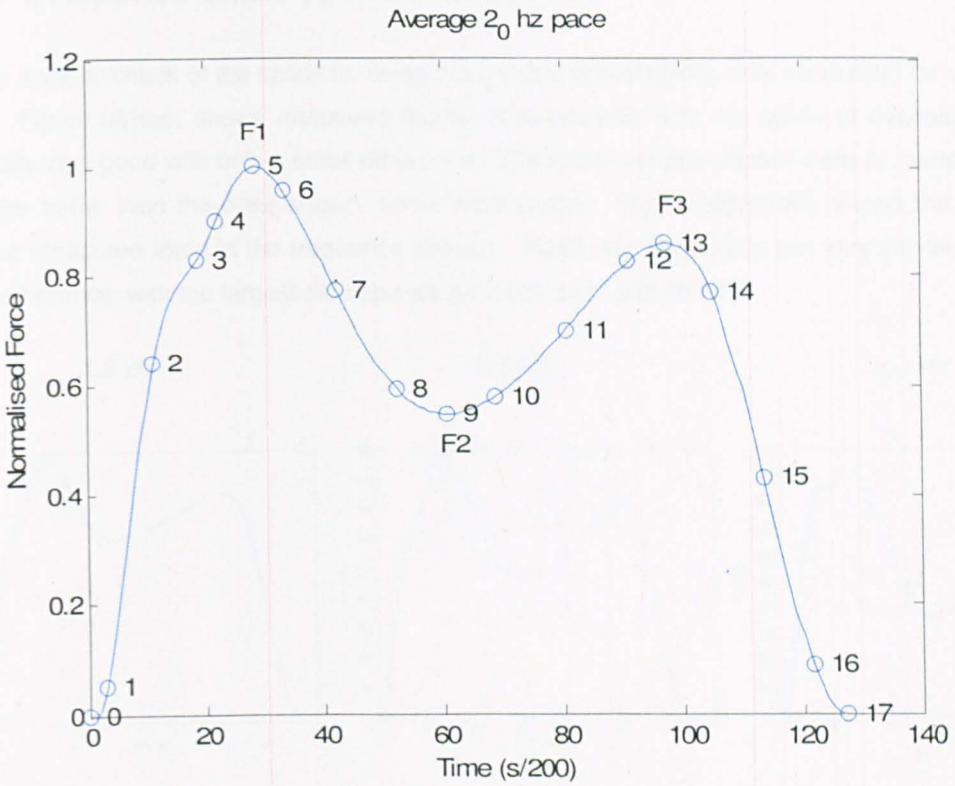

Point	Force Proportion
0	0
1	0.05 F1
2	0.64 F1
3	0.83 F1
4	0.9 F1
5	F1
6	0.9 (F1-F2)
7	0.5 (F1-F2)
8	0.1 (F1-F2)
9	F2
10	0.1 (F3-F2)
11	0.5 (F3-F2)
12	0.9 (F3-F2)
13	F3
14	0.9 F3
15	0.5 F3
16	0.1 F3
17	0

Figure 37 – Footfall force spline points

4.2.3 Evaluation of the Spline Fitted Force

Initially a visual check of the spline fit, using the generic spline points, was conducted for various pace rates. Figure 38(top) shows measured footfall time histories with the spline fit overlaid. The fit is generally very good with only a small difference. The three footfalls chosen were at random, as some fits were better than the ones shown, some were worse. Figure 38(bottom) shows the spline force and the measured force in the frequency domain. Again, the two forces are very similar, with only a slight difference, with the largest discrepancy between 5 Hz and 15 Hz.

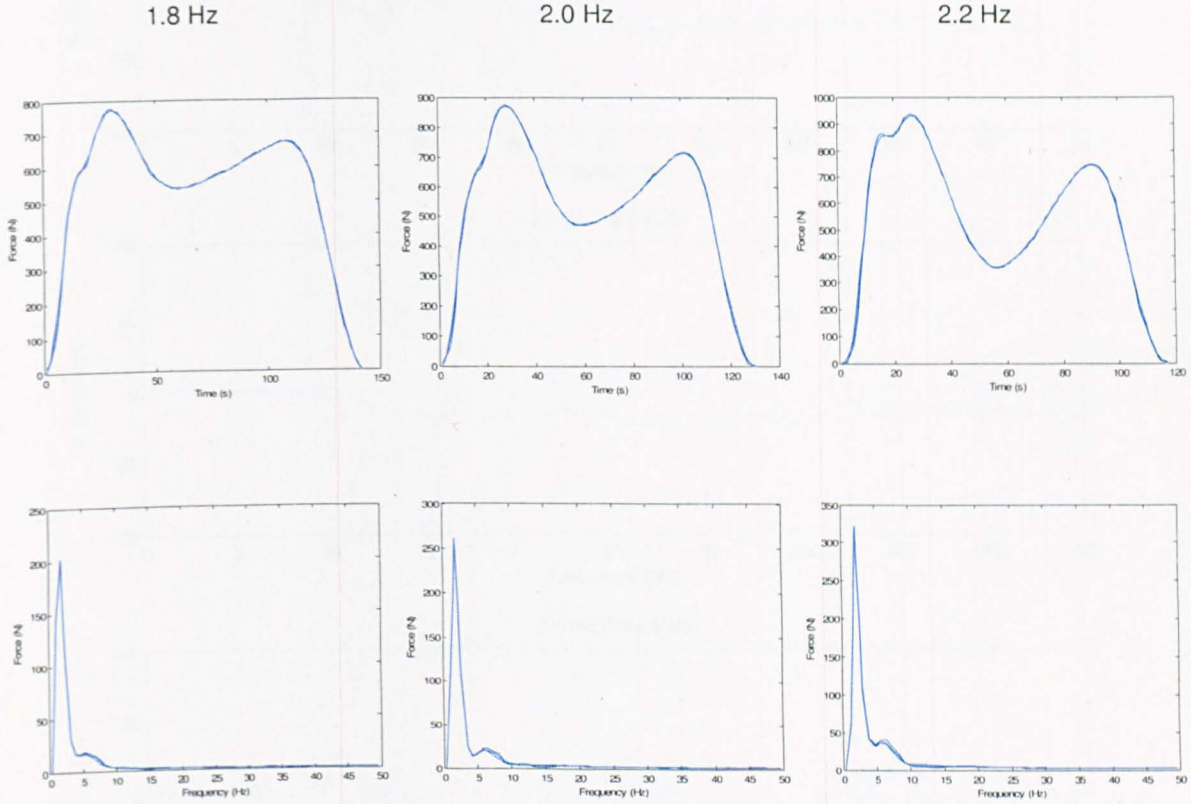

Figure 38 - Overlaid forces in the time domain (top) and frequency domain (bottom), recorded GRF and the spline force

Next, the spline fitted forces were analysed in the same manner as the force models in Chapter 3. A complete footfall force time history has a unique spline created for each pace using the points as shown in Figure 37. The simulated and measured forces were both applied to an SDOF oscillator of varying frequency to obtain response spectra. Figure 39 shows the percent difference in response spectra. The response is not exactly the same, with a maximum difference of about 20%. Compared with the methods shown in Chapter 3 this error is small. It is also clear that the method accurately reproduces the response over the whole frequency range. The results could be improved further with optimisation of the spline points. The points have been optimised for a fixed location (in amplitude) to fit a wide range of pace rates, however, each pace rate has its own optimal points. In Figure 38 it is possible to see how the location of the high frequency spike changes with increasing pace rate, it

becomes more pronounced and moves towards the first maximum, F1. It is the reproduction of this spike that causes the errors as using fixed spline points the spike cannot be accurately reproduced for every pace rate.

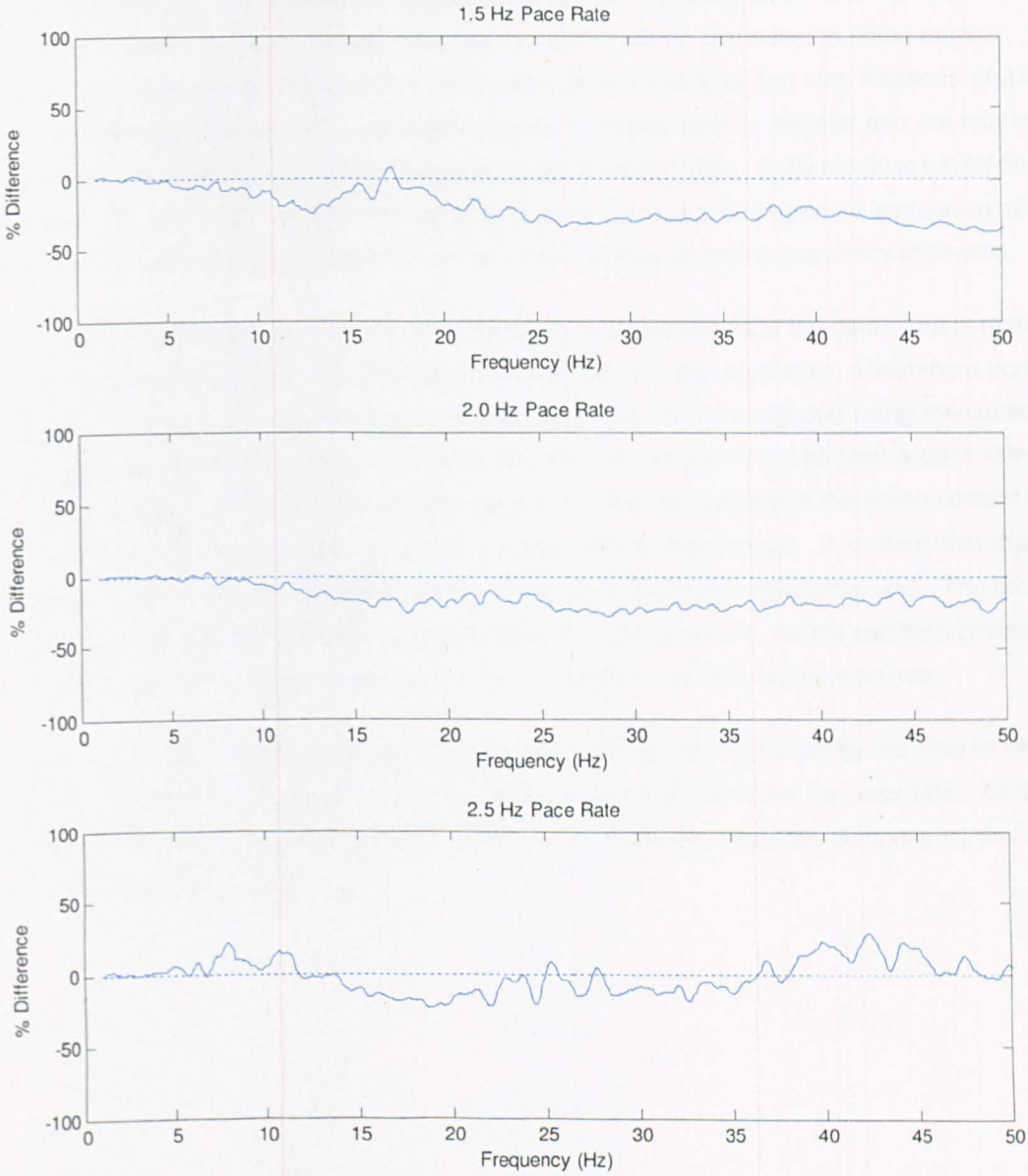

Figure 39 ***(From top to bottom)*** **– Percentage difference between the velocity response spectra using the measured force and the spline fitted force, for 1.5 Hz pace rate; 2.0 Hz pace rate; 2.5 Hz pace rate, the dotted line represents the measured force**

4.2.4 Spline Point Correlations and Variances

After the position of the spline points had been decided, an investigation was conducted into the various correlations the points have with each other. If the points exhibit any type of correlation then assuming that they act as independent random variables will introduce errors and the force will not be modelled accurately. It is logical to assume that the points will be correlated in some manner. If one considers time, it stands to reason that if the contact time is reduced, the time locations of all other points must also be reduced. Also considering force, if contact time is reduced and the total energy stays the same, it stands to reason that the peak forces must increase. If the model is based on these hypotheses then all points in time and amplitude must have some degree of correlation with the contact time. It also stands to reason that contact time reduces as pacing frequency increases.

In all the figures in this section, the thick line represents a polynomial fit of the data. The fit represents the mean at that specific pace rate, the standard deviation will also be shown, assuming a normal fit. Initially the possible correlation of contact time to pace rate was investigated using measured force time histories of the author walking. The time histories contain many paces over a pace rate range from 1.5 Hz to 2.5 Hz. Figure 40 shows the correlation, the line represents the mean contact time at each pace rate, and the standard deviation is shown in the table below. It is clear that there is a definite correlation and that the fitted quadratic curve represents the relationship well. The properties of the curve can be used to estimate the contact time for any pace rate. As the standard deviation and the mean is known, assuming a normal distribution, a random variable can be obtained.

All other points will be shown to be correlated with the contact time (defined by the time in which the foot is in contact with the floor, i.e. the length of the force), and therefore the pace rate. As such, all correlation plots will be shown in terms of contact time. Each point has two components that need to be estimated: force and time.

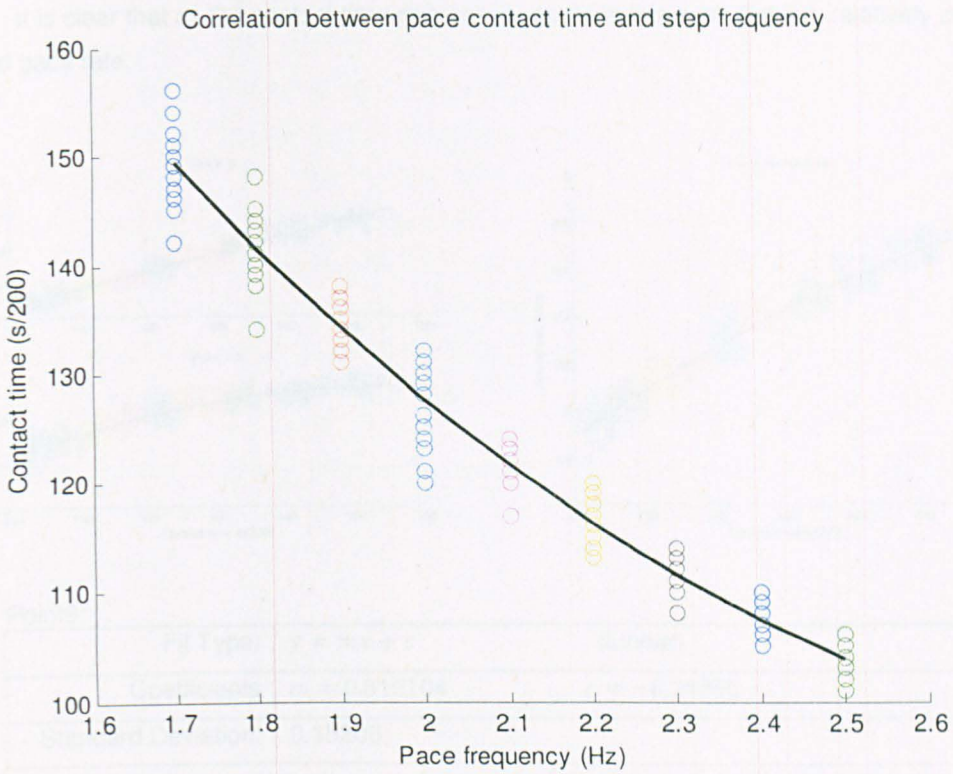

Fit Type:	$y = ax^2 + bx + c$	(Quadratic)	
Co-efficients:	$a = 30.8378$	$b = -186.525$	$c = 377.3792$
Standard deviation:	$\frac{y}{68.348}$		

Figure 40 - Correlation between the force contact time and the average pace rate; measured data are overlaid by the fit

4.2.4.1 Force Component Correlations

In this section all plots have a similar layout: a line represents the mean value of a correlation, dots of a constant colour represent a constant pace rate and at the bottom of each plot is a table showing the type of fit, the co-efficients and the standard deviation.

As shown in Figure 37 all force components of the spline are related to the force components of points 5, 9 and 13. As the force is normalised so that the peak force is 1, which is always at point 5, only two unknowns remain, the forces at points 9 and 13. Figure 41a shows the correlation between the contact time and the force magnitude at points 9 and 13 with each colour represent data from a fixed pace rate. The correlation is very clear: as the contact time decreases (and the pace frequency increases) the force for both points decreases. Figure 41b shows the correlation between the contact

time and the sum of points 5, 9 and 13. This sum is a crude representation of the energy in the footfall force. It is clear that as the contact time decreases, as does this sum, but it is relatively constant over a fixed pace rate.

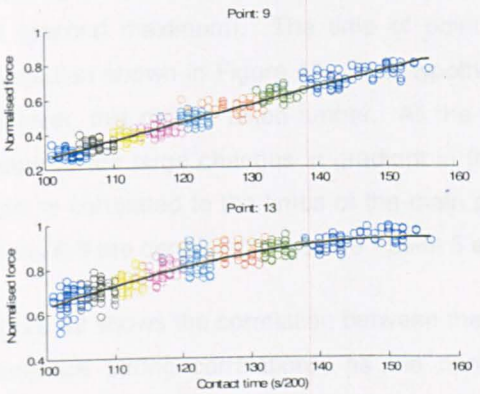

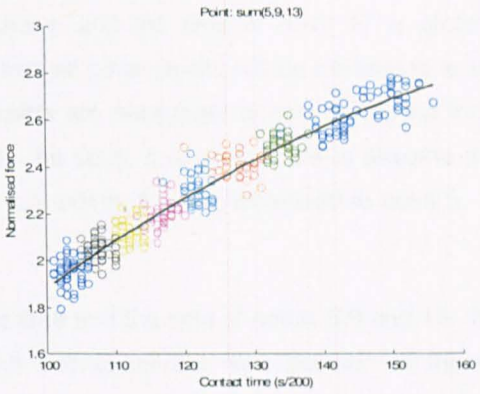

Point9:

Fit Type:	$y = mx + c$	(Linear)
Coefficients	$m = 0.010104$	$c = -0.74995$
Standard Deviation:	0.15206	

Point13:

Fit Type:	$y = ax^2 + bx + c$	(Quadratic)	
Coefficients	$a = -8.9423 \times 10^{-5}$	$b = 0.028352$	$c = -1.3111$
Standard Deviation:	0.095927		

Sum of points 5, 9 and 13:

Fit Type:	$y = ax^2 + bx + c$	(Quadratic)	
Coefficients	$a = -0.0001063$	$b = 0.042683$	$c = -1.3217$
Standard Deviation:	0.24255		

Figure 41a - Correlation between contact time and normalised force of points 9 and 13

b - Correlation between contact time and the sum of the normalised force of points 5, 9 and 13

4.2.4.2 Time Component Correlations

As stated earlier, each point located on Figure 37 contains force and time components. In this section, correlations regarding the time components are investigated. There are 5 main points that make up the spline: point 0 (start), point 17 (end), point 5 (first maximum), point 9 (minimum) and point 13 (second maximum). The time of point 0 is known and the time of point 17 is given by the correlation shown in Figure 40. The hypothesis is that all other points will be correlated to point 17, however, this can be taken further. All the other points are necessary to give the spline the correct shape at the large changes in gradient in the force. As such, it is reasonable to assume that each point is correlated to the times of the main points. E.g. points 1-4 are correlated to point 5 - point 0, points 6-8 are correlated to point 9 - point 5 etc.

Figure 42 shows the correlation between the contact time and the time of points 5,9 and 13. It is clear there are strong correlations, as the contact time decreases the time position of these points decreases, as expected.

Figure 43 shows the correlation between point 5 and points 1-4. These points are also well correlated, however, there is more variation and a noticeable discrepancy at points 3 and 4. This can be explained with the position of the high frequency heel strike spike. In these data, as the pace rate increases (and therefore contact time decrease) the position of this spike moves towards the first maximum. The discrepancy is due to when the spike passes the location of the points 3 and 4.

Figure 46 show the correlations of the other points. It is clear that there is a strong correlation at all points, but with a different degree of variation.

The colours on each plot represent a number of paces at a certain prompted frequency. The values from the curve fitting shown in the correlation figures represent the mean value at the corresponding contact time. Along with the standard deviation, a random variable can be obtained assuming a normal distribution. These values can then be used to estimate values for spline fitting.

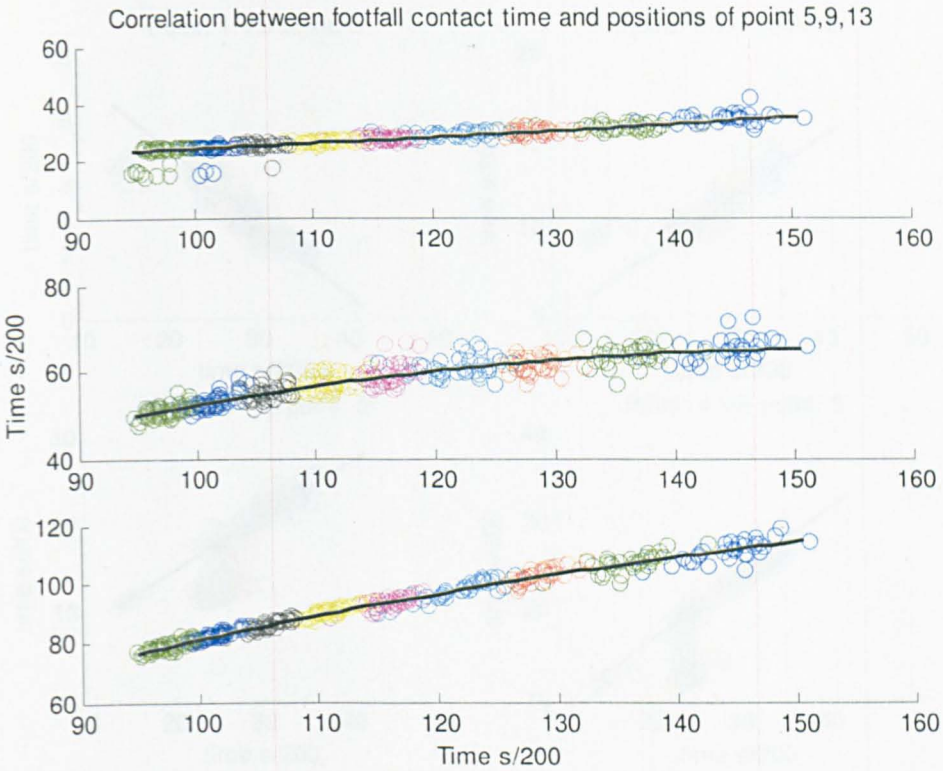

Fit type:	$y = ax^2 + bx + c$ (Quadratic)		
Point5 coefficients:	$a = 0.00083206$	$b = 0.01382$	$c = 14.310$
Standard deviation:	$\frac{y}{23.270}$		
Point9 coefficients:	$a = -0.0042632$	$b = 1.3254$	$c = -37.6604$
Standard deviation:	$\frac{y}{29.634}$		
Point13 coefficients:	$a = -0.0035052$	$b = 1.548$	$c = -38.9381$
Standard deviation:	$\frac{y}{44.289}$		

Figure 42 - Correlation between contact time and points 5, 9 and 13

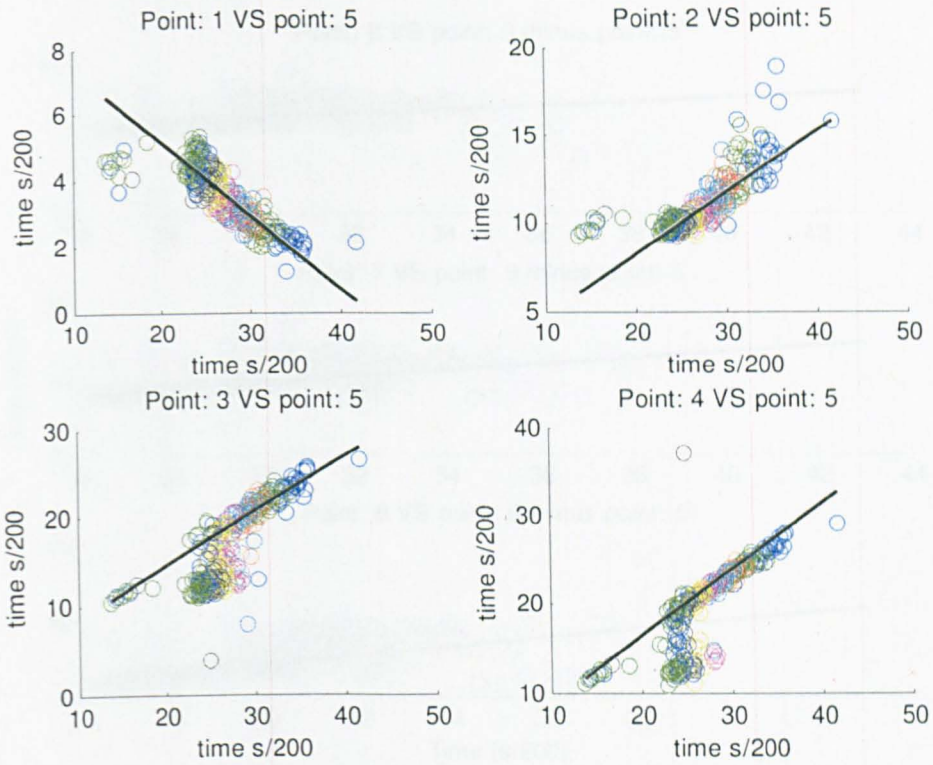

Fit type:	$y = mx + c$	(Linear)
Point1 coefficients:	$m = 0.2226$	$c = 9.586$
Standard deviation:	0.4127	
Point2 coefficients:	$m = 0.349$	$c = 1.219$
Standard deviation:	0.5981	
Point3 coefficients:	$m = 0.6278$	$c = 1.853$
Standard deviation:	0.8959	
Point4 coefficients:	$m = 0.7518$	$c = 1.358$
Standard deviation:	0.6239	

Figure 43 - Correlations of point 5 VS points 1, 2, 3 and 4

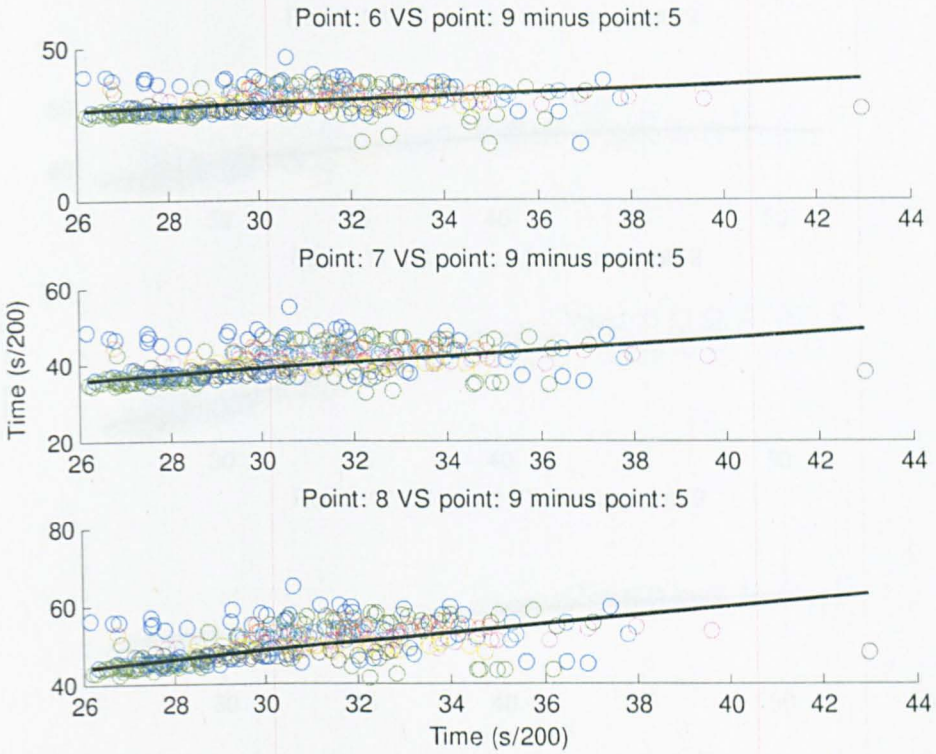

Fit type:	$y = mx + c$ (Linear)	
Point6 coefficients:	$m = 0.61455$	$c = 12.989$
Standard deviation:	3.9182	
Point7coefficients:	$m = 0.80005$	$c = 14.938$
Standard deviation:	3.8435	
Point8 coefficients:	$m = 1.1024$	$c = 15.181$
Standard deviation:	4.297	

Figure 44 - Correlations between (point 9 minus point 5) and points 6, 7 and 8

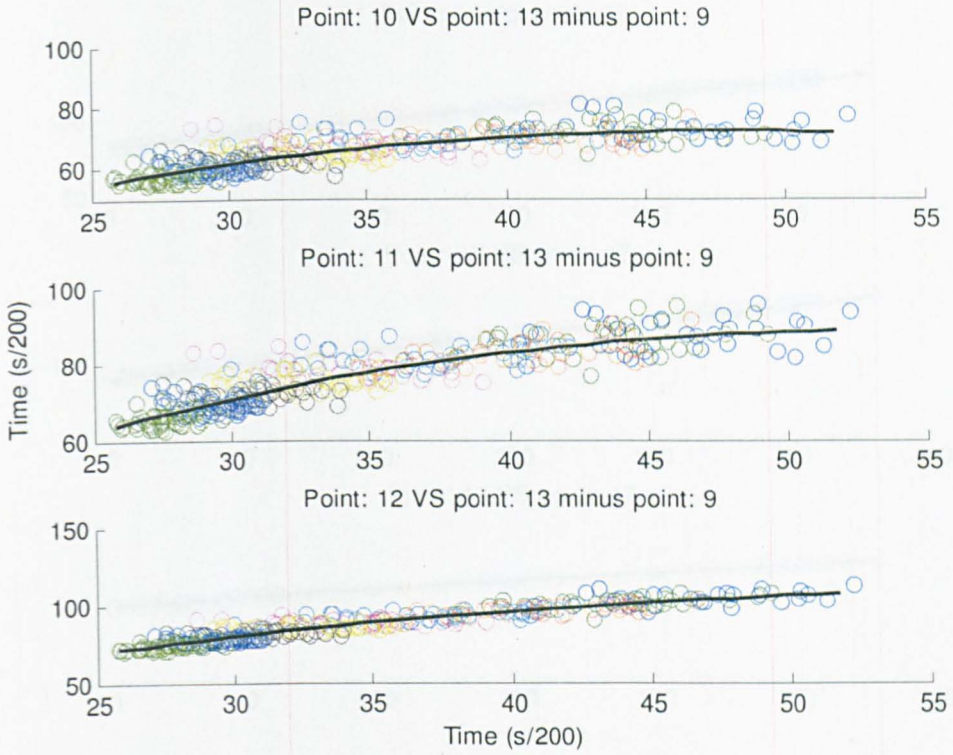

Fit type:	$y = ax^2 + bx + c$ (Quadratic)		
Point10 coefficients:	$a = -0.033338$	$b = 3.1994$	$c = -4.7204$
Standard deviation:	5.8995		
Point11 coefficients:	$a = -0.032328$	$b = 3.4598$	$c = -3.8687$
Standard deviation:	7.7207		
Point12 coefficients:	$a = -0.025494$	$b = 3.3305$	$c = -2.5593$
Standard deviation:	9.7897		

Figure 45 - Correlations between (point 13 minus point 9) and points 10, 11 and 12

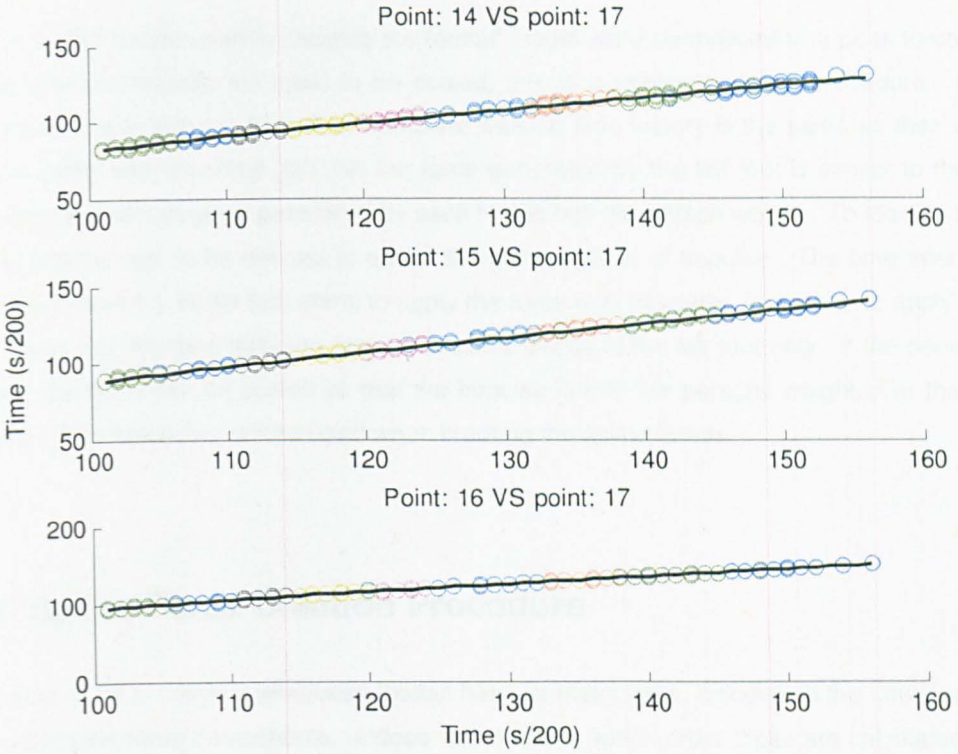

Fit type:	$y = ax^2 + bx + c$ (Quadratic)		
Point14 coefficients:	$a = -0.001452$	$b = 1.2204$	$c = -26.634$
Standard deviation:	12.564		
Point15 coefficients:	$a = -0.00057186$	$b = 1.0874$	$c = -1.0874$
Standard deviation:	13.819		
Point16 coefficients:	$a = -1.4476 \times 10^{-5}$	$b = 1.0242$	$c = 1.0242$
Standard deviation:	14.937		

Figure 46 - Correlations between 17 and points 14, 15, 16

4.2.5 Amplitude Scaling of the Spline Force

As the footfall forces used in creating the footfall model were normalised to a peak force of unity, any forces that are created will need to be scaled, this is a relatively simple procedure. For a person walking, the total impulse from their complete walking time history is the same as their weight. If the person walks with a normal gait, i.e. the force generated by the left foot is similar to the force of the right foot, then the impulse generated by each foot is half the person weight. To identify a single pace, a time interval has to be defined to obtain the correct value of impulse. The time interval is defined from the moment a single foot starts to apply the force until the same foot starts to apply a force of the next pace, e.g. the time between two consecutive paces of the left foot only. If the person's weight is known, the force can be scaled so that the impulse is half the persons weight over the defined time interval. This procedure will be used when creating the spline forces.

4.3 Spline Force Creation Procedure

The procedure to create a simulated footfall has two main steps, calculating the time components and calculating the force components. It does not matter in which order these are calculated, but for both, a contact time must first be estimated. The procedure for each is outlined below, with the points defined in Figure 37.

Contact Time:

1) Estimate contact time from Figure 40 using a random variable

Force Components:

2) Assume amplitude at point 5 = 1
3) Estimate amplitude of point 9 using correlation in Figure 41a
4) Estimate amplitude of point 13 using sum correlation in Figure 41b
5) Estimate all other amplitudes using table in Figure 37
6) Add point 0 and 17 with force=0

Time Components:

2) Estimate times at points 5, 9 and 13 using correlations in Figure 42
3) Estimate times at points 1, 2, 3 and 4 using correlations in Figure 43
4) Estimate times at points 6, 7 and 8 using correlations in Figure 44
5) Estimate times at points 10, 11 and 12 using correlations in Figure 45
6) Estimate times at points 14, 15 and 16 using correlations in Figure 46
7) Add point 0 and 17 at time=0 and time=contact time respectively

Spline Creation:

8) Create spline using time = x co-ordinates and force = y co-ordinates
9) Scale force using: $\frac{Impulse\ of\ the\ measured\ force}{contact\ time+time\ to\ next\ footfall} = 0.5 \cdot weight\ of\ person$

Each pace can then be added into a walking time history, obtaining the pace timings using the distribution shown in Chapter 3 (Figure 17).

4.4 Evaluation of the Simulated Spline Force

This section analyses the performance of the simulated spline force which include variation in amplitude and pace rate. As such, it should estimate responses at all frequencies well. As the force has random characteristics, a direct comparison with measured responses is not a fair test: it is unknown if the measured responses represent an average response, it could just as likely be an uncharacteristic high or low response. The same applies for the simulated spline force, no two forces will be the same.

The comparison conducted consists of two parts: evaluation of spectra and evaluation of time domain response. The analysis for each part begins the same, with 100 simulated spline forces are created, consisting of many paces. As the force uses random variables, each simulated force, and the corresponding response, is unique. The simulated forces are applied to the system being analysed (which will be described in more detail shortly). A velocity response spectrum will be obtained from each system, for each simulated force. At each frequency point, a maximum and minimum value from all the response spectra will be obtained and plotted, forming a response envelope. A real response will then be measured. The measured response spectrum should then fit within the response envelope. Regarding the time histories, a time history will be chosen at random from one of the one hundred simulated responses and compared with the measured response. Due to the randomness of the spline force it is highly unlikely that the two responses will match, in the same manner that two individual measured responses would not match. Finally, to show that the variation predicted by the spine force envelope exists, a measured response envelope will be obtained for one of the systems.

Three systems are analysed: a simulated SDOF oscillator with a fixed mass and varying frequency, a real resonant response floor and a real transient response floor, each is analysed using a number of pace rates. Due to the different nature of each system, and the variety in pace rate, the analyses are a good test of the performance of the simulated spline force.

4.4.1 SDOF Response Analysis

The measured and simulated spline forces were applied to a SDOF oscillator with varying frequency to create response spectra. Due to the variation of the spline force, it was applied 100 times, each with a unique force, and maximum and minimum values were obtained from all spline force spectra to form a response envelope. The plots are shown in Figure 47 with various frequency bandwidths, the solid line represents measured force and the dotted lines represent the range of the simulated force. The response from the measured force fits within the envelope created by the spline forces, therefore, it estimates the response well.

Although the spectrum reports good correlations for maximum responses, this does not necessarily mean that the time domain response is comparable. To check this, Figure 48 shows comparisons of the response of the measured and spline force overlaid in the time domain. It must be stressed that these responses will not be the same due to the variation of the simulated force, in the same way that if the response of a structure was measured to a person walking, two measurements would not yield the same results, but they would be similar. The figure shows time domain plots at three four different oscillator frequencies to demonstrate the resonant and transient accuracy of the simulated force. Blue represents the real force, black represents the simulated force.

The two time histories match well. However, there is a difference in phase due to the different variation in timing between each step. There is also a difference in amplitude due to the difference in each pace's contact time, pace rate, and therefore the harmonic amplitudes, which all the correlations are based on.

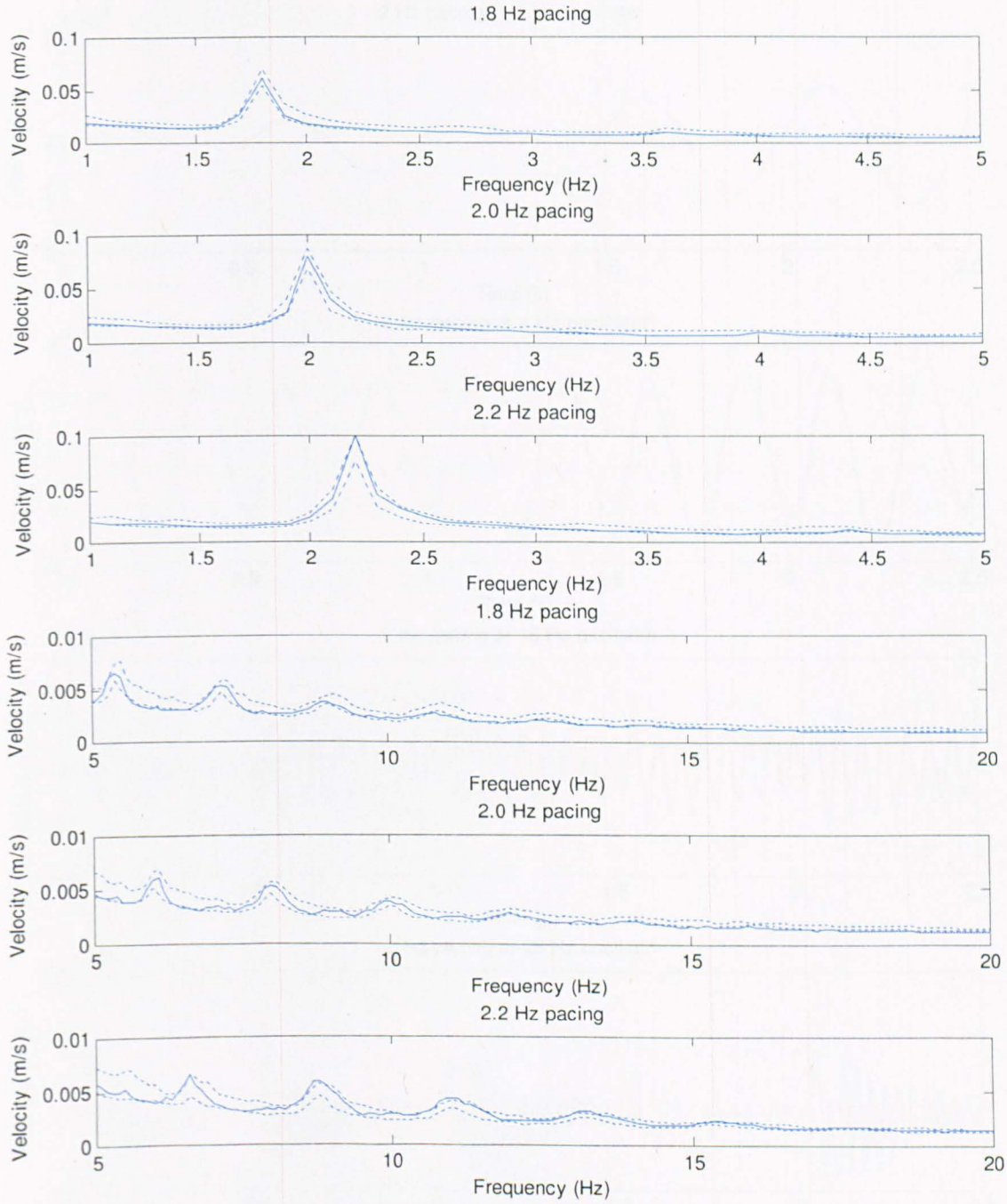

Figure 47 - SDOF spectrum comparisons of the recorded and simulated force for various pace rates and bandwidths

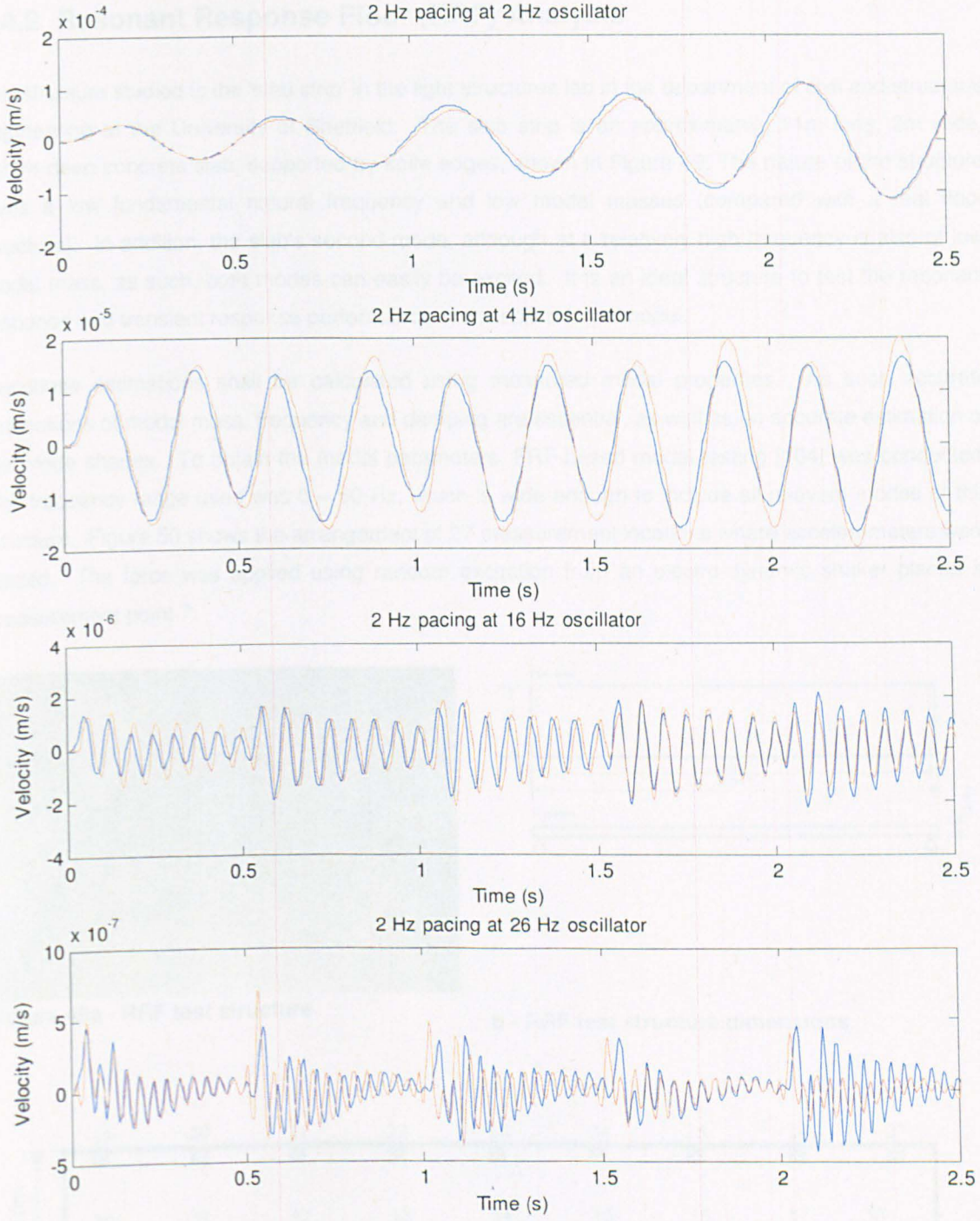

Figure 48 – Time history response of simulated and measured forces; blue is from the measured force, red is from the spline force.

4.4.2 Resonant Response Floor (RRF) Analysis

The structure studied is the 'slab strip' in the light structures lab in the department of civil and structural engineering at the University of Sheffield. The slab strip is an approximately 11m long, 2m wide, 0.27m deep concrete slab, supported by knife edges, shown in Figure 49. The nature of the structure gives a low fundamental natural frequency and low modal masses (compared with a real floor structure). In addition, the slab's second mode, although at a relatively high frequency is also of low modal mass, as such, both modes can easily be excited. It is an ideal structure to test the resonant response and transient response performance of the spline force model.

Response estimations shall be calculated using measured modal properties. As such accurate estimations of modal mass, frequency and damping are essential, as well as an accurate estimation of the mode shapes. To obtain the modal parameters, FRF-based modal testing [104] was conducted. The frequency range used was 0 – 50 Hz, which is wide enough to include all relevant modes of this structure. Figure 50 shows the arrangement of 27 measurement locations where accelerometers were placed. The force was applied using random excitation from an electro-dynamic shaker placed at measurement point 7.

Figure 49a - RRF test structure

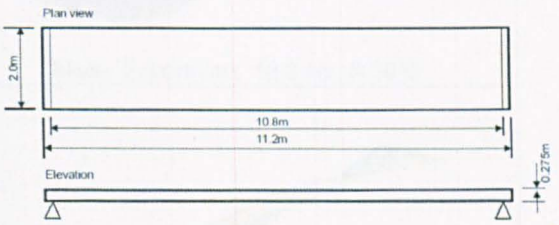

b - RRF test structure dimensions

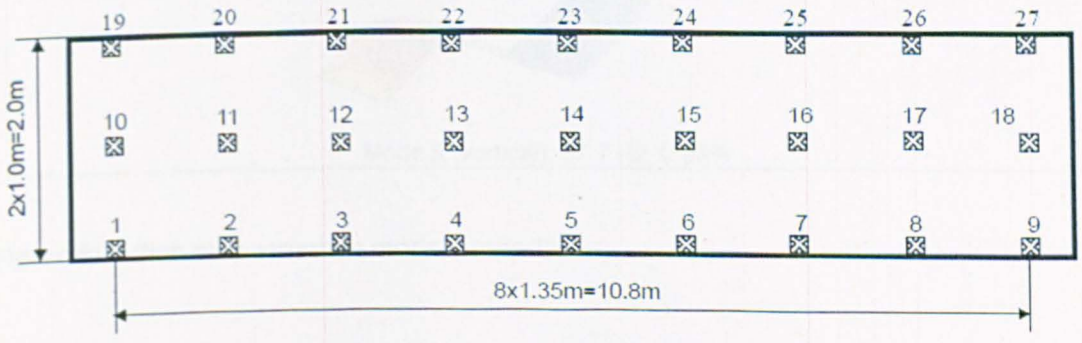

Figure 50 – Measurement points used for modal analysis

Figure 51 shows the estimated modal properties with five very clear modes identified. The fundamental modal frequency is 4.5 Hz with a modal mass of approximately 4000 kg and the second

mode has a frequency of 16.8 Hz and a modal mass of approximately 5900 kg. The author has experience in measurements on this structure and it is apparent that the first two modes govern the response, due to the low damping and low mass of each mode. Mode 3 and mode 4 are torsional with a nodal line down the centre of the slab in the longitudinal direction and as the walking path is along this nodal line these modes will not be excited. Mode 5 is also a vertical mode, however due to the high frequency it is unlikely to feature in the response much.

Although not shown in this study, it is known that the damping and frequency are non-linear and depend on the amplitude of the response, and due to the low mass, the number of people on the structure. The modal properties shown are for an empty structure. For a detailed investigation into the non-linearites of the structure refer to Zivanovic *et al.* [105].

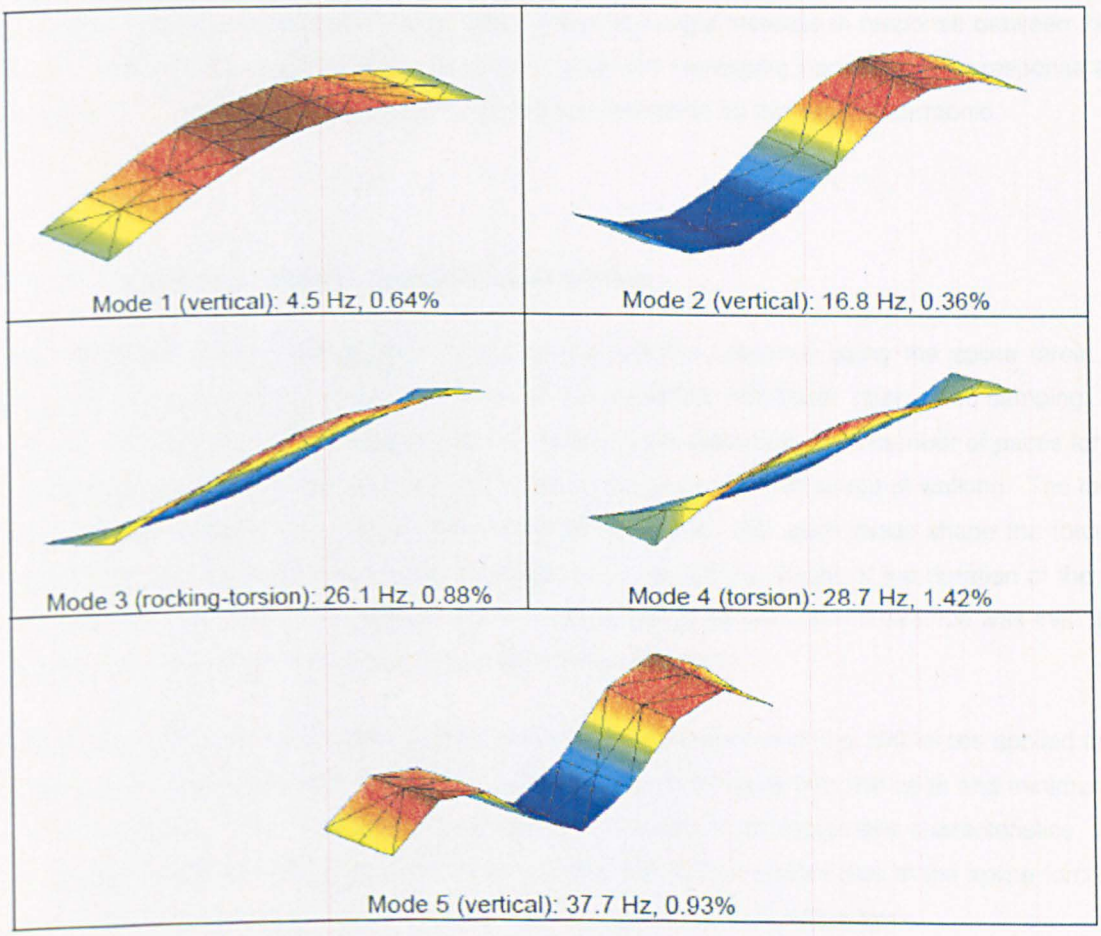

Figure 51 – Slab strip structure modal properties

4.4.2.1 Response Measurements

The response of the structure was measured while the author performed a number of walking tests at different pace rates. The measurement point used for the analysis was at quarter span to ensure there was a response from all three vertical modes. The walking path began at a structurally disconnected platform at one end of the slab and finished at a structurally disconnected platform at the other end. The pace rates walked at were 1.8 Hz, 2.0 Hz and 2.2 Hz with each pace rate repeated once.

Figure 52a, Figure 53a, and Figure 54a show one of the measurements for each pace rate at quarter span, with the solid line in Figure 52c, Figure 53c, and Figure 54c, the corresponding spectrum. There are clear maxima at 4.5 Hz and 16.8 Hz which are due to the first two vertical modes. The torsional modes are not excited due to the walking path being in the centre of the slab, and the response of the 3rd vertical mode is so low that it is negligible. There is a slight increase in response between the 1.8 Hz and 2.0 Hz pacing due to a slight increase in force with increasing pace rate. The response at 2.2 Hz pace rate is the largest due to an almost resonant excitation by the second harmonic.

4.4.2.2 Response Estimation Using the Spline Force

The measured modal properties were used to estimate the response using the spline force. The damping values were increased according to the expected non-linear change in damping. 100 different simulated force time histories were created at each pace rate. The number of paces for each pace rate was estimated with a relationship between the pace rate and speed of walking. The method of modal superposition was used in calculating the response. For each mode shape the force was scaled in time to the magnitude of the mode shape, i.e. at half the length of the duration of the force, the force was scaled by the magnitude of the mode shape at centre span. The force was then scaled again by the magnitude of the mode shape at the response point.

Figure 52b, Figure 53b, and Figure 54b shows one of the responses of the 100 forces applied at each pace rate, with the dotted lines in Figure 52c, Figure 53c, and Figure 54c, the peak and minimum hold for all the spectra. It is clear that the time histories are similar in amplitude and characteristics. Again, it must be made clear they should not match exactly due to the randomness of the spline force. The measured spectra also fit between the response envelopes from the spline force.

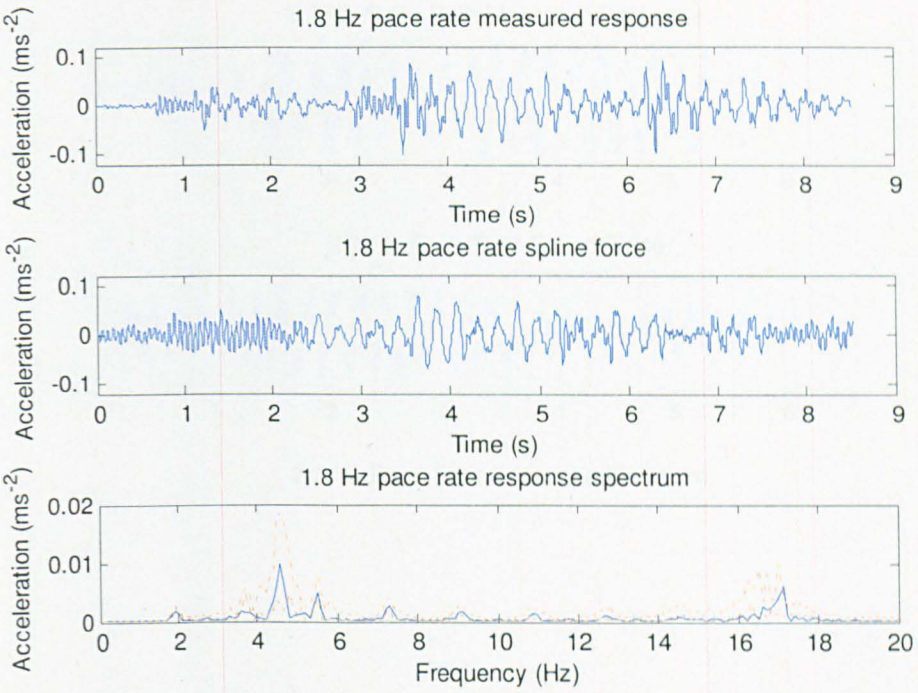

Figure 52 (from top to bottom) – a) test structure measured response, b) test structure spline force c) response spectrum (the red dots represent the response envelope from the spline force); all 1.8 Hz pace rate

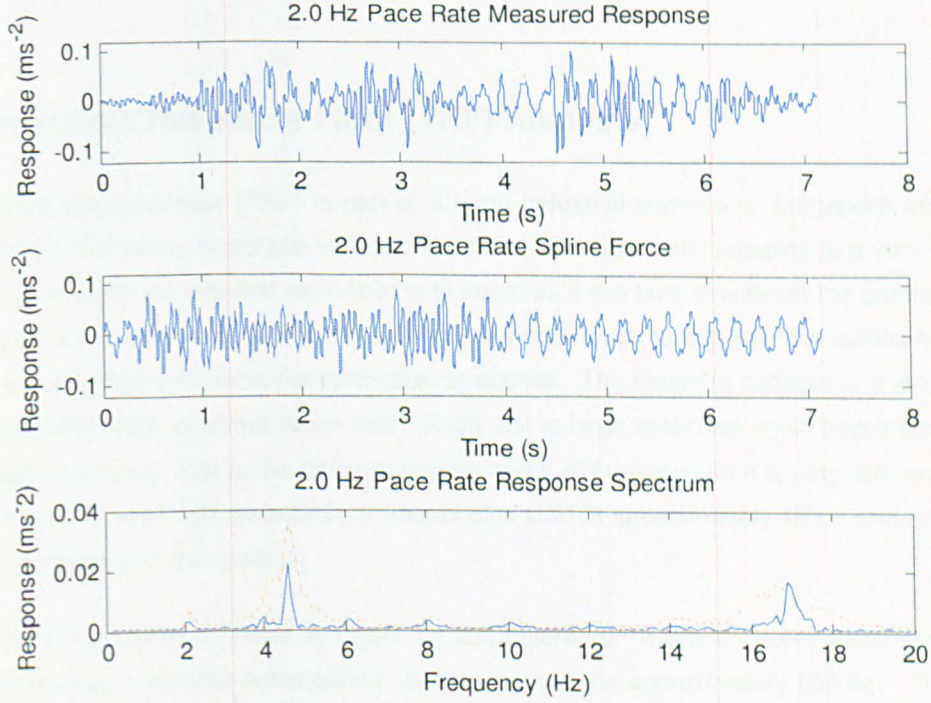

Figure 53 (from top to bottom) – a) test structure measured response, b) test structure spline force c) response spectrum (the red dots represent the response envelope from the spline force); all 2.0 Hz pace rate

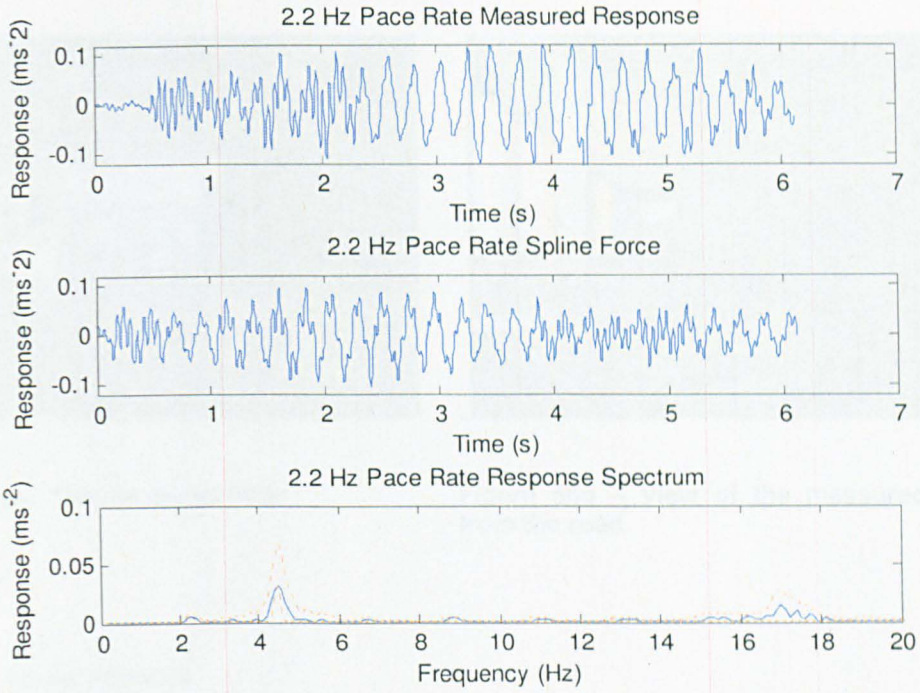

Figure 54 (from top to bottom) – a) test structure measured response, b) test structure spline force c) response spectrum (the red dots represent the response envelope from the spline force); all 2.2 Hz pace rate

4.4.3 Transient Response Floor (TRF) Analysis

The transient response floor (TRF) is part of a large industrial complex in Singapore which houses many different industries, some are vibration sensitive. The industrial complex is a very large multi-storey structure, with the aim that each floor is to seem as if it is built directly on the ground. As such, the structure is massive for its size with each floor strong enough to support fully loaded heavy goods vehicles with seemingly no vehicular restriction on access. The structure consists of a long main road with the industrial units attached either side. Each unit is large detached, multi-bayed floor, and only connected to the road. Due to the strength requirements of the structure it is very stiff, and even with beam spans up to 12m, fundamental floor frequencies start at approximately 10 Hz and are ideal for a transient response floor comparison.

The floor that was tested is shown in Figure 55 and Figure 56. It is a 4th storey warehouse which, at the time of testing, contained some pallets (each pallet weighs approximately 500 kg). The total floor (including the parking areas) is 3 bays wide (1 large centre span with two smaller spans each side) and 8 bays long. The building is situated on area 2 x 7 bays, as shown in Figure 58. Spanning in the short direction, the floor is made up from a number of precast hollow core slabs with a span of 7.5m. A structural layout is shown in Figure 58.

Figure 55a – The measured floor

Figure 56b – View of the measured floor from the road

4.4.3.1 Modal Analysis

Only one bay was tested: a bay towards the centre of the building, with a low number of pallets. It was decided that this location would give the highest response and give a good representation of the rest of the floor. FRF based modal testing was conducted using roving hammer excitation, a brief report of the modal analysis can be found in Appendix B. Figure 57 shows a photograph of the hammer test in progress. A grid of 11 test points was used (shown in Figure 58), with reference accelerometers at points 4, 5 and 11. During the hammer testing there were un-measureable external sources of excitation from the other industrial units, however, modal parameters all agreed with other units measured and finite element analysis.

Figure 57 – Hammer testing of the floor bay

Figure 59 shows the mode shapes and modal parameters obtained. The fundamental mode was estimated to be 10.3 Hz with a modal mass of 139 tonnes and 9 modes, in total, were found in the frequency range 10 – 50 Hz and is ideal for the TRF analysis. Later, the mode shapes obtained will be used in the response estimation from the spline force.

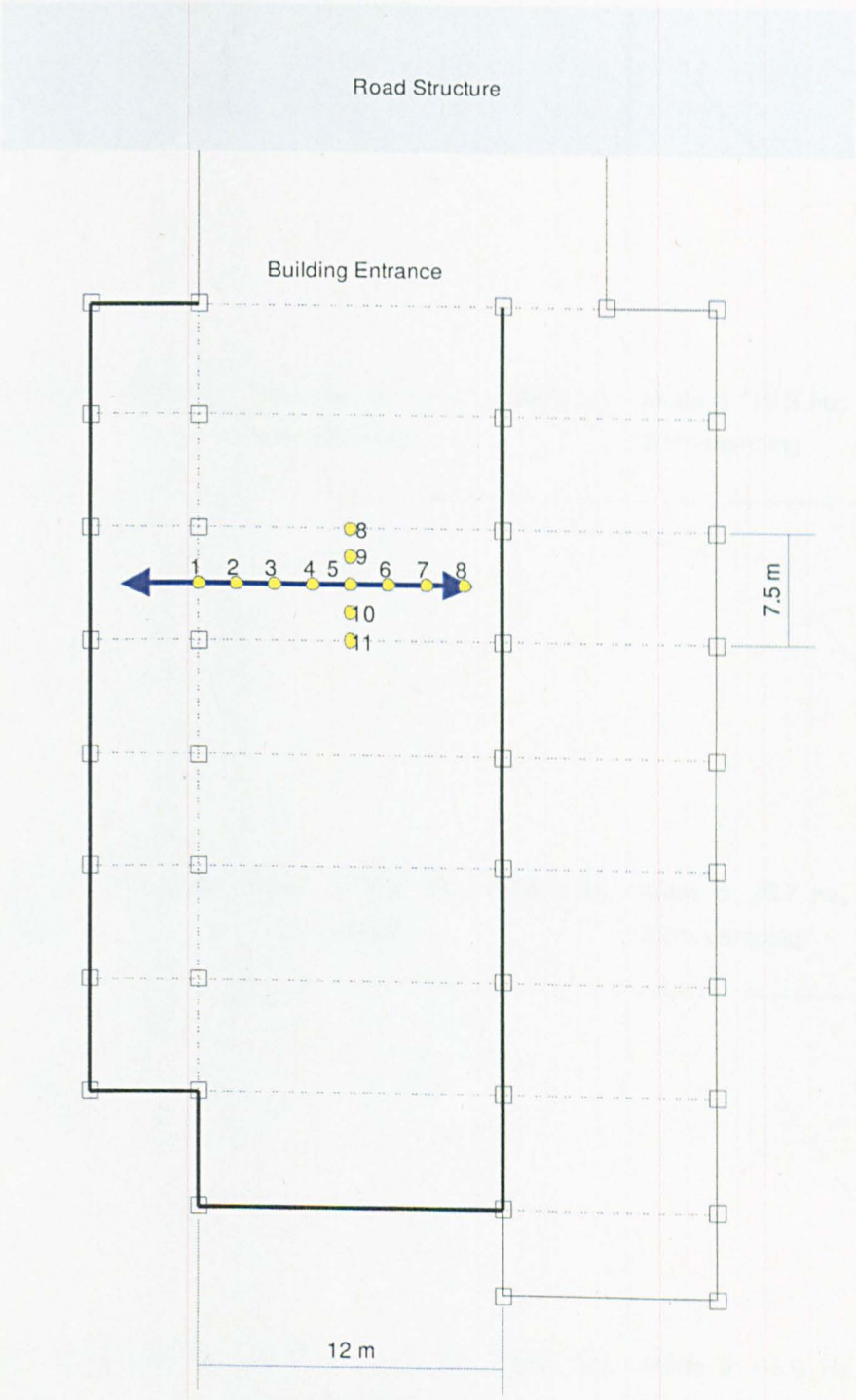

Figure 58 – Test points used for modal analysis; the thick black line represents the walls of the structure, the thin black lines the structures edge, the dotted lines represent beam lines (there are also beams along the other lines), the squares represent columns, the blue arrow represents the walking path and the yellow dots represent test points.

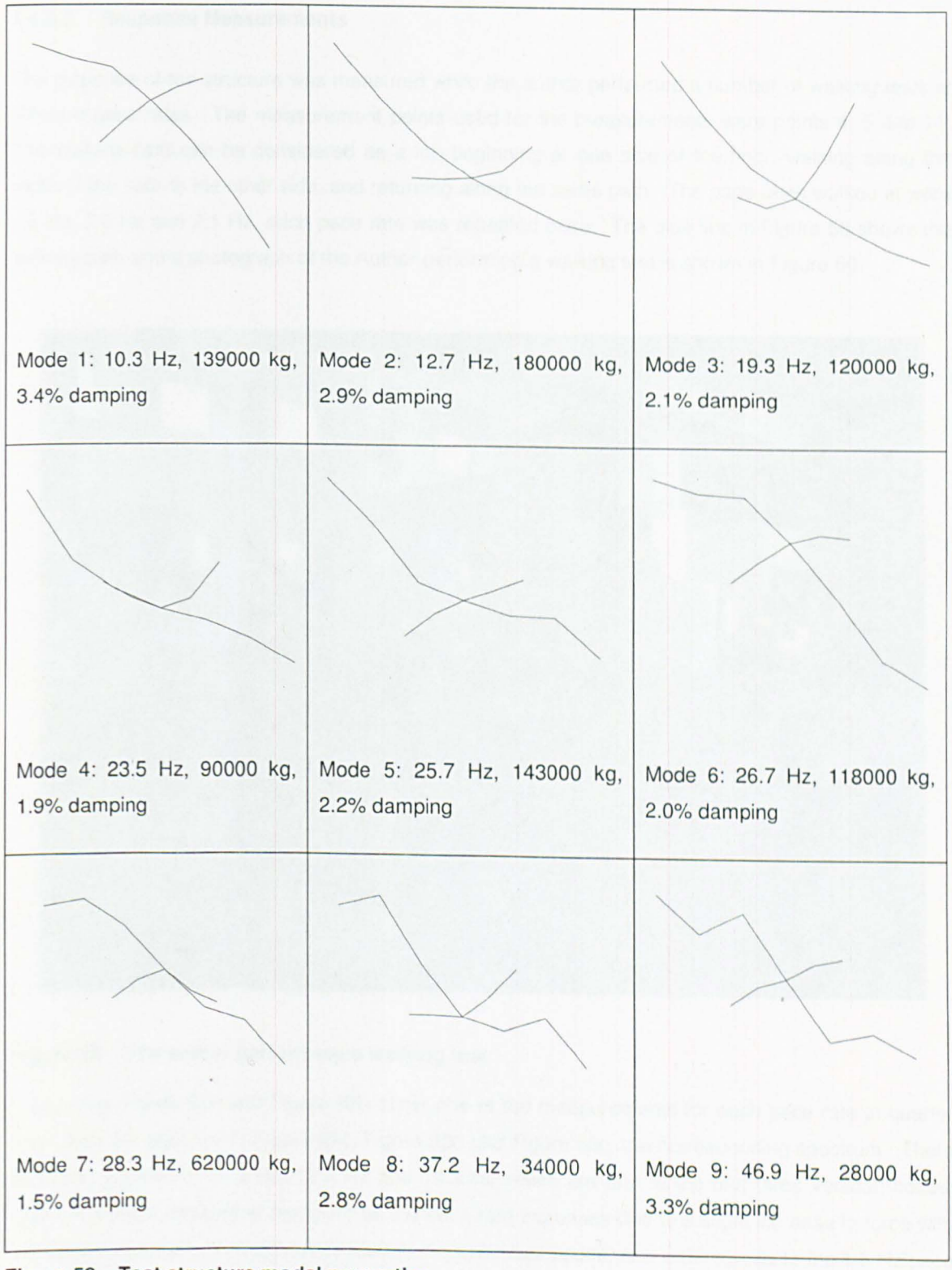

Figure 59 – Test structure modal properties

4.4.3.2 Response Measurements

The response of the structure was measured while the author performed a number of walking tests at different pace rates. The measurement points used for the measurements were points 4, 5 and 11. The walking path can be considered as a lap beginning at one side of the floor, walking along the width of the floor to the other side, and returning along the same path. The pace rates walked at were 1.8 Hz, 2.0 Hz and 2.1 Hz, each pace rate was repeated once. The blue line in Figure 58 shows the walking path and a photograph of the Author performing a walking test is shown in Figure 60.

Figure 60 – The author performing a walking test

Figure 61a, Figure 62a and Figure 63a show one of the measurements for each pace rate at quarter span, with the solid line in Figure 61c, Figure 62c and Figure 63c, the corresponding spectrum. There are clear maxima at 10.3 Hz, 12.7 Hz and 19.3 Hz which are due to the first three vertical modes. There is a slight increase in response as the pace rate increases due to a slight increase in force with increasing pace rate. It is difficult to identify the individual paces, and with regards to the 1.8 Hz pace rate, it is even difficult to identify the walking. To identify the footfalls, the reponses were filtered to remove high frequency noise. During the measurements, all practical measures were taken to reduce any external noise. However, it was an industrial unit on a large industrial complex, surrounding units were still in operation, creating un-measurable broadband noise, which is present in the measurements.

4.4.3.3 Response Estimation Using the Spline Force

The measured modal properties were used to estimate the response using the spline force. 100 different simulated force time histories were created at each pace rate. The number of paces for each pace rate was estimated with a relationship between the pace rate and speed of walking. The method of modal superposition was used in calculating the response. The force was scaled again by the magnitude of the mode shape at the response point as well as being modulated by the mode shapes along the walking path.

Figure 61b, Figure 62b and Figure 63b shows one of the responses of the 100 forces applied at each pace rate, with the dotted lines in Figure 61c, Figure 62c and Figure 63c, the maximum and minimum hold for all the spectra. The measured time histories have had a low pass filter applied to them at 35 Hz. The filtering was required due to the presence of broadband noise which made the footfalls indistinguishable. The broadband noise is clearly present in the spectrum, which is identified by a larger response in frequencies where there are no modes. The measured response is, in places, slightly larger than the upper bound estimated response. However, where this is the case, the extra response seems no larger than the response caused by the broadband noise.

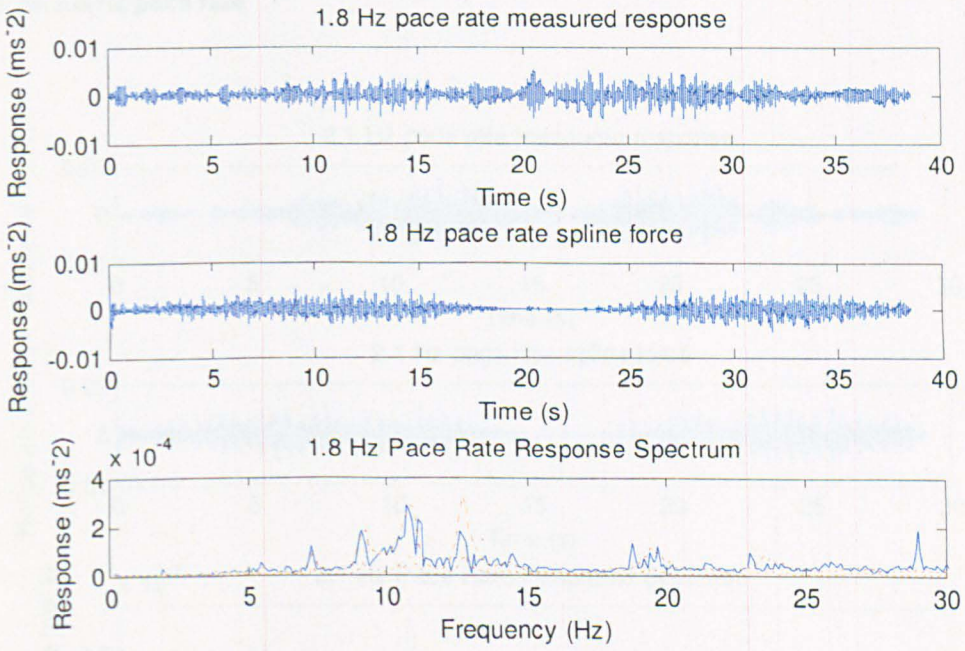

Figure 61 (from top to bottom) – a) test structure measured response, b) test structure spline force c) response spectrum (the red dots represent the response envelope form the spline force); all 1.8 Hz pace rate

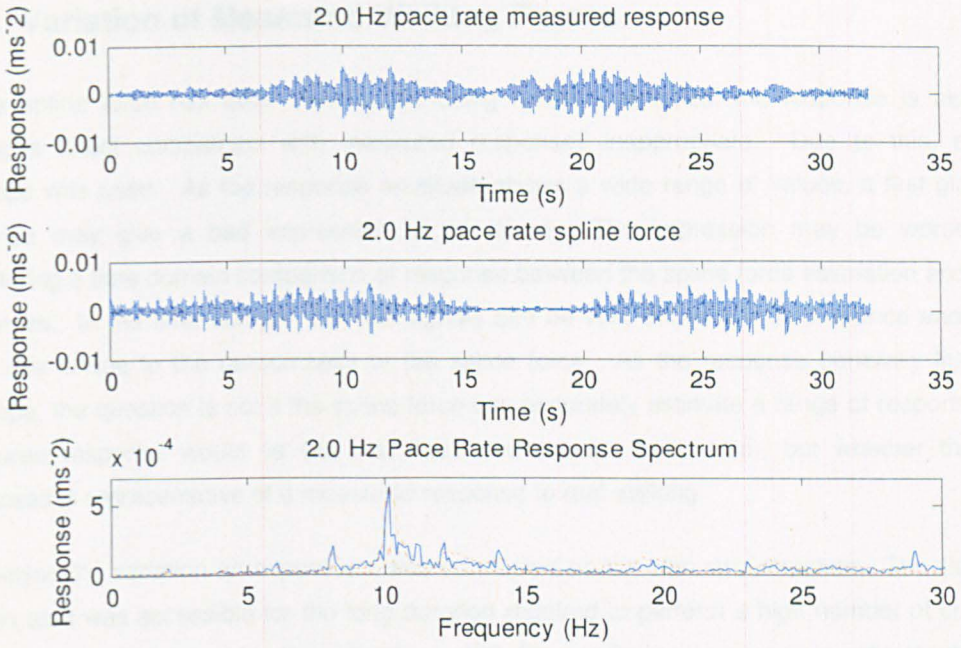

Figure 62 (from top to bottom) – a) test structure measured response, b) test structure spline force c) response spectrum (the red dots represent the response envelope form the spline force); all 2.0 Hz pace rate

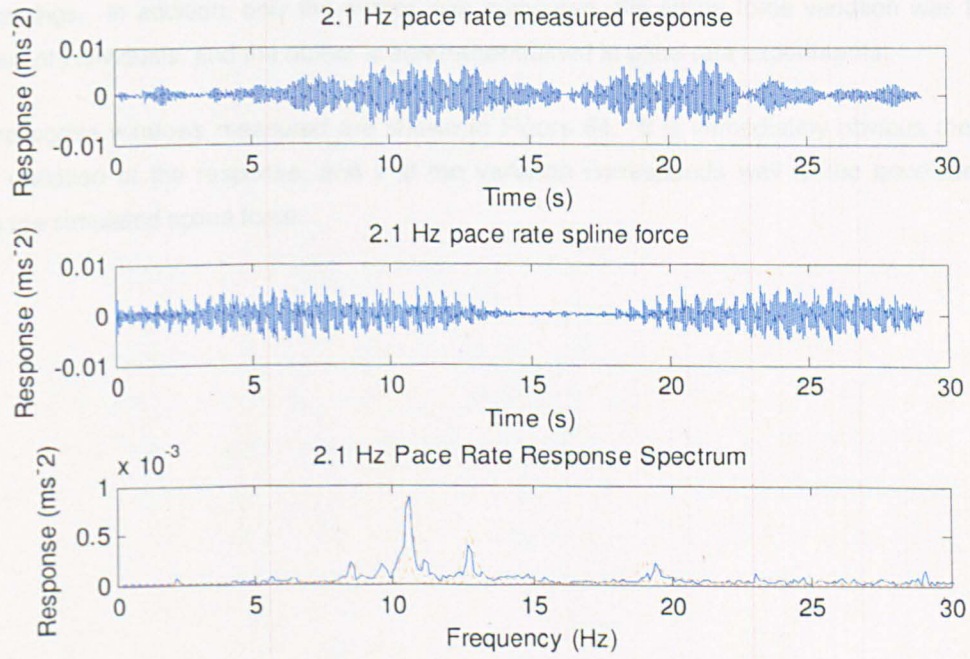

Figure 63 *(from top to bottom)* – a) test structure measured response, b) test structure spline force c) response spectrum (the red dots represent the response envelope form the spline force); all 2.1 Hz pace rate

4.4.4 Variation of Measured Walking Forces

As the spline force has been constructed using random variables, the response is also random, making a direct comparison with measured responses inappropriate. Due to this, a response envelope was used. As the response envelope shows a wide range of values, a first glance at the response may give a bad impression of the force. The impression may be worsened when considering a time domain comparison of response between the spline force estimation and measured responses. In the time domain, the two signals can be very different in appearance and amplitude, again this is due to the randomness of the spline force. As the response generally fits within the envelope, the question is not if the spline force can accurately estimate a range of responses within a measured response would lie (as that has been proven to be true), but whether the range of responses is representative of a measured response to real walking.

To analyse the variation an experiment was conducted on the slab strip structure. The slab strip was chosen as it was accessible for the long duration required to perform a high number of crossings. In the response estimation using the spline force 100 different forces were used to estimate the response window. If this were to be matched in reality the slab strip would need to be crossed 100 times at each pace rate used. This amount of walking was not practical, as such, less crossings were used. The slab was crossed approximately 30 times for each pace rate, which still accumulated almost 1 km of walking. The variation is likely to be less than the spline force in this case due to the lower number of crossings. In addition, only the author was measured, the spline force variation was based on a number of individuals, and the author is somewhat trained in pace-rate experiments.

The response windows measured are shown in Figure 64. It is immediately obvious that there is a large variation of the response, and that the variation corresponds well to the envelope estimated using the simulated spline force.

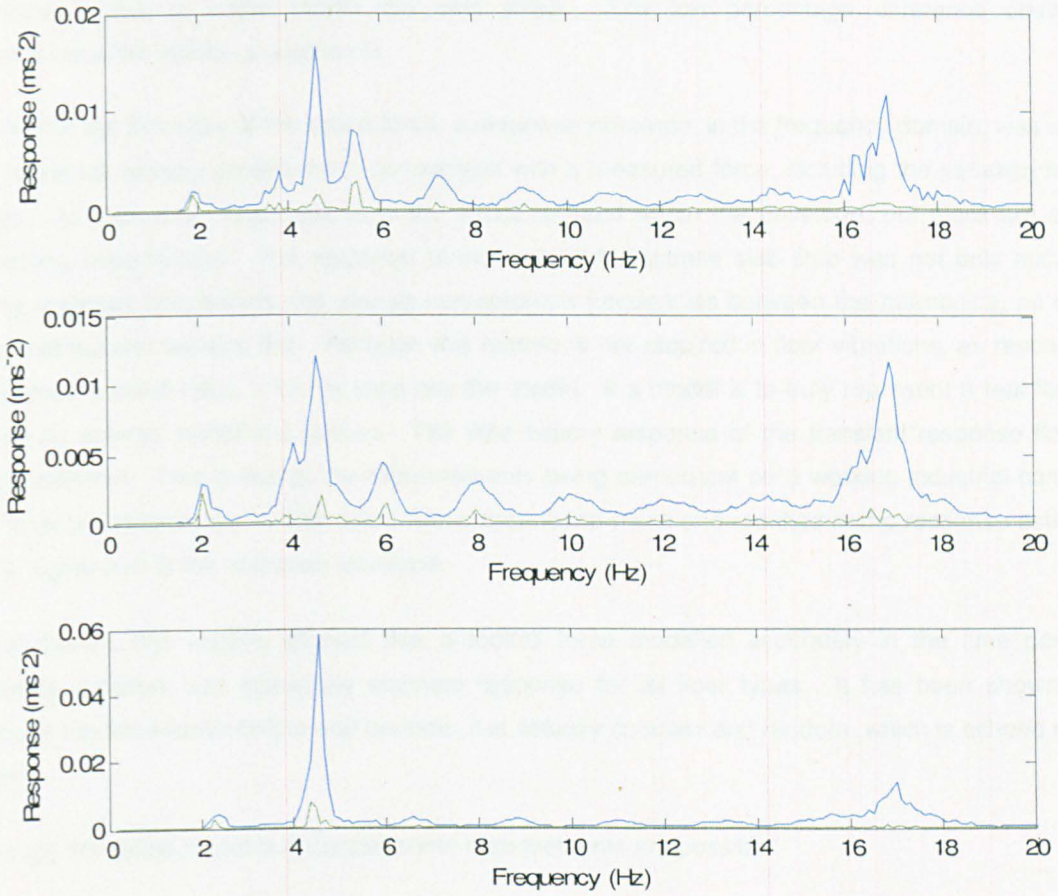

Figure 64 ***(from top to bottom)*** **– Measured response envelope for walking on the slab strip structure for 1.8 Hz, 2.0 Hz and 2.1 Hz pace rates**

4.5 Discussion and Conclusion

This chapter investigated the possibility of a universal footfall force model that is suitable for all floor types and analysis methods. A force model in the time domain was created by fitting a cubic spline through a number of important, statistically defined points on the footfall force. As the statistical properties of important points are known, each one can be obtained randomly, which introduced randomness into the model. The resulting model is in the time domain and visually looks like a measured footfall force.

To analyse the accuracy of the method a number of procedures were used. Firstly a walking time history for a individual footfall was modelled with its own unique spline fit (although the fit points remained constant). This was then used to construct a simulated force. The response spectra of the two forces were compared, using the same procedure used to analyse the existing methods in Chapter 3. The maximum percent difference was approximately 25%, less than any existing method. The difference could be considerably reduced if the location of the points was optimised for each

individual footfall to better model the heel strike. The low percentage difference observed demonstrates the validity of a spline fit.

To analyse the accuracy of the spline force, a response envelope, in the frequency domain, was used. The response window allowed for a comparison with a measured force, including the variation in the forces. All measured responses from the structure fitted within the envelope, but there are some interesting observations. The response of the resonant response slab strip was not only accurate during resonant frequencies, but also at non-resonant frequencies between the harmonics, no other force method can achieve this. Although this feature is not required in floor vibrations, as resonance would be the worst case, it further validates the model. If a model is to truly represent a real force it should be able to model this feature. The time history response of the transient response floor is clearly different. This is due to the measurements being carried out on a working industrial complex with a lot of external noise. This noise was a broadband noise and resulted in the response estimate at the higher end of the response envelope.

In conclusion, this section showed that a footfall force modelled accurately in the time domain, including variation, can accurately estimate response for all floor types. It has been shown that although the force looks simple and periodic, it is actually complex and random, which is echoed in the model.

Although the spline model is accurate, some improvements are possible:

1. The heel strike could be modelled more accurately. Currently the spline points that model it are fixed for all pace rates, which introduces a small error. A function of the location of the points could be correlated to the pace rate, which would improve the accuracy.

2. Different people have different walking characteristics. Although the person's weight is the main factor in the force produced, the small variation between individuals alter the frequency distribution of the force. To model this in detail, many models of different people would be required. The analysis would then consist of generating a certain number of random people, then applying a large number of simulated walking forces across the structure to form a response envelope. This method of analysis is very complex, with too many variables to list in a design guide and would be limited to software.

3. Complex correlation is not considered; i.e. correlation such as an uncharacteristic slow pace followed by an uncharacteristic fast pace, which in reality would cause a limp.

4. All distributions are considered to be normal; this is not strictly true, with data exhibiting a slight log normal distribution.

Although more complex than other methods, the spline method has been shown to be more accurate than all other published methods, and could still be presented in a design guide and programmed in a software code.

5 Modelling of Transient Response Floors

Although accurate forcing models of human walking have been the subject of much research, an accurate force is useless unless the structure can be modelled approximately to obtain accurate response estimates. Chapter 2.2.1.2 described how the current guidance [3, 5, 6, 17-19, 60, 106] estimates the dynamic properties of floors. The most popular method is to estimate modal parameters either to design the floor above a minimum frequency or to perform a response analysis using modal superposition.

Traditionally, serviceability problems in footbridges and floors caused by human walking were due to a build up of resonance [107-115]. As a result, much research has been focused on determining the fundamental natural frequency of the structure in an effort to minimise resonance [54, 56, 116, 117]. There was a basic knowledge that excessive floor vibrations could also be caused by a transient event, from a single footfall, which was designed against using a limit of static deflection. Static deflection seemed, in principle, to be a valid method of limiting transient response. However, as the static displacement could be reduced (and therefore the floor response apparently improved) by reducing the floor mass, the effect could be counterproductive. Two references highlight the issue which are studies conducted in 1962 by Lenzen [118] and in 1988 by Ohlsson [119]. Both studies dealt with floors that would not have a resonant response: the floors would respond in a transient manner. Lenzen explicitly states that problematic floors are due to "insufficient stiffness", i.e. deform too much in static loading. Ohlsson presents a method based on static stiffness, with a more rigorous analysis, using the contribution of modes up to 40 Hz in response estimation. In his method he states that increasing mass will increase response. He argues that this increases the static deformation and also decreases the fundamental modal frequency, which increases the number of modes below 40 Hz and therefore increases the response. Both these methods are flawed and, unfortunately, the lack of knowledge carried through to industry. Three reports from the same company (Branz) highlight further problems [120-122]. They produced a literature review in 1991 [120] followed by a report on heavy floors also in 1991 [121] and a report on lightweight timber floors in 1998 [122]. All but one of the floors, in both reports, have fundamental frequencies above 10 Hz so resonant response is not considered. The main point made in the literature review is that there is a harmonic and transient excitation from humans, and that the transient response is governed by modal mass, which contradicts Ohlsson [119]. The analysis for both floors then consists of determining the fundamental natural frequency, but with no mention of modal mass. Response estimation was then created using a harmonic excitation model, but transient excitation was not considered. Response measurements were also obtained from the real floors using heel drop tests and from a dropped mass, but not from walking. It is not clear why, although they were concerned with excessive vibration due to walking, walking was not measured. These examples illustrate that, not only was the force model not suitable, there was a lack of knowledge of how the floor would respond and its dynamic properties (due to not considering mass). Since these analyses were done, the general knowledge of floor vibration has improved, however mistakes are still being made.

Guidance for all types of floor vibration has generally been concerned with an accurate estimation of the fundamental natural frequency. The accuracy of the estimation of modal mass has been neglected as it was considered to be less influential for the floor response. In addition, it cannot be as accurately determined experimentally as frequency. When considering transient response floors modal mass can often be crucial parameter in response estimation, with the importance of frequency diminishing as the modal frequency increases [61]. Another issue is the response estimation of multi-bayed floors. Transient response floors (TRFs) commonly have many bays and the response reduces as a structure becomes larger. Current guidance cannot accurately determine how the dynamic properties vary as the number of bays varies.

This section investigates how to estimate accurately the dynamic properties of floors for estimating response from human walking. All structures, for any type of analysis, are simplified. The degree of abstraction is not important, whether it is a hand calculation or an FE model with thousands of DOFs, so long as the abstraction accurately represents the real structure. This section begins by investigating how the simplified analyses, in the current guidance, estimates TRFs response to walking. The most appropriate method is then analysed in further detail to see exactly where the inaccuracies lie. A large parametric study, with over 500 floors, was conducted to improve empirically the simplified guidance. From the results of the parametric study a method of equivalent modes was developed to estimate the response at the structures centre (i.e. the centre of the central bay of a multi-bayed structure). The parametric study was then used to consider modelling detail of multi-bayed floors: how the response changed with respect to the number of bays in the structure and how far the response of a footfall would 'travel', i.e. the decay with respect to distance. Due to the large size and computing time of multi-bayed floors, an investigation of modelling detail was conducted and a method of partial modelling of floors was developed. A second parametric study, with over 17000 configurations, was developed to investigate the importance of columns in floor response. A similar study of columns has been conducted in the past, but was only concerned with natural frequency [59]. Finally the procedure of estimating the transient response is investigated: modal superposition is compared to a full integration method. It is shown that for large multi-bayed floors many hundreds of modes can be obtained, which can be problematic. A method of mode participation is demonstrated, clearly showing that the total number of modes can be vastly reduced to a subset of fewer modes.

5.1 Evaluation of Current Design Guide Methods

There have been many different design guides published in the UK [3, 5, 17, 18, 106], and are used throughout the world, that help an engineer design for floor vibration. In the USA the AISC design guide [19] is widely used, even though it is out-dated. Chapter 2.3 discusses in detail how each relevant design guide estimated the dynamic properties of floor. The most recent design guides [5] [6] are similar in their recommendations on response estimation for TRFs:

- Use FEA, if possible, to estimate modal properties of the floor. Then, using an appropriate force model, estimate the response using modal superposition (this is not true for the AISC design guide which recommends using the kf method).

- If FEA is not possible, each design guide offers simplified analysis, suitable for hand calculations, to estimate response.

Simplified guidance is desirable for a number of reasons: it allows quick initial designs of structures in the tender stage when it is not cost effective to create many detailed designs, and it is useful for small low-key structures where an FEA would significantly increase the cost of design. Also, although structural dynamics can be a complex subject, due to a general lack of knowledge within the industry the design guides must be accessible to all. However, due to the complex nature of dynamic analyses, simplification introduces many inaccuracies and restricts the structural layout.

This section evaluates the SCI guidance and the Concrete Centre guidance and compares each method with finite element analysis. The section begins by examining how accurately each method estimates the modal properties of the structure (i.e. modal frequency, modal mass and mode shape). Response estimates are then calculated using each method and compared.

The method in which the simplified analyses, offered by the design guides, estimates modal properties is discussed. Although one guide is written for steel design and the other for concrete design they are still comparable. If the methods are based on first principles the material should be irrelevant, the calculation floor properties should be independent of material.

5.1.1 Estimation of Modal Properties

In accurately estimating the response of TRFs an understanding of how the dynamic properties affect the response is essential. The key point is that the response is significantly different when compared to a resonant response floor, as such, the dynamic properties that govern the response are also different. When concerned with a RRF, the response is governed by the mode of vibration that matches with a forcing harmonic from the walking force. This single mode of vibration generally governs the response. The magnitude of the force is frequency dependant: there is a large reduction in force with a relatively small increase in frequency. As such, the fundamental modal frequency often governs the design.

For example, if a hypothetical floor with a fundamental mode at 5 Hz, which would be excited by the third harmonic of the force, had an excessive response, a number of methods could be applied to reduce the response. If a 20% increase in mass is considered (which, with all other things including frequency were unchanged, reduce response by 20%) and it was then estimated that the modifications would reduce the fundamental frequency to 4.4 Hz the mode could now be excited by

the second harmonic of the force. The increase in force would be much larger than 20%, with a net effect of an increase in response.

When considering the response of a TRF the floor responds very differently. The frequency content of a footfall force has an inverse power law reduction with an increase in frequency. With a RRF a small change in frequency can result in a large change in force through switching harmonics. However, for a TRF, where the fundamental frequency is higher, the same change in frequency will result in a smaller change in force. Another effect is that within a specific frequency range there could be a number of modes. As for TRFs the effects of frequency differences in the modes would have a gradual change in force applied to them. As such all modes within a frequency range may have a similar force applied to them. Due to this, frequency as well as mass is equally as likely to govern the response and more modes will need to be considered in the analysis.

Due to the nature of a TRF, the prerequisites for an accurate assessment of floor response are:

- Multiple modes must be obtained - the fundamental modal properties are not enough to estimate the response.
- Accurate frequency estimates. The degree of accuracy can decrease as the modal frequencies increase.
- Accurate modal mass estimates.
- Accurate modal amplitude estimates.

Each method, and how the modal properties are estimated, was shown in detail in Chapter 2.3. As a reminder, each method evaluated here will have its methods repeated.

5.1.1.1 Modal Frequency Estimation

The SCI [6] recommend using total static displacement to evaluate the fundamental natural frequency:

$$f_0 \approx \frac{18}{\sqrt{\Delta}}$$ **Equation 55**

where Δ is the static deflection. They also suggest that the frequency of the floor can be made from its components frequencies using Dunkerly's method:

$$\frac{1}{f_0^2} \approx \frac{1}{f_1^2} + \frac{1}{f_2^2} + \cdots + \frac{1}{f_c^2}$$ **Equation 56**

where f_c are the component frequencies for $1 \leq n \leq t$ where t is the total number of components. This method can only estimate the fundamental frquency.

The Concrete Centre [5] use a plate abstraction to estimate natural frequencies:

$$f_n = \frac{\pi}{2W^2}\sqrt{\frac{j^4 D_x^2 + 2Hj^2k^2\left(\frac{W^2}{L^2}\right) + k^4 D_y\left(\frac{W^4}{L^4}\right)}{m}}$$ **Equation 57**

where D_x and D_y are the flexural stiffness of the plate in the x and y directions respectively, H is a parameter related to the flexural stiffness, W and L are the length and width of the slab respectively, m is the total mass of the slab and j and k are the number of half sine waves that make up the mode in the x and y directions respectively. This method allows estimations of the frequencies for the higher modes of vibrations and is accurate so long as the structure acts as a simply supported plate.

5.1.1.2 Modal Mass Estimation

The SCI guidance [6] uses empirically derived effective widths and lengths to estimate modal mass. The guidance has different formulae depending on which of their flooring systems is being designed, and is outlined in Table 3. The Concrete Centre guidance [5], analysing a floor as a simply supported plate, uses one quarter of the total floor mass.

5.1.1.3 Mode Shape Estimation

If FEA is not available, SCI guidance [6] conservatively recommends not to use mode shape scaling of the force and response. If one mode governs the response, as the SCI guidance assumes, this is a reasonable assumption. However, for TRFs more than one mode often significantly contributes to the response and assuming no mode shape scaling for each mode may introduce a significant error.

When considering TRFs, where multiple modes contribute to the response, assuming unit amplitude for all mode shape displacements will overestimate the response. In response to this the Concrete Centre guidance has offered a a formula based on the summation of sine waves to estimate the modal displacements [123]:

$$u_{j,k}(x,y) = sin\left(\frac{j\pi x}{W}\right) sin\left(\frac{k\pi y}{L}\right)$$ **Equation 58**

where W and L are the width and length of the slab respectively, x and y are the position on the slab in the x and y co-ordinates respectively and j and k represent the number of half sine waves that make up the mode shape in the x and y direction respectively.

5.1.2 Comparison of the Concrete Centre [5] and the SCI [6] methods

The methods presented by the Concrete Centre [5] and the SCI [6] will be compared with an FEA analysis of an imaginary, but representative, multi-bay floor structure. The AISC design guide [19] shall not be used as it is for TRFs is outdated. The modal properties obtained using the simplified guidance will be directly compared with modal properties estimated by FEA. For each method, the modal properties will be used in a walking response estimation to ascertain the importance of accurate modal properties. Brief descriptions of the key assumptions in the methodologies are described below:

Concrete Centre:

- The simplified guidance requires a uniform construction, i.e. all bays are of the same construction and size.
- The accuracy of using an equivalent flat slab reduces as the spacing between the slab down-stands increases.
- Only the slab is considered to affect the dynamic properties of the floor
- Modal superposition is recommended up to "twice the fundamental natural frequency".
- Modal mass is assumed to be one quarter of the total slab mass for each mode.
- Multiple natural frequencies are estimated using a plate equation.
- Response is estimated using the effective impulse

SCI

- The simplified guidance requires a uniform construction, i.e. all bays are of the same construction and size.
- The accuracy of using an equivalent flat slab reduced as the spacing between the slab down-stands increases.
- Only the slab is considered to affect the dynamic properties of the floor
- Modal mass is estimated using an effective width and length which is based on the size of the floor. There are two different modal mass equations depending on the floor type, with each mass is apparently adjusted to "include contributions from higher modes"
- The fundamental natural frequency is estimated from the static deflection of the floor. Only the fundamental mode can be estimated.
- The response is estimated using the effective impulse. However, the impulse has been modified, which results in a more conservative response.

FEA

- Any floor type can be modelled, to any degree of accuracy.
- The whole structure can be considered, with other parts of the structure contributing to the dynamic properties of the floor.
- Modal superposition can easily be used with any frequency range.

- Modal properties are estimated from an eigen-value solution, the accuracy of which is dependent on accurate modelling of the structure.
- The response is estimated using the effective impulse described in the Concrete Centre guide

Due to the fact the simplified methods require a simple uniform structure for an accurate estimation of modal properties a very simple structure is used. The structure is based on a real structure with experimentally determined properties. The floor slab and column details are the same as the real structure but the bay layout has been simplified. The FE model is assumed to be a reasonable approximation of the real structure due to similarities in the fundamental natural frequency. The test structure is shown in Figure 65. The structure consists of 10x1, 5.4m square bays of a waffle style construction. For the simplified analyses, the waffle ribs are closely spaced and are therefore suitable for an approximation using an equivalent slab. The distributed stiffness of the uniform slab in this case would be uniform and isotropic. For the FEA, the slab, including the waffle down-stands, were modelled using shell elements. The floor is very stiff, with a fundamental modal frequency above 25 Hz.

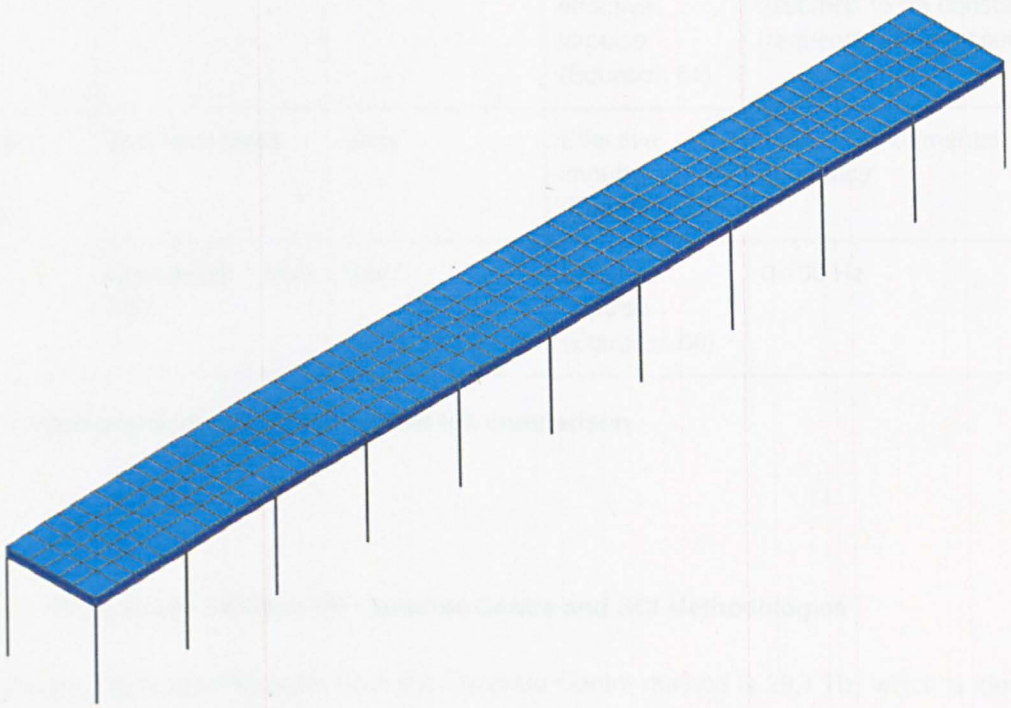

Figure 65 – 10x1 bays waffle style structure: FE model

Due to the SCI method only estimating modal properties for the fundamental mode, the response of that mode shall be considered constant for all frequencies of the response spectrum. Estimation of modal amplitudes is impossible without a FEA, excluding the Concrete Centre method. Due to this mode shapes shall be ignored and no mode shape scaling of the force or response is carried out. There is a small difference in analysis between the FEA and the simplified methods: the FEA includes columns, and a frequency range up to 100 Hz shall be considered for the FEA.

As a reminder from Chapter 2, the formula for the effective impulse in the Concrete Centre guidance is:

$$I_{eff} = 54 f_p^{1.43} / f_n^{1.3}$$ **Equation 59**

and the simplified SCI version is:

$$I_{eff} = \frac{190}{f_n^{1.3}}$$ **Equation 60**

A summary of the assumptions and values used in this analysis is presented in Table 7.

	Modal mass	Modal amplitude	Force	Bandwidth
SCI guidance	Table 3	Unity	Simplified effective impulse (Equation 61)	Single mode (response will assumed to be constant for all frequencies in the spectrum)
Concrete Centre Guidance	0.25 floor mass	Unity	Effective impulse (Equation 60)	Twice fundamental natural frequency
FEA	Calculated from FEA	Unity	Effective impulse (Equation 60)	0-100 Hz

Table 7 - Summary of assumptions used in the comparison

5.1.2.1 Comparison between the Concrete Centre and SCI Methodologies

The fundamental modal frequency from the Concrete Centre method is 29.1 Hz, which is identical to the value from the SCI method. As the displacement of the slab was estimated from a Navier's solution to the differential equation describing the plate dynamics [123], both methods are now essentially based on the plate equation the frequency would be expected to be similar. If there were beams between the columns the estimation from each method would likely be different.

The modal mass for each mode estimated by the Concrete Centre method is 123,900 kg. Using the SCI method both deck types were used: the modal masses for the shallow and deep deck are 102,900 and 150,100 kg respectively. The mass estimated by the Concrete Centre method is approximately the mean of the two SCI values.

Figure 66 shows the RMS velocity response using the Concrete Centre and SCI methods, the frequency range is set at twice the fundamental natural frequency. Due to the assumptions made, the SCI response is constant over all frequencies, which clearly overestimates the response. The assumption clearly over-estimates the response at higher frequencies. However, the response could be allowed to reduce with increasing frequency, as the effective impulse is a function of frequency. The response using the Concrete Centre reduces asymptotically with increasing frequency. This is due to the variation of the forcing function of the effective impulse also reducing asymptotically with increasing frequency. As there is no change in mass the response is a function of the frequency, via the effective impulse.

When comparing the maximum response of each method, the fundamental mode has the highest response. Although the frequencies are equal, and the modal mass is similar, it may be expected that each method may have similar responses. It must be clarified that the SCI method has modified the effective impulse, which increases the response estimation. In this case the difference in response is considerable.

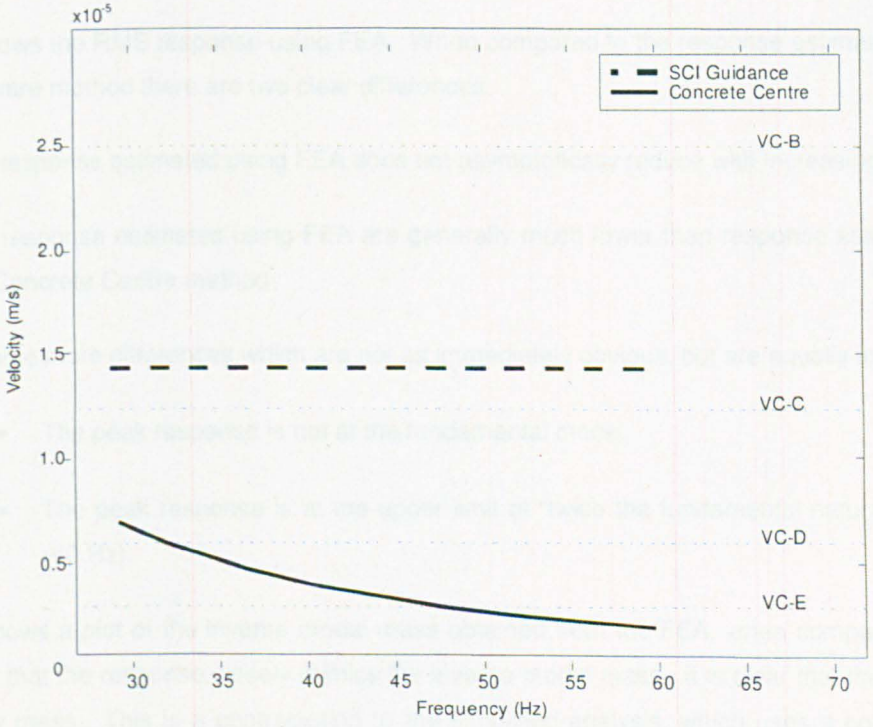

Figure 66 – Peak RMS velocity response of the floor for each mode using the Concrete Centre and SCI's methods

5.1.2.2 Comparison between the Concrete Centre Method and FEA

Table 8 shows a comparison of the modal masses and modal frequencies for all modes up to twice the fundamental natural frequency. The correlation of modal frequencies is good, there is a slight over-estimation using the Concrete Centre method but this would only cause a negligible change in

force. The modal mass estimates are clearly very different, with values estimated using the Concrete Centre guidance are less than half the estimates from the FEA.

Frequency (Hz)		Modal Mass (Kg)	
FEA	Concrete Centre	FEA	Concrete Centre
27.1	29.1	409000	124000
27.4	29.3	297000	124000
27.7	30.0	277000	124000
28.4	30.8	265000	124000
29.3	32.0	295000	124000
29.4	33.8	475000	124000
30.5	36.3	340000	124000
32.0	39.5	287000	124000
33.9	43.4	283000	124000
36.0	48.1	276000	124000
37.9	53.6	259000	124000
53.4	59.9	54000	124000
53.9		45000	

Table 8 – Comparison of modal properties estimated using the Concrete Centre method and FEA

Figure 67 shows the RMS response using FEA. When compared to the response estimated using the Concrete Centre method there are two clear differences.

1. The response estimated using FEA does not asymptotically reduce with increasing frequency.
2. The response estimates using FEA are generally much lower than response estimates using the Concrete Centre method.

There are some more differences which are not as immediately obvious, but are equally important:

- The peak response is not at the fundamental mode.
- The peak response is at the upper limit of "twice the fundamental natural frequency" (60 Hz).

Figure 68 shows a plot of the inverse modal mass obtained from the FEA, when compared to Figure 67 it is clear that the response closely mimics the inverse modal mass. It is clear that the response is governed by mass. This is a contradiction to the simplified analysis, which uses a constant modal mass (i.e. quarter of the total floor mass), and therefore variations in force can only change the response, which is governed by frequency. At high frequencies the change in force with an increase in frequency is small. Figure 66 shows that doubling the frequency (from 30 Hz to 60 Hz) approximately halved the force. However, as a footfall can be considered as an impulse for a TRF the velocity response is governed by:

$$V = I/m$$ **Equation 61**

where I is the value of the impulse and m is modal mass. It is clear from Equation 61 that the response is directly related to the modal mass. This explains why the FEA response plot is more erratic then the Concrete Centre response plot, and why the response is generally lower.

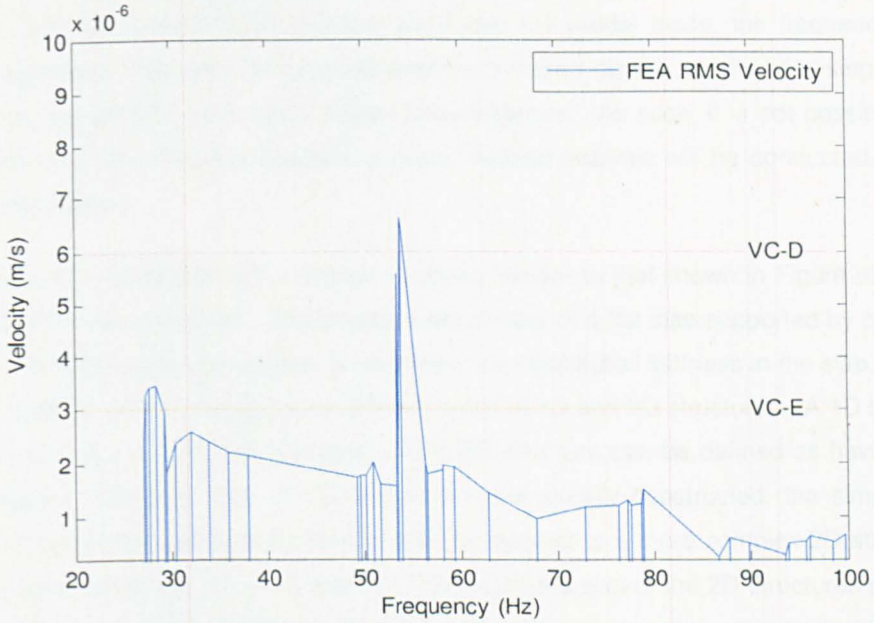

Figure 67 – RMS response of the floor using FEA with the vertical lines representing each RMS modal response

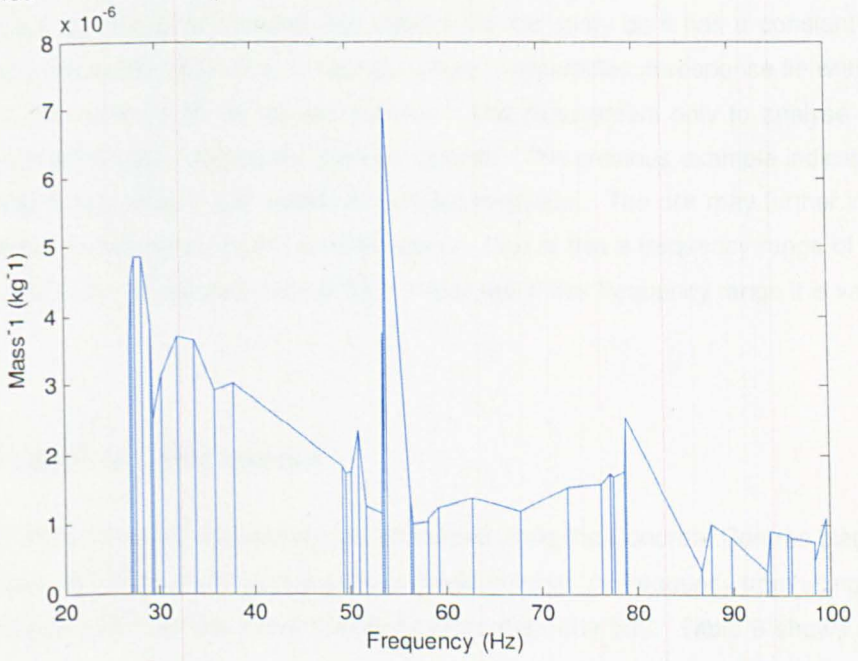

Figure 68 – Inverse modal mass from the FEA with the vertical lines representing each inverse modal mass

5.1.3 Detailed Investigation of the Concrete Centre Method [5]

It has been shown that TRFs require analysis of multiple modes of vibration for accurate response estimation. As only the Concrete Centre method can do this, it shall be investigated in more detail Although the Concrete Centre method poorly estimates the modal mass, the frequency estimates seem to be accurate. However, these conclusions are based on the results of a single test floor. Often, methods can perform well under certain circumstances. As such, it is not possible to form a general opinion from the previous analysis, a more detailed analysis will be conducted to ascertain any further inaccuracies.

A new test structure will be defined, a simple structure, similar to that shown in Figure 65, which is a typical application of the guidance. The structure will consist of a flat slab supported by columns, with no ribs, which removes inaccuracies due to assuming any distributed stiffness in the slab. The size of the structure shall be varied, investigating different sizes of 1D and 2D structures. A 1D structure can be defined by having 1 x n bay configuration and a 2D structure can be defined as having an m x n bay configuration. Although large 1D structures are not usually constructed, the simplicity allows identification of floor characteristics which can then be applied to a more complex 2D structure. The size of 1D structures shall be: 1x1, 1x3 and 1x11 bays and the size of the 2D structures shall be: 1x1, 3x3 and 11x11 bays. Each structure will have the natural frequency estimated, comparing the accuracy against FEA. The response of the structure to an impulse will also be investigated, including mode shape scaling. A perfect impulse was chosen for the study as it has a constant force over a frequency range and is therefore ideal to identify where inaccuracies in response lie without the need to worry about the accuracy of the forcing function. The requirement only to analyse modes up to twice the fundamental natural frequency shall be ignored. The previous example indicated that a low mass mode above this range might exhibit the largest response. The risk may further increase if the structure does not have such a simple, uniform layout. Due to this a frequency range of 0-100 Hz will be assumed, which, as the relevant criteria [8] is presented in this frequency range it is valid.

5.1.3.1 Multi-Bay Frequency Analysis

The 1D and 2D floor's natural frequencies are estimated using the Concrete Centres plate equation up to 100 Hz. Figure 69 to Figure 72 shows plots of mode number vs. frequency from using the Concrete Centres method and FEA for the floors that have more than one bay. Table 9 shows a summary of the results.

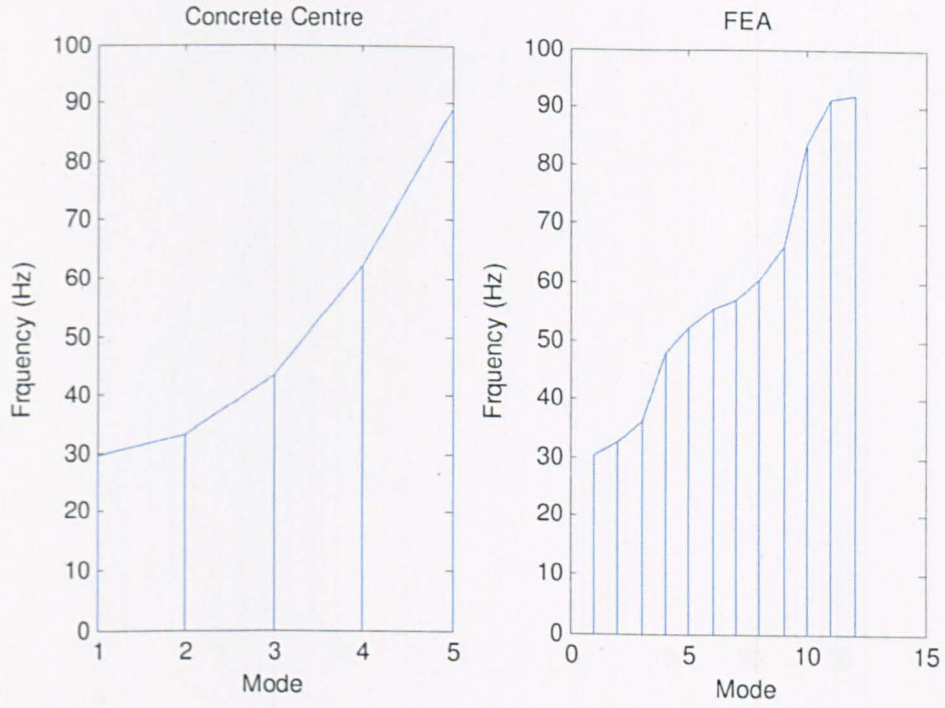

Figure 69 (*From left to right*) – Frequency Vs mode, Concrete Centre guidance and using FEA (1x3 bays) with the vertical lines representing each mode

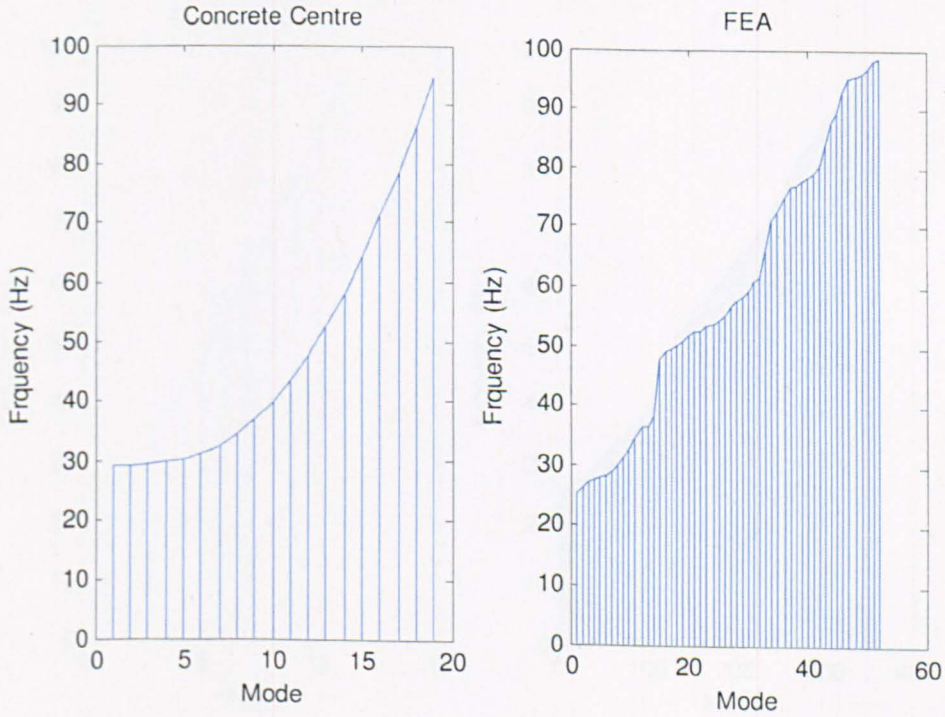

Figure 70 (*From left to right*) – Frequency Vs mode, Concrete Centre guidance and using FEA (1x11 bays) with the vertical lines representing each mode

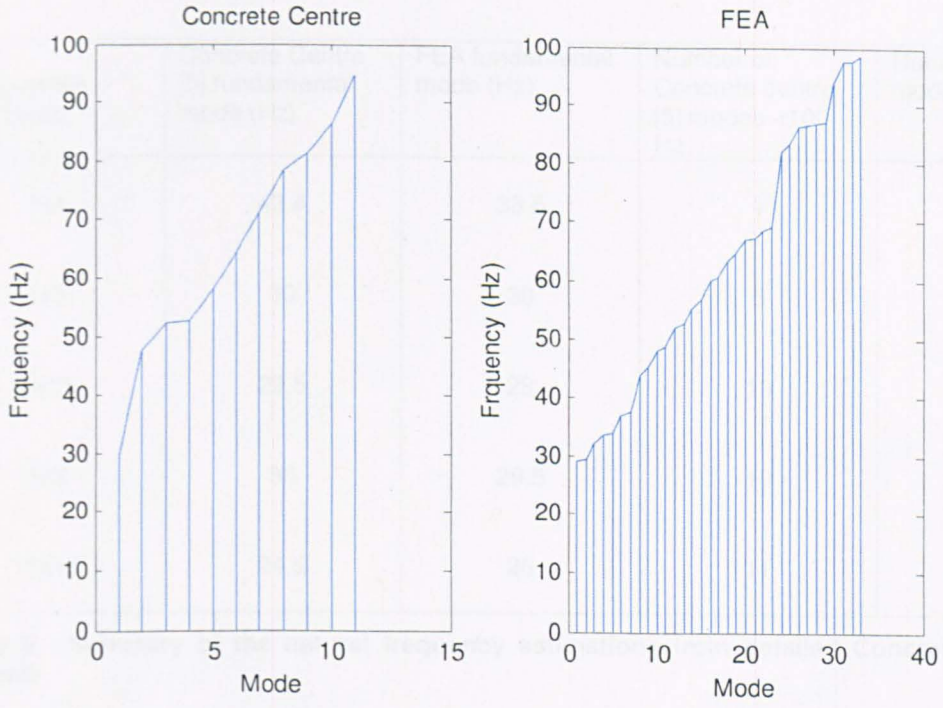

Figure 71 (*From left to right*) – Frequency Vs mode, Concrete Centre guidance and using FEA (3x3 bays) with the vertical lines representing each mode

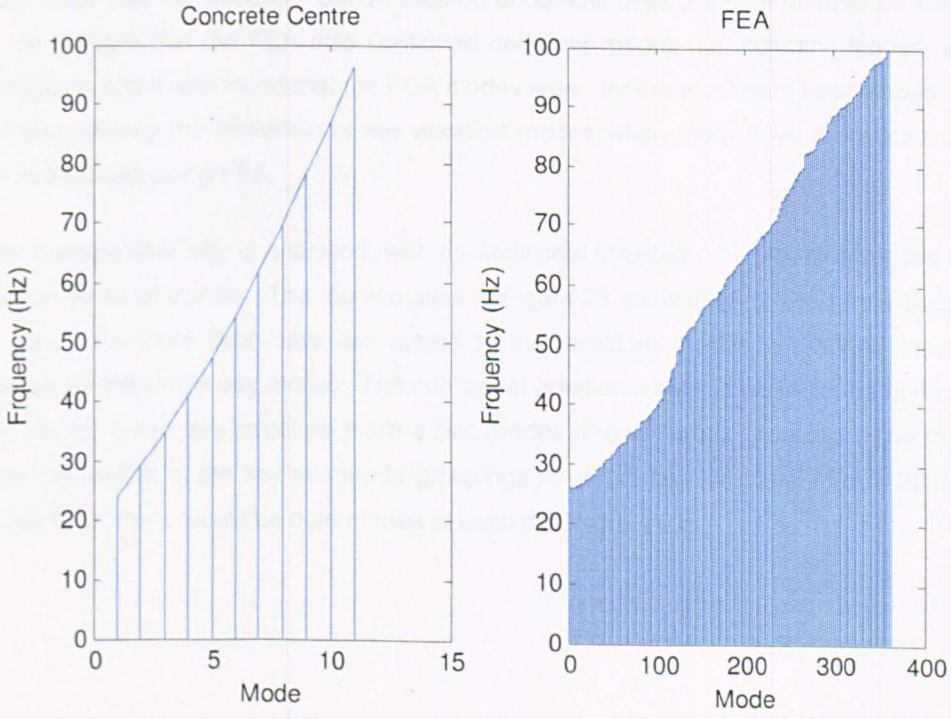

Figure 72 (*From left to right*) – Frequency Vs mode, Concrete Centre guidance and using FEA (11x11 bays) with the vertical lines representing each mode

Floor configuration (mxn bays)	Concrete Centre [5] fundamental mode (Hz)	FEA fundamental mode (Hz)	Number of Concrete centre [5] modes <100 Hz	Number of FEA modes <100 Hz
1x1	43.4	33.5	1	5
1x3	30	30	5	12
1x11	29.5	28	19	51
3x3	30	29.5	10	32
11x11	24.5	26	11	362

Table 9 - Summary of the natural frequency estimations from detailed Concrete Centre [5] analysis

From Table 9 it is possible to see that for a single bay the Concrete Centre does not estimate the fundamental mode well, overestimating the frequency considerably. For all the other configurations the fundamental mode was estimated reasonably well. However, Table 9 and Figure 69 to Figure 72 clearly show that the Concrete Centre method underestimates the total number of modes. Initially, it may be thought that the FEA also contained non-floor modes, i.e. columns modes, etc.. This was investigated and it was found that the FEA modes were, for the most part, floor modes. Due to such a large discrepancy the formation of the vibration modes when more bays are added to the structure was investigated using FEA.

When a single floor bay is analysed, with no additional structure, the vibration modes of the floor are similar to those of a plate. The top two plots in Figure 73 show the first two mode shapes for a single bay floor. As more floor bays are added to the structure modes are added around the modes identified by the single bay model. The number of additional bays is equal to the number of additional bays, i.e. for a 1x5 bay structure there a five modes at each mode grouping. The rest of Figure 73 shows the modes of the first two mode groupings for a 1x5 bay structure. For a 2D floor, such as a 3x3 bay floor, there would be nine modes at each mode grouping.

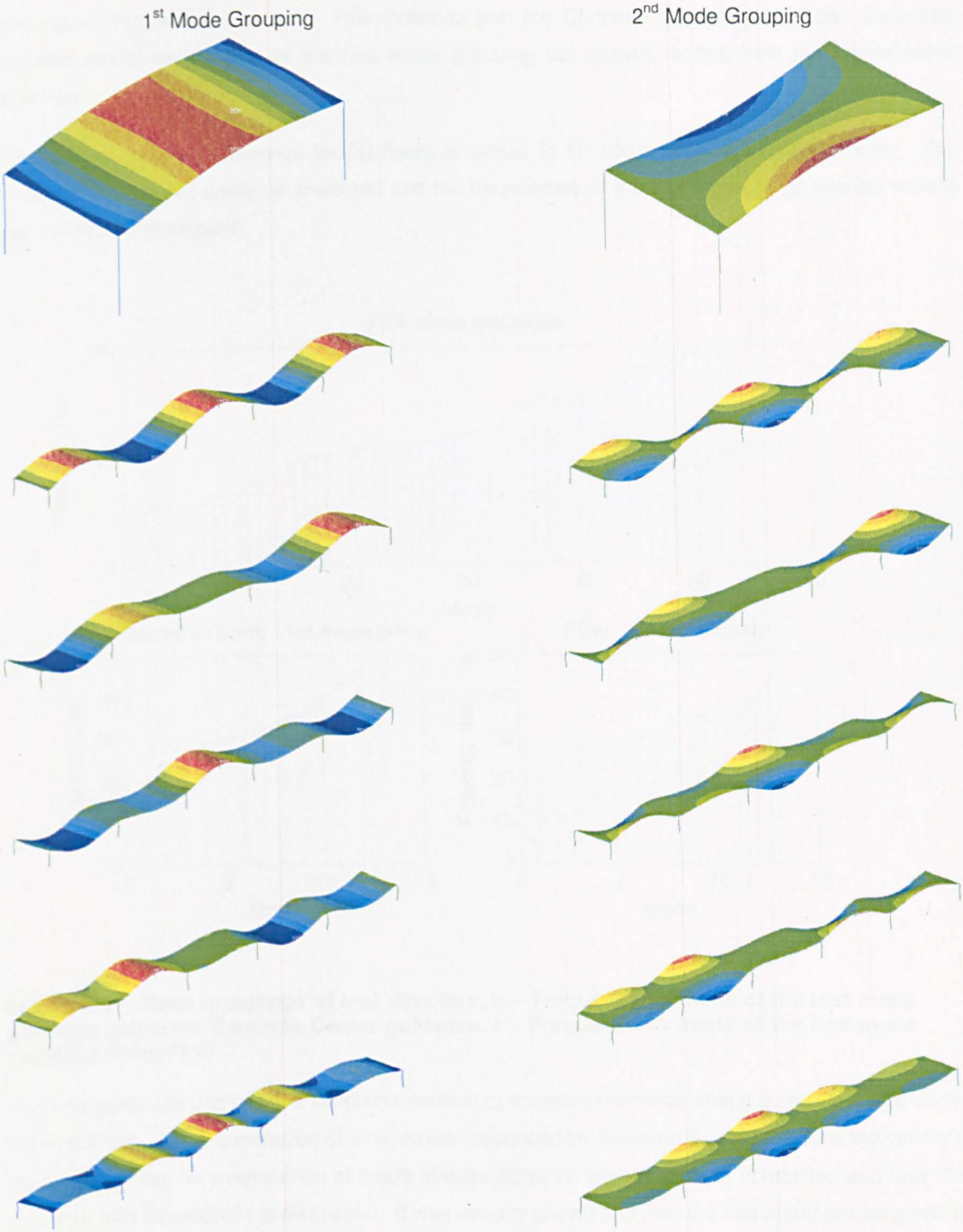

Figure 73 – First and second mode groupings for a 1x5 bay structure; from top to bottom: single bay mode, 5 modes of the first two mode groupings

Figure 74a shows a plot of modes vs. frequency from FEA of a 1D structure with the mode groupings clearly defined. Between each mode group there is a clear jump in frequency. Figure 74c shows a plot of modes vs. frequency from the same FEA but just for the first mode grouping. Figure 74b shows a plot of modes vs. frequency from using the Concrete Centre method. When compared, Figure 74b

and Figure 74c are very similar. This indicates that the Concrete Centre method can accurately estimate modal frequencies of the first mode grouping but misses modes from the higher mode groupings.

The process of mode groupings for 2D floors is similar to 1D floors but much more complex. The mode shapes cannot easily be predicted and the frequencies of the mode groupings overlap making them difficult to distinguish.

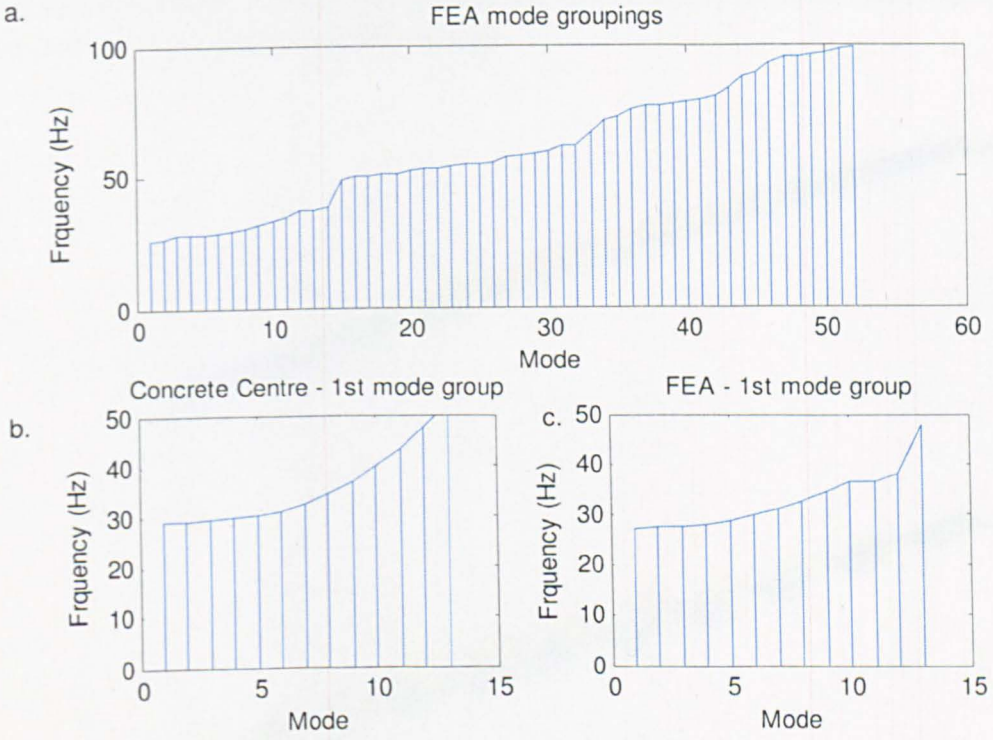

Figure 74a – Mode groupings of test structure, b – Frequency Vs mode of the first mode grouping using the Concrete Centre guidance, c - Frequency Vs mode of the first mode grouping using FEA

The only guidance that offers a simplified method to estimate the mode shape is the Concrete Centre method which uses a summation of sine waves, described by Equation 51. To examine the validity of the simplification, an examination of mode shapes obtained using FEA was conducted and how they compare with Equation 51 is discussed. It was already shown that only the first mode grouping can be estimated using the Concrete Centre method and, as such, only the first mode grouping shall be considered. A 21x1 bay structure was considered, the structure is unusually long and thin, but a long simple structure illustrates the behaviour and trend of multi-bay floors, more clearly then less bays, and can then be applied to any bay configuration. Figure 75(top) shows the first mode shape of the first mode grouping. The simplified method would estimate this mode as a half-sine wave acting over the entire floor area matching the FEA well. Figure 75(bottom) shows the last mode of the first mode grouping. The simplified method, in this case, would estimate the mode as 21 half-sine waves, over

the entire floor area, each having amplitude of 1. This correlates reasonable well with the FEA, however, the amplitudes of each half-sine are not 1. It appears as if the shape of the mode has been superimposed on a half-sine spanning the entire structure. This trend continues with the second mode grouping of this structure, with each mode superimposed over a full sine wave spanning the whole structure. This would cause an overestimation of response over a large area of the structure when using the simplified method with the response only being accurate in the centre for the first mode, quarter points for the second mode and so on. It may be noticed that in Figure 75 there is some significant column flexure. Note that this model is based on a real measured structure with sensible proportions. In reality the columns are likely to deform as shown, however, the structure is very stiff so the magnitude would be very low.

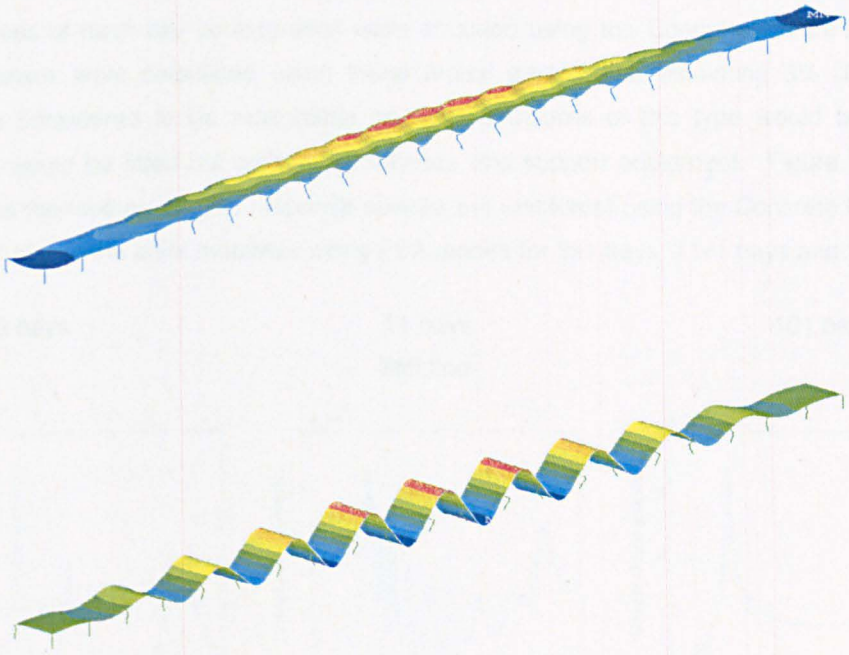

Figure 75 ***(from top to bottom)*** **- Mode shapes of a 21x1 bay structure: first mode shape of the first mode grouping; last mode shape of the first mode grouping**

5.1.3.2 Multi-Bay Impulse Response Estimation

To examine the various inaccuracies that the Concrete Centre's simplified method introduces into modal parameter estimation and how the number of bays affects the response of a floor, response to an impulse shall be considered for a number of test structures. An impulse is used as an excitation as it contains an equal level of force for the considered frequency range. This results in a lack of bias, with all modes having an equal excitation, which will allow for a clear identification of any errors and their magnitude. An impulse is also very simple and therefore will remove any complication due to inaccuracies resulting in choosing a force model.

Two simple TRF structures shall be examined: a 'soft' and 'stiff' structure, with fundamental natural frequencies at approximately 8 Hz and 22 Hz respectively. In reality a floor of 8 Hz is likely to have maximum response due to resonance. However, any conclusions made using this structure are valid for TRFs due to the impulsive excitation. The structure consists of a flat slab supported by columns and is therefore the simplest structure possible. The stiffness of the structure was varied by increasing the length of the bay in the long structural direction. The stiff floor is a 5x5 m configuration and the soft floor is a 10x5 m configuration. The structures considered will be 3x1 bays, 11x1 bays and 101x1 bays. The very largest structures are unlikely to exist in reality, but they serve a purpose in estimating the response of an infinite length structure for comparisons. Incidentally, in the authors experience number of rare structures do exist approaching 100 bays in size, but due to bays extending in x and y spatial directions.

Modal properties of each bay configuration were obtained using the Concrete Centre's method and FEA. Responses were calculated using these modal parameters, assuming 3% damping. 3% damping was considered to be reasonable as most structures of this type would be made from concrete and would be fitted out with many services and support equipment. Figure 76 shows the point mobilities (defined as velocity response spectra per unit force) using the Concrete Centre modes and Figure 77 shows the point mobilities using FEA modes for 3x1 bays, 11x1 bays and 101x1 bays.

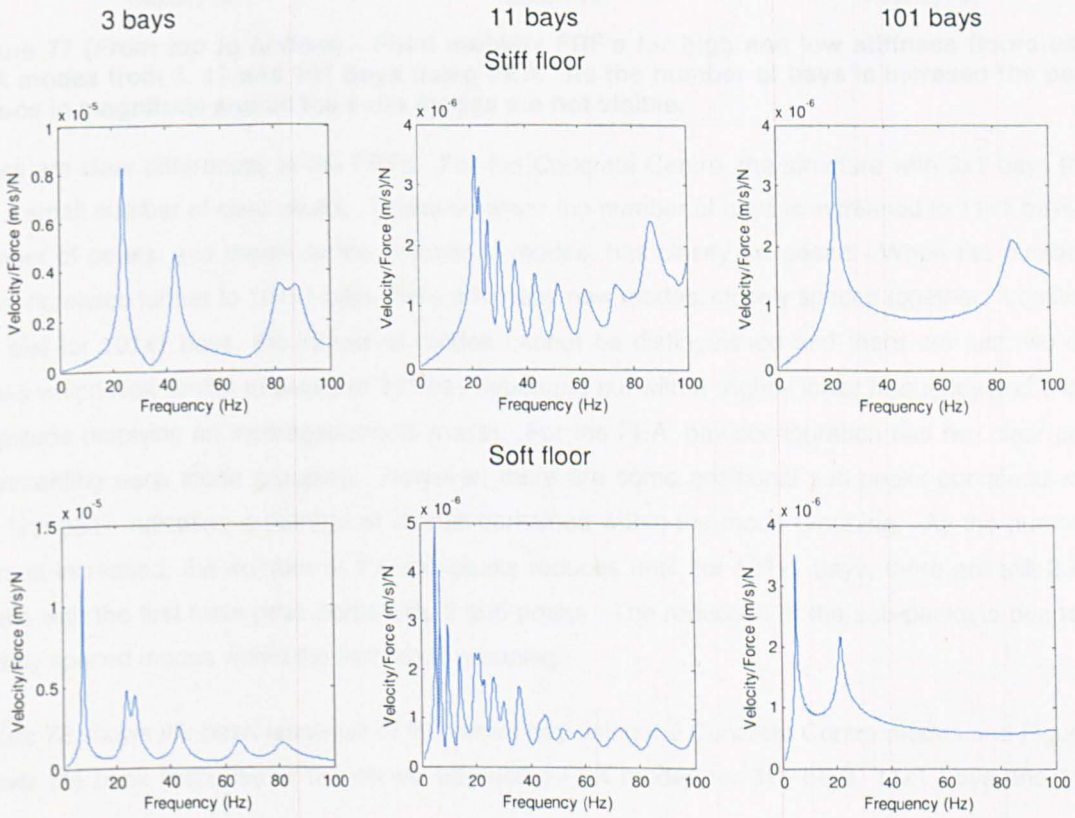

Figure 76 (*From top to bottom*) - Point mobility FRF's for stiff (top) and soft (bottom) floors using Concrete Centre modes from 3, 11 and 101 bays using the Concrete Centre's method. As the number of bays is incresed the peaks reduce in magnitude. At 101 bays, all the extra modes are not visible.

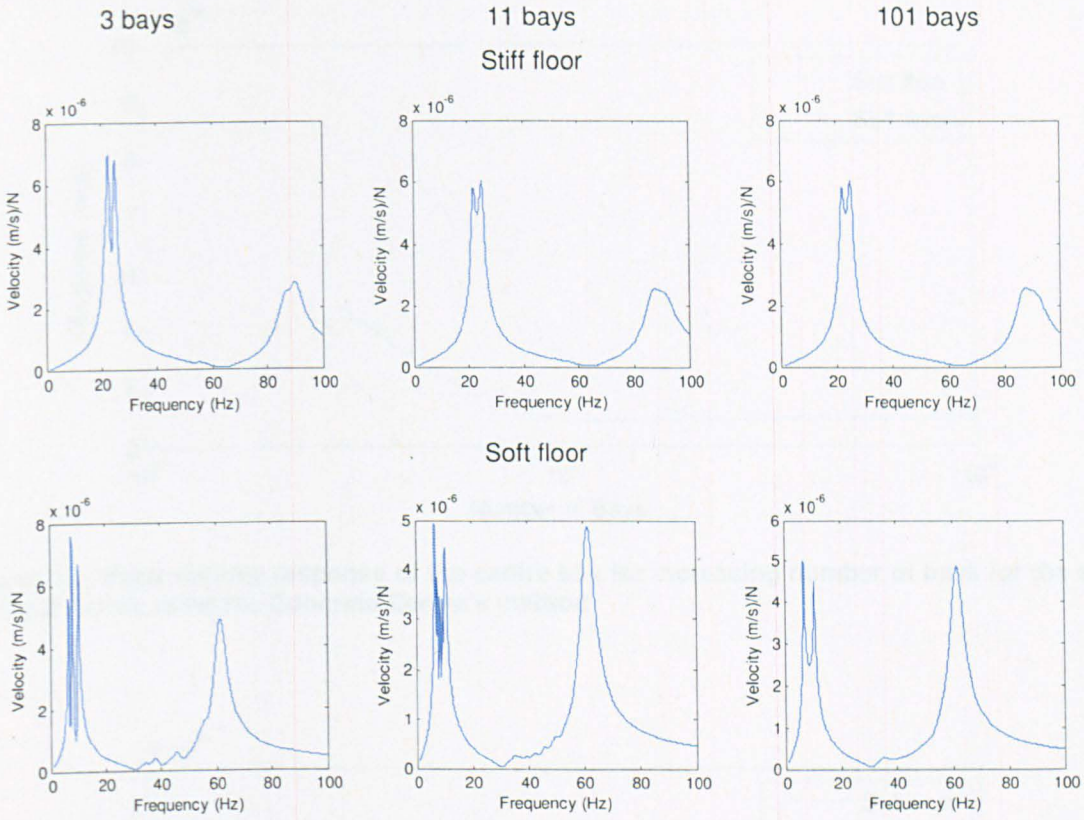

Figure 77 (*From top to bottom*) - Point mobility FRF's for high and low stiffness floors using FEA modes from 3, 11 and 101 bays using FEA. As the number of bays is incresed the peaks reduce in magnitude and all the extra modes are not visible.

There are clear differences in the FRFs. For the Concrete Centre, the structure with 3x1 bays there are a small number of clear peaks. However, when the number of bays is increased to 11x1 bays the number of peaks, and therefore the number of modes, has clearly increased. When the number of bays increases further to 101x1 bays there are many new modes, closely spaced together. Looking at the plot for 101x1 bays, the individual modes cannot be distinguished and there are just two clear peaks which look similar to peaks of 3x1 bay structures but with a slightly lower frequency and a lower amplitude (implying an increased modal mass). For the FEA, bay configuration has two clear peaks representing each mode grouping. However, there are some additional sub-peaks contained within the first peak indicating a number of modes contained within the mode grouping. As the number of bays is increased, the number of the sub-peaks reduces until, for 101x1 bays, there are still 2 main peaks with the first main peak containing 2 sub-peaks. The reduction of the sub-peaks is due to the closely spaced modes within the first mode grouping.

Figure 78 shows the peak response of the centre bay using the Concrete Centre modes and Figure 79 shows the peak response of the centre bay using FEA modes for 3x1 bays, 11x1 bays and 101x1 bays.

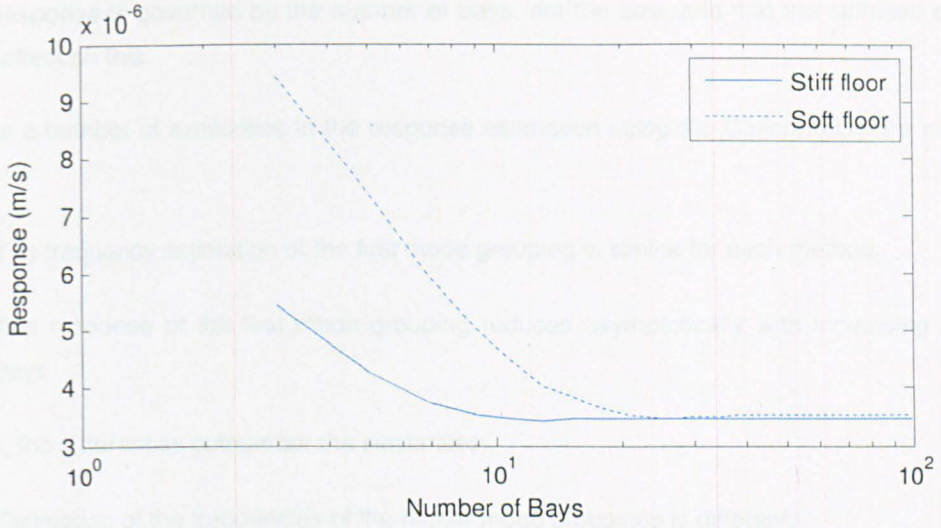

Figure 78 - Peak velocity response of the centre bay for increasing number of bays for the soft and stiff floors using the Concrete Centre's method

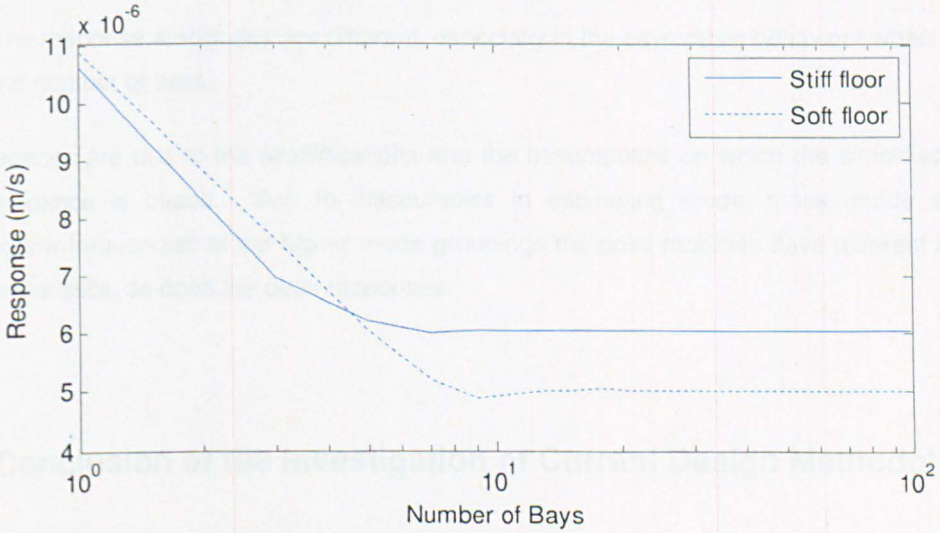

Figure 79 - Peak velocity response of the centre bay for increasing number of bays for the soft and stiff floors using the Concrete Centre's method

There are clear differences in peak responses. Using the Concrete Centre modes, for both floor stiffnesses the responses asymptotes to a similar level, which in this case is almost identical, however, the stiff floor reaches this level much quicker. The stiff floor asymptotes at approximately 10 bays, whereas the soft floor requires 20 bays, suggesting that the asymptotic behaviours is dependent on the size of the structure. Using the FEA modes, for both floor stiffnesses the response asymptotes to a certain response, which in this case is lower for the soft floor. The soft floor has a lower response due to a higher average modal mass as it is twice as long as the stiff floor. What is interesting to note is at what point the response asymptotes. For both floors, this is approximately 10 bays, suggesting

that the response is governed by the number of bays, not the size, and that the stiffness of the floor has little effect on this.

There are a number of similarities in the response estimation using the Concrete Centre method and FEA:

- The frequency estimation of the first mode grouping is similar for each method.
- The response of the first mode grouping reduces asymptotically with increasing number of bays.

However, the differences outnumber the similarities:

- Estimation of the frequencies of the higher mode groupings is different.
- The closely spaced modes are not formed in the same manner. The Concrete Centre estimates the closely spaced modes of the first mode grouping, but cannot estimate higher mode groups.
- The response amplitudes are different, especially in the asymptotic behaviour when increasing the number of bays.

The differences are due to the simplifications and the assumptions on which the simplified Concrete Centre guidance is based. Due to inaccuracies in estimating modal mass, mode shape and estimating the frequencies of the higher mode groupings the point motilities have different amplitudes and characteristics, as does the peak responses.

5.1.4 Conclusion of the Investigation of Current Design Methodologies

This section has reviewed the current guidance for estimating response of transient response floors (TRFs). Primarily in the past, but also to some degree today, there has been a general lack of knowledge when it comes to floor design for vibration performance. Even when previous knowledge has been documented and published in the form of technical papers and literature reviews it has often not been used. However, this experience does eventually trickle through into design although it may take many years. As such, there has been a relatively recent improvement in design guides with respect to TRFs.

Unfortunately, design guides historically have primarily been written in mind for a resonant response, i.e. with a single mode governing the response. This background has influenced modern design guides. Although detailed provisions now exist for the analysis of TRFs they are based on single

mode estimates with accuracy focused on estimating parameters that govern resonant response, i.e. frequency.

This section showed that TRFs require a multi-mode analysis, with many modes considered in response estimation. Most guidance does not offer a simplified solution for this and recommends FEA using modal superposition including modes up to twice the fundamental natural frequency. It was shown that this frequency limit might be inadequate, with the risk increasing with non-uniform structures. The exception to this is the Concrete Centre method, which offers simplified guidance to estimate modal parameters of multiple modes. Formulae are given for the estimation of modal frequency, modal mass and mode shape. An interesting point is that this is the only method to offer an estimation of mode shape.

It was also shown that the focus on accuracy in estimating natural frequency is not valid for TRFs. It was shown that as the modal frequency increases modal mass becomes more important when calculating response, becoming the governing factor before 20 Hz due to the energy content of a footfall reducing slowly with increasing frequency. All the current guidance poorly estimates modal mass, and in the examples in this section it was underestimated by a factor of two. This is due to assuming the mode shapes are similar to a simply supported slab. Although this is an conservative assumption, and may sometimes be true, a quick observation of FE mode shape will show this is not valid in this case. Empirical formulae have been developed, and can be used, to estimate the modal mass, but this is not suitable for a general guidance. The mode shape is a function of the mass and stiffness distribution (of the columns as well as the floor) and accurate knowledge of the stiffness distribution is required. If an empirical formula is developed using a floor type, as that mass and stiffness distribution is unique to that floor type, the empirical formula is only suitable for that individual floor.

Due to the Concrete Centre method being the only method suitable for TRF analysis the method was examined in more detail. A number of hypothetical floors were compared with FEA to identify inaccuracies and errors in the method. The errors can be categorised into three forms: modal frequency, modal mass and response estimation.

Modal frequency: The estimates for a single bay floor were inaccurate due to the inaccurate assumptions in the boundary conditions. The method assumes the floor is a simply supported plate, which is not the case. For a single bay the floor just has four corner supports and is not supported in between. As the number of bays increases the columns can be assumed to act as a distributed supports and approximate the assumed boundary condition better (similar to a beam on an elastic foundation). It was shown that floors with three or more bays could have their frequency estimated reasonably well, for multiple modes. A further investigation into frequency revealed that multi-bay floors have characteristic mode groupings, and it was shown that only the first mode grouping could be accurately estimated and for higher mode groupings the estimations were poor

Modal mass: All estimates for modal mass are very poor, considerably underestimating the mass. This is due to the mode shapes being estimated as being identical to a simply supported plate and neglecting column deformation (in reality this is not the case). As a flat slab is used in the examples, the mass distribution in this case was not the problem, it was limited to the mode shape.

Response estimation: There was a large difference in the response estimations when comparing the Concrete Centre method to FEA. Although both methods showed asymptotically decreasing response when increasing the number of bays in the structure, the characteristics of the asymptote were different for each method. The stiffness of the floor was the key factor when using the Concrete Centre method, whereas the FEA showed that the number of bays was the key factor. Also the final response was different due to the errors in mass estimation using the Concrete centre method. There was also a large difference in the point mobility plots, with the Concrete Centre method producing more peaks. This, again, was due to poor estimation of mass and the poor estimation of modal frequencies for the higher mode groupings.

5.2 Parametric Study of Multi-Bayed Floors

Previously in this chapter, it has been shown that for accurate response estimations of TRFs multiple modes he need to be included in the analysis. The simplified methods in the current guidance cannot estimate the parameters of these floors very well. It was also shown the multi-bayed floors have closely spaced modes and characteristic mode groupings, which makes modal properties even harder to estimate.

Multi-bayed floors are common in many building types, e.g. car parks, shopping centres, hospitals, office buildings, fabs, etc., appearing in any structure that requires a large floor plan. TRFs often, due to their occupancy, require a large floor plan and as such are often multi-bayed floors. This section investigates some interesting and unique dynamic properties of multi-bayed floors. Once the characteristics of multi-bayed floors have been determined, accurate methods of modelling them can be developed.

A parametric study was conducted on floors with constant bay properties, but the number of bays was always an odd number to maintain a centre bay. Two types of floors were analysed, a soft floor and a stiff floor. The stiffness of each floor was achieved by varying the length of the bay in the x direction from 5m to 10m. Each bay consisted of a flat slab supported by four columns. Each bay was 5m long in the y direction, and either 5m or 10m long in the x direction, depending on the floor stiffness. The type of floor was chosen due to its simplicity and would serve as a good base for any future analysis. Two types of structures were considered, known as 1D and 2D floors. The 1D floor consisted of 1 x X bays, where X was varied to change the number of bays, as such, the structure only changed length in

one dimension. The 2D floor consisted of X x Y bays, where both X and Y were varied to change the number of bays, as such, the structure changed length in two dimensions.

Regular floor bays were chosen for a number of reasons. Firstly, many buildings are constructed with regular bay spacings making design simpler and quicker. They are also quicker to construct, reducing the overall cost of the structure. Secondly, floors with regular bays are simpler to analyse. Irregular floor bays exhibit many local modes of vibration (i.e. a mode that engages a single bay rather than the whole structure) which are unique to the floors layout, it would be incredibly difficult, if not impossible, to generalise the properties of such floors.

The section begins by examining 1D floors, to use the analysis of 1D floors to speculate what will happen in 2D floors. A number of the structures dynamic characteristics were analysed as the number of bays were increased, these are:

- The number of modes within a specified frequency range.
- How modal mass and frequencies vary.
- Properties of the mode groupings.
- Response estimated in terms of peak responses and response spectra.

Similar comparisons are then conducted for 2D floors and the properties are compared with the 1D floors. Finally, from the trends observed, empirical modifications can be suggested for simplified guidance based on single bay analysis.

5.2.1 1D Floors

The 1D floor consisted of a bay which is repeated along one spatial axis. The number of bays was varied from 1 to 101, effectively showing how the floors properties and characteristics change as the floor length can be considered to tend to infinity. There were two types of floor: soft and stiff. The different stiffnesses were obtained by varying the length of the bay along the dimension i.e. 5m x 5m bay for the stiff floor and 10m x 5m for the soft floor.

5.2.1.1 Mode Characteristics

Figure 80 shows how the number of modes within a frequency range of 0-100 Hz varies when the number of bays is increased. As can be seen, for both floor types the increase in modes is linear. If one imagines the properties of the mode groupings as described earlier in the chapter, for a single bay the modes correspond to plate modes. As more bays are added, mode groupings appear around the

modes of a single bay. If *n* bays are added, each plate mode now represents a mode grouping with *n* modes at each mode grouping, which is clearly a linear increase in the number of modes.

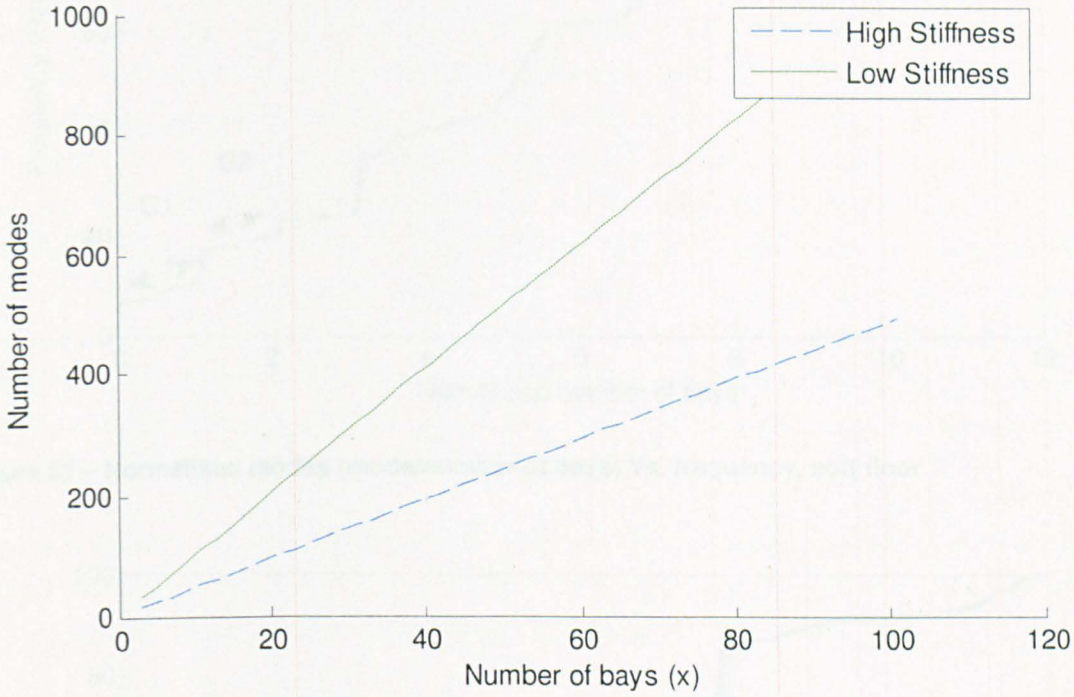

Figure 80 – Number of modes vs. number of bays

It is known that mode groupings exist, and that the number of modes within the mode groupings increases proportionally with the number of bays. Figure 81 and Figure 82 show plots of normalised modes versus the frequency. The normalisation in this case is the mode number divided by the number of bays. For each plot, as the line becomes darker the number of bays increases. Due to how well the plots over-lay, it is confirmed that the number of bays has a linear relationship to the number of modes, so this is a valid normalisation. In each plot, the mode groupings are clear with the first two mode groupings for each floor indentified and labelled as G1 and G2 respectively. What is interesting is that as more bays are added the plots over-lay themselves better, demonstrating further that after so many bays, adding more does not change the characteristics of the mode groupings.

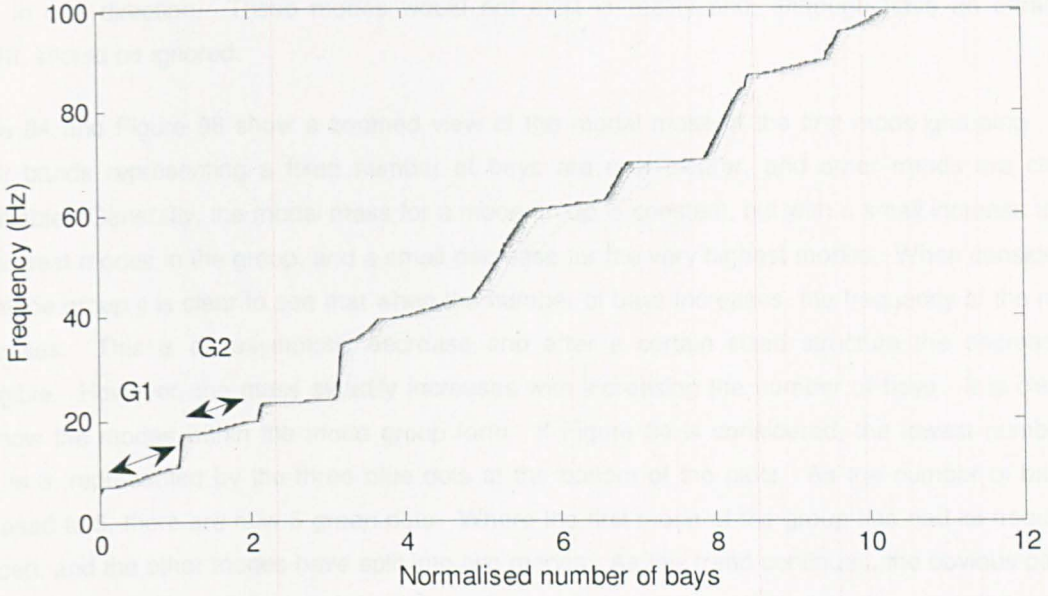

Figure 81 – Normalised modes (mode/number of bays) Vs. frequency, soft floor

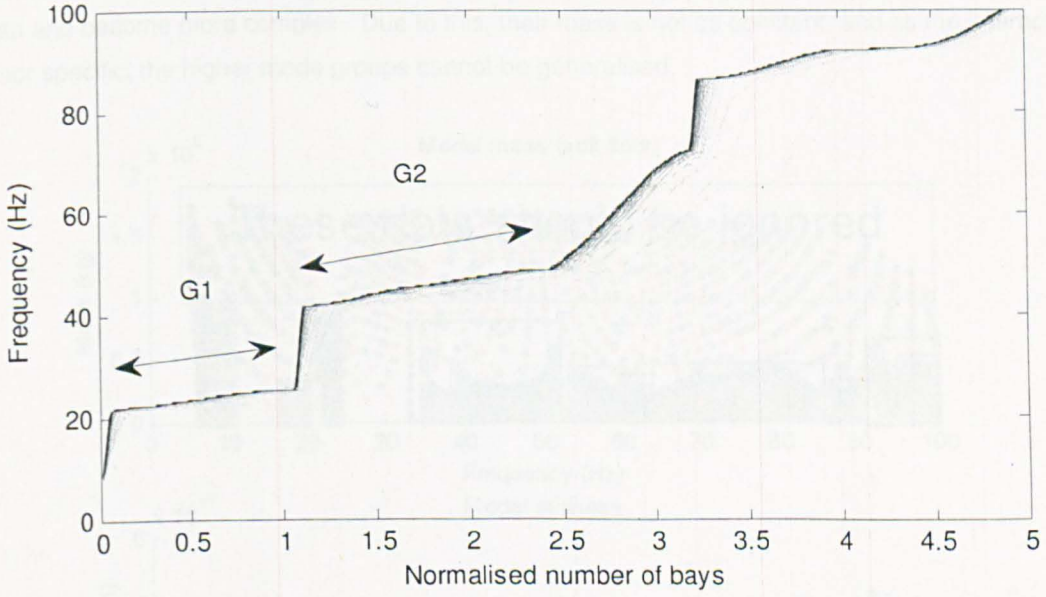

Figure 82 – Normalised modes (mode/number of bays) Vs. frequency, stiff floor

Figure 83 and Figure 85 show plots of the modal masses and stiffnesses versus the modal frequency as the number of bays is increased, with each dot representing a mode. On each plot, there are regions of densely packed dots, which have been identified with rectangles, representing a mode grouping. Within these densely packed regions, stripes of a single colour, representing a fixed number of bays, are apparent. The remaining dots, outside of the rectangles, represent other modes. Due to their high modal mass it indicates that most of the structure is engaged in these additional modes. These modes are lateral sway modes which only exist because a long 1D floor is relatively

weak in one direction. These modes would not exist in reality and, although have an attractive pattern, should be ignored.

Figure 84 and Figure 86 show a zoomed view of the modal mass of the first mode grouping. The colour bands representing a fixed number of bays are now clearer, and other trends are clearly identifiable. Generally, the modal mass for a mode group is constant, but with a small increase at the very lowest modes in the group, and a small decrease for the very highest modes. When considering this mode group it is clear to see that when the number of bays increases, the frequency of the mode decreases. This is an asymptotic decrease and after a certain sized structure the decrease is negligible. However, the mass steadily increases with increasing the number of bays. It is clear to see how the modes within the mode group form. If Figure 84 is considered, the lowest number of bays is 3, represented by the three blue dots at the bottom of the plots. As the number of bays is increased to 5, there are now 5 green dots. Where the first mode of the group has had its frequency reduced, and the other modes have split into two modes. As this trend continues, the obvious pattern is formed. Figure 86 shows a dip in mass within the mode grouping, this dip is floor specific and not characteristic of the first mode groupings.

The second mode group has similar characteristics as the first. However, the higher mode groupings overlap and become more complex. Due to this, their mass is not as constant, and as the interactions are floor specific, the higher mode groups cannot be generalised.

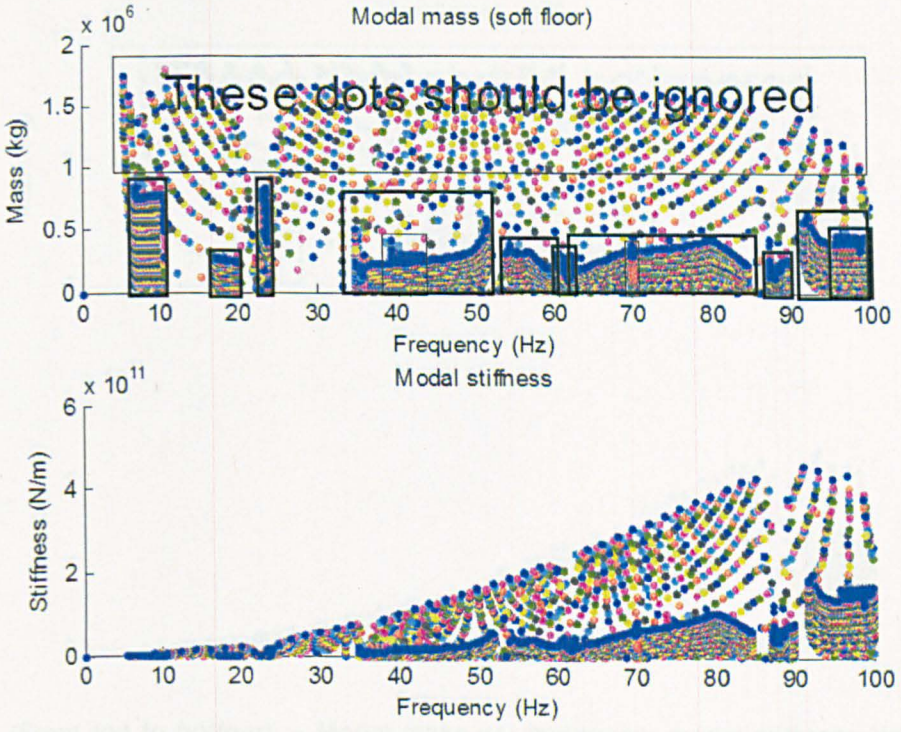

Figure 83 ***(From top to bottom)*** **– Modal mass vs. frequency; modal stiffness Vs. frequency (soft floor)**

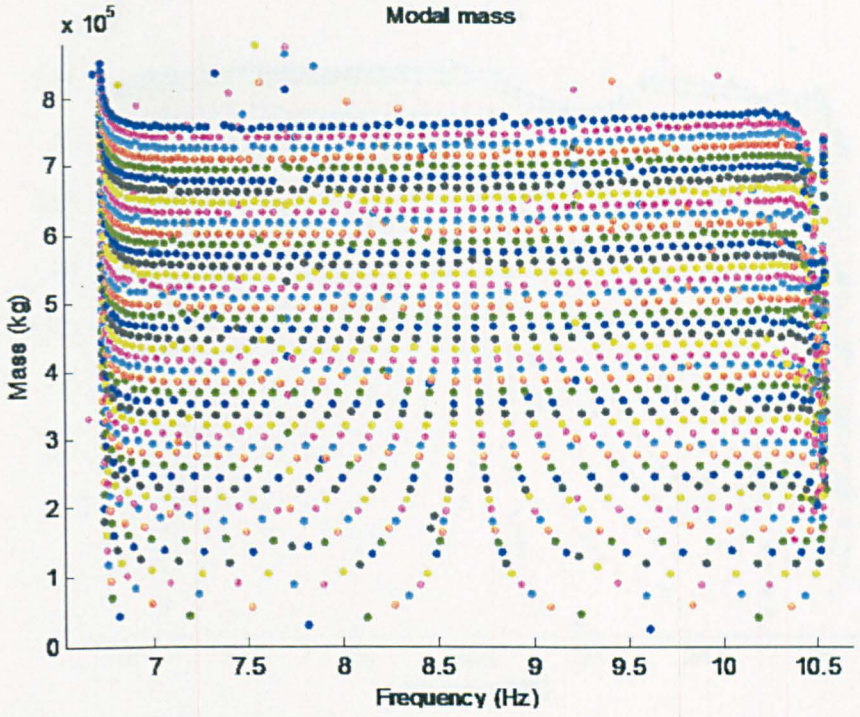

Figure 84 - Zoomed modal mass plot of the first mode grouping for the soft floor

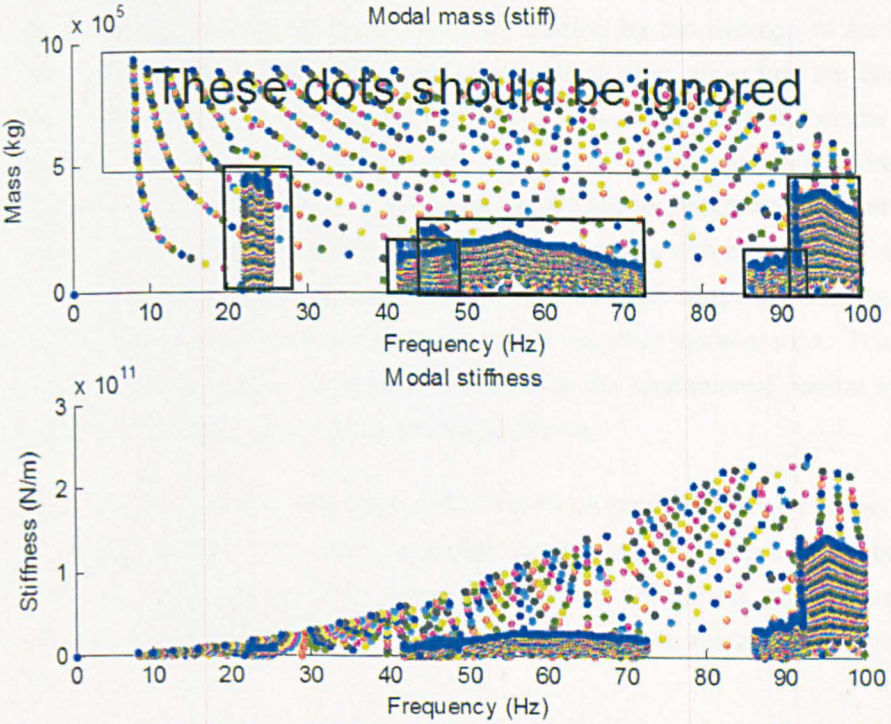

Figure 85 *(From top to bottom)* – Modal mass vs. frequency; modal stiffness Vs. frequency (stiff floor)

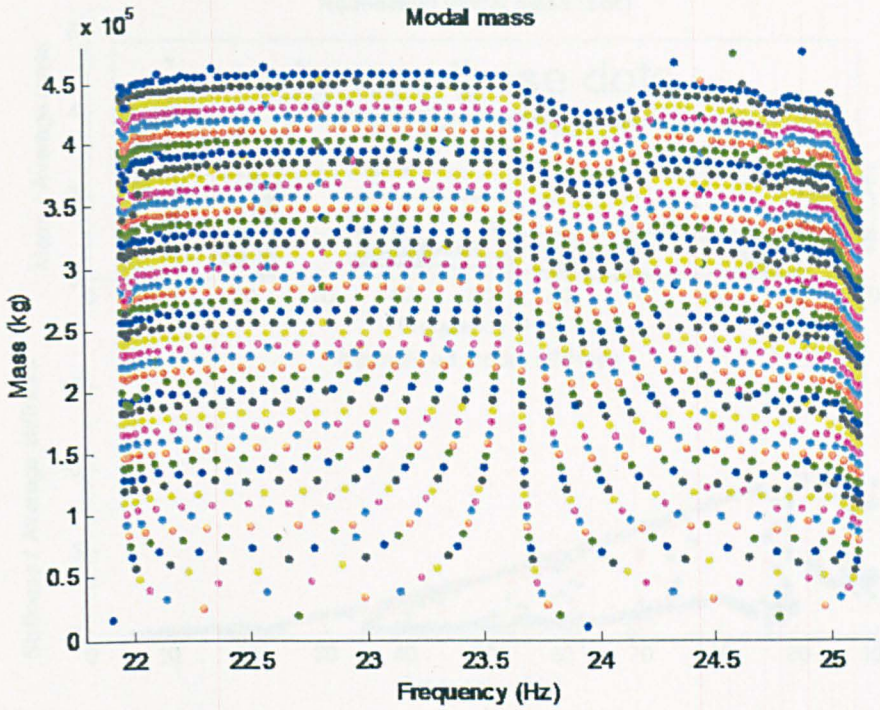

Figure 86 - Zoomed modal mass plot of the first mode grouping for the stiff floor

Figure 87 and Figure 89 shows the normalised mass and normalised stiffness with respect to frequency of each mode with increasing bays. Again, mode groups have been identified with rectangles. The normalisation has been achieved by dividing by the average of each metric, i.e. normalised mass = modal mass / average modal mass. Both plots show that the bands of mode groupings form a single line after normalisation, making it clear to see how the modal mass varies within mode groups. For the first two mode groups of each floor, the mass is quite constant through the group. The small change that does occur could be ignored for response estimates with only a small drop in accuracy. The higher mode groups are more complex, with modal mass increasing and decreasing, with no obvious trend. An interesting observation can also be made here: the modal mass of the first mode group is approximately twice that of the other mode groups. This could cause an underestimation of response if only modes up to 'twice the fundamental natural frequency' are considered in analysis, which is recommended in the guidance.

Figure 88 and Figure 90 show zoomed plots of the first mode group of the normalised modal mass. These plots show an important point: there is a slight change in ratio between the modal mass and average modal mass. This indicates that the normalisation is not perfect, and although the modal mass characteristics will be very similar to the characteristics of the average mass, they will not be exactly the same.

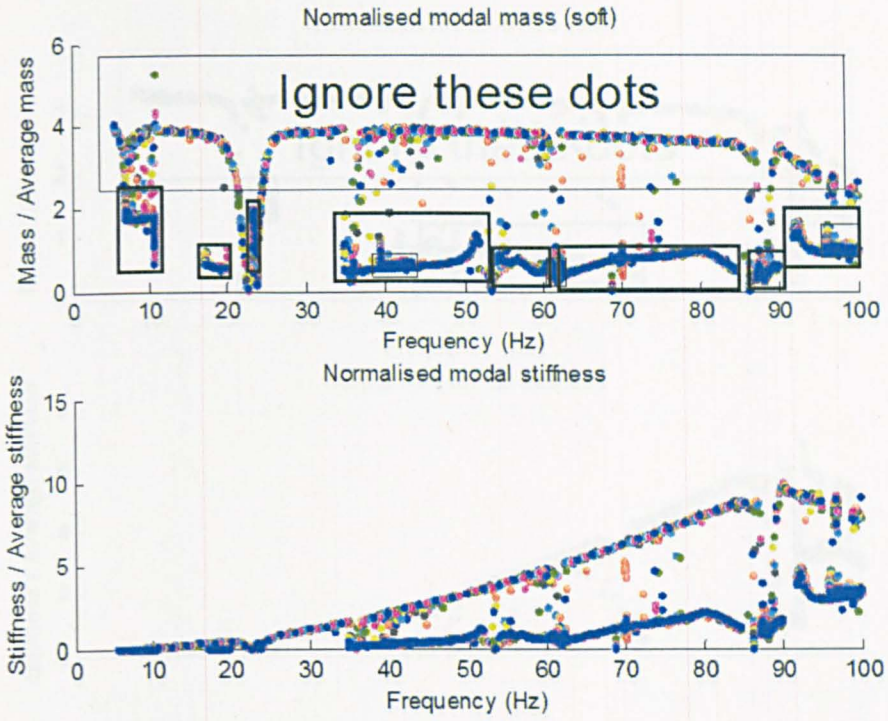

Figure 87 *(From top to bottom)* – Normalised modal mass vs. frequency; normalised modal stiffness Vs. frequency (soft floor)

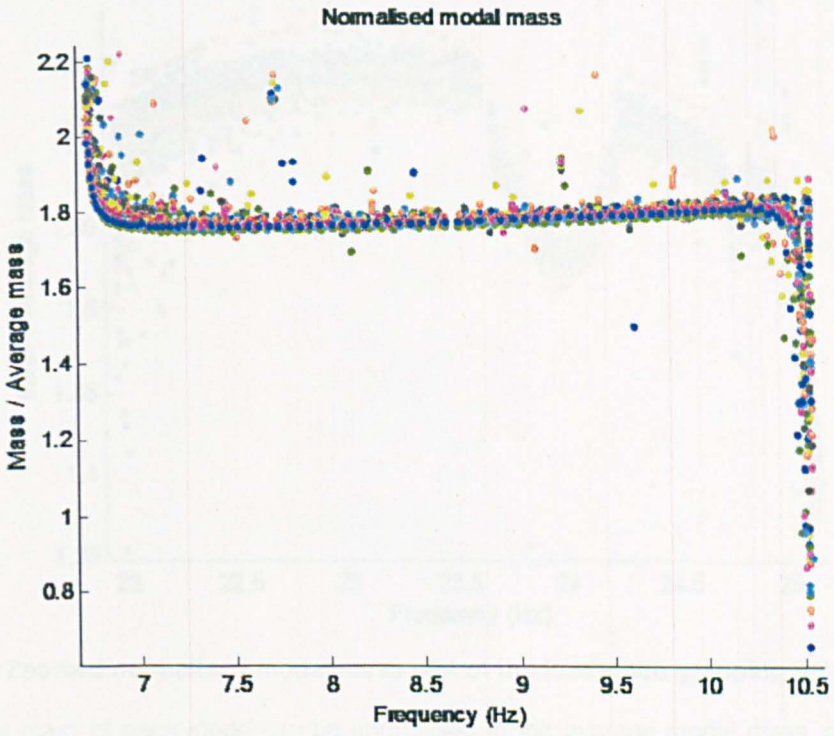

Figure 88 - Zoomed normalised modal mass plot of the first mode grouping for the soft floor

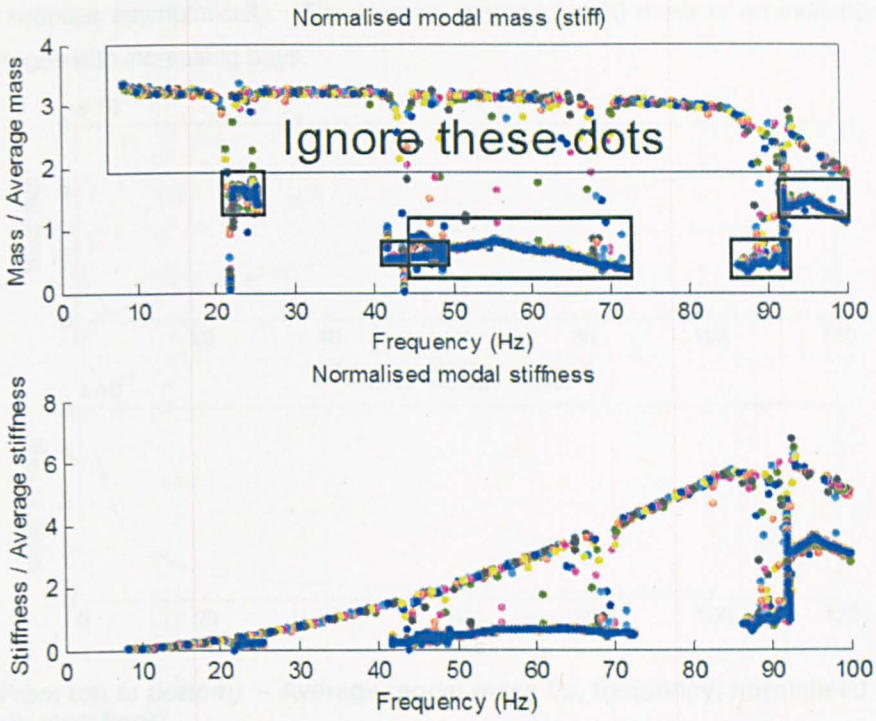

Figure 89 *(From top to bottom)* – Normalised modal mass vs. frequency; normalised modal stiffness Vs. frequency (stiff floor)

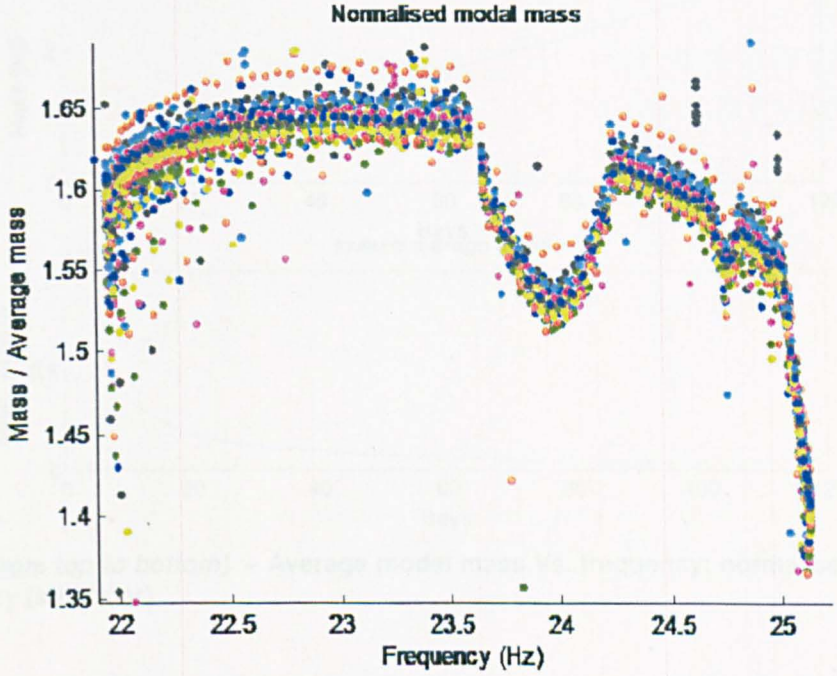

Figure 90 - Zoomed normalised modal mass plot of the first mode grouping for the stiff floor

As the modal mass of each mode can be normalised to the average modal mass, characteristics of the average mass will loosely translate to the individual modal masses. Figure 91 and Figure 92 show how the average modal mass and inverse average modal mass change with increasing bays. For both floors, the average modal mass increases linearly with increasing bays, and the inverse average

modal mass reduces asymptotically. The inverse average modal mass is an indicator of how the response changes with increasing bays.

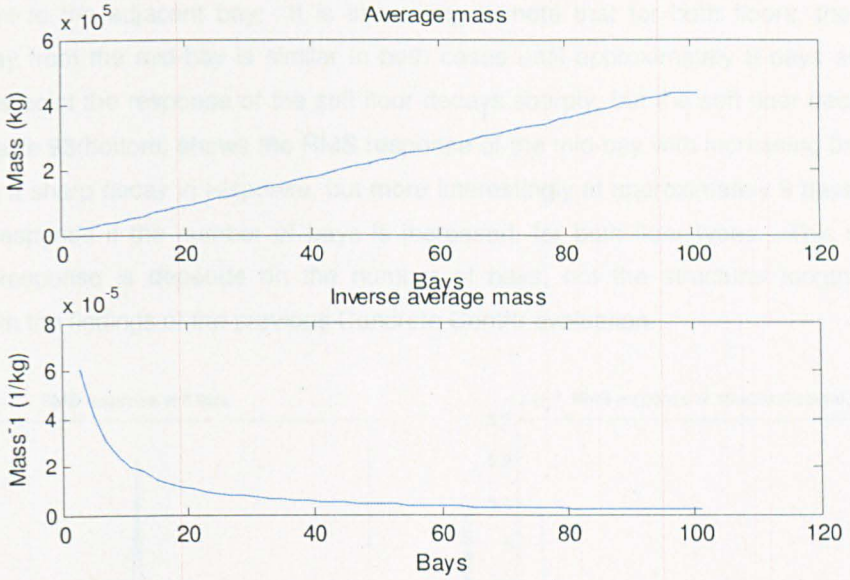

Figure 91 ***(From top to bottom)*** **– Average modal mass Vs. frequency; normalised modal mass Vs. frequency (soft floor)**

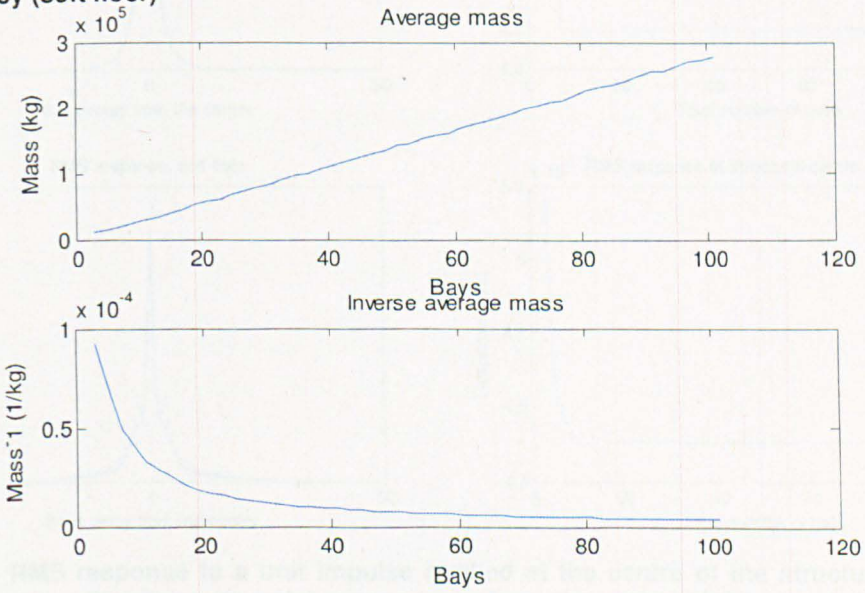

Figure 92 ***(From top to bottom)*** **– Average modal mass Vs. frequency; normalised modal mass Vs. frequency (stiff floor)**

5.2.1.2 Response to a Unit Impulse

Figure 93(top) shows the maximum RMS response, with 0.5 s window, of each bay to a unit impulse applied at the centre of the structure (the centre of the central bay). On the x axis, 0 represents the response at the midpoint of the structure and the values represent the number of bays away from the midpoint (i.e. +10 and -10 represent 10 bays in one direction, and 10 bays in the other, a 21 bay

structure). The responses from increasing the number of bays are overlaid on top of each other. It is clear to see that increasing the number of bays does not reduce the response as much as moving the response point to the adjacent bay. It is interesting to note that for both floors, the reduction in response away from the mid-bay is similar in both cases until approximately 8 bays away from the centre. At this point the response of the stiff floor decays sharply, but the soft floor decay somewhat levels off. Figure 93(bottom) shows the RMS response of the mid-bay with increasing bays. For both floors there is a sharp decay in response, but more interestingly at approximately 9 bays there is little reduction is response if the number of bays is increased, for both floor types. This suggests that reduction of response is depends on the number of bays, not the structural length, which is in agreement with the findings of the previous Concrete Centre evaluation.

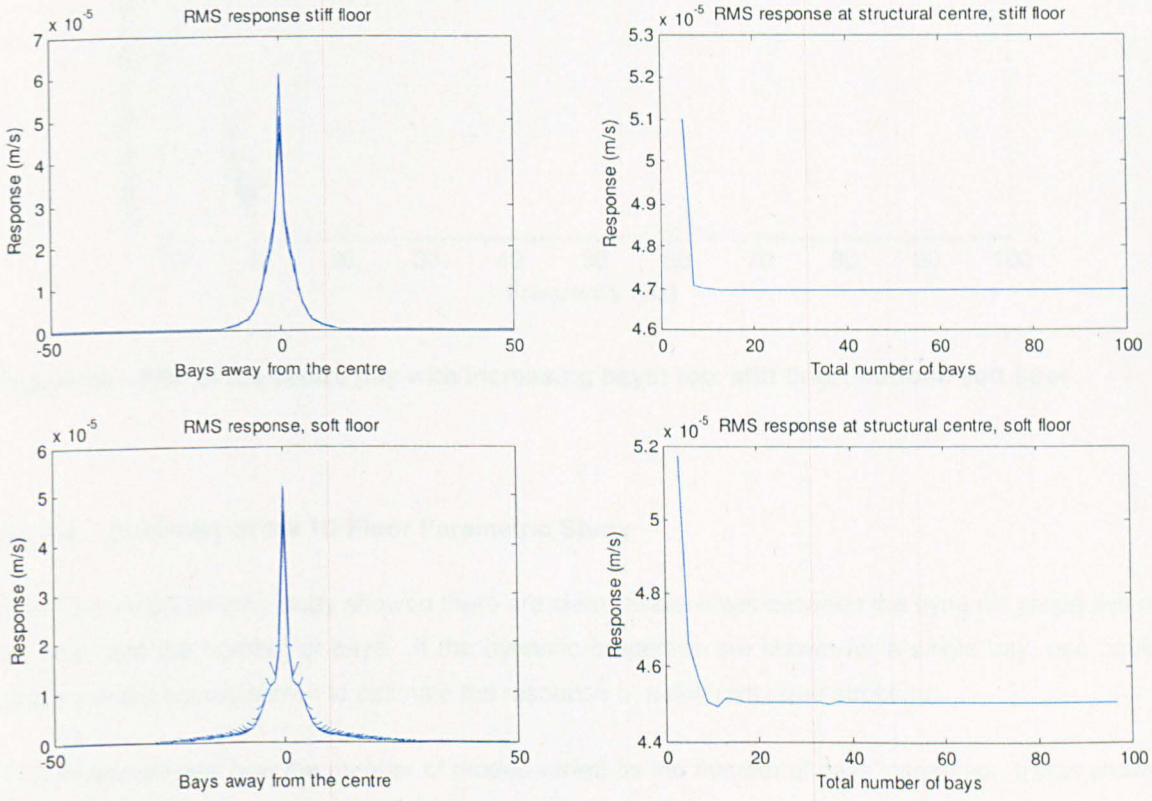

Figure 93 - RMS response to a unit impulse applied at the centre of the structure; *left*: peak RMS response as the response point moves away from the centre of the structure; *right*: peak RMS response at the centre of the structure with increasing bays.

Figure 94 shows the FRFs of the soft and stiff floors with increasing bays overlaid on one another; the darker line represents more bays within the structure. It is clear that for both floors each FRF is similar, but the amplitude changes with increasing bays. All the extra modes associated with increasing the number of bays are not apparent.

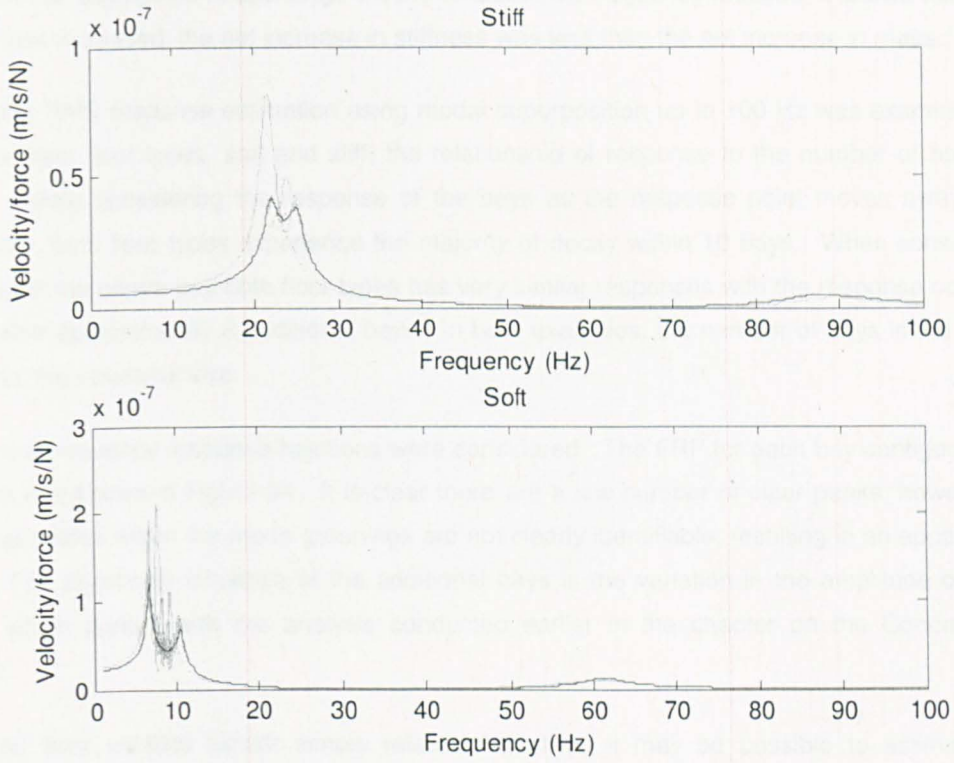

Figure 94 – FRF of the centre bay with increasing bays; *top*: stiff floor; *bottom*: soft floor

5.2.1.3 Summary of the 1D Floor Parametric Study

The 1D floor parametric study showed there are clear relationships between the dynamic properties of the floor and the number of bays. If the dynamic properties are known for a single bay, one could easily use the figures shown to estimate the response of a different sized structure.

First examined was how the number of modes varied as the number of bays increased. It was shown that there is a linear relationship, with the assitional modes appearing as closely spaced modes, forming mode groupings.

Next, the modal mass, stiffness and frequencies were evaluated. Mass also increases with a linear relationship with the number of bays. This makes sense, if the number of bays is doubled, so will the amount of mass participating in the mode shape. Doubling the mass, however, did not halve the response. This may initially seem strange as the response is governed by an inverse relationship to the mass (Equation 61). What has to be remembered is that if the bays are doubled, the mass is double, but so are the number of modes that contribute to the response, demonstrating another reason why multi-modal analysis is essential for large TRFs. It was also shown that if the mass is normalised to the size of the structure, the normalised mass is relatively constant, which is in agreement with the simplified guidance. The stiffness, and as such, the fundamental frequency, both

varied with an asymptotic relationship. As the fundemental frequency reduced, it shows that although the stiffness increased, the net increase in stiffness was less than the net increase in mass.

Next, peak RMS response estimation using modal superposition up to 100 Hz was examined (Figure 93). For both floor types, soft and stiff, the relationship of response to the number of bays is very similar. When considering the response of the bays as the response point moves away from the centre bay, both floor types experience the majority of decay within 10 bays. When considering the response of the centre bay both floor types has very similar responses with the response not reducing further after approximately 8 additional bays. In both examples, the number of bays is the governing factor, not the structural size.

Finally, the frequency response functions were considered. The FRF for each bay configuration were over laid and shown in Figure 94. It is clear there are a low number of clear peaks, however all the individual modes within the mode groupings are not clearly identifiable, resulting in an apparent single mode. The significant influence of the additional bays is the variation in the amplitude of the main peaks, which agrees with the analysis conducted earlier in the chapter on the Concrete Centre method.

If the 2D floor exhibits similar simple relationships then it may be possible to estimate the 2D behaviour from the relationships discovered in the 1D analysis. Eventually, the final goal would be able to extrapolate the dynamic properties of a single bay to a uniform bay configuration of any size.

5.2.2 2D Floors

The 2D floor consisted of a bay which is repeated along two spatial axes. The number of bays along each axis was varied from 1 to 21, effectively showing how the floors properties and characteristics change as the floor length tends towards infinity (recall that for 1D floors that after approximately 10 bays, additional bays have little effect). Again, there were two types of floor: soft and stiff. The different stiffnesses were obtained by varying the length of the bay along one dimension i.e. 5m x 5m bay for the stiff floor and 10m x 5m for the stiff floor.

5.2.2.1 Mode Characteristics

Figure 95 and Figure 96 show how the number of modes increases with the number of bays (up to 100 Hz). It is clear that the number of modes is more or less a product of the linear relationship shown with 1D floors, i.e. doubling the number of bays doubles the number of modes. As expected the soft structure has more modes then the stiff structure, but both have the same trend.

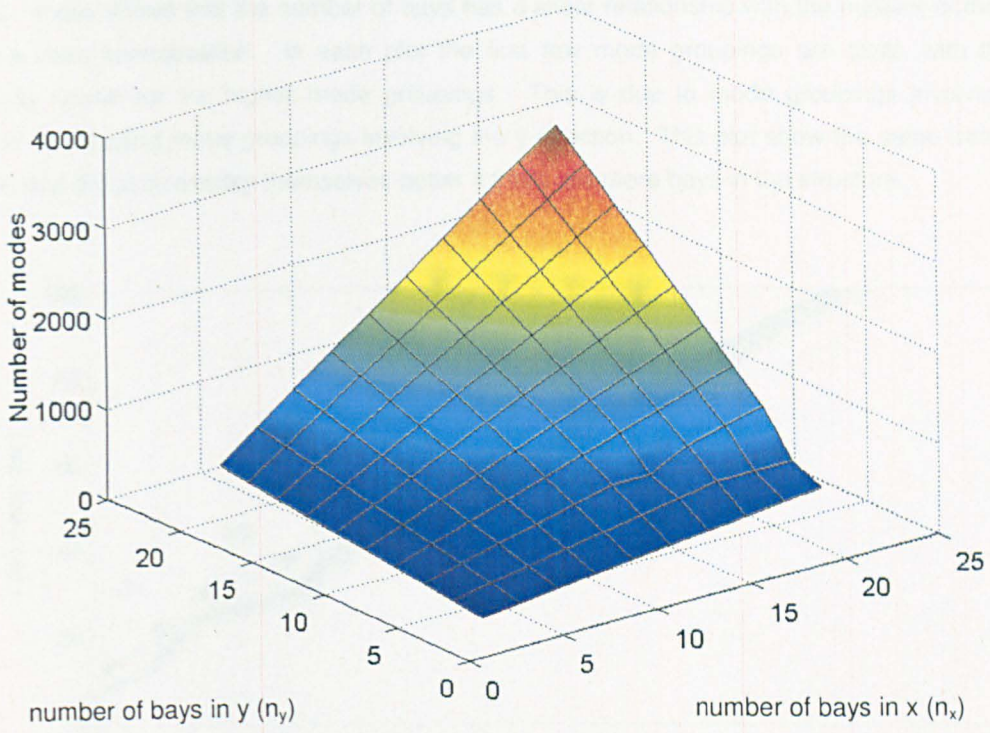

Figure 95 - Number of modes Vs. number of bays (soft floor)

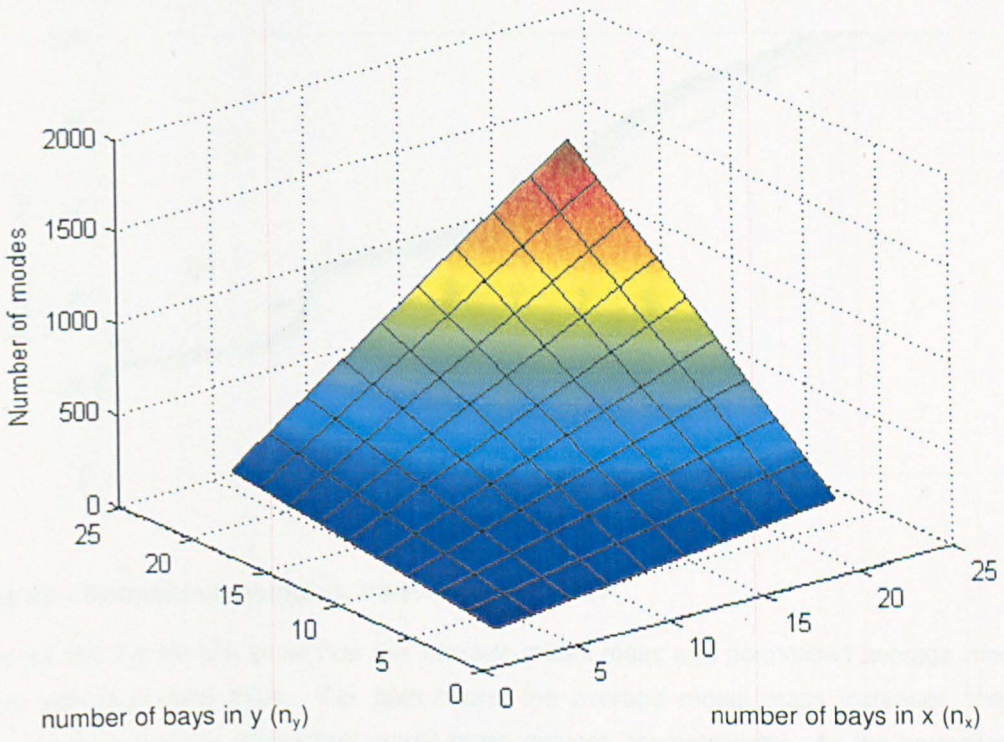

Figure 96 - Number of modes vs. number of bays (stiff floor)

Figure 97 and Figure 98 show plots of normalised mode number versus the frequency where G represent the mode group. The normalisation in this case is the mode number divided by the number

of bays. It was shown that the number of bays has a linear relationship with the number of modes, so this is a valid normalisation. In each plot the first few mode groupings are clear, with the plots becoming noisier for the higher mode groupings. This is due to mode groupings involving the x direction overlapping mode groupings involving the y direction. This plot show the same trend as 1D floors in that the plots overlay themselves better if there are more bays in the structure.

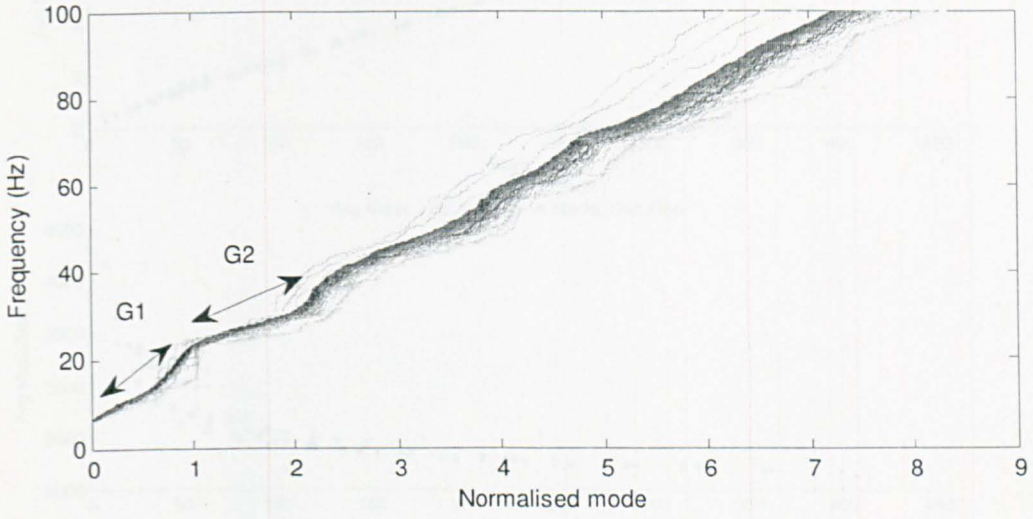

Figure 97 – Normalised modes vs. frequency, soft floor

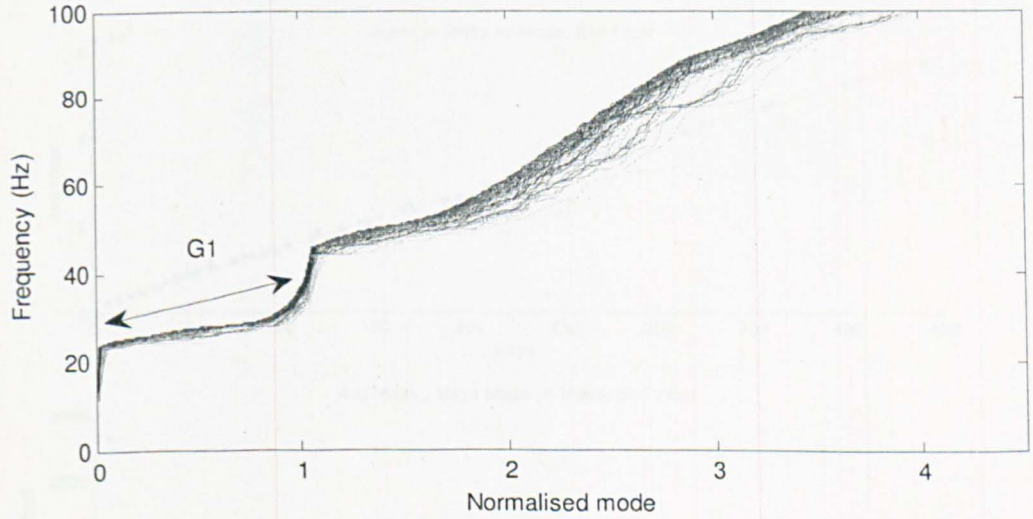

Figure 98 – Normalised modes vs. frequency, stiff floor

Figure 99 and Figure 100 show how the average modal mass and normalised average modal mass change with increasing bays. For both floors, the average modal mass increases linearly with increasing bays and the normalised modal mass reduces asymptotically. As the normalised modal mass is somewhat inversely proportional to the floor's response it serves as an indicator of how the response changes with increasing bays. Due to there being two different increases in mass for the soft floor, (whether n_x or n_y is increased) there can be multiple masses at explicit total number of bays.

It is interesting that this relationship is the same as the 1D floor even though the floor allows for more complex mass estimations.

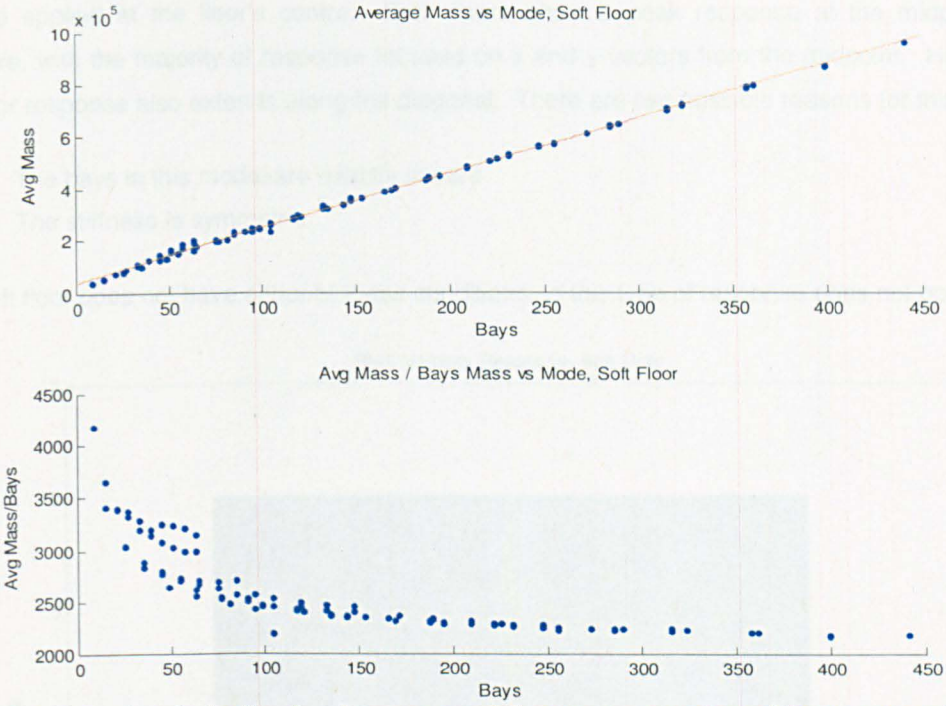

Figure 99 (*from top to bottom*) – Average modal mass vs. number of bays; normalised modal mass vs. number of bays (soft floor)

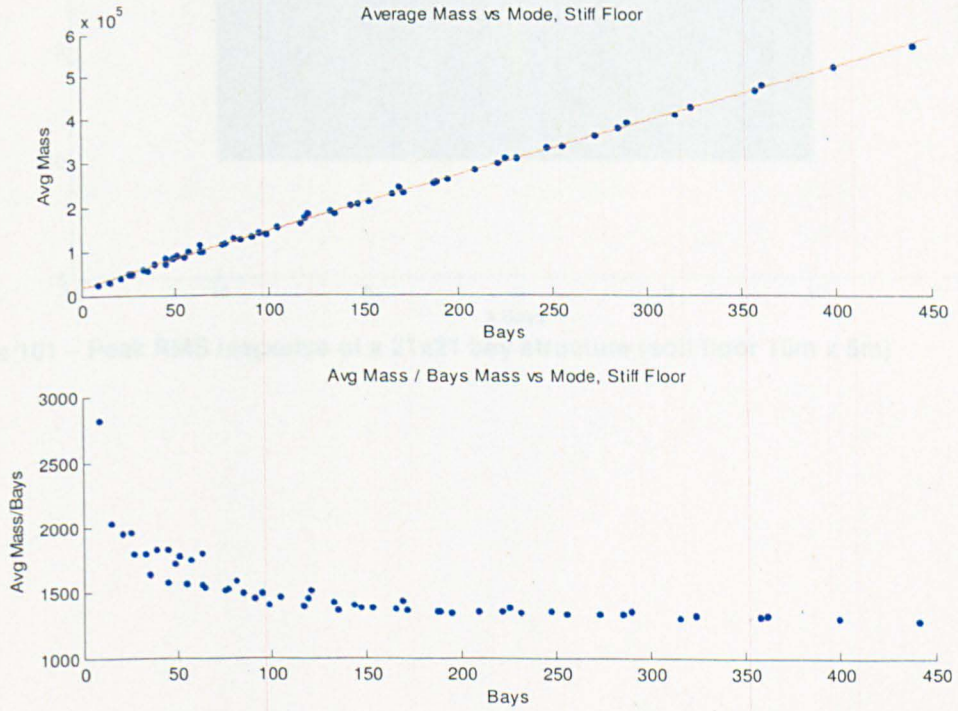

Figure 100 (*from top to bottom*) – Average modal mass vs. number of bays; normalised modal mass vs. number of bays (stiff floor)

5.2.2.2 Response to a Unit Impulse

Figure 101 and Figure 102 show the RMS responses of the largest 2D structures analysed to a unit impulse applied at the floor's centre. Both floors show a peak response at the midpoint of the structure, with the majority of response focused on x and y vectors from the midpoint. However, the stiff floor response also extends along the diagonal. There are two possible reasons for this:

1. The bays in this model are exactly square
2. The stiffness is symmetric

The soft floor does not have either of these conditions so this type of response does not occur

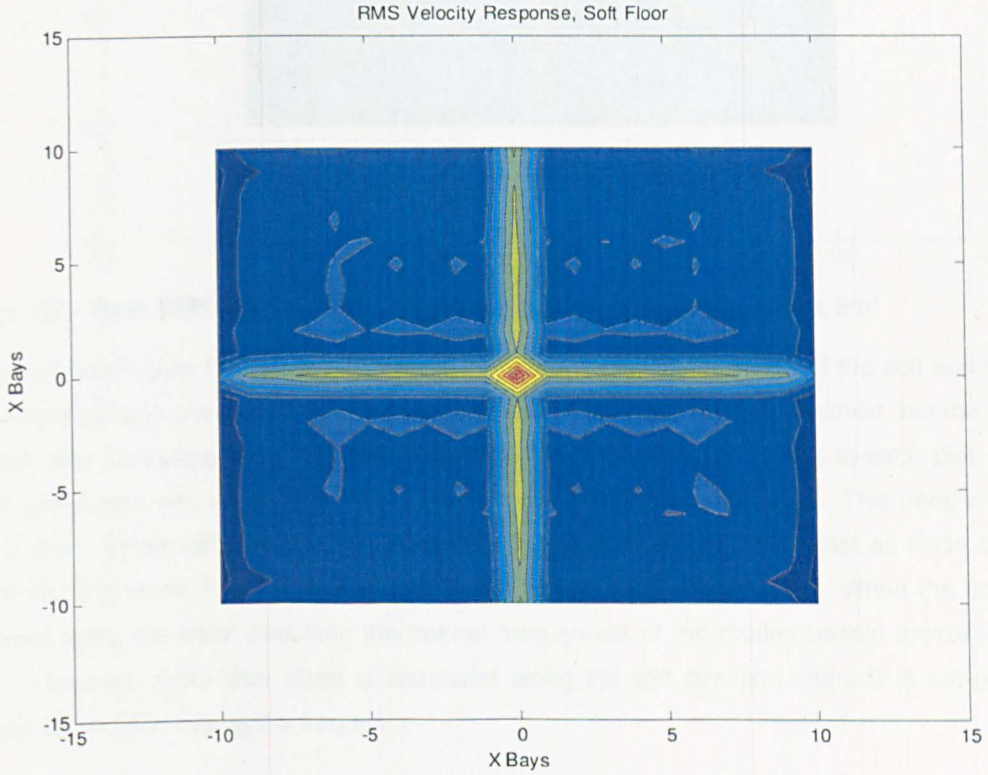

Figure 101 – Peak RMS response of a 21x21 bay structure (soft floor 10m x 5m)

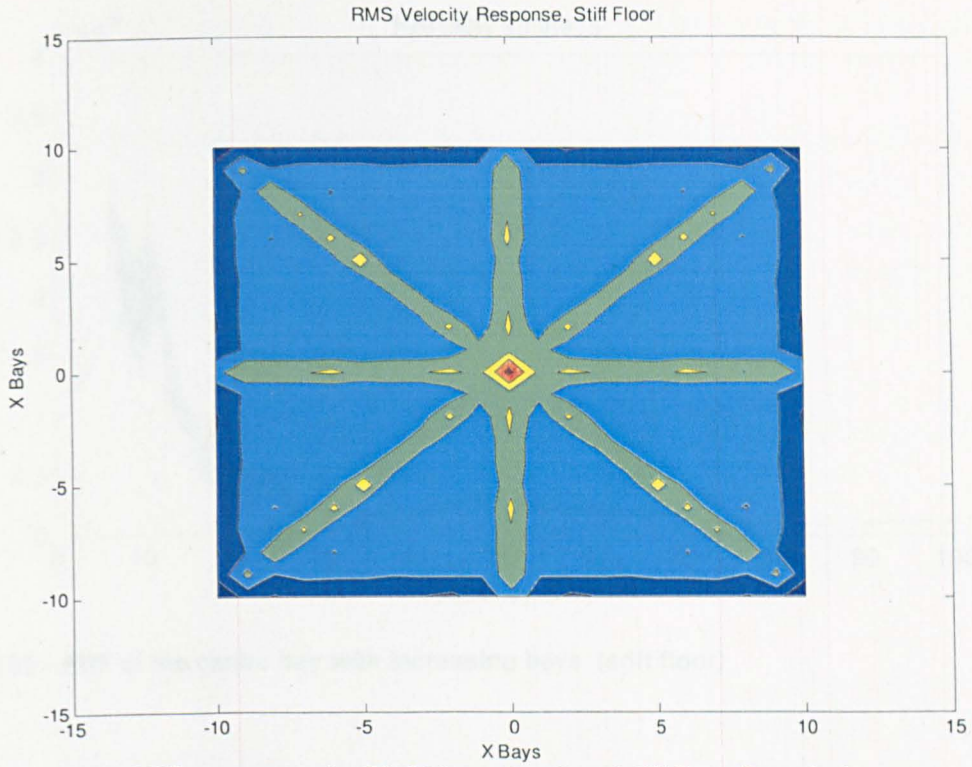

Figure 102 – Peak RMS response of a 21x21 bay structure (stiff floor 5m x 5m)

Figure 103 and Figure 104 show the (frequency response functions) FRFs of the soft and stiff floors with increasing bays overlaid. It is clear that with each floor type the FRF is similar, but the amplitude changes with increasing bays. Considering there are thousands of modes in each plot, the extra modes associated with increasing the number of bays are also not apparent. This trend is similar to the 1D floor. When considering the soft floor in Figure 103, the FRFs are not as clean due to the orthotropic (the whole floor mimics an orthotropic plate) nature of the floor. When the floor size is increased along the weak direction, the natural frequencies of the modes remain approximately the same. However, if the floor sized is increased along the stiff direction, there is a net gain in the stiffness of the floor, raising the frequency.

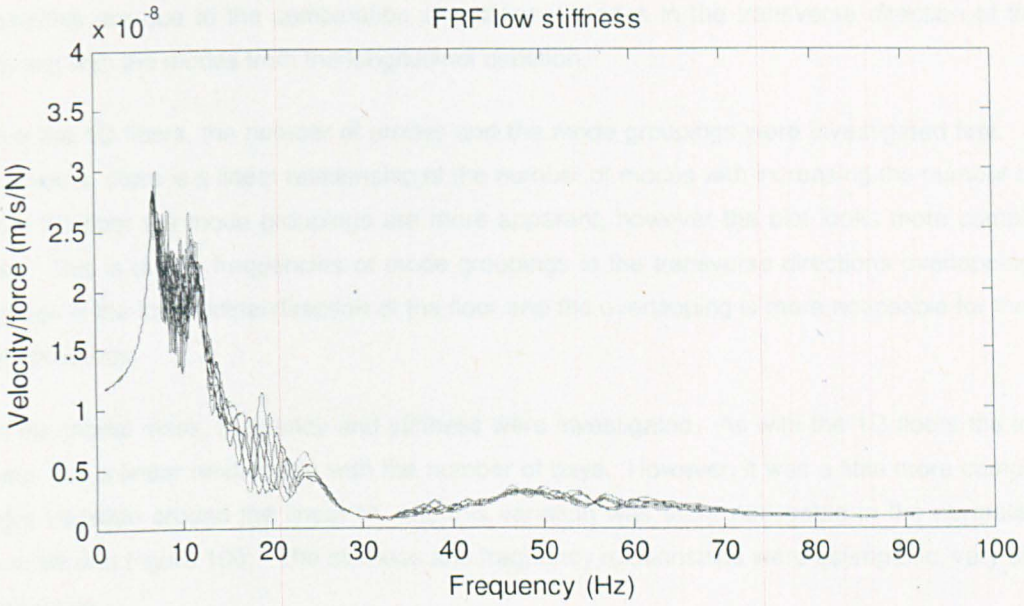

Figure 103 – FRF of the centre bay with increasing bays (soft floor)

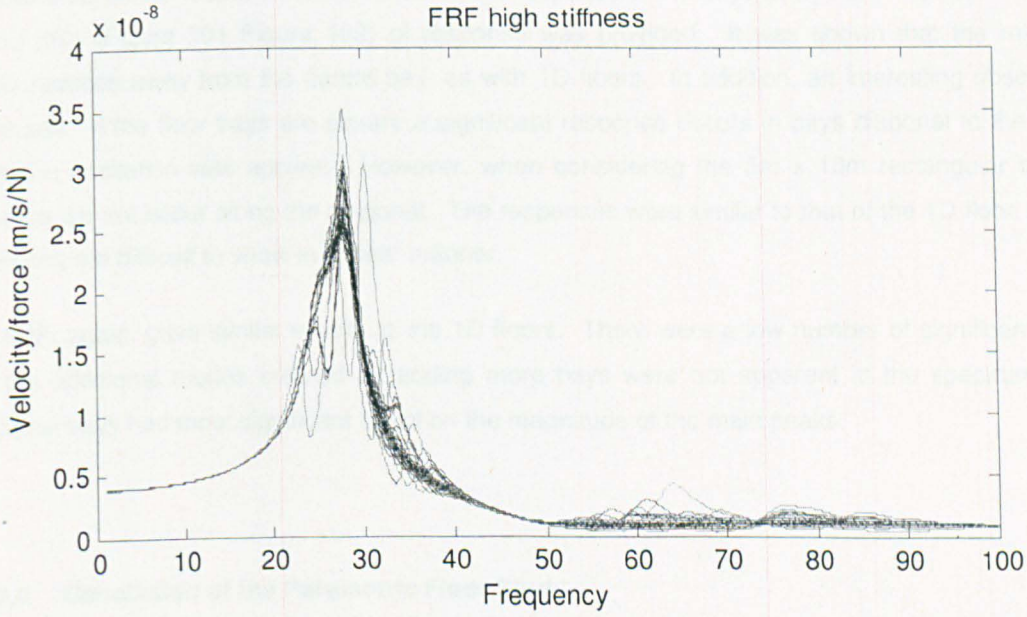

Figure 104 – FRF of the centre bay with increasing bays (stiff floor)

5.2.2.3 Summary of the 2D Floor Parametric Study

The 2D floor parametric study showed that the relationship between the 2D floor's dynamic properties and the number of bays was similar to that for the 1D floors. However, there are some differences, with the relationships of the 2D floor being more complex then the relationships of the 1D floors. The

complexities are due to the combination of additional modes in the transverse direction of the floor combining with the modes from the longitudinal direction.

As with the 1D floors, the number of modes and the mode groupings were investigated first. As with the 1D floors, there is a linear relationship of the number of modes with increasing the number of bays. For the 2D floor the mode groupings are more apparent, however the plot looks more complex and messy. This is due to frequencies of mode groupings in the transverse directions overlapping mode groupings in the longitudinal direction of the floor and the overlapping is more noticeable for the higher mode groupings.

Next, the modal mass, frequency and stiffness were investigated. As with the 1D floors the increase in mass had a linear relationship with the number of bays. However, it was a little more complex with a slight variation around the linear fit, and this variation was more noticeable in the normalised plot (Figure 99 and Figure 100). The stiffness and frequency relationships were asymptotic, very similar to the 1D floors.

Next, the maximum RMS response, with a 0.5s window, was investigated. Due to the nature of the 2D floor having two dimensions, similar plots with the 1D floor analysis are not possible. A 2D floor requires a 3D plot of response to demonstrate the response of the bays away from mid-bay. Hence, a contour plot (Figure 101 Figure 102) of response was provided. It was shown that the response rapidly reduces away from the centre bay, as with 1D floors. In addition, an interesting observation was made. If the floor bays are square a significant response occurs in bays diagonal to the bay in which the excitation was applied. However, when considering the 5m x 10m rectangular bay the response did not occur along the diagonal. The responses were similar to that of the 1D floor, but the responses are difficult to show in a clear manner.

The FRF, again, gave similar results to the 1D floors. There were a low number of significant peaks and the additional modes created by adding more bays were not apparent in the spectrum. The additional bays had most significant effect on the magnitude of the main peaks.

5.2.2.4 Conclusion of the Parametric Floor Study

It was shown that the 1D and 2D floors exhibit similar relationships of their dynamic properties and the number of bays making up the floor, although the 2D floor was a little more complex. All the relationships are relatively simple and can easily be curve fitted. Due to this curve fitting, it may be possible to extrapolate from a single bay the properties of a floor with any number of uniform bay configurations. Due to the similarities of the 1D and 2D relationships, it may also be possible to use the relationships from the simpler 1D analysis to estimate the properties of the 2D structure.

The next section will explore the possibility of estimating the properties of multi-bayed structures from the properties of a single bay. If it is possible to obtain reasonably accurate results from extrapolation, it may be possible to offer an alternative simplified method, more accurate than the current published design guidance. It is unlikely that the accuracy will come close to that of a complete FEA, however. the goal would be to achieve better accuracy than the best current simplified guidance, i.e. the Concrete Centre guide.

5.3 Improved Simplified Guidance

Previously in this chapter, it has been shown that natural frequencies can be reasonably accurately obtained for the first mode group of a multi-bayed structure. It has also been shown that in regular, uniform floors, the first mode grouping will dominate the response to walking excitation. However, modal mass estimates were shown to be very poor due to assumptions of the mode shape. If the accuracy of the modal mass can be improved, then as the first mode grouping governs the response, it would be possible to obtain an accurate response estimation of the floor using the first mode grouping.

When considering the FRF spectra of multi-bay floors, the individual modes of the mode groupings are not apparent, however, there are clear peaks in the FRF at approximately the modal frequencies of a single bay. As the number of bays is increased the frequency of the peak remains relatively constant, however the amplitude reduces. An additional observation is that if the second, or higher mode grouping is considered, the reduction in the peak's amplitude reduces less than that of the first mode grouping. This suggests that the reduction has some dependence on frequency.

Another consideration is the contribution of columns in modal mass estimation. A floor with no columns would have a free body mode, with a modal mass equal to the total mass of the structure. If the floor were supported by springs at the edges with zero stiffness, the mode would still be a free body mode. As the spring stiffness is increased, the modal mass reduces until it is equal to a floor with fixed supports at the column locations. As such, one would assume softer columns would therefore increase the modal masses. Any modal mass variations are likely to be due to vertical deformation of the columns, which has been observed in global floor modes of real structures. The contribution of columns is sometimes overlooked as they have been shown not to influence natural frequency much, with the influence depending on the relationship of column stiffness and slab point stiffness. However, columns have never been considered when evaluating the accuracy of modal mass estimations.

This section investigates how to estimate a single equivalent mode for response estimations by estimating an equivalent modal mass that includes modal amplitudes and modal masses of the

individual modes within a mode group. The section also investigates vertical column stiffness and its relationship with the floors modal mass.

5.3.1 Equivalent Mode Estimation

It was shown earlier in the chapter that increasing the number of bays within a floor structure creates mode groupings which contain the same number of modes as there are bays. When looking at a point mobility from the floor, the additional modes from increasing the bays are not apparent with the point mobility similar to a 1 bay floor but with different amplitudes. As such, if the excitation point is considered to be fixed, the mode grouping could be considered as a single mode that approximates the contribution of all the modes within a mode grouping. This is a logical extension to a design guide that uses one mode to estimate the response. As it was also shown that for uniform bay spacings the first mode group governs the response, only mode that is required for response estimation. For this section, when peak values are stated they are for the first mode group. If the force is constant for all frequencies (i.e. has a flat power spectral density), the amplitude of point mobility is a function of mode shape and modal mass. If, for the equivalent mode, the mode shape is assumed to have unity normalised mode shape [124], and the force is kept constant, the variation of the FRF amplitude can be achieved by varying the modal mass of the equivalent mode. As modal mass has a linear relationship with the amplitude of the FRF, if the FRF is normalised so that the peak value is 1 for a 1 bay structure, the value for the other bay configurations will be the inverse of the increase in modal mass. Therefore, if this relationship can be obtained, an equivalent mass for additional bays can be obtained if the modal mass of a single mode can be estimated. Regarding the dominant frequency of the mode group, there is a variation with increasing the number of bays but the variation is small.

Figure 105 shows the FRF with increasing number of bays overlaid for the soft and stiff floors, Figure 106 shows the peak amplitudes of the first mode grouping from the FRF with increasing number of bays for the soft and stiff floors and Figure 107 shows their inverse, normalised so that a single bay has a value of 1. This effectively gives a multiplier of the modal mass obtained from a single bay for the equivalent mass.

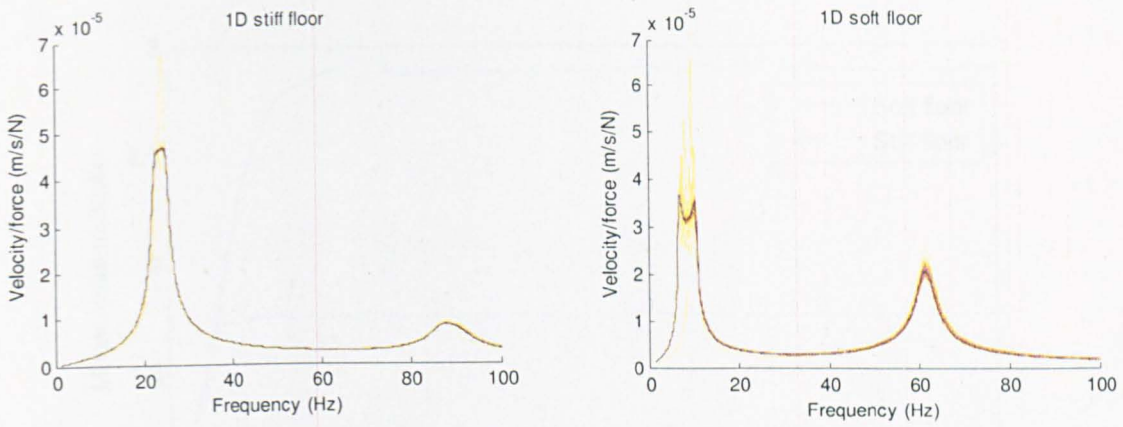

Figure 105 ***(From left to right)*** **– Point mobility for 1D stiff floor with increasing bays; point mobility for 1D soft floor with increasing bays**

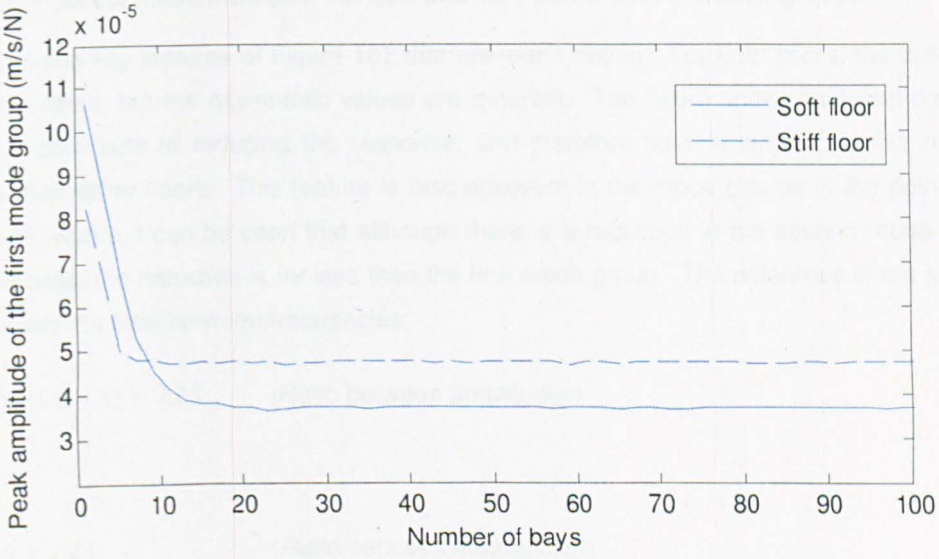

Figure 106 – Peak response of the first mode group with increasing bays for the soft and stiff floors

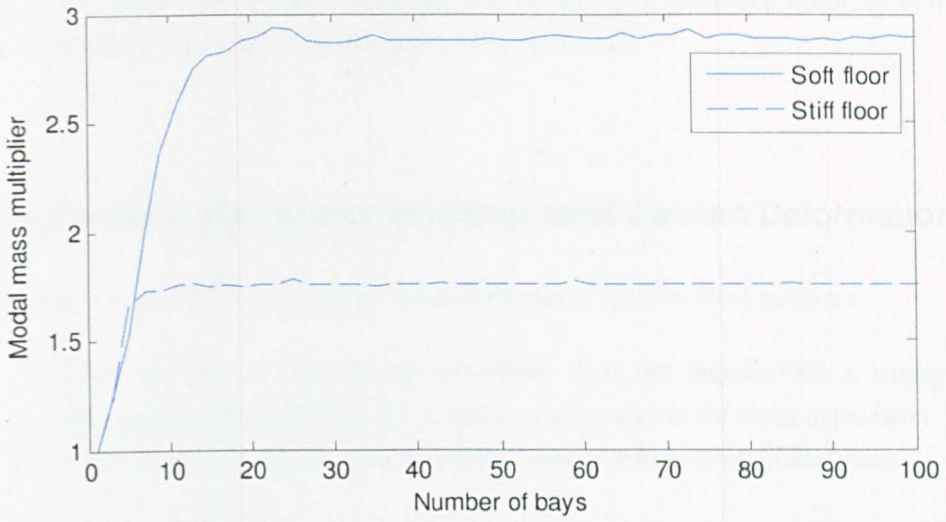

Figure 107 – Modal mass multiplier for soft and stiff floors with increasing bays

There are some key features of Figure 107 that are worth noting. For both floors, the initial gradient roughly the same, but the asymptotic values are different. The figure shows that with the soft floor more bays contribute to reducing the response, and therefore have a larger possible reduction in response than stiffer floors. This feature is also apparent in the mode groups in the point mobilities (Figure 105) where it can be seen that although there is a reduction in the second mode group with increasing bays, the reduction is far less than the first mode group. The difference in the amplitude is approximately the ratio between frequencies:

$(2.8 - 1)/(1.8 - 1) = 2.25$ (Ratio between amplitudes)

and

$21.58/9.6 = 2.25$ (Ratio between frequencies)

Due to this relationship it is possible to simply curve fit the multiplier, A_{mass}, for any frequency:

$$A_{mass} = 0.0073 f_n - 1.1e^{4.3 n_{bays}}$$ **Equation 62**

where f_n is the fundamental floor modal frequency of a single bay and n_{bays} is the number of bays in the structure. When estimating an equivalent mass for a 2D structure the multiplier must be applied twice, e.g. if there are 11 bays in the x direction and 3 bays the y direction and the modal mass of the fundamental mode of a single bay is m with a frequency of f_n, the equivalent mass would be:

$$A_{mass\_1} = 0.0073 f_n - 1.1e^{4.3 \times 11}$$
$$A_{mass\_2} = 0.0073 f_n - 1.1e^{4.3 \times 3}$$
$$m_{equiv} = m \cdot A_{mass\_1} \cdot A_{mass\_2}$$

The only problem now remaining is the initial estimate of modal mass, which with current methods is notoriously poor. The next section investigates the possibility of increased accuracy in modal mass estimate by including axial column deformation in the calculation.

5.3.2 Modal Mass Estimation Including Axial Column Deformation

There are two reasons for the poor modal mass estimates in the simplified guidance:

1. The edge of the floor slab in the simulation does not approximate a simply supported boundary condition or the boundary condition used to create the mass expression.
2. Column deformation, which is not considered, has an influence on modal mass.

As the approximation of the slabs supports and boundary conditions would be specific to the floor type it is not considered. This section investigates the influence of column stiffness and examines how axial deformation of the column contributes to the modal mass.

Due to a simple method being required, there is a limited complexity that can be adopted in the modification. Modal mass is obtained from the mass distribution and the mode shape. An accurate estimation of the mode shape is not possible without detailed calculations, and as such is not within the scope of this work. Any change in modal mass will be related to the stiffness of the column.

The columns are square and their stiffness will be varied by changing real life parameters, i.e. that column length, and the column width. The axial stiffness of the column can be defined by:

$$k_a = \frac{EA}{L}$$ **Equation 63**

and the flexural stiffness by:

$$k_f = \frac{12EI}{L^3}$$ **Equation 64**

where E is the Young's modulus of the material, A is the cross-sectional area of the column, L is the column length and I is the second moment of area of the column. Changing either of the column parameters will change both column stiffnesses, but as the stiffnesses can be quantified, it is possible to assess k_a and k_f affect on modal mass separately.

If one considers a slab supported along the edge by vertical springs with zero stiffness, the fundamental mode of the slab would be a rigid body mode with a modal mass equal to the total mass of the slab. If the spring stiffness is increased the modal mass will decrease. As the spring stiffness approaches infinity, the slab will become more like a simply supported slab, as such the modal mass will approach the modal mass of a simply supported slab, i.e. 25% of the total mass. With this is mind, it is likely that the vertical deformation of the column will have the largest influence on the floors modal

mass. In reality, the slab spring analogy is not exactly comparable. Firstly, the columns only support the slab at the corner points and are not continuous supports along the slab length. Secondly, due to strength limitations of the columns, a low enough stiffness would never be achieved for the modal mass to approach the total mass (i.e. a near rigid body mode).

A parametric study of over 17,000 floors was conducted, varying the slab depth, column length and column diameter. It was shown that the column size influences modal mass due to both the axial deformation and the column bending. A variation of modal mass will be shown by evaluating ratios of deflection, which can then be used to improve the modal mass estimation.

5.3.2.1 Column Parametric Study

The parametric study was conducted on a 7m square flat slab with a depth that ranged from 0.1m to 0.5m at 0.01m intervals. The slab was supported at four corners by columns, which had lengths ranging from 2m to 4m at 0.1m intervals. The columns were square with widths ranging from 0.05m to 1m at 0.05m intervals. The columns with the smallest widths are not realistic; however, they do demonstrate an interesting relationship with modal mass.

Figure 108 shows how the modal mass varies with changes in slab depth and column dimensions. The top plot shows how the modal mass varies with each run and the bottom two plots show zoomed sections of the primary plot. A number of clear observations can be made: as the column diameter increases the modal mass decreases asymptotically, as column length increases there is a linear increase in the modal mass, as the slab depth increases the modal mass increases with a slight curve, but a linear fit could be assumed with little error. The observations are consistent with the hypothesis that the modal mass is influenced by the (axial) column deformation.

Figure 109 shows how the modal mass varies with changes in slab depth and column dimensions with respect to axial column stiffness. The top plot shows the results from all runs, whereas the bottom plot shows a zoomed in section. Each plot can be split into bands and rows with each band containing the modal masses for a certain column width and each row containing the modal masses for a certain slab depth. There is a clear relationship between the axial column stiffness and the modal mass, with the modal mass asymptotically reducing with increasing axial stiffness, meaning the modal mass does not increase linearly with slab depth. The top plot of Figure 110 shows this by dividing the modal mass by the total slab mass to form a modal mass ratio. It is clear that there is no single value of ratio for any individual column stiffness and that the variation increases as the axial column stiffness decreases. For very low (and unrealistic) column stiffnesses it can be seen that the modal mass ratio asymptotically approaches 1, i.e. the modal mass equals the total mass where rigid body motion is achieved. Another interesting point is the value of the ratio, usually between 0.44 and 0.5, which is a variation of approximately 12%. Using recommendations from the Concrete Centre guide, which gave similar values to the SCI guide, the ratio would be 0.25, approximately half of the value obtained here.

The variation decreases as the axial column stiffness increases, further agreeing with the hypothesis that the modal mass is influenced by the axial column deformation.

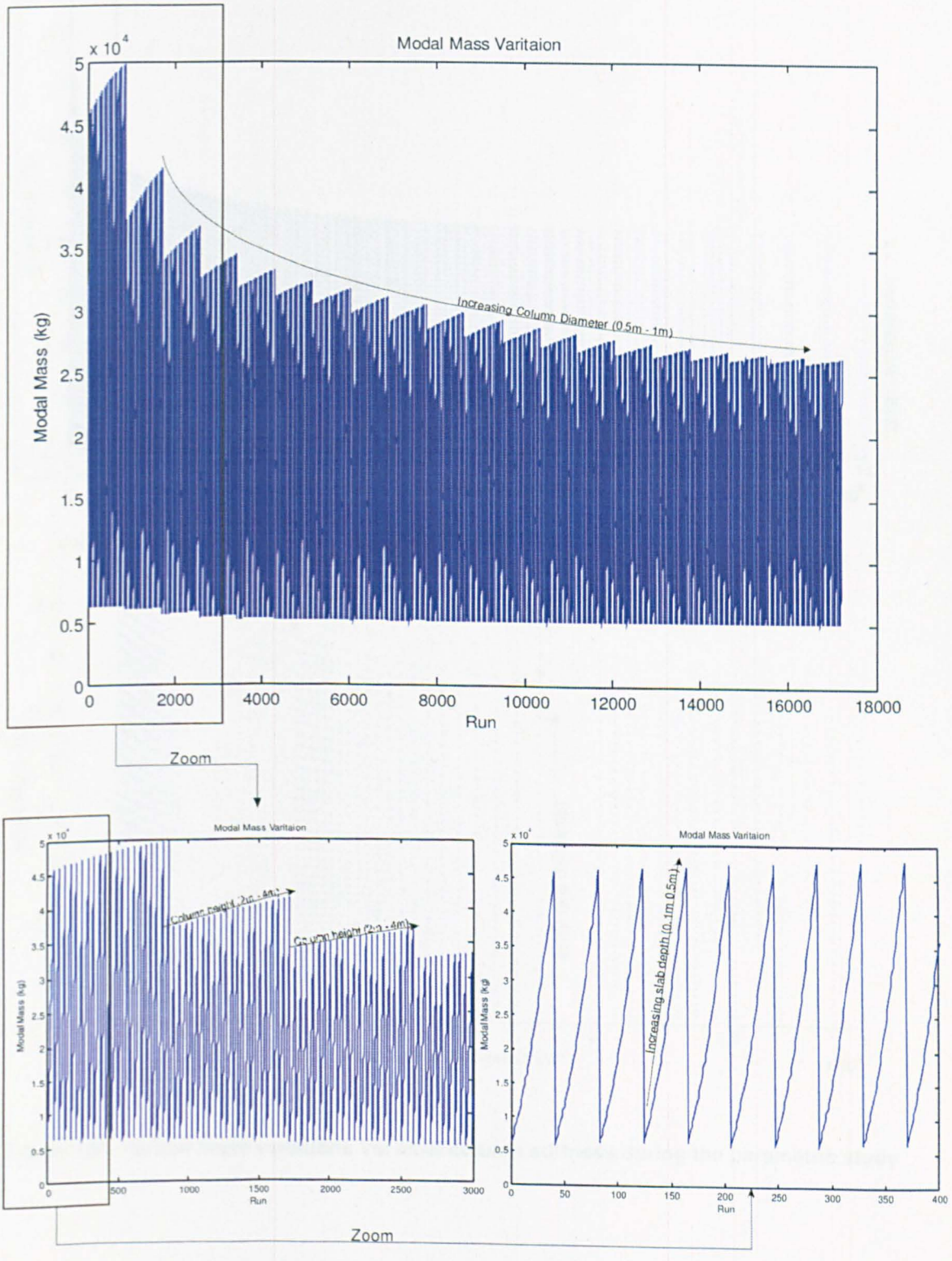

Figure 108 – Modal mass variations during the parametric study; (*top)* change in column diameter; (*bottom left)* change in column height; *(bottom right)* change in slab depth

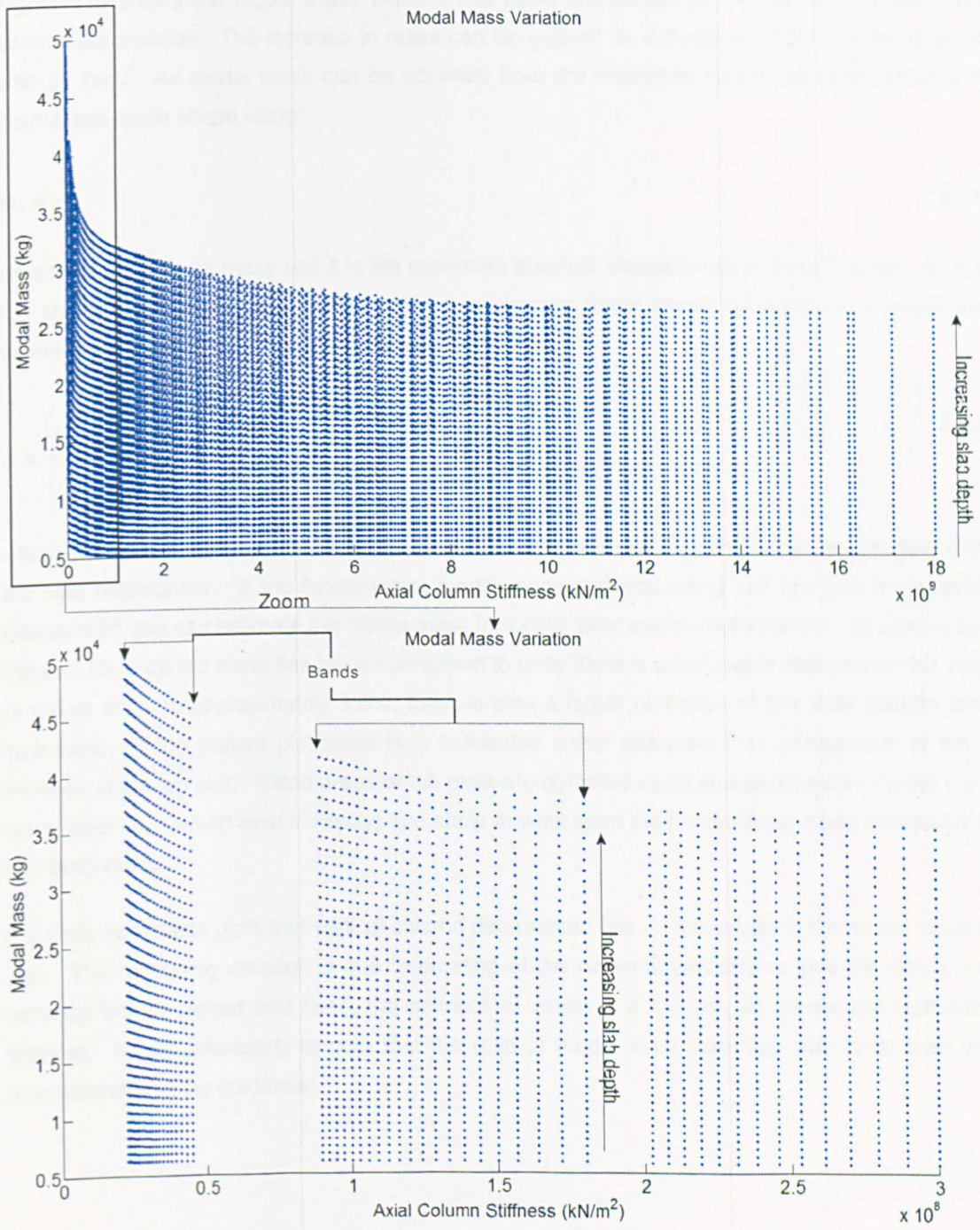

Figure 109 – Modal mass variations Vs. axial column stiffness during the parametric study

To illustrate further the contribution to modal mass, the mass was normalised. The bottom plot of Figure 110 shows the modal mass when it has been normalised by the increase in mass due to column deformation. The increase in mass can be defined as a multiplier to the modal mass of the slab by itself. As modal mass can be obtained from the maximum modal displacement of a mass normalised mode shape using:

$$m_i = \frac{1}{\Delta_i^2}$$ **Equation 65**

where m is the modal mass and Δ is the maximum absolute displacement of the i^{th} mode. As such, if the static deflected shape is similar to the fundamental mode shape, an increase in mass can be obtained from a ratio between the static displacements:

$$A = \frac{\left(\frac{1}{\Delta_{total}^2}\right)}{\left(\frac{1}{\Delta_{slab}^2}\right)}$$ **Equation 66**

where the subscripts total and slab represent the complete structure including the columns and just the slab respectively. If the fundamental modal mass obtained using just the slab is multiplied by Equation 66 one can estimate the modal mass including axial column deformation. As can be seen in Figure 110, once the mass has been normalised to unity there is a noticeable reduction in the variation of modal mass to approximately 7.5%, there is also a larger reduction as the axial column stiffness increases. In the bottom plot there is a noticeable sharp reduction that corresponds to the large increase in the top plot. These areas of the plots are obtained using unrealistic column sizes (i.e. they are smaller then would exist in reality) and show at what point the fundamental mode transforms into a free body mode.

It is clear from these plots that vertical column deformation has an influenced in the modal mass of the slab. The remaining variation is due to bending of the columns and slab to give the slab a support between that of pinned and fixed, the stiffness of which is a function of column stiffness and slab stiffness. It also interesting to note that the ratio of modal mass and total slab is far from what is recommended in the guidance.

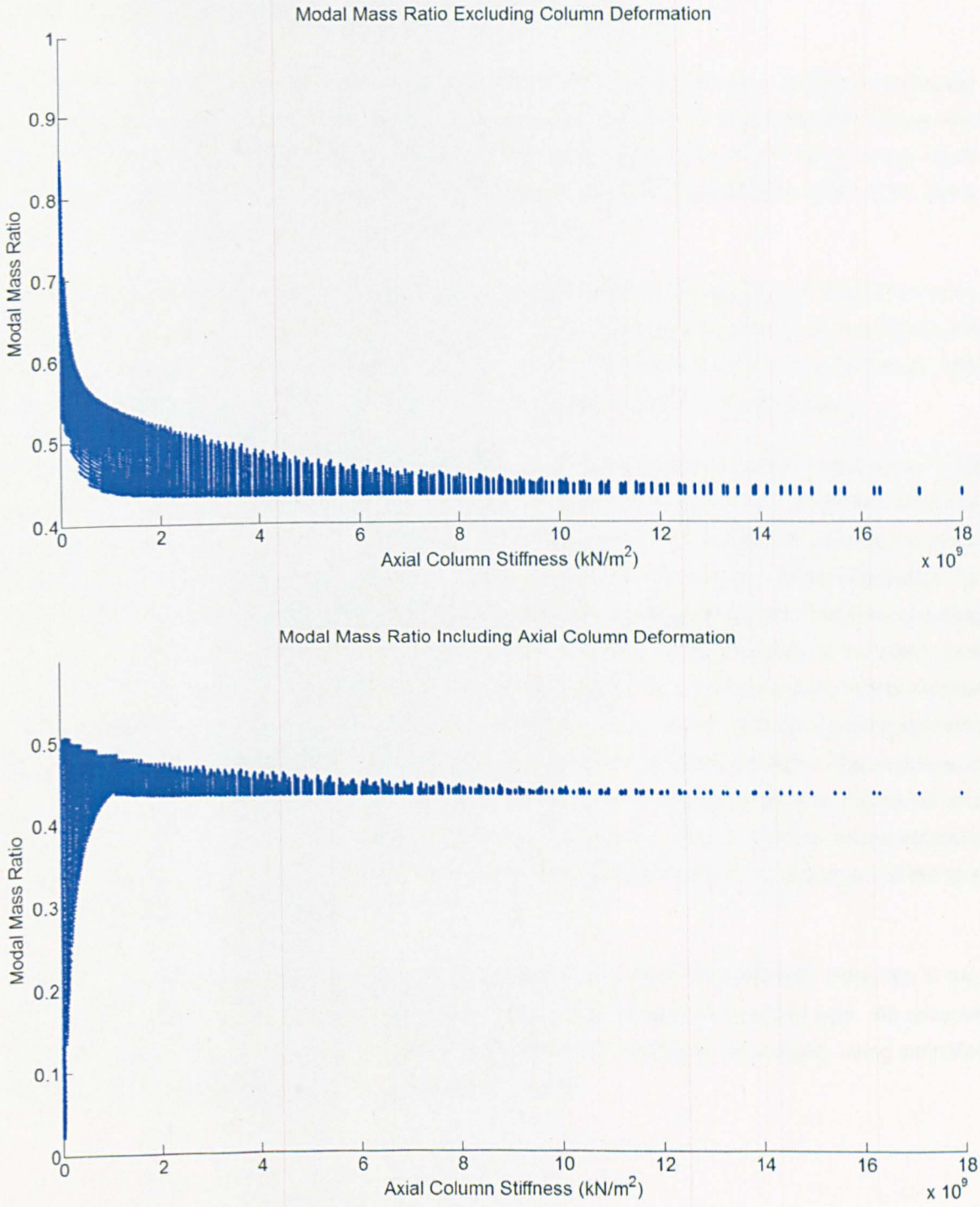

Figure 110 – Ratio of modal mass and total slab mass with increasing column stiffness, not including axial column deformation *(top)* and with modal mass adjusted to include axial column deformation *(bottom)*; the variation present after axial column deformation is due to flexural motion of the column

5.3.3 Conclusion of Improved Simplified Guidance

This section has shown that the closely spaced modes within a mode grouping can be approximated as a single equivalent mode if the excitation point is fixed. For uniform structures with regular bay sizes the response is governed by the first mode group, requiring analysis of just this mode group is sufficient to represent the structure. The method presented uses the modal properties of a floor with a single bay to estimate properties of a floor with multiple bays.

Although a single bay can be used to estimate an equivalent mode of multiple bays, the problem of an initial accurate mass estimate still remained. A parametric study was conducted to investigate the influence of columns on the modal mass of the floor. It was shown that there is a clear influence, with bending and axial deformation of the column contributing to the variation in modal mass.

It was also shown that the amount of the total slab mass that contributes to the modal mass is far greater then reported in the guidance, with approximately 43% of the slab mass contributing, whereas the guidance recommends 25%. This is due to the stiffness and mass distribution causing the mode shape not to match a simply supported plate. Depending on the stiffness and mass distribution, for other floors, the mode shape may be more similar to a simply supported plate, and therefore reducing the modal mass. As such a slab's modal mass should be between 25% and 43% of the slab's total mass. One may think that a 1D floor acts similar to a beam, and this is the reason why modal mass is similar to a beam, and with a 2D floor, this would not be the case. When considering the parametric study of the number of bays it was shown that even for a 2D floor, doubling the size of the structure, in any direction, approximately doubled the modal mass and total mass (top plots of Figure 99 and Figure 100). As such, if a floor with 10 x 1 bays (with modal mass 43% of the total mass) structure was extended to 10 x 10 bays, the modal mass would increase by a factor of 10, but so would the total mass, so the ratio remains constant.

It is likely that small empirically alterations could be made to the simplified guidance. However, to gain any sufficient accuracy, the empirical alterations would have to be specific to a floor type. An accurate simplified guidance for all floors is not possible with the current methods. As a result, using simplified methods will give conservative overestimation of responses.

5.4 Investigation of Modelling Detail

So far, this chapter has shown that modal mass is difficult to estimate. Various methods have been proposed, but these methods are still inaccurate and will only work for a simple uniform structure. FEA is currently the only accurate method for modal mass estimates and it can also be used for more complex structures, which simplified methods cannot. As such, if time and cost allows FEA should be used.

Often time may not be available, or it may not be financially viable, to create a full FE model, but more accurate results from the simplified methods are required. In such circumstances, a more simple abstraction of the model is desired, but there is no published method for an accurate implementation of this. This section investigates the loss of accuracy when reducing the modelling detail away from points of interest (i.e. excitation and response points) on the FE model.

5.4.1 Mesh Density of Floor Bays

Often in response estimation of floors it is reasonable to select an area of the floor which is likely to have a large response, then, response estimation can be calculated at that point and assumed to be a worst case for the rest of the floor. The area where the force and response are located requires a reasonable level of modelling detail. However, the rest of the structure serves to create the required boundary conditions of the area of interest. Does the rest of the structure require such a high degree of detail?

The floor used in this example was the same as used in the parametric study from previous in the chapter. Figure 111 shows the mesh layout of the floor for the centre 5 bays. It can be seen that the centre bay is modelled in detail. The 5^{th} bay, and all bays beyond, are meshed in low detail, with just 4 shell elements representing the floor. The 3^{rd} bay can be considered a transitional bay, modelled in half detail. The transitional bay is required to allow and acceptable element shapes while decreasing the mesh density.

The procedure to be applied obtains the velocity (mobility) FRF at the centre bay using a fully meshed model. A second point mobility will be obtained using the partial modelled floor. The two FRFs will then be compared, if there is a significant difference in response the detail of the model will be increased and the procedure repeated until the FRFs match.

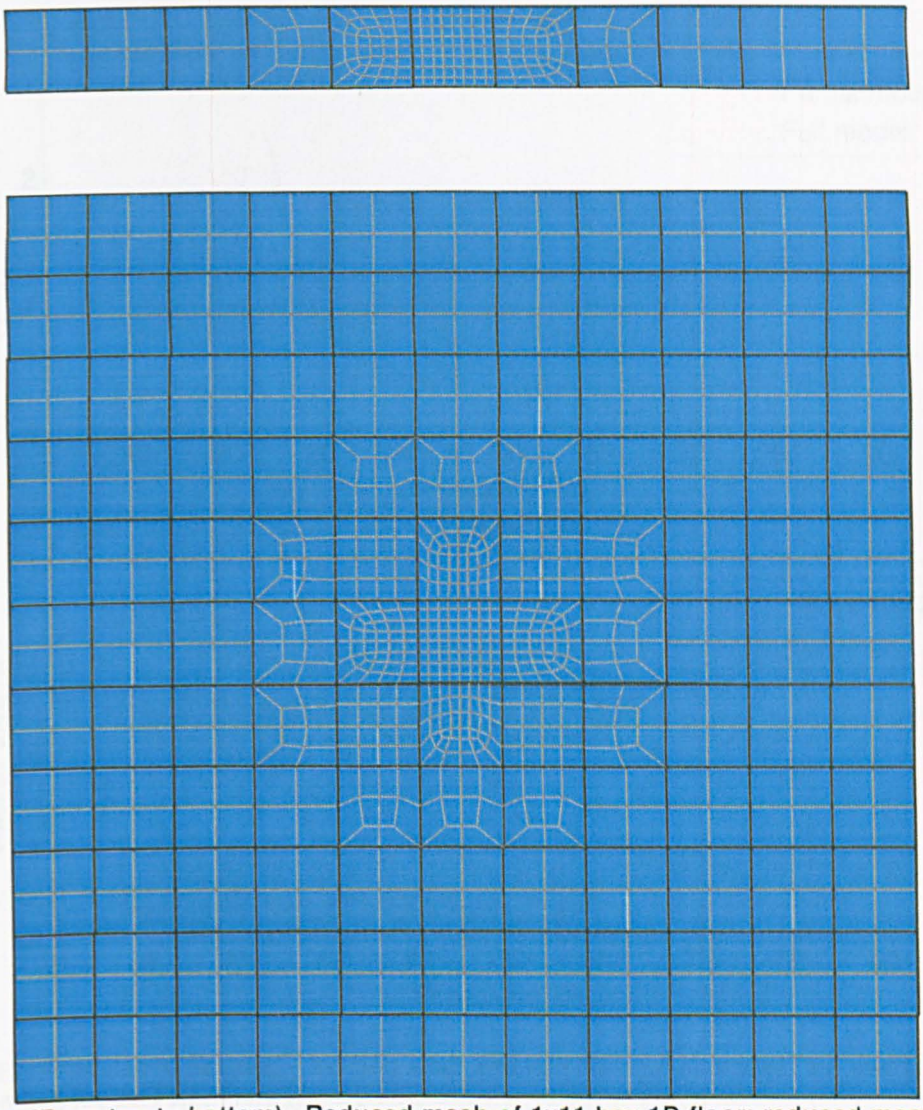

Figure 111 ***(From top to bottom)*** **- Reduced mesh of 1x11 bay 1D floor; reduced mesh of 11x11 bay 2D floor**

Figure 112 and Figure 113 show the FRFs for the 1D and 2D floors respectively. As can be seen there is very little difference between the FRFs, and therefore, no increase in mesh detail is required. The largest differences occur at the higher frequency end of the bandwidth. This is expected as more nodes are required to form the mode shapes at those frequencies. At the centre, enough nodes exist, whereas there are not at the rest of the structure.

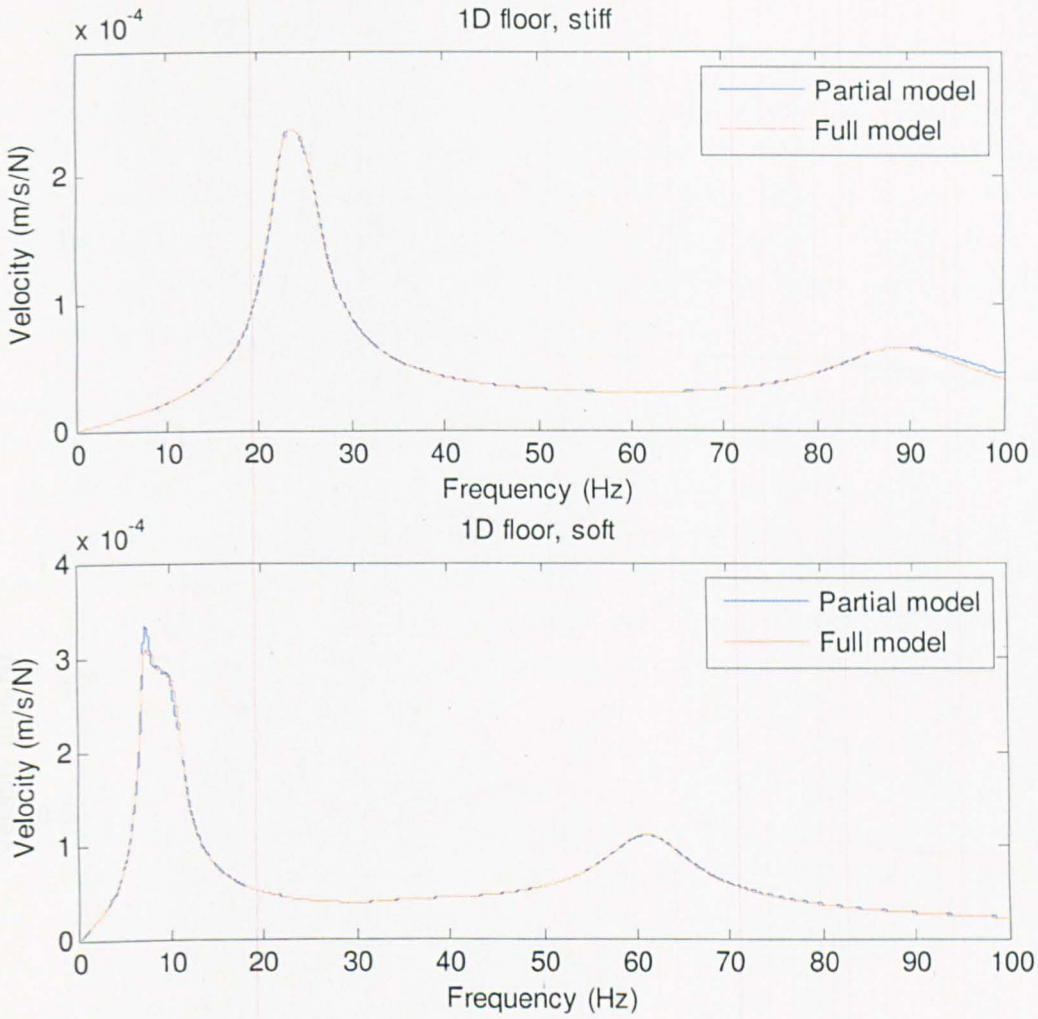

Figure 112 ***(From top to bottom)*** **– 2D Soft floor and stiff floor; Full model FRF overlaid with the reduced mesh model FRF, there is very little difference between the two**

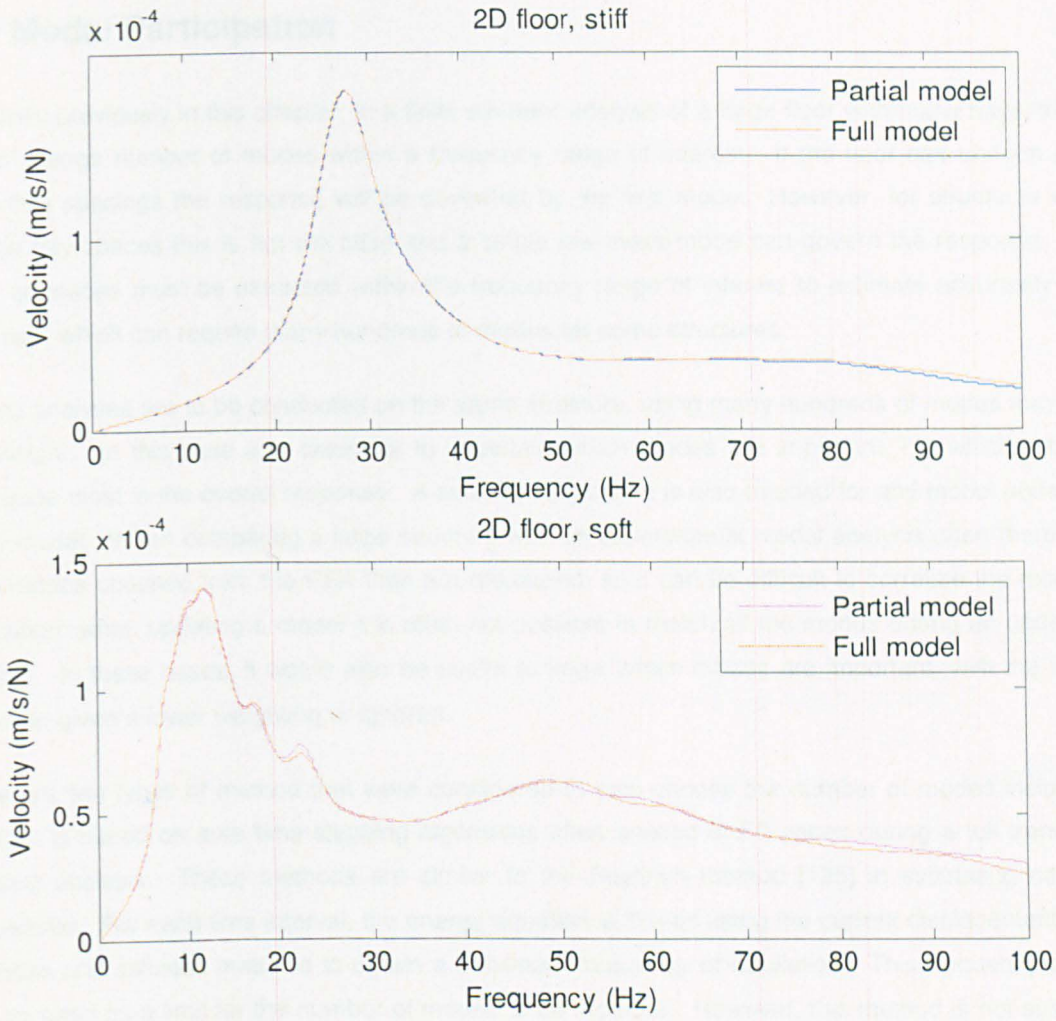

Figure 113 ***(From top to bottom)*** **– 2D Soft floor and stiff floor; Full model FRF overlaid with the reduced mesh model FRF, there is very little difference between the two**

5.4.2 Conclusion of Modelling Detail

It was shown that for 1D and 2D floors the entire floor area does not need to be modelled in detail to estimate responses accurately. Modelling the bay of interest in detail, with the rest of the structure modelled relatively crudely is sufficient. A transition between the crude modelling and the detailed modelling is necessary to avoid any issues with ill-conditioned element shapes. For the stiff floor there was no noticeable difference between the fully meshed floor and the reduced mesh, however, there was a small difference in the soft floor in the first mode group. This is likely due to more bays contributing to the amplitude of the FRF of the first mode group. As such, the crude modelling of the rest of the structure had more influence. The difference in the soft floor, however, is negligible.

5.5 Modal Participation

As shown previously in this chapter, in a finite element analysis of a large floor with many bays, there will be a large number of modes within a frequency range of interest. If the floor has uniform and equal bay spacings the response will be governed by the first mode. However, for structures with uneven bay spaces this is not the case and a single low-mass mode can govern the response. As such, all modes must be extracted within the frequency range of interest to estimate accurately the response, which can require many hundreds of modes for some structures.

If many analyses are to be conducted on the same structure, using many hundreds of modes may not be efficient. In this case it is desirable to ascertain which modes are important, i.e. which modes participate most in the overall response. A similar requirement is also needed for any model updating of the model. When comparing a large structure with an experimental modal analysis often there are more modes obtained from the FEA than are measured, so it can be difficult to correlate the modes. In addition, when updating a model it is often not possible to match all the modes during an updating process. In these cases, it would also be useful to know which modes are important, with the least important given a lower weighting or ignored.

There are two types of method that were considered to help choose the number of modes included. The first is based on auto time-stepping algorithms often applied in FE codes during a full transient dynamic analysis. These methods are similar to the Rayleigh method [125] in estimating natural frequencies. For each time interval, the energy equation is solved using the current displacement and the mass and stiffness matrices to obtain a maximum frequency of oscillation. This frequency could then be used as a limit for the number of modes to be included. However, this method is not suitable for a number of reasons. Firstly, the mass and stiffness matrices are required for the calculations, which can be difficult to obtain from commercially available FE software. Secondly, the method only obtains a frequency limit of the system. As this is often well over 100 Hz and because in floor structures the maximum frequency of concern is generally less than 100 Hz, it is unlikely to prove useful. The second method is a method briefly described by NAFEMS [44, 126] (shown in Chapter 2.3.4.2.4).

The rest of this section evaluates the NAFEMS method. Due to this brevity in which this method was published a derivation of the method is attempted. The method is then applied to a simple beam structure to show how the participation factors can be visualised. Finally, the method is adjusted to remove any dependence on the system matrices' and factored by Arup's effective impulse [127, 128] to give a frequency weighting more consistent for transient response floors.

5.5.1 Method Description

This is a description and example of the method presented by NAFEMS [126] to estimate the importance of modes for analysis by modal superposition..

The force input of a structure can be written as a summation of all the forcing functions:

$$\{f(t)\} = \sum_i [\cdots \quad F_i \quad \cdots] \begin{Bmatrix} \vdots \\ a_i(t) \\ \vdots \end{Bmatrix} \qquad \textbf{Equation 67}$$

where $a_i(t)$ are the scalar time histories, F_i is one spatial distribution of forces over the structure and $f(t)$ is the distribution of the time histories over the structure, curly brackets, { }, represent a column vector and square brackets, [ ] , represent a matrix. If there is a single forcing function this can be written as:

$$\{f(t)\} = \{F\}a(t) \qquad \textbf{Equation 68}$$

A work quantity can be obtained if the force is multiplied by the maximum displacement:

$$(WD) = \{F\}^T\{max|u(t)|\} \qquad \textbf{Equation 69}$$

where (WD) is a measure of energy in Nm and $u(t)$ is the displacement time history vector and max represents the maximum value over time. The maximum displacement can be found using the Duhamel integral:

$$\{u(t)\} = \int_0^t [h(t-\tau)]\{f(\tau)\}d\tau \qquad \textbf{Equation 70}$$

where h is an impulse response function matrix. If Equation 70 is substituted into Equation 69 this will yield:

$$(WD) = \underbrace{\{\mathrm{F}\}^T max}_{\mathrm{A}} \underbrace{\left| \int_0^t [h(t-\tau)]\{f(\tau)\}d\tau \right|}_{\mathrm{B}} \qquad \textbf{Equation 71}$$

This can be split into a spatial varying part, A and a time varying part, B. Equation 71 can be represented in the modal domain as follows.

The velocity response of an oscillator due to an impulse is:

$$\dot{u} = \sum_{r=1}^{m} \{\phi_r\}\{\phi_r\}^T \frac{I}{m} \sin(\bar{\omega}_r t)\, e^{\omega_r \xi t} \qquad \textbf{Equation 72}$$

which, for a unit impulse and converting to displacement is given by:

$$u = \sum_{r=1}^{m} \{\phi_r\}\{\phi_r\}^T \frac{\sin(\bar{\omega}_r t)}{m_r \bar{\omega}_r} e^{\omega_r \xi_r t} \quad \textbf{Equation 73}$$

where ϕ is the mode shape vector, ω and $\bar{\omega}$ are the circular and damped circular frequencies respectively, ξ is the modal damping ratio, m is the modal mass and the subscript r represents the current mode. This provides the IRF, h, in Equation 71.

Equation 68 and Equation 73 are substituted into Equation 71 to form:

$$(WD) = \sum_{r=1}^{m} F \cdot max \left| \int_0^t \{\phi_r\}\{\phi_r\}^T \frac{\sin(\bar{\omega}_r t)}{m_r \bar{\omega}_r} e^{\omega_r \xi_r t}(t-\tau) F_i a(\tau) d\tau \right| \quad \textbf{Equation 74}$$

Since a modal force is defined as:

$$P_r = \{\phi_r\}^T \{F\} \quad \textbf{Equation 75}$$

the space varying terms can be removed from the integral so Equation 74 can be written as:

$$(WD) = \sum_{r=1}^{m} P_r P_r \cdot max \left| \int_0^t \frac{\sin(\bar{\omega}_r t)\, e^{\omega_r \xi_r t}(t-\tau) a(\tau)}{m_r \bar{\omega}_r} d\tau \right| \quad \textbf{Equation 76}$$

where P_r is the scalar modal force of the rth mode.

5.5.2 Investigation of Spatially Varying Part, A

5.5.2.1 Modal Force Convergence

A form of convergence is required so that the addition of mode, r, into Equation 76 has convergence properties that need to be investigated. This convergence can be written as:

$$Q = \sum_{r=1}^{m} Q_r = \sum_{r=1}^{m} P_r P_r \rightarrow \{F\}^T [M]^{-1} \{F\} \quad \textbf{Equation 77}$$

where Q is the scalar modal participation and $[M]$ is the mass matrix.

Equation 77 can be verified as follows:

Since $P_r = \{\phi_r\}^T\{F\}$

It is possible to write:

$$P_r P_r = \{\phi_r\}^T\{F\}\{\phi_r\}^T\{F\} = \{F\}^T\{\phi_r\}\{\phi_r\}^T\{F\}$$

For a set of mass-normalised mode shapes:

$$[\Phi]^T[M][\Phi] = \begin{bmatrix} \vdots \\ \{\phi_r\}^T \\ \vdots \end{bmatrix}[M][\cdots \quad \{\phi_r\} \quad \cdots] = [I]$$

where $[I]$ is the identity matrix. The inverse mass matrix $[M]^{-1}$ can be expressed as:

$$[M]^{-1} = [\Phi][\Phi]^T = [\cdots \quad \{\phi_r\} \quad \cdots]\begin{bmatrix} \vdots \\ \{\phi_r\}^T \\ \vdots \end{bmatrix} = \sum_{r=1}^{m}\{\phi_r\}\{\phi_r\}^T$$

therefore:

$$\sum_{r=1}^{m} P_r P_r = \sum_{r=1}^{m}\{F\}^T\{\phi_r\}\{\phi_r\}^T\{F\} = \{F\}^T[M]^{-1}\{F\}$$

5.5.2.2 Participation Factor Representation using Energy

The modal participation is represented by $Q_r = P_r P_r$ but what does this value represent? Assuming work done can be calculated for a constant force, F, as:

$$(WD) = \int_0^u F\,du$$ **Equation 78**

Elastic (potential) energy stored for displacement, u, is:

$$= \frac{1}{2}ku^2 = \frac{1}{2}Fu = (PE)$$ **Equation 79**

where k is stiffness, u is displacement, F is force and (PE) is potential energy. Therefore it can be shown using Equation 79:

$$(WD) = 2(PE)$$ **Equation 80**

As kinetic energy in an oscillator is given by:

$$(KE) = \frac{1}{2} m\dot{u}^2$$ **Equation 81**

Over a cycle of vibration for an oscillator (PE) represents the maximum potential energy and (KE) represents the maximum kinetic energy and $(KE) = (PE)$. Hence if the time varying part of Equation 71 is considered to be unity, Equation 71, Equation 77, Equation 80 and Equation 81 together give:

$$(WD) = 2(PE) = 2(KE) = P_r P_r = \mathrm{Q_r}$$ **Equation 82**

As the modal participation is directly related to the maximum kinetic energy, a peak velocity can be obtained, which, if considering harmonic motion, can be easily transformed to acceleration and displacement:

$$Q_{vel} \equiv \dot{u}_r = \sqrt{Q_r/m_r}$$ for velocity **Equation 83**

$$Q_{disp} \equiv u_r = \frac{1}{\omega_r}\sqrt{Q_r/m_r}$$ for displacement **Equation 84**

$$Q_{acc} \equiv \ddot{u}_r = \omega_r\sqrt{Q_r/m_r}$$ for acceleration **Equation 85**

As the modal participation directly relates to each metric of response Q_r can be used to show clearly the importance of a mode in each metric required, this is important as vibration criteria are not always specified in a standard manner. The next section will show how the participation works in the response of a simple structure.

5.5.2.3 MDOF Simulation

An MDOF simulation of the participation factors has been conducted where one force distribution was represented by a single impulse at node 5. The beam has a uniform mass of 1kg/m, stiffness of 1000 N/m and no damping. The beam is shown in Figure 114 and natural frequencies are given in Table 10.

A number of values will be obtained: Q_r is the modal participation, the sum of which should be one if all modes are excited, Q_{disp} and Q_{vel} are displacements and velocities respectively calculated from the modal participation using Equation 83 and Equation 84. The maximum velocity and maximum displacements calculated in the analysis will also be shown for comparison.

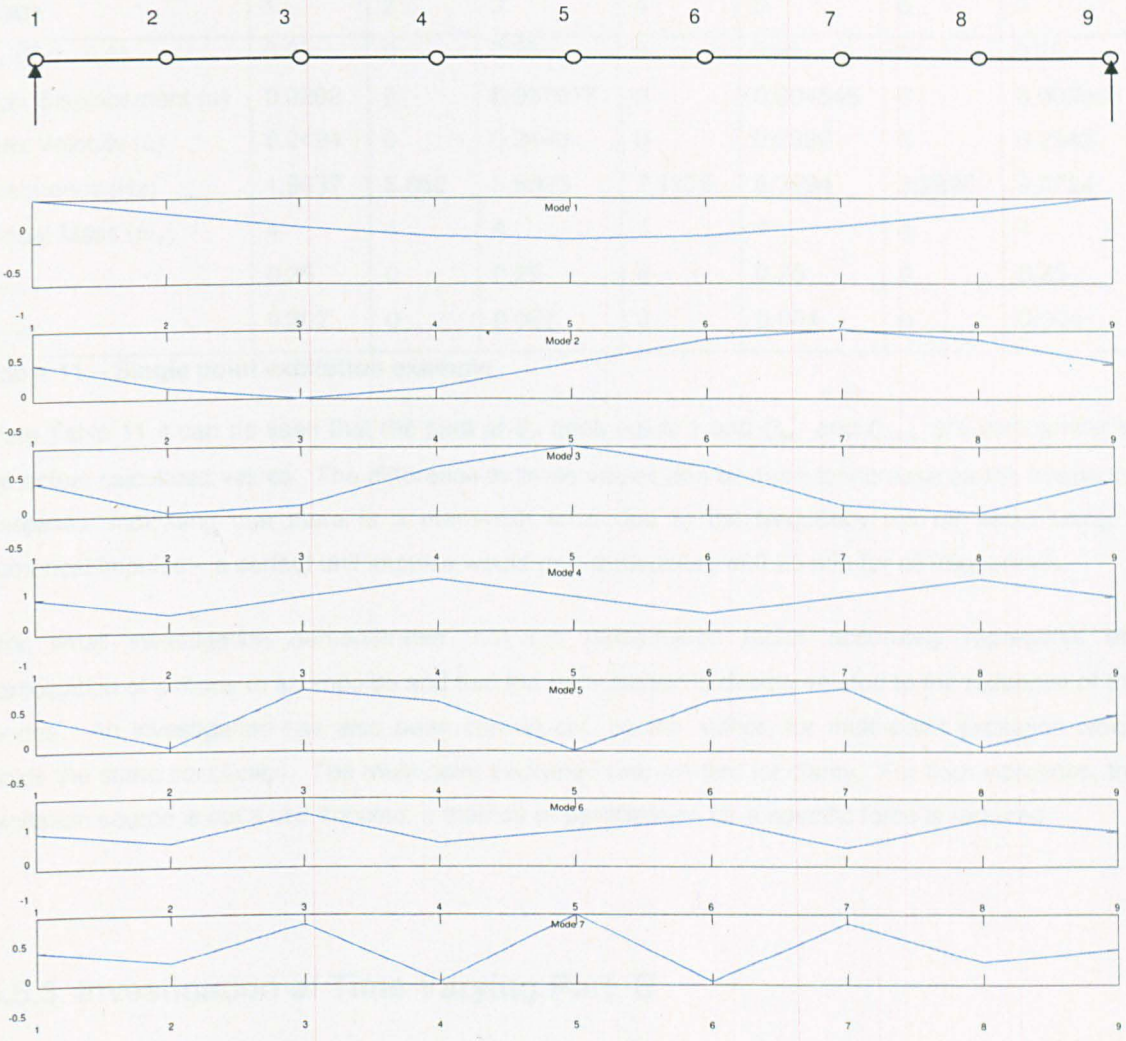

Figure 114 - NDOF beam simulation and mode shapes

Mode	1	2	3	4	5	6	7
Frequency (Hz)	1.9637	3.852	5.5923	7.1176	8.3694	9.2996	9.8724
Modal mass (kg)	4	4	4	4	4	4	4

Table 10 - Natural frequencies of the MDOF example

Single Point Excitation:

A single excitation point was used in this example, where a unit impulse was applied at the beam's mid span. The unit impulse was applied with a value of 100N with duration of 0.01s, dt was 0.01s.

Mode	1	2	3	4	5	6	7
Q_r ($\Sigma Q_r = 1$)	0.25	0	0.25	0	0.25	0	0.25
Max Displacement (u)	0.0202	0	0.007078	0	0.004546	0	0.003965
Max Velocity ($\dot{u}$)	0.2494	0	0.2449	0	0.2386	0	0.2343
Frequency (Hz)	1.9637	3.852	5.5923	7.1176	8.3694	9.2996	9.8724
Modal Mass (m_r)	4	4	4	4	4	4	4
Q_{vel}	0.25	0	0.25	0	0.25	0	0.25
Q_{disp}	0.202	0	0.007	0	0.004	0	0.004

Table 11 – Single point excitation example

From Table 11 it can be seen that the sum of Q_r does equal 1 and Q_{vel} and Q_{disp} are very similar to the actual calculated values. The difference in these values can be seen to increase as the frequency increases, indicating that there is a numerical error due to the frequency roll off when using a numerical impulse – a perfect unit impulse would give a response of 0.25 m/s for all frequencies.

This small investigation demonstrates that the participation factor accurately represents the participation of a mode to an impulse and that the participation is directly related to the response of the modes. An investigation has also been carried out, by the author, for multi-point excitation which yields the same conclusion. The multi-point excitation was omitted for clarity. For floor vibrations, the excitation source is not a unit impulse, a method of participation for a specific force is required.

5.5.3 Investigation of Time Varying Part, B

As the modal participation shown up to this point does not include a force dependent factor, the modal participations are only valid for an impulse excitation, with equal force at all frequencies. When considering a real footfall force, the force is not equal at all frequencies, but is weighted towards the low frequency range, which the modal participation must account for. The time varying part of Equation 76 includes the frequency content of the force.

The time varying part of the Equation 76 is given as:

$$B = max\left|\int_0^t \frac{\sin(\bar{\omega}_r t)\, e^{\omega_r \xi_r t}(t-\tau)a(\tau)}{m_r \bar{\omega}_r} d\tau\right| \qquad \textbf{Equation 86}$$

Equation 86 calculates the peak displacement for a SDOF oscillator, with a fixed mass of unity, using the Duhamel integral. If the damping is set to an appropriate value a response spectrum can be obtained ranging through a number of frequencies shown in Figure 115.

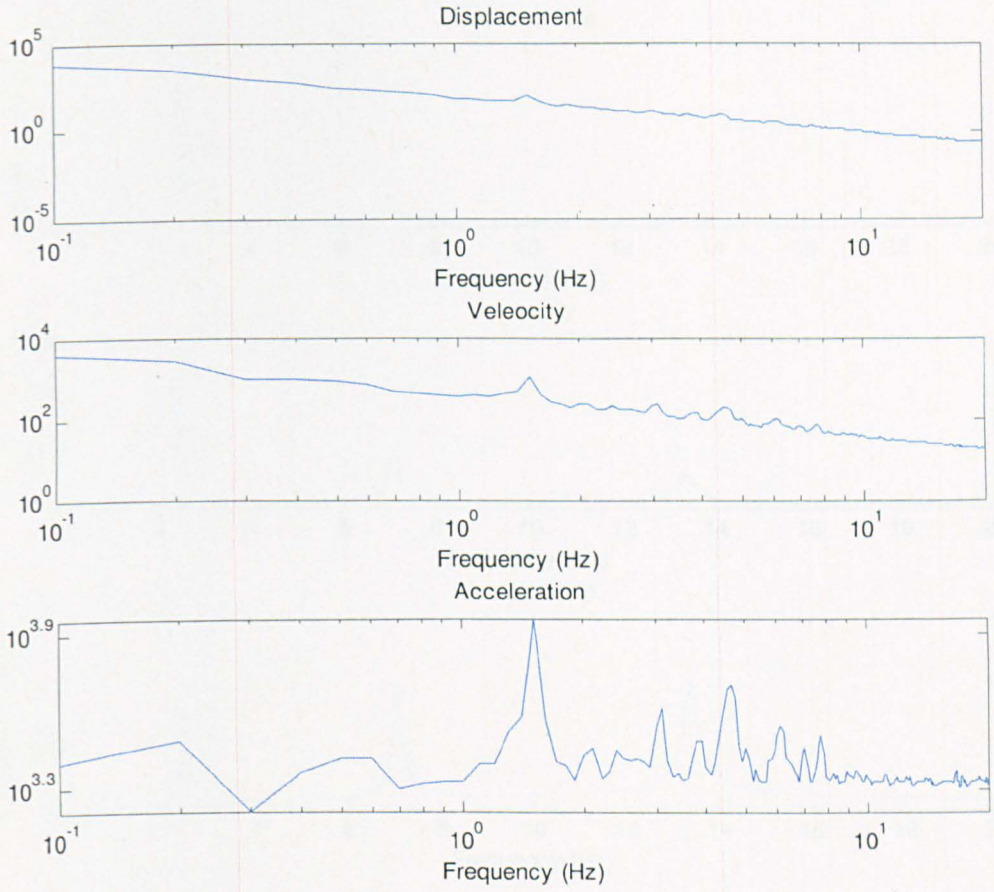

Figure 115 - Response spectra of a typical footfall time history

An initial velocity of a mass as a force is applied can be represented as:

$$\dot{u} = \frac{F}{m}$$ **Equation 87**

As the mass of the SDOF oscillator is 1, each value on the velocity spectrum can be considered an 'effective impulse' for the corresponding frequency of the input force. Due to the fact that the modal participation is based on a unit impulse, the peak velocity obtained by the participation factor can be multiplied by the effective impulse from the spectrum resulting in the peak velocity of the oscillator. The peak velocities can then be scaled to obtain response spectra can obtained for the system, shown in Figure 116, the peak values of which are very close to values calculated by the MDOF analysis.

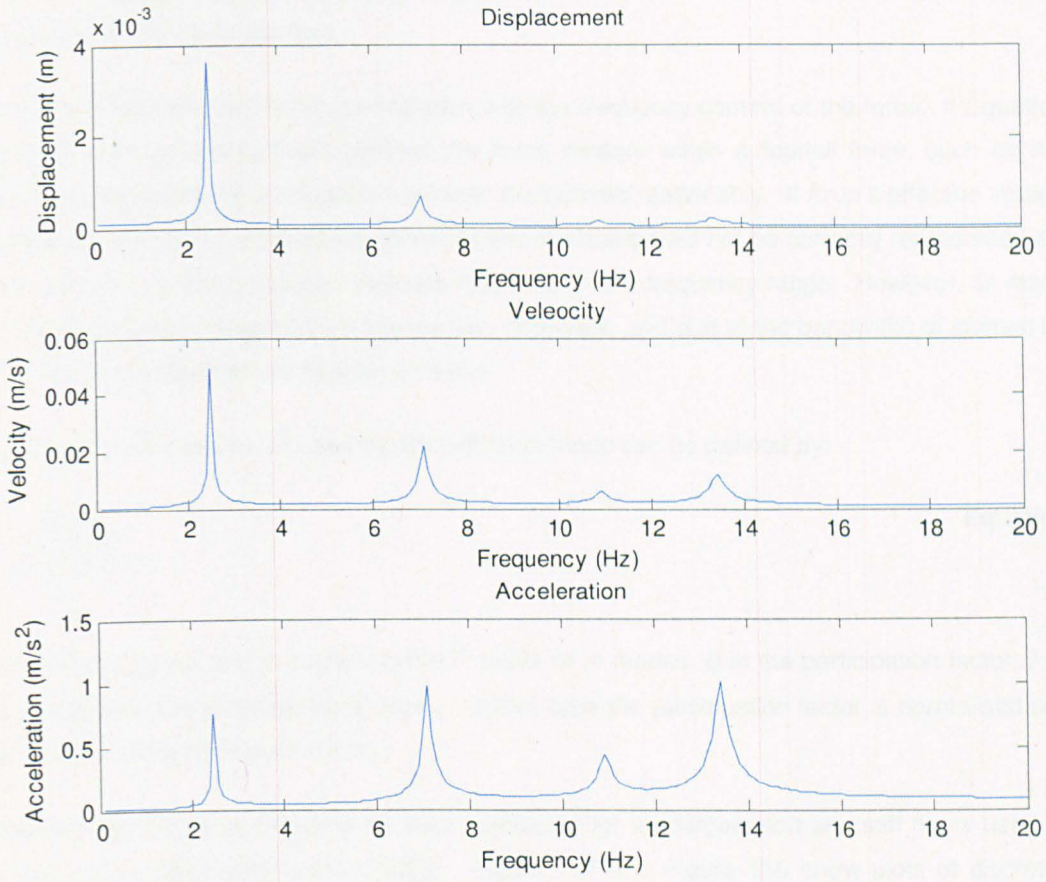

Figure 116 - Response spectra of the MDOF system obtained using the modal participation

5.5.4 Application of Modal Participation to Multi-Bay Floors

To apply the participation factor to multi-bay floors, with modal properties obtained from FEA, a number of modifications to the procedure are necessary. Firstly, the mass matrix is difficult to obtain, therefore a method that does not use the mass matrix is needed. Secondly, the energy contained within a footfall force is not constant at all frequencies, i.e. there is less energy at higher frequencies.

Equation 77 shows that the cumulative sum of the participation of each mode tends towards $\{F\}^T[M]^{-1}\{F\}$. The limit of participation is for all modes, however, in floor vibrations, a certain frequency bandwidth is of interest, as such a new limit can be defined. If $\sum_{r=1}^{m} P_r P_r$, where m is the number of modes within the bandwidth of interest, is evaluated then the participation can be obtained of each mode with respect to the bandwidth used. However, if such a summation is to be computed, a more sensible solution would be to obtain a modal participation directly in the form of the metric used in the vibration criteria, i.e. velocity. As the peak velocity is inversely proportional to the mass, the modified summation would simply divide each modal mass by the modal force. The modified

summation, although not as neat as the original solution, is a trivial computation and will have a negligible impact on computer time.

Equation 86 effectively factors the participation with the frequency content of the force. If Equation 86 is replaced with something that represent the force content within a footfall force, such as Arup's effective impulse [128], the participation will then be factored reasonably. If Arup's effective impulse is used, the participation of resonant response modes of vibration will not be correctly represented as the effective impulse cannot accurately estimate response in this frequency range. However, as resonant response is generally governed by a low number of modes, and due to the bandwidth of interest being smaller, modal participation is not such an issue.

Using the two modifications, the participation of each mode can be defined by:

$$Q_r = \frac{I_r/M_r}{\sum_{r=1}^{m} I_r/M_r}$$ **Equation 88**

where the subscripts r and m represent the i^{th} mode of m modes, Q is the participation factor, I is the effective impulse and M is the modal mass. In this case the participation factor is normalised so that all the mode contributions sum to unity.

Participation factors using Equation 88 were calculated for the largest soft and stiff floors used in the parametric study previously in the chapter. Figure 117 and Figure 118 show plots of discrete and cumulative participation factors for the soft and stiff floors for the 1D and 2D arrangements.

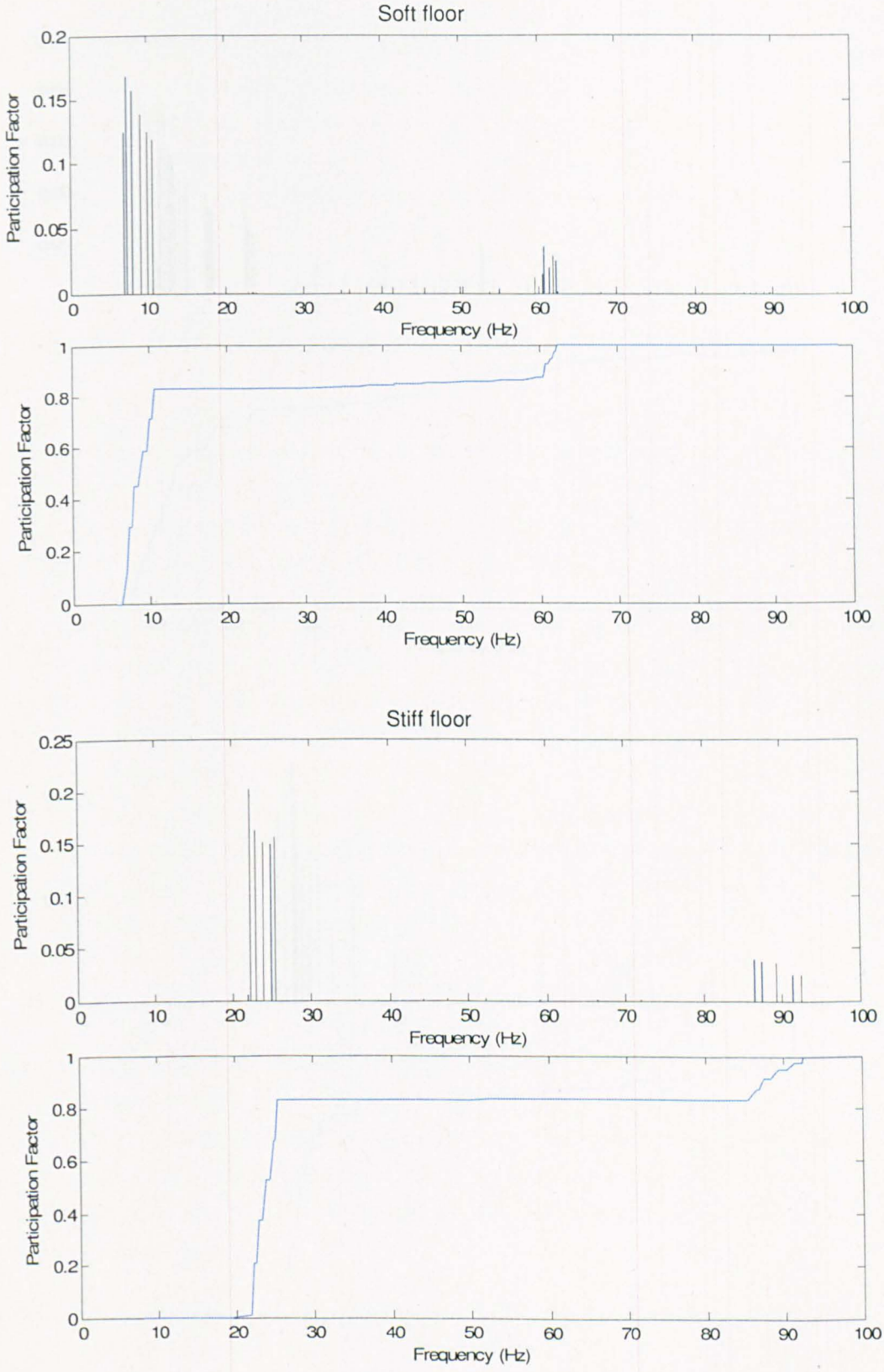

Figure 117 ***(from top to bottom)*** **– Participation factors for the soft and stiff floors respectively**

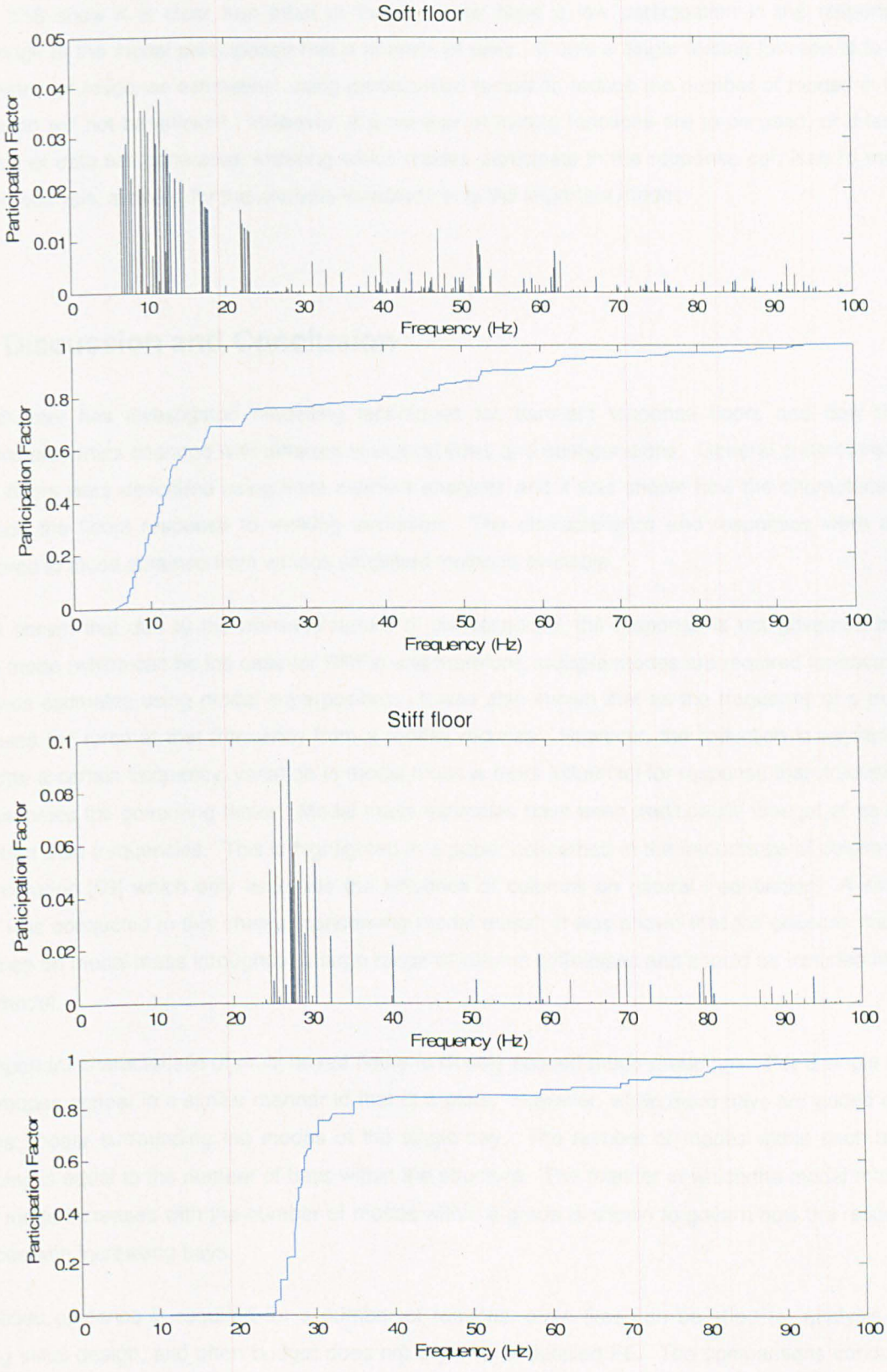

Figure 118 ***(from top to bottom)*** **– Participation factors for the soft and stiff floors respectively**

Referring to the previous section in the chapter describing the parametric studies, it is shown that each of the floors used has many hundreds of modes within the frequency range used. Figure 117 and

Figure 118 show it is clear that most of these modes have a low participation in the response. Knowledge of the modal participation has a number of uses. If only a single forcing function is to be considered for response estimation, using participation factors to reduce the number of modes in the calculation will not be efficient. However, if a number of forcing functions are to be used, or if large amounts of data are generated, knowing which modes participate in the response can lead to more efficient analysis, allowing for the analysts to include only the important modes.

5.6 Discussion and Conclusion

This chapter has investigated modelling techniques for transient response floors and how their dynamic properties changed with different structural sizes and configurations. General characteristics of the floors were described using finite element analyses and it was shown how the characteristics influence the floors response to walking excitation. The characteristics and responses were also compared to those obtained from various simplified methods available.

It was shown that due to the transient nature of the response, the response is not governed by a single mode (which can be the case for RRFs) and therefore, multiple modes are required for accurate response estimates using modal superposition. It was also shown that as the frequency of a mode increases the force at that frequency from a footfall reduces. However, the reduction is asymptotic and after a certain frequency, variation in modal mass is more influential for response than frequency, and becomes the governing factor. Modal mass estimates have been traditionally thought of as less important than frequencies. This is highlighted in a paper concerned in the importance of columns in floor vibration [59] which only assesses the influence of columns on natural frequencies. A similar study was conducted in this chapter concerning modal mass. It was shown that the columns had an influence on modal mass throughout a large range of column stiffnesses and should be included in the floor model.

An important characteristic of multi-bayed floors is closely spaced mode groupings. For a single floor bay, modes appear in a similar manner to that of a plate. However, when more bays are added extra modes appear surrounding the modes of the single bay. The number of modes within each mode grouping is equal to the number of bays within the structure. The manner in which the modal mass of each mode increases with the number of modes within a group is shown to govern how the response reduces with increasing bays.

Simplified guidance is required for a number of reasons: often time can be short for analysis, e.g. during initial design, and often budget does not allow for a detailed FE. The comparisons conducted here used a simple structure with uniform, regular bay sizes and spacings for which the simplified methods were developed. The guidance recommends estimating modal properties and then, using modal superposition, estimating responses.

Natural frequency estimation is generally obtained through static deformation of the structure to estimate the fundamental natural frequency, the accuracy of which depends on how well the deformed shape represents the fundamental mode shape. The exception of this is the Concrete Centre guide which uses a plate equation and can estimate higher modes of vibration. It was shown that for the fundamental mode the frequency estimates from both methods were very similar to each other and the FEA predictions. Although this is only the case when there are three or more floor bays as assuming simply supported boundary condition of the plate did not represent the structure well. It was also shown that for the first mode grouping the plate equation estimates the frequencies reasonably well when there are three or more bays. However, above the fist mode grouping the accuracy reduces considerably with the plate equation missing modes.

Modal mass estimates are generally derived from empirical studies using FEA, such as in the SCI guide, however, the Concrete Centre guide again uses a plate equation. The two methods were compared and, although the SCI guide has two expressions depending on the floor type, both methods produced similar modal masses. When compared with modal mass values obtained from FEA it is clear that both simplified guidance are inaccurate, underestimating masses by approximately a factor of 2. This may seem surprising since the SCI guide is based on empirical FEA studies. However, each floor type will have an individual mass and stiffness distribution and therefore a different mode shape and modal mass. As such, modal mass is much more sensitive to small changes in the mass and stiffness distributions than frequency, and will be floor specific and could be inaccurate for other floor types. The modal masses are generally underestimated and, therefore, would give conservative response estimates.

Mode shapes are an important property for scaling the magnitude of the force and response and are generally not considered in the guidance, except for the Concrete Centre guide. The mode shape used in the guide is calculated from an expression based on the summation of sine waves. Due to the manner in which the mode shapes manifest within mode groupings it was shown that the sine wave summation can be inaccurate for the first mode group and not at all suitable for higher mode groups. However, the inaccuracies are generally significant away from the structural centre and generally over estimate the modal amplitude, which would give a conservative response estimate. It was shown that when including the mode shape, the simplified method was more accurate.

The point mobility FRFs obtained using the Concrete Centre method were clearly different to the FRFs obtained using FEA, indicating inaccuracies due to poor estimation of modal mass and mode shape amplitudes. Using FEA the extra modes within the mode groupings, as the number of floor bays increased, were not clearly visible, and the occurring FRFs remained smooth with peaks similar to the single bay structure.

A large parametric study was conducted on floors of different stiffnesses and sizes with various column sizes to quantify empirically the dynamic properties of multi-bayed floors and the relationship of column size and modal mass. It was found that the number of modes within a fixed bandwidth increases linearly with the number of bays within the structure, which matches the relationship of the

modes contained within each mode group. The average modal mass was also found to increase linearly with increasing bays which, as response can be assumed to be proportional to the inverse of the modal mass, would lead to a asymptotic relationship with response. It was also shown that the response of uniform floors with a constant bay size is governed by the first mode group.

From the results of the parametric study a number of empirical improvements were investigated for the simplified guidance. Although minor improvements are possible for general structures, these improvements are small. To realise major improvements, emprical alterations would be specific to certain floor types and could not be used for generalised guidance.

Due to the difficulty in accurately estimating modal masses of floors using simplified guides finite element analysis is recommended. Also, simplified guides are only suitable for structures with regular bay spacings. As developing a full FE model can be time consuming and expensive, a crude model that is simple and quick to develop, but still accurate, is desirable. For large multi-bayed structures the area of interest for response estimates is often small, the rest of the structure serves to apply boundary conditions to the area of interest. As such, it is likely that the rest of the structure need not be modelled in such detail. This modelling detail was investigated for the largest structures from the parametric studies. It was shown that only the bay of interest is required to be modelled in detail, the rest of the structure can be modelled very crudely.

If a full structure is modelled using finite elements, modal analysis can produce many hundreds of floor modes, depending on the size of the structure. If multiple floors are modelled this number will increase further. Although this results in accurate mass estimates, the amount of data produced is difficult to deal with for a number of reasons. Firstly, modal superposition, which is efficient for structures where a small number of modes govern the response becomes less efficient, and can result in many gigabytes of data for even a short analysis. Secondly, many of the modes are not important and when compared with experimental modal analysis seem not to exist. This can cause problems when mode correlation is required for such things as model verification of model updating. To aid in these issues a method of mode participation was developed based on a method published (but very poorly described) by NAFEMS. This improved method identifies which modes contribute significantly to the response and which modes do not. If the modes with low participation are excluded, the number of modes reduces considerably.

Modal analysis and modal superposition is a great technique for simple structures when one mode governs the response. The mode shape, in this case, clearly shows how the structure vibrates making it easy to visualise. For large TRFs, where many modes make up the response, this visualisation is not as clear as a summation of modes is required to make the response. The next chapter analyses large multi-bayed floors using wave propagation techniques. Considering a structure in terms of wave propagation allows an analyst to easily visualise how the vibrational waves propagate through the structure. This, in turn, allows for a comprehension of the spatial dissipation of the wave energy, which for transient vibrations, governs the decay. For large floors, the problem of many closely spaced modes is also removed.

6 Wave Propagation Analysis of Transient Response Floors

Traditionally, in floor vibrations, response predictions have been performed using modal superposition. In most aspects of structural dynamics, a low number of modes will govern the response, so modal superposition is an efficient method in these cases. Also, when a single mode governs response it is easy to visualise how the structure will respond to the excitation, with the response being factored by the mode shape. It was shown in Chapter 5 that multi-bay floors have a large number of modes, and when considering a transient response a large number of these modes needs to be considered. In this case, the efficiency of modal superposition is lost. In addition, it is no longer possible to visualise how the vibration will manifest itself by simply considering the mode shapes. If a hypothetical floor structure is infinitely large, with an infinite number of bays, there will be an infinite number of modes within a mode grouping, making for a purely wave propagation problem.

If the time history response of a multi bay floor to a transient impulse is considered over a short duration (e.g. <0.5s) it is possible to see how a the vibration propagates throughout the structure. The response is similar to a pebble dropped in a pond, with the maximum response at the excitation point, and waves propagating away from the excitation point. As such, the problem becomes a wave propagation problem.

When considering the response in terms of wave propagation, a number of characteristics of the response immediately become clear. It is now possibly to visualise how the vibration changes with time, with the amplitude generally reducing away from the excitation point, the magnitude of the wave reducing at stiffer parts of the structure, and reflections at structural boundaries, columns and large changes in stiffness. How the vibration amplitude decreases away from the excitation point is worth considering in more detail. When considering harmonic excitation, the response is equal for points on the mode shape with the same amplitude, and damping governs the response. When considering transient vibrations, damping is less influential, and spatial dissipation of energy governs the decay of the response. This is not easily appreciated when considering response using modal superposition.

As many structural dynamic analysts do not work in terms of wave propagation various terms may be unfamiliar, Table 12 contains a glossary of terms for this type of analysis.

The solution method used in this chapter is the spectral element method (SEM). The SEM considers elements as connected wave guides, channelling waves along them. The method is build up by solving partial differential equations governing the wave motion using the spectral method and fast Fourier transform (FFT). The procedure is transformed into a matrix method, similar to the finite element method (FEM). As the SEM is a matrix method, it has the same advantages, i.e. complex structures can be created, including complex boundary conditions. A key difference of the SEM is the possibility of a semi-infinite element. In classical FEA energy dissipation out of the system is only

possible through damping, the SEA allows spatial dissipation into an infinite medium. The solution method involves solving pseudo-static problems at explicit frequencies to obtain a complex displacement at that frequency. A number of the frequencies are solved to obtain a spectrum. As the method is based on the FFT, the spectrum can be passed through the IFFT to obtain a time history response.

As TRFs have, by definition, a transient response, and they are often multi-bay floors they are ideal for wave propagation analysis. This chapter begins with a simple wave propagation analysis of a beam supported on an elastic foundation and shows how the results can be related to floor vibrations. The spectral element method is then derived in detail, showing the formation of the dynamic stiffness matrices. A computer program, called *SPECTRAL,* with a spectral element solver is introduced. *SPECTRAL* is then used to solve a number of grillage representations of multi-bay floors, including the use of semi-infinite elements, with the results directly compared with FEA using ANSYS. It is found that for a equivalent analysis, the SEM is more efficient than FEA, as it requires less elements for similar accuracy, less memory and less computer time.

Term	Definition
Wave number, k	Spatial domain version of period, i.e. number of waves per unit length
Wavelength, $\lambda = \frac{2\pi}{k}$	Length of the propagating wave
Phase velocity, $c = \frac{\omega}{k}$	The speed of an individual wave
Group speed, $c_g = \frac{d\omega}{dk}$	The speed of a group of waves. If the phase velocity and group velocity are not equal (which is the case for flexural waves in beams), when the wave appears to go off the end of the group, it will appear at the other end.

Table 12 - Glossary of terms for wave propagation analysis

6.1 Floor Represented as a Beam on Elastic Foundation

In the previous chapter it was shown that beyond a certain number of bays within a floor structure, the addition of more bays does not influence the response. As such, it can be assumed at this size that the structure acts as an infinite structure, with an infinite number of bays. If a 1D floor is considered to be infinitely long it would be reasonable to assume an abstraction of a beam on an elastic foundation, where the floor is modelled by the beam and the columns are modelled by the elastic foundation. Such problems are difficult to solve with modal analysis due to the large number of modes, however, using a wave propagation approach is efficient. If a threshold value is decided below which response can be taken as negligible, wave propagation equations can be used to estimate the distance, at which this will occur, from the excitation location. This section investigates this hypothesis and investigates if it can actually accurately be applied to a floor structure.

Although the response could not be used for accurate estimation of response magnitude, it serves as a simple solution to estimate how far the response will travel from the excitation point. The better visualisation of the problem using wave propagation techniques will provide a better understanding of the problem and its variables than was possible using the modal analysis procedures described in the previous chapter.

To ensure the simplicity of the solution, only flexural waves of 1D floors of infinite length shall be considered. The characteristics of 2D floors should be possible to obtain from a 1D solution using superposition. The 1D structure used in the parametric study in the previous chapter is used for the basis of this analysis.

6.1.1 Wave Propagation of an Infinite Euler Beam on an Elastic foundation

The derivation of the equations are described in detail by Doyle [129] and will only briefly be repeated here. The displacement wave propagation of an Euler beam can be described by:

$$\frac{\partial^2}{\partial x^2}\left[EI\frac{\partial^2 u}{\partial x^2}\right] + \rho A\frac{\partial^2 u}{\partial t^2} + \eta A\frac{\partial u}{\partial t} = q(x,t) \qquad \textbf{Equation 89}$$

where x is the distance away from the excitation point, ρ is the density of the beam, A is the cross-sectional area η is a loss factor, t is time and q is the force. Equation 89 can be solved using a spectral solution with:

$$u(x,t) = \sum [Ae^{-ikx} + Be^{-kx} + Ce^{ikx} + De^{kx}]\, e^{i\omega t} \qquad \textbf{Equation 90}$$

where A, B, C and D are constants depending on the boundary conditions, ω is the angular frequency of the current frequency and k is the wave number. Equation 90 is summed over the frequency range of interest to form the total response. Equation 89 can be modified to include a distributed stiffness, K, to represent the elastic foundation:

$$\frac{\partial^2}{\partial x^2}\left[EI\frac{\partial^2 u}{\partial x^2}\right] + \rho A\frac{\partial^2 u}{\partial t^2} + Ku + \eta A\frac{\partial u}{\partial t} = q(x,t) \qquad \textbf{Equation 91}$$

This does not affect the solution in Equation 90, but modifies the wave number. How to calculate the wave number from the wave propagation PDE is described in the next section. However, for a beam with an elastic foundation including damping it is found to be:

$$k = \pm\left[\frac{\rho A}{EI}\omega^2 - \frac{K}{EI} - \frac{i\omega\eta A}{EI}\right]^{1/4} \qquad \textbf{Equation 92}$$

Equation 92 can then be substituted into Equation 90, which then takes the form:

$$u(x,t) = \sum \frac{\hat{P}}{2EIi(k^2 - ik^2)} \left(e^{-ikx} - \frac{k}{ik} e^{kx} \right) e^{i\omega t}$$ **Equation 93**

which can be simplified to:

$$u(x,t) = \sum \frac{-i\hat{P}}{4EIk^3} (e^{-ikx} - ie^{-kx}) e^{i\omega t}$$ **Equation 94**

where $\hat{P}$ is the spectral amplitude of the force at frequency ω. Equation 93 can be solved for any distance from the excitation point for any specific frequency and time.

6.1.2 1D Floor Example

Equation 93 was solved using MATLAB for various floor and column stiffnesses. The floor stiffness was adjusted by varying both the slab depth and the slab length, and the distributed column (foundation) stiffness was adjusted by varying the size of the columns and length of the floor bay.

Firstly the stiff and soft floor were compared using the same floor properties as the parametric study from (the same floor as Chapter 5.2). Figure 119 shows how the wave propagates with respect to time along the length of the beam due to a unit impulse. It is clear that the stiff beam has a higher wave speed then the soft beam. This is due to higher frequency waves propagating faster than lower frequencies. For both beams, the crest of the wave, for each oscillation, at the excitation point initially travels with a high wave speed and then the speed reduces. Away from the excitation point there is an interval before the wave propagates to this location. Preceding the main wave a series of lower amplitude, higher frequency waves appear, which dissipate quickly, leaving the main lower frequency wave to dominate, this is a characteristic of a dispersive wave (as are flexural waves). An important observation is that the frequencies of the waves are higher than were obtained using the FE model. This is due to the crude assumption that the column stiffness can be distributed over the floor area. This assumption effectively overestimates the stiffness, and if thought of in modal terms, also overestimates the modal mass, the consequence of which will be shown shortly.

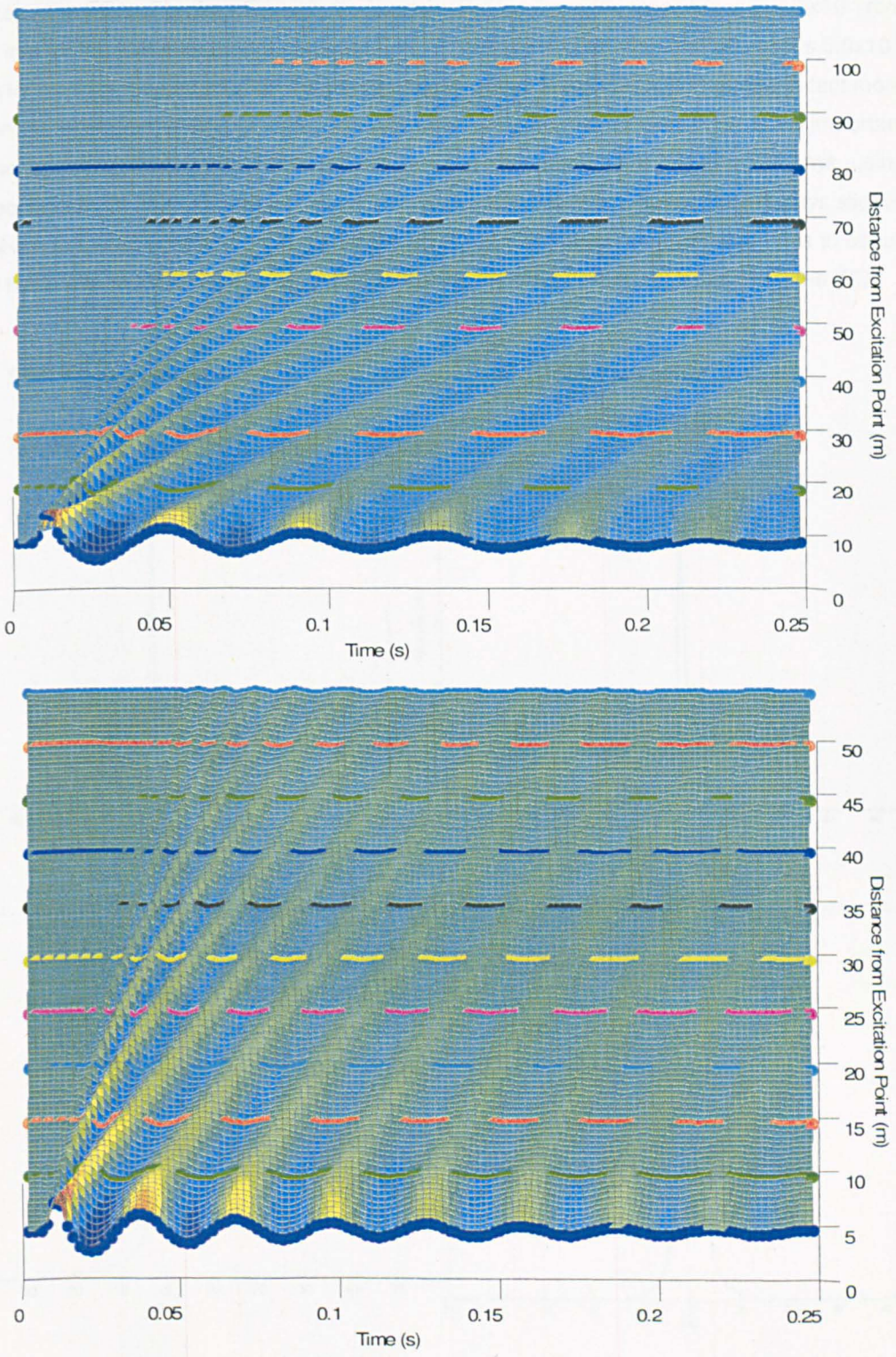

Figure 119 ***(From top to bottom)*** **- Flexural wave propagation of the soft floor, flexural wave propagation of the stiff floor; the horizontal dots represent the centre of bays**

The peak RMS over a 0.5s averaging window was calculated for the mid-bay location of each bay in the same manner as the parametric study of the previous chapter and is shown in Figure 120 next to the equivalent figure from the parametric study. The wave propagation analysis is similar in shape

and amplitude to the FEA. For the FEA with the largest 1D floor the peak response was $4.5x10^{-5}$ m/s and $4.7x10^{-5}$ m/s for the soft and stiff floor respectively. The wave propagation analysis yields $5.0x10^{-5}$ m/s and $4.5x10^{-5}$ m/s for the soft and stiff floor respectively, which is reasonably close and in fact more accurate then the simplified design guides. Although the two plots are similar, there is an important difference: the response decay away from the excitation point is not the same. In terms of bays, using FEA, both floors decay at approximately 10 bays, although the stiffer (and shorter) floor decays slightly faster. However, the wave propagation analysis shows that the stiff floor requires more bays to decay then the soft floor, and that the wave propagation is more sensitive to structural length than the FEA.

SEM Wave Propagation

FEA Parametric Study

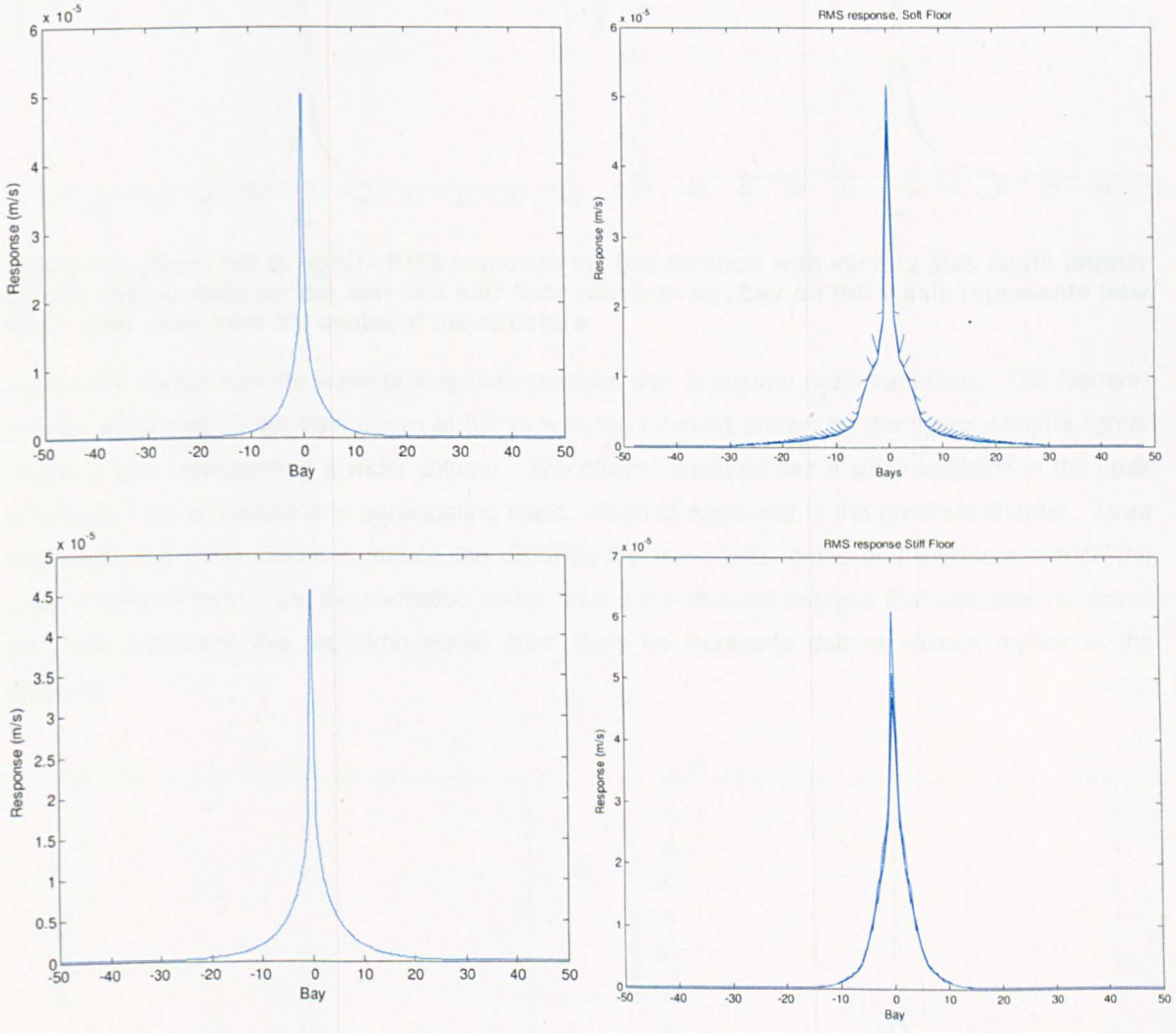

Figure 120 (*From top to bottom*) - RMS response vs. bay location soft floor, RMS response Vs. bay location stiff floor; bay on the x axis represents how many bays away from the centre of the structure

Although the wave propagation model does not perform exactly as the FEA, for a fixed floor length changes in the floor properties using the wave propagation model should be characteristic of the floor. As such, it is simple to see how sensitive the propagation is to the floor properties.

Figure 121 shows how the wave propagation changes due to slab depth variations. The slab depth was varied from 0.3 m to 0.5 m with ten intervals shown by the lighter shade of grey representing a deeper slab. It is clear that the slab depth changes the peak amplitude at the excitation point considerably, however the amplitudes away from the excitation change very little.

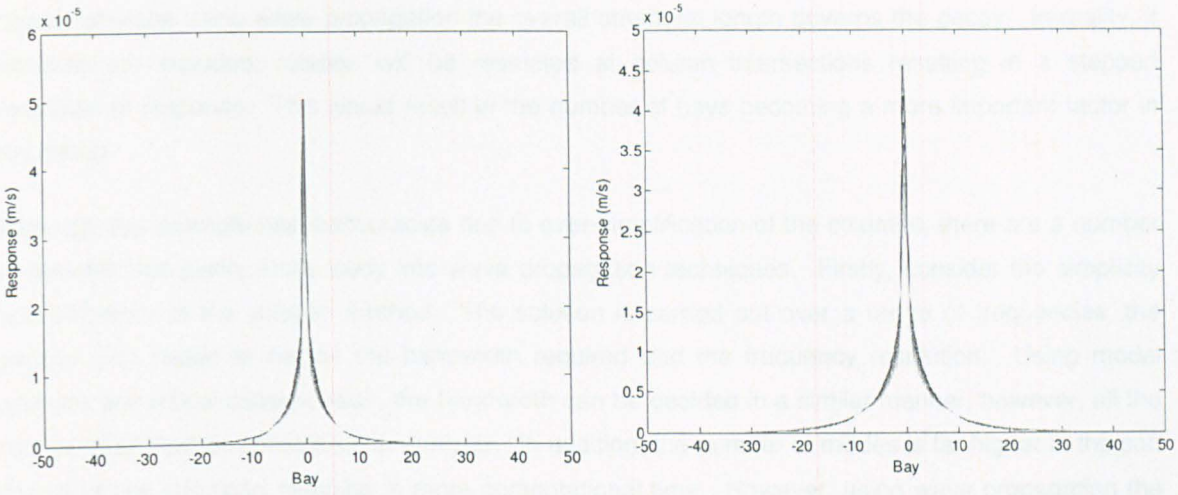

Figure 121 ***(From left to right)*** **- RMS response vs. bay location with varying slab depth (lighter grey is deeper slab) for the soft and stiff floor respectively; bay on the x axis represents how many bays away from the centre of the structure**

Figure 122 shows how the wave propagation changes due to column width variations. The (square) column width was varied from 0.3 m to 0.5 m with ten intervals shown on the figure with the lighter shade of grey representing a wider column. The column variation has a small variation in the peak amplitude, due to variations in participating mass, which is explained in the previous chapter. More noticeably, the stiffer columns reduce the distance the wave propagates and therefore reduce the peak amplitude away from the excitation point. In a more detailed analysis that included the actual structural members, this reduction would most likely be increased due to flexural motion of the columns.

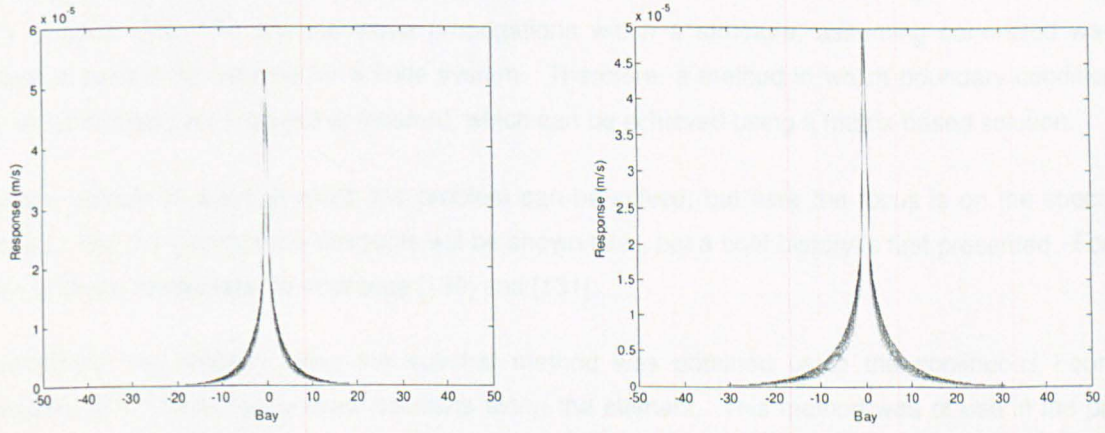

Figure 122 ***(From left to right)*** **- RMS response vs. bay location with varying column diameter (lighter grey is wider column) for the soft and stiff floor respectively; bay on the x axis represents how many bays away from the centre of the structure**

It was shown that the wave propagation technique offers a reasonably simple solution for decay of response with distance from the excitation point. Using the simplified guidance, a solution of this kind is not possible, and would require a rigorous analysis. The solution is relatively simple using wave propagation techniques and is based on first principles. However, the decay does not exactly match that of the FEA due to the column simplifications. Using the FEA the number of bays governs the decay, whereas using wave propagation the overall structural length governs the decay. In reality, if columns are included, rotation will be restricted at column intersections resulting in a stepped reduction of response. This would result in the number of bays becoming a more important factor in the decay.

Although this example has inaccuracies due to over-simplification of the columns, there are a number of benefits that justify more study into wave propagation techniques. Firstly, consider the simplicity and efficiency of the solution method. The solution is carried out over a range of frequencies, the analyst only needs to decide the bandwidth required and the frequency resolution. Using modal analysis and modal superposition, the bandwidth can be decided in a similar manner, however, all the modes must then be considered in analysis. In addition, the number of modes is far higher in the soft floor than the stiff floor, resulting in more computational time. However, using wave propagation the bandwidth and frequency resolution do not change, so neither will the computational time.

This small study showed that there are clear benefits when looking at transient responses of floor structures using a wave propagation perspective, justifying further study. A more detailed approach necessary to provide accurate results is covered in the next section using the spectral element method.

6.2 Spectral Element Method (SEM)

Generally simple solutions for wave propagation are based on infinite continua, e.g. beam (1D), shell (2D) or solid (3D). To analyse wave propagations within a structure, assuming connected wave guides, a solution is required for a finite system. Therefore, a method in which boundary conditions and discontinuities are included is required, which can be achieved using a matrix-based solution.

There a number of ways in which the problem can be solved, but here the focus is on the spectral method. The derivation of the elements will be shown later, but a brief history is first presented. For a more in-depth review refer to reference [130] and [131].

Traditionally, the solution using the spectral method was obtained using the continuous Fourier transform (CFT) which gave exact solutions along the element. This method was of use in the past since the method could be applied by hand and computers were not readily available. However, there was a major limitation: due to the nature of the CFT, the excitation had to be periodic and describable using a mathematical function, so an arbitrary time varying force could not be considered.

Doyle [129] solved this problem by using the fast Fourier transform. Indeed, the FFT had been available for a while at this point, and even before that the DFT. However, both procedures are too computationally intense for hand calculation, so implementation using the FFT was not possible. Although the methods required computer implementation, complex signals could now be analysed and the basis for the spectral element method was developed. The problem remained of connecting the individual elements as a series of wave guides to build a complete structure. The solution was solved in a similar manner as FEA, but using a dynamic stiffness matrix in the frequency domain.

When considering a beam element, two main forms exist: the Euler-Bernoulli beam and the Timoshenko beam. The Euler beam is much simpler to formulate then the Timoshenko beam and its dynamic stiffness matrix was first developed in 1941 [132], although a practical implementation was not possible due to lack of computer facilities. As computer power became more widely available, more research was carried out into Euler beams [130, 133, 134] where the stiffness matrix was developed using the FFT and a number of elements was created and simple structures analysed. Generally, the types of structures analysed were pipe and frame structures. Doyle also formulated a semi-infinite element to analyse the traditional wave propagation problems, such as infinite long pipes. The Euler beam performed well for structures of low frequency, but became less accurate as the frequency increased. This is due to the wave speed increasing with frequency: an infinite frequency results in an infinite speed, which is impossible. Low frequency in this case is in wave propagation terms which includes frequencies of many kHz. All frequencies in civil structures would be considered low frequency in these terms

The dynamic stiffness matrix for a Timoshenko beam was first developed in 1970 [132]. Much research has been carried out into the Timoshenko beam [135], comparing its accuracy with the Euler beam. The comparisons again consisted of pipes and frame structures, with the inclusion of a Timoshenko semi-infinite element. Due to the Timoshenko beam including shear deformation, a different wave number is formulated. The nature of this wave number limited the maximum wave speed with a cut of frequency, with the wave speed asymptotic to this value, which gave a much better accuracy at higher frequencies than the Euler beam.

To model a civil structure, plate elements are highly desirable, as well as beam elements, and therefore have been the focus of much research [129, 133]. The solution for a plate element is generally based on either a Navier's solution or Levy's solution to the governing equations. The continuing issue with plate elements is how to apply boundary conditions accurately and efficiently. When considering a beam element, the boundary condition is applied at a point and is easy to describe mathematically. Along the beam element is an exact formulation of the shape function, resulting in the need for only one element per beam. This results in efficiency in both analysis time, but also greater accuracy, and is one of the key benefits of the SEM. It is desirable to have the same efficiency for plate elements. However, a plate's boundary conditions often exist along its edges, requiring a function for a continuous boundary condition. The boundary conditions are usually defined with some sort of Fourier expansion, or summation of sine waves; however, these methods are only

exact for a small number of special cases. As such, nearly all of the research in these elements is on application of arbitrary boundary conditions with minimal error. Because of introducing these errors, discretisation is required to minimise them, in the same manner as FEA. Although the discretisation reduces the influence of one of the key benefits of the SEM, for an equal mesh density the SEM is still more accurate then the FEM [133].

In most of the literature, damping has not been included in the elements, usually with dissipation only included with semi-infinite elements. The only reference found to damping in the literature [136] somewhat over complicates the matter. Doyle introduced a loss factor into the formulation, which can easily be estimated from a viscous damping ratio.

An important characteristic of the SEM must be considered to ensure accurate analysis. Due to the method using the FFT, and because of the nature of the discrete Fourier Transform, a wrap around effect, akin to leakage, can occur in the response. Essentially, the magnitude of the start of the response is the same as the magnitude at the end. If there is any response at the end, it will also appear at the beginning of the response time history. The solution to this problem is to ensure that the time window is long enough for the response to reduce to zero, with either the inclusion of semi-infinite elements to remove energy from the system, or the introduction of damping.

The remainder of this section will develop spectral elements and, a computer program to create and solve problems using them. Then responses predictions will be compared with standard finite elements. Within the timescale of this research and the significant problems with plate spectral elements, these will not be studied. Also, due to the nature of civil structures having low frequency bandwidth (in terms of wave propagation) for serviceability issues, the Euler beam element will suffice for the analyses. To assess the performance, the computer program developed is somewhat emulate ANSYS. The program is written in MATLAB to read an ANSYS script and supports a subset of commands, enabling a direct comparison with ANSYS. To model a floor with the beam elements, a simple grillage shall be designed. The author has been involved in consultancy work where modal analysis of grillages corresponded very well to measured results, justifying the method.

The spectral element method has not previously been used to model transient responses in large civil structures, this investigation will serve as a test to assess the benefits. If significant benefit is obtained, future research can include plate elements, and spectral super elements (a spectral method of reduction for large finite element matrices).

6.2.1 Spectral Element Formulation

In this section, a dynamic stiffness matrix for an Euler beam element shall be formulated. For this formulation three subsets of the beam are required: a longitudinal (axial rod) deformation, a torsional deformation and the bending (flexural) deformation. This section shall develop the element in that

order. The formulation of the axial deformation will be considered in detail, whereas the basic formulation of the other subsets is similar in form, and therefore will be omitted. Finally it shall be described how the global dynamic stiffness matrix is defined and how the solution is obtained. First some general procedures and notations are outlined.

6.2.1.1 General Solution

In a 2D plane a degree of freedom, u, is a function of x, y and t, where x and y are spatial co-ordinates and t is time:

$$u(x,y,t) = f_1(t). \qquad \textbf{Equation 95}$$

Equation 95 can be represented in the frequency domain by:

$$u(x,y,t) = \sum_{\omega} \hat{C}_n \, e^{i\omega t} \qquad \textbf{Equation 96}$$

where $\hat{C}$ represents the spatial frequency domain displacement at node n and ω is the circular frequency. At an arbitrary position, Equation 96 can be rewritten as:

$$u(x,y,t) = \sum_{\omega} \hat{u}_n(x,y,\omega) \, e^{i\omega t} \qquad \textbf{Equation 97}$$

where $\hat{u}_n$ represents the spatially dependant Fourier co-efficient of displacement at an arbitrary point along an element. For simplification and clarity in notation writing $\sum$, n, and $e^{i\omega t}$ will be omitted. As such Equation 97 would become:

$$u(x,y,t) = \hat{u}_n(x,y,\omega). \qquad \textbf{Equation 98}$$

When considering derivatives of Equation 98 it can be shown that:

$$\frac{\partial^m u}{\partial t^m} = \frac{\partial^m}{\partial t^m} \sum_{\omega} \hat{u}_n e^{i\omega t}$$

$$\frac{\partial^m u}{\partial t^m} = i^m \omega_n^m \hat{u} \qquad \textbf{Equation 99}$$

and

$$\frac{\partial^m u}{\partial x^m} = \frac{\partial^m}{\partial x^m} \sum_{\omega} \hat{u}_n e^{i\omega t}$$

$$\frac{\partial^m u}{\partial x^m} = \frac{\partial^m \hat{u}}{\partial x^m}. \qquad \textbf{Equation 100}$$

A solution to an equation of the form:

$$u + a\frac{\partial u}{\partial x} + b\frac{\partial u}{\partial t} + c\frac{\partial^2 u}{\partial x^2} + d\frac{\partial^2 u}{\partial t^2} + \cdots = 0$$ **Equation 101**

where *a,b,c* and *d* are time independent variables can be found by first substituting in Equation 99 and Equation 100 to form:

$$\hat{u}_n + a\frac{\partial \hat{u}_n}{\partial x} + b(i\omega_n)\hat{u}_n + c\frac{\partial^2 \hat{u}_n}{\partial x^2} + d(i\omega_n)^2\hat{u}_n + \cdots = 0$$ **Equation 102**

which can be rearranged to form:

$$[1 + (i\omega_n)b + (i\omega_n)^2 d + \cdots]\hat{u}_n + [a + (i\omega_n)e + \cdots]\frac{\partial \hat{u}_n}{\partial x} + \cdots = 0.$$ **Equation 103**

On grouping terms Equation 102 can be expressed as:

$$A_1\hat{u}_n + A_2\frac{\partial \hat{u}_n}{\partial x} + A_3\frac{\partial^2 \hat{u}_n}{\partial x^2} + \cdots = 0$$ **Equation 104**

A solution to Equation 104 can be found in the form $e^{\lambda x}$ where $\lambda = -ik$, where *k* represents the wave number. If the solution is applied to Equation 104 the following is obtained:

$$A_1\lambda^0 + A_2\lambda^1 + A_3\lambda^2 + \cdots = 0$$ **Equation 105**

As the *A* are known, and $\lambda = -ik$, Equation 105 can be solved to find solutions of the wave number, *k*. This can then be substituted into the solution:

$$\hat{u}(x) = C_1 e^{-ik_1 x} + C_1 e^{-ik_2 x} + \cdots + C_n e^{-ik_n x}$$ **Equation 106**

where C_n are constants dependant on the boundary conditions.

6.2.1.2 Formulation of a Rod Element (Axial Deformation)

The general solution is applied to a specific problem. Figure 123 shows a representation of an axial rod element where *E* is the Young's modulus of the material, ρ is the density, *A* is the cross-sectional area, *L* is the element length and *F* represents the force. Deformation in the rod is assumed to only act in the axial (x) co-ordinates.

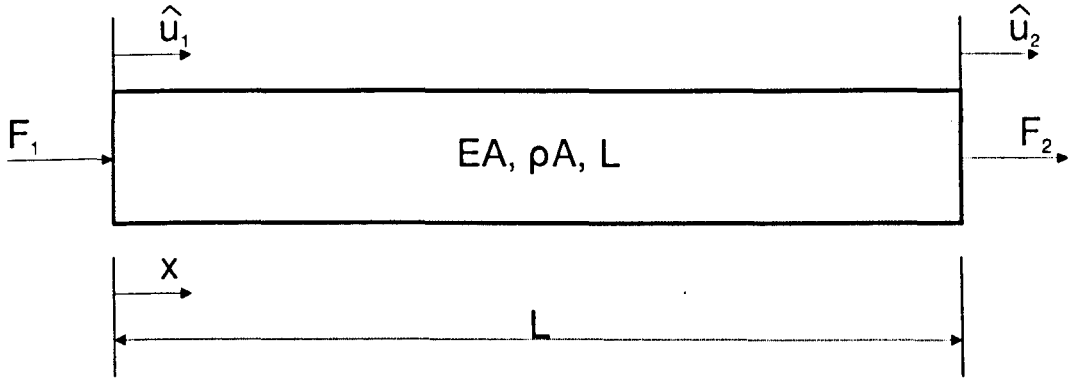

Figure 123 - Rod element representation

The axial deformation of a rod can be described by:

$$EA\frac{\partial^2 u}{\partial x^2} - \rho A\frac{\partial^2 u}{\partial t^2} - \eta A\frac{\partial u}{\partial t} = -q \qquad \textbf{Equation 107}$$

where η is a loss factor and q is a function of force. The spectral form of Equation 107 can be obtained by substituting Equation 99 and Equation 100 to form:

$$EA\frac{\partial^2 \hat{u}}{\partial x^2} - \rho A\omega^2\hat{u} - \eta Ai\omega\hat{u} = -q \qquad \textbf{Equation 108}$$

which can be simplified to:

$$EA\frac{\partial^2 \hat{u}}{\partial x^2} - (\rho A\omega^2 - \eta Ai\omega)\hat{u} = -q \qquad \textbf{Equation 109}$$

If:

$$A_1 = \rho A\omega^2 - \eta Ai\omega \qquad \textbf{Equation 110}$$

then

$$A_2 = EA. \qquad \textbf{Equation 111}$$

Equation 110 and Equation 111 can be substituted into Equation 109 to form:

$$-A_1\hat{u} + A_2\frac{\partial^2 \hat{u}}{\partial x^2} = -q. \qquad \textbf{Equation 112}$$

In the same manner that Equation 105 was developed:

$$-A_1 + A_2\lambda^2 = 0. \qquad \textbf{Equation 113}$$

As $\lambda = -ik$, the wave number can be expressed as:

$$k = \pm\sqrt{\frac{A_1}{A_2}} = \pm\sqrt{\frac{\rho A\omega^2 - \eta A i\omega}{EA}}$$ **Equation 114**

Equation 114 can then be inserted into the final solution to form:

$$\hat{u}(x) = Ae^{-ikx} + Be^{ikx}$$ **Equation 115**

where A and B are values depending on boundary conditions. Equation 115 consists of two parts, the part factored by the co-efficient A represents a forward propagating wave, whereas the part factored by the co-efficient B represents a backward propagating wave.

A number of examples show now be given to show how the simple rod element can be modified to include boundary conditions, excitation conditions and additional physical conditions.

Introduction of hysteretic damping:

To introduce a hysteretic damping, which is proportional to the displacement of system, via co-efficient *K*, the governing differential equation changes to:

$$EA\frac{\partial^2 u}{\partial x^2} - \rho A\frac{\partial^2 u}{\partial t^2} - \eta A\frac{\partial u}{\partial t} - Ku = -q$$ **Equation 116**

If the wave number is then obtained using the same procedure as described previous the following expression is found:

$$k = \pm\sqrt{\frac{\rho A\omega^2 - \eta A i\omega - K}{EA}}$$ **Equation 117**

The rest of the solution would be the same, demonstrating the simplicity of this method.

Force applied at the end of a semi-infinite rod:

One the main benefits over the FEA is the ability to extend easily the element to infinity, therefore removing energy from the system in a different manner to damping, which is ideal for large structures. Consider the force applied to the rod, as shown in Figure 124.

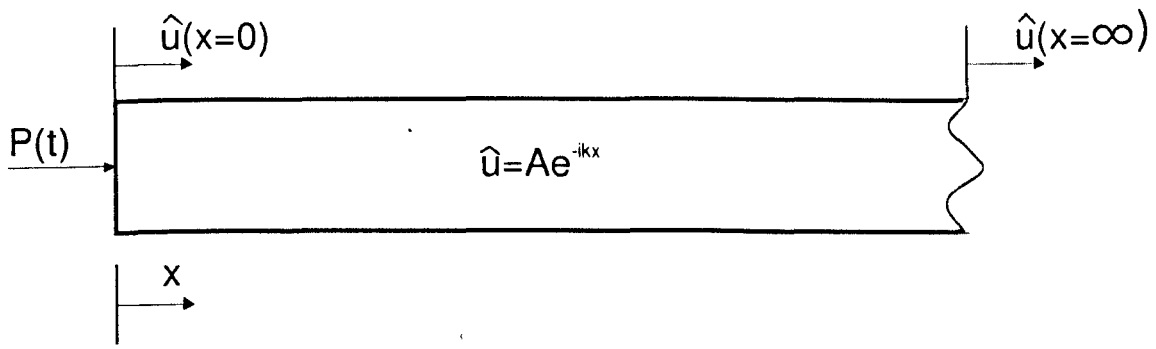

Figure 124 - Semi-infinite rod element representation with force applied at one end

If the force is represented by:

$$F = -P(t) = EA\frac{\partial u(x,t)}{\partial x}$$ **Equation 118**

where $P(t)$ is the force time history, the spectral representation is:

$$F = -\hat{P}(t) = EA\frac{\partial \hat{u}(x,\omega)}{\partial x}$$ **Equation 119**

As this is a semi-infinite rod with the force applied at one end, the wave propagates in a single direction; as such, the solution of governing differential equation (Equation 115) is reduced to:

$$\hat{u}(x) = Ae^{-ikx}$$ **Equation 120**

where the wave number, *k*, is obtained using Equation 114. At x=0, using Equation 120:

$$\frac{\partial u(0,\omega)}{\partial x} = ik_1 A\,.$$ **Equation 121**

If Equation 121 is then substituted into Equation 119 the following expression is obtained:

$$EA[-ik_1 A] = -\hat{P}$$ **Equation 122**

which can be rearranged to obtain:

$$A = \frac{\hat{P}}{ik_1 EA}.$$ **Equation 123**

Equation 123 can then be substituted into Equation 120 to obtain the particular solution.

Spring boundary condition at one end:

To demonstrate the solution of the rod with some kind of fixity at one end, a spring support will be used as an example. Using this example it is also easy to examine free and fixed boundary conditions by varying the spring constant. The spring boundary condition is shown in Figure 125.

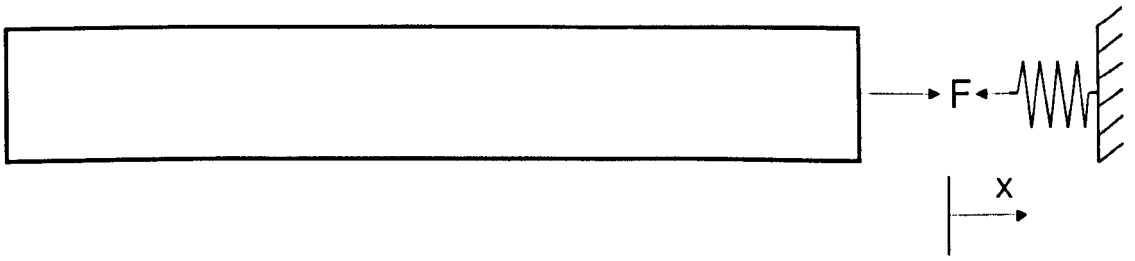

Figure 125 - Spring boundary condition of a rod

The force applied by the spring is defined by:

$$EA\frac{\partial u(0,t)}{\partial x} = -Ku(0,t) \qquad \textbf{Equation 124}$$

where K is the spring stiffness. The spectral representation of Equation 124 is given by:

$$EA\frac{\partial \hat{u}(0,\omega)}{\partial x} = -K\hat{u}(0,\omega)\,. \qquad \textbf{Equation 125}$$

Substituting Equation 115 into Equation 125 yields:

$$EA(-ik_1\boldsymbol{A} + ik_2\boldsymbol{B}) = -K(\boldsymbol{A} + \boldsymbol{B}) \qquad \textbf{Equation 126}$$

Equation 126 can be written to determine the reflective wave, $\boldsymbol{B}$, in terms of the incident wave, $\boldsymbol{A}$:

$$\boldsymbol{B} = \frac{ik_1EA - K}{ik_1EA + K}\boldsymbol{A}\,. \qquad \textbf{Equation 127}$$

To obtain a solution with a force input, obtain $\boldsymbol{A}$ from Equation 123. Notice that for a very stiff spring, where K approaches infinity (fixed condition), $\boldsymbol{B} = -\boldsymbol{A}$, and for a soft spring, where K approaches zero (free condition), $\boldsymbol{B} = \boldsymbol{A}$.

Rod spectral element:

The only method to handle large structures is to develop a matrix method assembled from individual elements. The approach of the spectral element method is similar to that of the finite element method: a force and stiffness matrix is obtained and solved for displacements. The solution of the original semi-infinite rod can be adapted to form its dynamic stiffness matrix.

Equation 115 can be modified to be an element of finite length, L:

$$\hat{u}(x) = Ae^{-ikx} + Be^{-ik(L-x)}$$ **Equation 128**

If $\hat{u}_1 = \hat{u}(0)$ and $\hat{u}_2 = \hat{u}(L)$ then:

$$\hat{u}_1 = A + Be^{-ikL}$$ **Equation 129**

and

$$\hat{u}_2 = Ae^{-ikL} + B\,.$$ **Equation 130**

In matrix notation Equation 129 and Equation 130 can be described as:

$$\{\hat{u}\} = \begin{Bmatrix}\hat{u}_1\\ \hat{u}_2\end{Bmatrix} = [D]\begin{Bmatrix}A\\ B\end{Bmatrix}$$ **Equation 131**

where

$$[D] = \begin{bmatrix}1 & e^{-ikL}\\ e^{-ikL} & 1\end{bmatrix}.$$ **Equation 132**

The axial force applied on the rod can be defined as:

$$F(x) = EA\frac{\partial u(x,t)}{\partial x}.$$ **Equation 133**

The spectral representation of Equation 133 in matrix form is given by:

$$\{\hat{f}\} = \begin{Bmatrix}\hat{f}_1\\ \hat{f}_2\end{Bmatrix} = [\hat{F}]\begin{Bmatrix}A\\ B\end{Bmatrix}$$ **Equation 134**

where

$$[\hat{F}] = EA\begin{bmatrix}-ik_1 & -ik_1e^{-ikL}\\ -ik_1e^{-ikL} & -ik_1\end{bmatrix}$$ **Equation 135**

which is obtained by differentiating Equation 129 and Equation 130. The dynamic stiffness matrix can be defined by:

$$\{\hat{f}\} = [\hat{K}]\{\hat{u}\}.$$ **Equation 136**

Substituting Equation 131 and Equation 134 into Equation 136 yields:

$$[\hat{F}]\begin{Bmatrix}A\\ B\end{Bmatrix} = [\hat{K}][D]\begin{Bmatrix}A\\ B\end{Bmatrix}$$

$$[\hat{F}] = [\hat{K}][D]$$

$$[\hat{K}] = [\hat{F}][D]^{-1}$$ **Equation 137**

where $[\hat{K}]$ is the symmetrical dynamic stiffness matrix, which can be shown explicitly as:

$$[\bar{K}] = EA\begin{bmatrix} -ik_1 & -ik_1 e^{-ikL} \\ -ik_1 e^{-ikL} & -ik_1 \end{bmatrix}\begin{bmatrix} 1 & e^{-ikL} \\ e^{-ikL} & 1 \end{bmatrix}^{-1}$$ **Equation 138**

which is reduced to:

$$[\bar{K}] = EA\frac{ik_1}{(1-e^{-2kL})}\begin{bmatrix} 1+e^{-i2kL} & -2e^{-ikL} \\ -2e^{-ikL} & 1+e^{-i2kL} \end{bmatrix}.$$ **Equation 139**

To have a full beam element, torsional and flexural components must also be derived. These components shall be derived next, but not in such detail as the rod element, as much of the process is the same.

6.2.1.3 Formulation of a Torsion Beam Element

Fortunately, the governing equation for torsion is the same as the axial deformation of a rod, but with different coefficients. This means that the axial deformation formulation of the rod can be used for torsion but with some minor changes. The governing differential equation is defined by:

$$GJ\frac{\partial^2 u}{\partial x^2} - \rho I\frac{\partial^2 u}{\partial t^2} - \eta I\frac{\partial u}{\partial t} = -q$$ **Equation 140**

and it can be shown that the wave number is:

$$k = \pm\sqrt{\frac{\rho I\omega^2 - \eta I i\omega - K}{GJ}}$$ **Equation 141**

where *GJ* is the torsional stiffness and *I* is the rotational inertia per unit length. From this point the solution is the same as the rod element so will be omitted.

6.2.1.4 Formulation of a Flexural Euler Beam Element

The beam formulated here is an Euler beam which includes elastic deformation of a beam. However, it does not include shear deformation, for which a Timoshenko beam is required. The Euler beam is simpler to formulate, and for civil applications the reduction in accuracy will be acceptable. The governing differential equation for flexural motion in an Euler beam is given by:

$$\frac{\partial^2}{\partial x^2}\left[EI\frac{\partial^2 u}{\partial x^2}\right] + \rho A\frac{\partial^2 u}{\partial t^2} + \eta A\frac{\partial u}{\partial t} = -q(x,t)$$ **Equation 142**

which, for a constant cross section, simplifies to:

$$EI\frac{\partial^4 u}{\partial x^4} + \rho A\frac{\partial^2 u}{\partial t^2} + \eta A\frac{\partial u}{\partial t} = -q(x,t).$$ **Equation 143**

The spectral representation of Equation 143 is given by:

$$EI\frac{\partial^4\hat{u}}{\partial x^4} - \rho A\omega^2\hat{u} + \eta Ai\omega\hat{u} = -q(x,t)$$

$$EI\frac{\partial^4\hat{u}}{\partial x^4} + (\eta Ai\omega - \rho A\omega^2)\hat{u} = -q(x,t) \qquad \textbf{Equation 144}$$

for which the wave number can be obtained as:

$$k = \sqrt[4]{\frac{\eta Ai\omega - \rho A\omega^2}{EI}} \qquad \textbf{Equation 145}$$

This leads to the general solution:

$$\hat{u}(x,\omega) = \sum_{\omega} Ae^{-ik_1x} + Be^{-ik_2x} + Ce^{-ik_3x} + De^{-ik_4x} \qquad \textbf{Equation 146}$$

where A, B, C, and D are dependent on the boundary conditions and excitation conditions. With the appropriate boundary conditions Equation 146 can be solved for an arbitrary force input.

Force applied in the centre of the beam:

One the main benefits of SEM over FEA is the ability to extend easily the element to infinity, therefore removing energy from the system in a different manner to damping, which is ideal for large structures. If a force is applied to the centre of the beam a free body diagram can be constructed, as shown in Figure 126. Where *M* and *V* are the moments and shear forces respectively, *P* and *T* are applied force and moment respectively and m is mass.

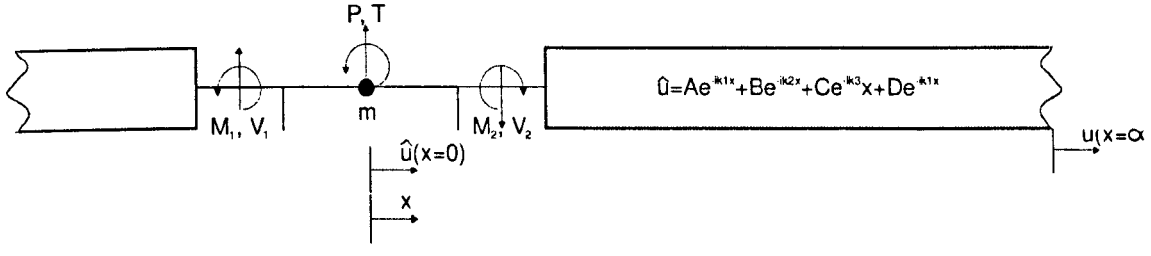

Figure 126 - Infinite beam element representation with force applied at the centre

The boundary conditions in this example are:

V_2=-V_1 $\qquad \partial u/\partial x = 0$

M_2=-M_1 $\qquad P + 2V_2 = m(x=0)\cdot\ddot{u}(x=0)$

which can be solved to find A:

$$A = \frac{-i\hat{P}}{4EAk^3}$$ **Equation 147**

and the other co-efficients are described by:

$B = -iA \qquad D = -iC \qquad C = A \qquad D = \mathrm{B}$

which then can be used to solve Equation 147.

Fixed boundary conditions:

To demonstrate the solution of the beam with some kind of fixity, a fixed support at one end will be used as an example. There are two boundary conditions, the displacement and slope at the support must be zero:

$u(0,t) = 0$ (displacement) **Equation 148**

$\partial u(0,t)/\partial x = 0$ (slope) **Equation 149**

When the boundary conditions are substituted into Equation 146, expressions can be formed to solve for A, B, C, and D:

$A + B + C + D = 0$ (displacement) **Equation 150**

$A(-ik_1) + B(-ik_2) + C(-ik_3) + D(-ik_4) = 0$ (slope) **Equation 151**

Beam spectral element:

Now the solution of the beam for a single, infinite length, element has been demonstrated, the formulation must now be used to construct a matrix solution method. Equation 146 can be modified to be an element of finite length, L:

$$\hat{u}(x,\omega) = Ae^{-ik_1x} + Be^{-ik_2x} + Ce^{-ik_3(L-x)} + De^{-ik_2(L-x)}.$$ **Equation 152**

However, to solve for a beam where moments will be transferred rotations are also required, these can be obtained by differentiating Equation 152:

$$\hat{\phi}(x,\omega) = -ik_1Ae^{-ik_1x} - ik_2Be^{-ik_2x} - ik_1Ce^{-ik_3(L-x)} - ik_2De^{-ik_2(L-x)}.$$ **Equation 153**

If $\hat{u}_1 = \hat{u}(0)$, $\hat{u}_2 = \hat{u}(L)$, $\hat{\phi}_1 = \hat{\phi}(0)$ and $\hat{\phi}_2 = \hat{\phi}(L)$ then:

$\hat{u}_1 = A + B + Ce^{-ik_1L} + De^{-ik_2L}$, **Equation 154**

$\hat{u}_2 = Ae^{-ik_1L} + Be^{-ik_2L} + C + D$, **Equation 155**

$\hat{\phi}_1 = -ik_1A - ik_2B - ik_1Ce^{-ik_1L} - ik_2De^{-ik_2L}$, **Equation 156**

$\hat{\phi}_2 = -ik_1Ae^{-ik_1L} - ik_2Be^{-ik_2L} - ik_1C - ik_2D.$ **Equation 157**

in matrix notation Equation 154, Equation 155, Equation 156 and Equation 157 can be described as:

$$\{\hat{u}\} = \begin{Bmatrix} \hat{u}_1 \\ \hat{\phi}_1 \\ \hat{u}_2 \\ \hat{\phi}_2 \end{Bmatrix} = [D] \begin{Bmatrix} A \\ B \\ C \\ D \end{Bmatrix} \quad \text{Equation 158}$$

where:

$$[D] = \begin{bmatrix} 1 & 1 & e^{-ik_1 L} & e^{-ik_2 L} \\ -ik_1 & -ik_2 & -ik_1 e^{-ik_1 L} & -ik_1 e^{-ik_2 L} \\ e^{-ik_1 L} & e^{-ik_2 L} & 1 & 1 \\ -ik_1 e^{-ik_1 L} & -ik_1 e^{-ik_2 L} & -ik_1 & -ik_2 \end{bmatrix}. \quad \text{Equation 159}$$

The forces applied to a beam are expressed in shear and moment contributions:

$$\hat{V} = -EI \frac{\partial^3 \hat{u}}{\partial x^3} \quad \text{Equation 160}$$

$$\hat{M} = EI \frac{\partial^2 \hat{u}}{\partial x^2} \quad \text{Equation 161}$$

which can be expressed in matrix form:

$$\{\hat{f}\} = \begin{Bmatrix} \hat{V}_1 \\ \hat{M}_1 \\ \hat{V}_2 \\ \hat{M}_2 \end{Bmatrix} = [F] \begin{Bmatrix} A \\ B \\ C \\ D \end{Bmatrix}, \quad \text{Equation 162}$$

where:

$$[F] = EI \begin{bmatrix} ik_1^3 & ik_2^3 & ik_1^3 e^{-ik_1 L} & ik_2^3 e^{-ik_2 L} \\ ik_1^2 & ik_2^2 & ik_1^2 e^{-ik_1 L} & ik_2^2 e^{-ik_2 L} \\ -ik_1^3 e^{-ik_1 L} & -ik_2^3 e^{-ik_2 L} & -ik_1^3 & -ik_2^3 \\ -ik_1^2 e^{-ik_1 L} & -ik_2^2 e^{-ik_2 L} & -ik_1^2 & -ik_2^2 \end{bmatrix}. \quad \text{Equation 163}$$

The dynamic stiffness matrix can then be obtained using Equation 137.

6.2.1.5 Formulation of the Complete Spectral Beam Element

After the individual dynamic stiffness matrices for the rod, torsional beam and flexural beam have been obtained they must be combined to form a complete beam dynamic stiffness matrix. In the case of a 3D beam (with six degrees of freedom per node), there exists a single axial rod element, a single torsional element and two flexural beam elements. The construction of the complete beam element is similar to that of an FE beam. The construction of the complete beam element is explicitly defined.

The dynamic displacements can be defined by:

$$\{\hat{u}\}^T = \{\hat{u}_{x1} \quad \hat{u}_{y1} \quad \hat{u}_{z1} \quad \hat{\phi}_{x1} \quad \hat{\phi}_{y1} \quad \hat{\phi}_{z1} \quad \hat{u}_{x2} \quad \hat{u}_{y2} \quad \hat{u}_{z2} \quad \hat{\phi}_{x2} \quad \hat{\phi}_{y2} \quad \hat{\phi}_{z2}\}. \quad \text{Equation 164}$$

Likewise, the dynamic forces can be defined by:

$$\{\hat{f}\}^T = \{\hat{P}_{x1} \quad \hat{P}_{y1} \quad \hat{P}_{z1} \quad \hat{T}_{x1} \quad \hat{T}_{y1} \quad \hat{T}_{z1} \quad \hat{P}_{x2} \quad \hat{P}_{y2} \quad \hat{P}_{z2} \quad \hat{T}_{x2} \quad \hat{T}_{y2} \quad \hat{T}_{z2}\}. \qquad \textbf{Equation 165}$$

Then, once knowing which column and row corresponds to each degree of freedom, the complete dynamic stiffness matrix can be constructed from the individual stiffness matrices.

$$[\hat{k}] = \begin{bmatrix} \hat{k}_{11}^R & 0 & 0 & 0 & 0 & 0 & \hat{k}_{12}^R & 0 & 0 & 0 & 0 & 0 \\ 0 & \hat{k}_{11}^B & 0 & 0 & 0 & \hat{k}_{12}^B & 0 & \hat{k}_{13}^B & 0 & 0 & 0 & \hat{k}_{14}^B \\ 0 & 0 & \hat{k}_{11}^B & 0 & \hat{k}_{12}^B & 0 & 0 & 0 & \hat{k}_{13}^B & 0 & \hat{k}_{14}^B & 0 \\ 0 & 0 & 0 & \hat{k}_{11}^S & 0 & 0 & 0 & 0 & 0 & \hat{k}_{12}^S & 0 & 0 \\ 0 & 0 & \hat{k}_{21}^B & 0 & \hat{k}_{22}^B & 0 & 0 & 0 & \hat{k}_{23}^B & 0 & \hat{k}_{24}^B & 0 \\ 0 & \hat{k}_{21}^B & 0 & 0 & 0 & \hat{k}_{22}^B & 0 & \hat{k}_{23}^B & 0 & 0 & 0 & \hat{k}_{24}^B \\ \hat{k}_{21}^R & 0 & 0 & 0 & 0 & 0 & \hat{k}_{22}^R & 0 & 0 & 0 & 0 & 0 \\ 0 & \hat{k}_{31}^B & 0 & 0 & 0 & \hat{k}_{32}^B & 0 & \hat{k}_{33}^B & 0 & 0 & 0 & \hat{k}_{34}^B \\ 0 & 0 & \hat{k}_{31}^B & 0 & \hat{k}_{32}^B & 0 & 0 & 0 & \hat{k}_{33}^B & 0 & \hat{k}_{34}^B & 0 \\ 0 & 0 & 0 & \hat{k}_{21}^S & 0 & 0 & 0 & 0 & 0 & \hat{k}_{22}^S & 0 & 0 \\ 0 & 0 & \hat{k}_{41}^B & 0 & \hat{k}_{42}^B & 0 & 0 & 0 & \hat{k}_{43}^B & 0 & \hat{k}_{44}^B & 0 \\ 0 & \hat{k}_{41}^B & 0 & 0 & 0 & \hat{k}_{42}^B & 0 & \hat{k}_{43}^B & 0 & 0 & 0 & \hat{k}_{44}^B \end{bmatrix} \qquad \textbf{Equation 166}$$

where the superscripts *R*, *S*, and *B* represent the stiffness matrix of the rod, shaft (torsional) and beam respectively and the subscripts represent the matrix cell of the individual elements dynamic stiffness. To build up a global stiffness matrix containing many elements, the procedure is exactly the same as in standard FEA. When the element local co-ordinate system is not the same as the global co-ordinate system a transformation matrix is used to convert between the two co-ordinate systems:

$$T = \begin{bmatrix} r & 0 & 0 & 0 \\ 0 & r & 0 & 0 \\ 0 & 0 & r & 0 \\ 0 & 0 & 0 & r \end{bmatrix} \qquad \textbf{Equation 167}$$

where

$$r = \begin{bmatrix} C_{Xx} & C_{Yx} & C_{Zx} \\ C_{Xy} & C_{Yy} & C_{Zy} \\ C_{Xz} & C_{Yz} & C_{Zz} \end{bmatrix} \qquad \textbf{Equation 168}$$

and

$$r = cos\,\theta_{Xx} \qquad \textbf{Equation 169}$$

and θ_{Xx} is the angle between the global x axis and the local x axis in a single plane. The transformation matrix is applied to the local stiffness matrix in the following manner:

$$[\hat{k}_t] = [T]^T[\hat{k}][T] \qquad \textbf{Equation 170}$$

6.3 Spectral Element Anlaysis of 1D Floors

To analyse a variety of floors efficiently a MATLAB program called *SPECTRAL* was developed. This software was then tested and used to obtain results using SEM and compare with the conventional FEM. This section begins by introducing the software, then continues by examining an initial test structure that was used to validate the program, and ends with a 3D grillage analysis of 1D floors. The investigations begins with focusing on full structures using standard beam elements, then investigates the possibility of reducing the size of the structure using semi-infinite elements.

6.3.1 The *SPECTRAL* Matlab Program

The Euler beam derived in the previous section has been implemented in the spectral element analysis software *SPECTRAL*. *SPECTRAL* assembles the global dynamic stiffness matrix in much the same way as standard FE analysis, however, there are some small differences. The problem must be solved for *N* pseudo static problems, where *N* represents a solution at an explicit frequency. The result is a displacement response spectrum with *N* frequency lines, for each node, which can be processed by the inverse FFT to obtain a time domain solution of displacement.

SPECTRAL was designed to be directly comparable with FE analysis, in this case ANSYS. *SPECTRAL* will read ANSYS script files, but with only a subset of commands and features, which allows for direct comparison with ANSYS. The reduced command and feature set is shown in Table 13. Spectral works by applying the spectral elements to the unmeshed geometry (e.g. keypoints, lines, etc.) and the mesh commands just applies the selected properties to the geometry, but does not split the geometry into smaller elements. Some additional features also needed to be added: finite and semi-infinite beams were included, and a frequency range for the solution was required.

AL	Maximum of four lines, will be used for a plate element in the future.
DK	Only supports displacements and rotations. Does not support DK,ALL.
*DO	Same as ANSYS.
ET	Only supports beam4. Use ET,4,SEMI for semi-infinite beam.
FK	Only supports keypoint and direction. The force applied will be unit impulse. The response can then be easily scaled in post processing for an arbitrary input.
K	Same as ANSYS.
L	Same as ANSYS.
LMESH	Only supports LMESH,ALL.
LSEL	Only supports select by line number. Only supports create new set or add to current set. Also, both line numbers must be specified.
MAT	Same as ANSYS.

MP	Only supports EX, GX and DENS.
NUMSTR	Only supports line, keypoints and areas.
R	Same as ANSYS, but for essential properties only.
REAL	Same as ANSYS.
SOLVE	Solves over frequency range, frequency range currently hard programmed into SOLVE.M.
TYPE	Same as ANSYS.

Table 13 - Spectral support for ANSYS commands

6.3.2 Initial Test Structure

Initially a small model was used to test *SPECTRAL* and complete the initial comparisons. This model was based on the parametric studies in Chapter 5.2, but the model complexity reduced considerably. The model was reduced to a single dimension, with a beam representing the slab and being supported by columns, shown in Figure 127. A unit impulse excitation was applied to the centre of the structure and compared with results from ANSYS. The response of each model at the excitation points is shown in Figure 128 with 3% damping.

As this example is not intended for analysing the accuracy of the simplification of the model, the results will not be compared with the corresponding model used in the parametric study. As seen from the responses of each method, they are almost identical. There is a small oscillation of the response when using the spectral element method due to leakage when using the Fourier transform. This problem can be eliminated by increasing the length of the time window, increasing the damping so the response decays faster or by adding semi-infinite elements to increase energy dissipation from the structure. However, the most interesting part of this initial comparison is the time for the analysis to run for the same resolution of data: 170s for ANSYS and 50s for the spectral elements.

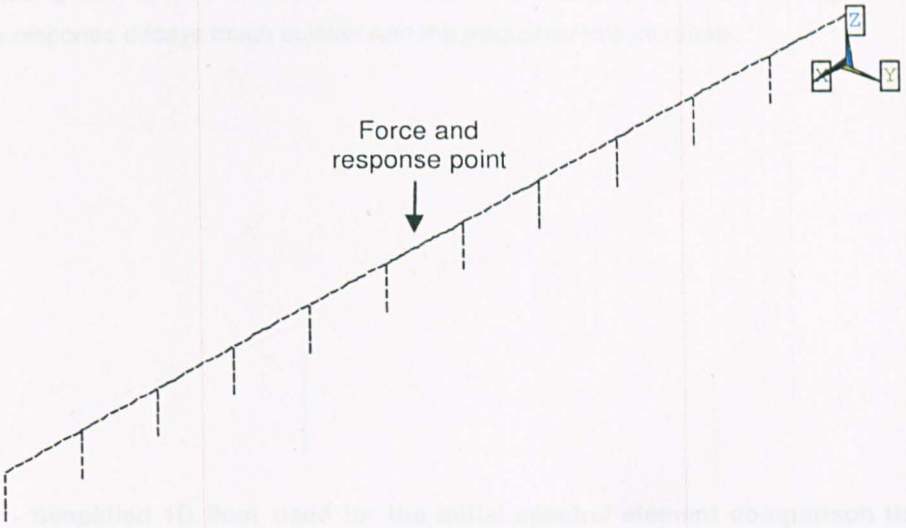

Figure 127 - Simplified 1D floor used for the initial spectral element comparison

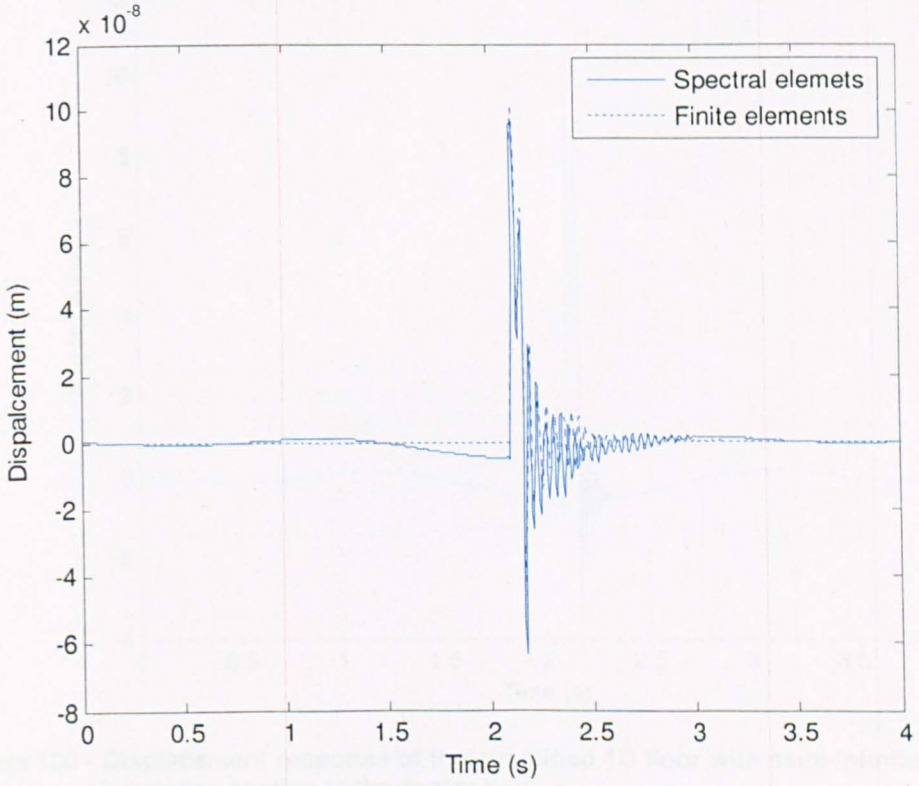

Figure 128 - Displacement response of the simplified 1D floor to a unit impulse applied at the centre bay

The simple structure was then adjusted to include semi-infinite elements in order to remove energy from the bay of interest, and the same analysis was rerun. The structure is shown in Figure 129 and the displacement time history in Figure 130.

Ideally, if this method could estimate the response of a floor of infinite bays the response should be similar to the 11 bay model (as after 10 bays there was generally little reduction in response when

further increasing the number of bays). It is clear that the amplitude of the response is similar, however the response decays much quicker and the frequency has increased.

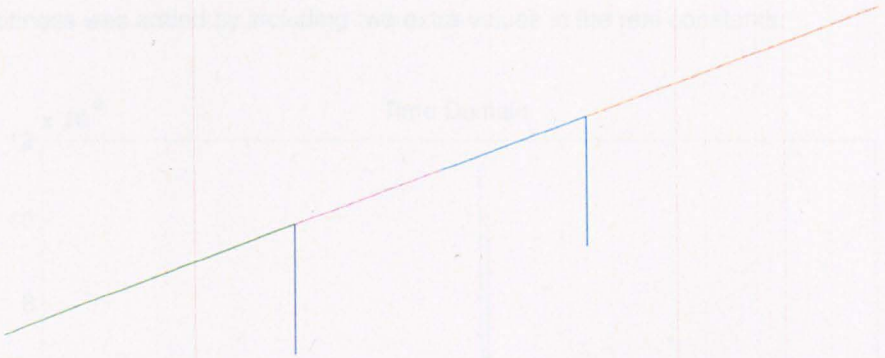

Figure 129 - Simplified 1D floor used for the initial spectral element comparison using semi-infinite elements at the ends; the force and response point is at the centre of the structure

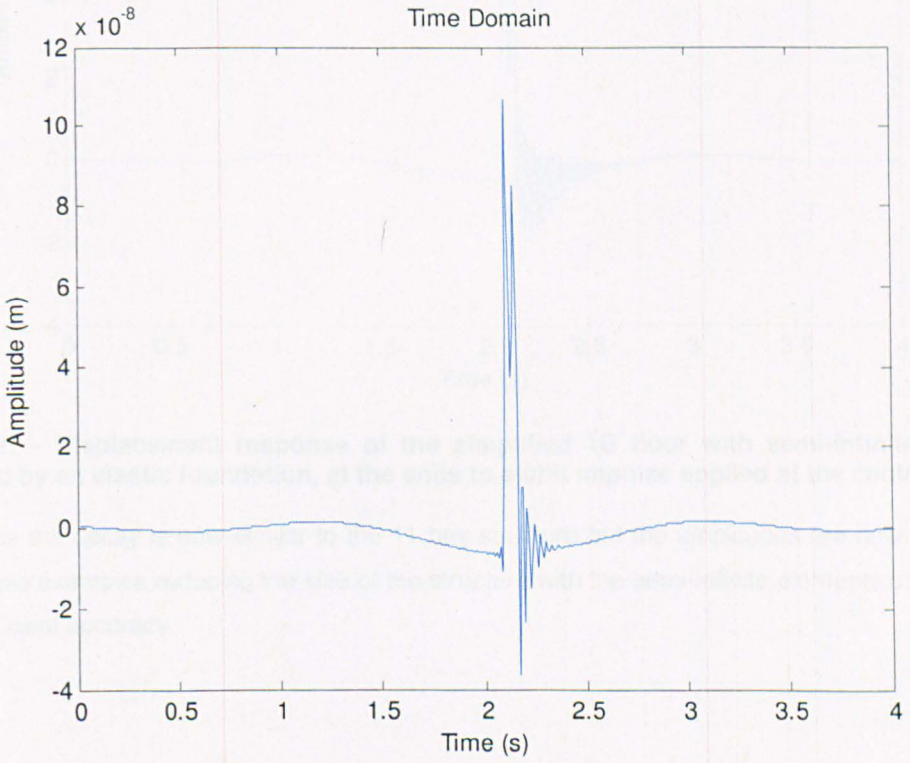

Figure 130 - Displacement response of the simplified 1D floor with semi-infinite elements at the ends to a unit impulse applied at the centre bay

To attempt to improve the accuracy, an additional element was created, one with a distributed stiffness support (i.e. an elastic foundation), similar to the first example in this chapter. Although in the previous example, the semi-infinite beam on the elastic foundation removed energy, the column stiffness of the floor could not accurately be described. In this example, as the centre bay is modelled, and it was shown in the previous chapter that parts of the structure away from the bay of interest could

be modelled crudely, the semi-infinite beam on elastic foundation may give an accurate solution. To incorporate the new element into the *SPECTRAL* program a new beam was created, known as beam5, where the Euler beam's wave number was altered to include the elastic support. The distributed stiffness was added by including two extra values in the real constants.

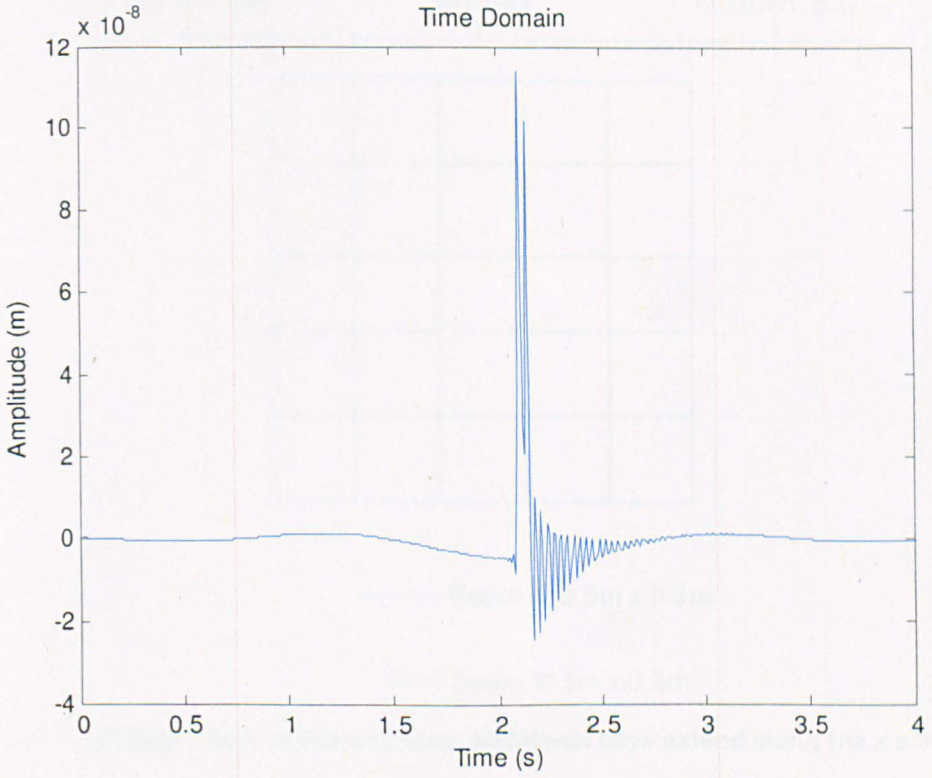

Figure 131 - Displacement response of the simplified 1D floor with semi-infinite elements, supported by an elastic foundation, at the ends to a unit impulse applied at the centre bay

In this case the decay is now similar to the 11 bay structure but the amplitudes are now different. In these simple examples reducing the size of the structure with the semi-infinite elements used does not retain sufficient accuracy.

6.3.3 Spectral Element Grillage Analysis of 1D Floors

As a plate element was not developed a grillage was created based on the floor used in the parametric study in Chapter 5.2. As the study investigates applications of the spectral element method, the grillage will be a very simple square mesh based on the work of Szilard [123].

The mesh of a single bay, with its corresponding elements, is shown in Figure 132. Beam 1 extends along the edge of the structure, as such it is half the width of beam 2. Beam 2 is 1m wide and 0.3m deep, which is the same depth as the slab. The grillage is somewhat coarse in its mesh and as such

accuracy will be lost. The accuracy could be improved with a finer mesh, or with the use of diagonal elements. However, due to limitations of the Spectral program, a limit based on the specifications of the computer would be exceeded with any more elements. However, as the study is concerned with the application of spectral elements, not the best practice of grillage design, it will suffice.

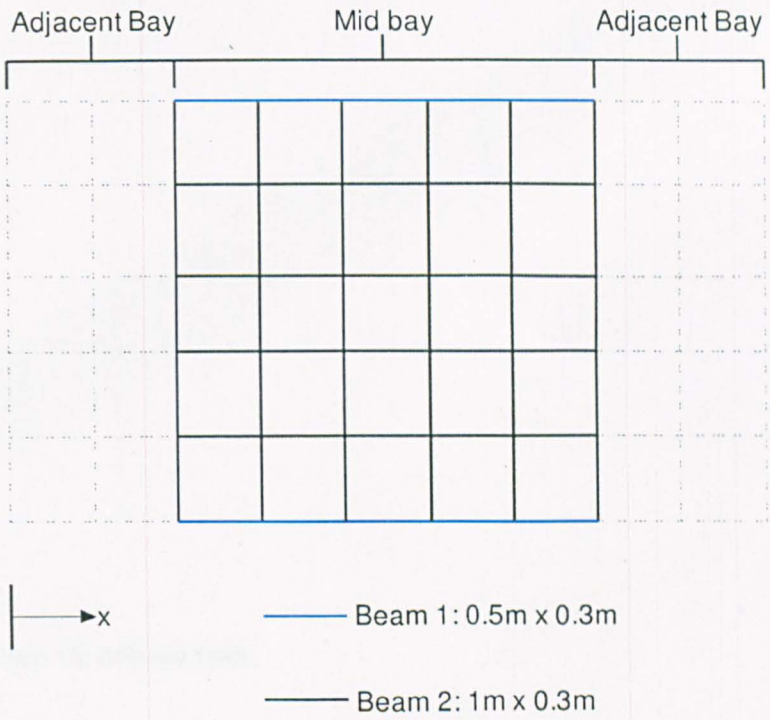

Figure 132 - 1D grillage mesh of the test floor, additional bays extend along the x axis

To begin with, an 11 bay 1D floor was analysed using finite elements and spectral elements, the floor is shown in Figure 133. As displacement spectra are the output from the SEM these will be compared, along with velocity time histories. Both of these are obtained for the centre of the structure.

Figure 134 shows a comparison of the displacement spectra. The two plots are very similar, however, there are some noticeable differences: the amplitudes of the peaks and troughs are slightly different. The differences can be attributed to the different levels in discretisation and the frequency resolution. Each beam in the FE model has been divided into two elements, whereas each spectral element is described by a continuous function. These differences, although small, can introduce small variances in the natural frequencies. As the spectra are constructed at 0.1 Hz frequency resolution it is possible that the peaks and troughs may not be described exactly and hence the variations.

Figure 135 shows the velocity time histories. Again, there are small differences; however, these are smaller than those of the displacement spectra, and are negligible. An interesting observation can be made. The previous section showed that the displacement time histories (such as Figure 130) were clearly affected by the wrap around effect, when considering velocity time histories this is not the case.

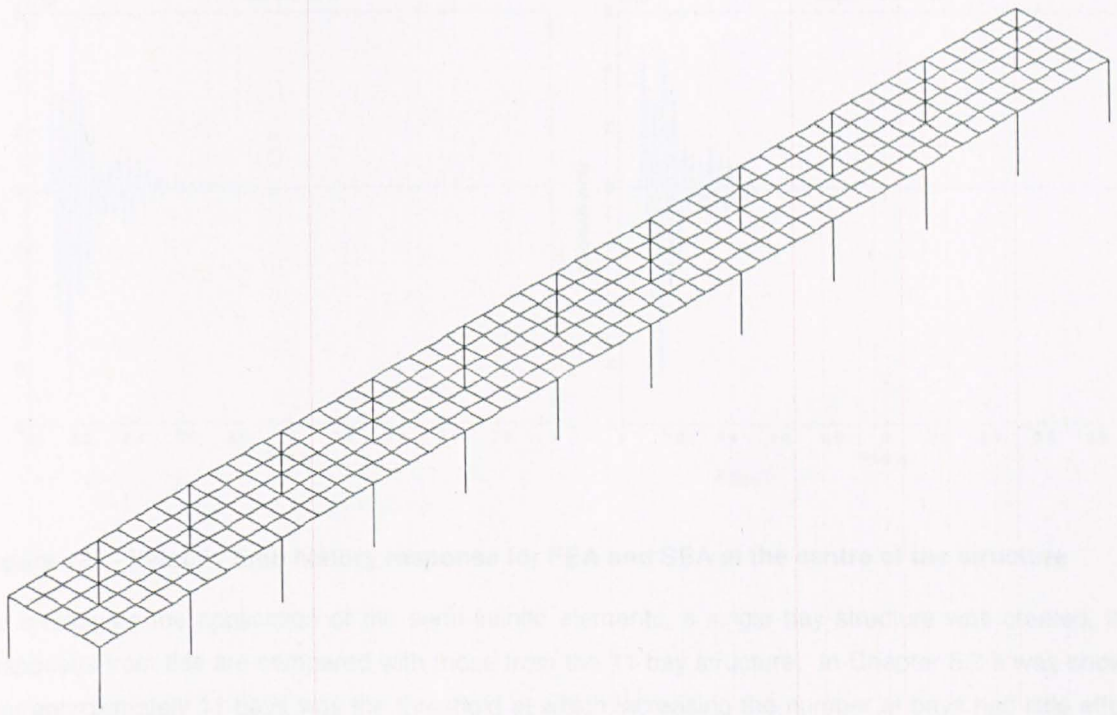

Figure 133 - 11 bay, 1D grillage floor

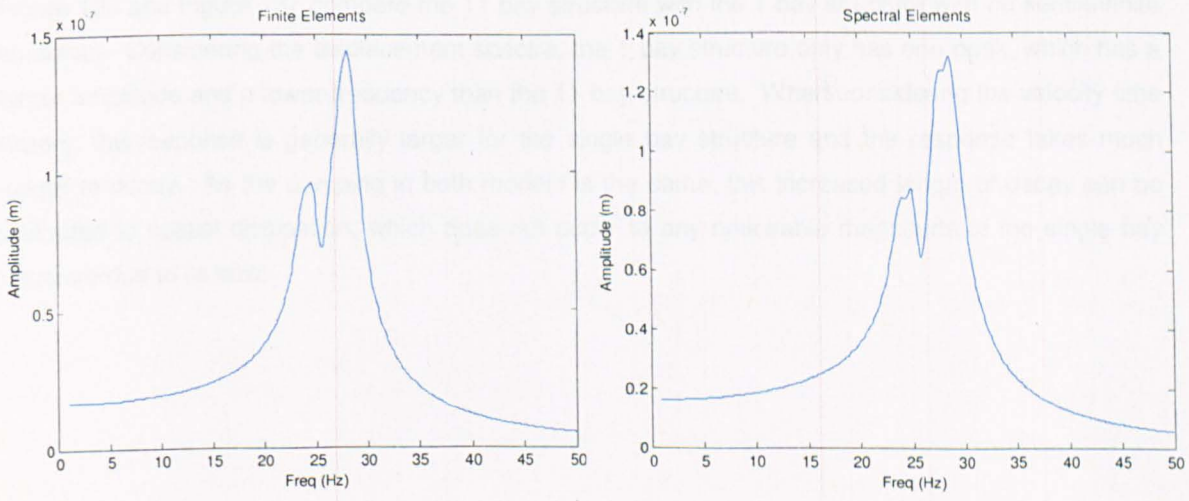

Figure 134 - Displacement spectra for FEA and SEA at the centre of the structure

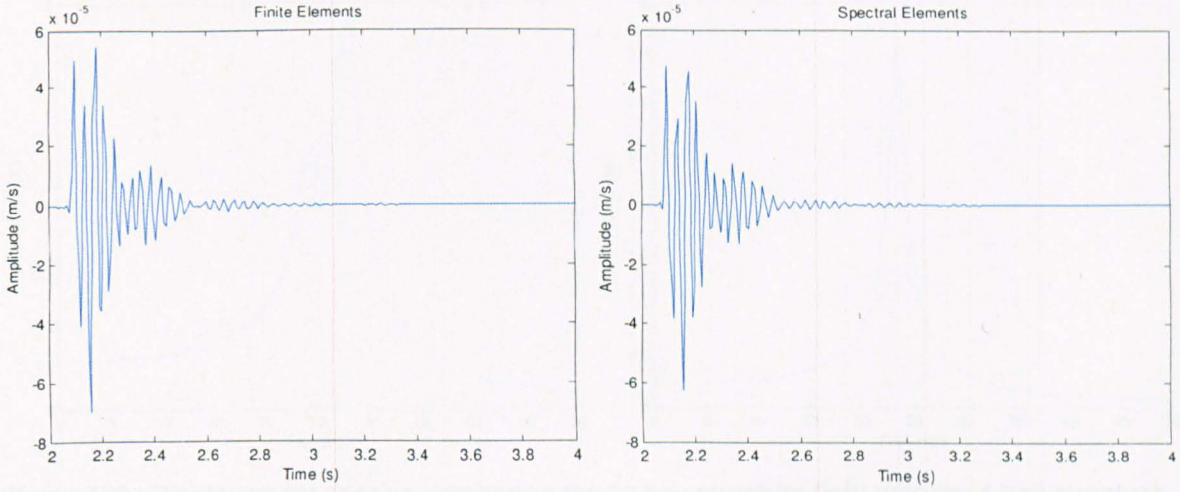

Figure 135 - Velocity time history response for FEA and SEA at the centre of the structure

To investigate the application of the semi infinite elements, a single bay structure was created, the responses from this are compared with those from the 11 bay structure. In Chapter 5.2 it was shown that approximately 11 bays was the threshold at which increasing the number of bays had little effect on the response. At this point, a structure of infinite length would have a response similar to that of the 11 bay structure, as such, the semi-infinite elements may be able to model this. In all subsequent figures the 11 bay response will be presented on the left for easy comparison with the spectral element response on the right.

Figure 136 and Figure 137 compare the 11 bay structure with the 1 bay structure with no semi-infinite elements. Considering the displacement spectra, the 1 bay structure only has one peak, which has a larger amplitude and a lower frequency than the 11 bay structure. When considering the velocity time history, the response is generally larger for the single bay structure and the response takes much longer to decay. As the damping in both models is the same, this increased length of decay can be attributed to spatial dissipation, which does not occur to any noticeable magnitude in the single bay structure due to its size.

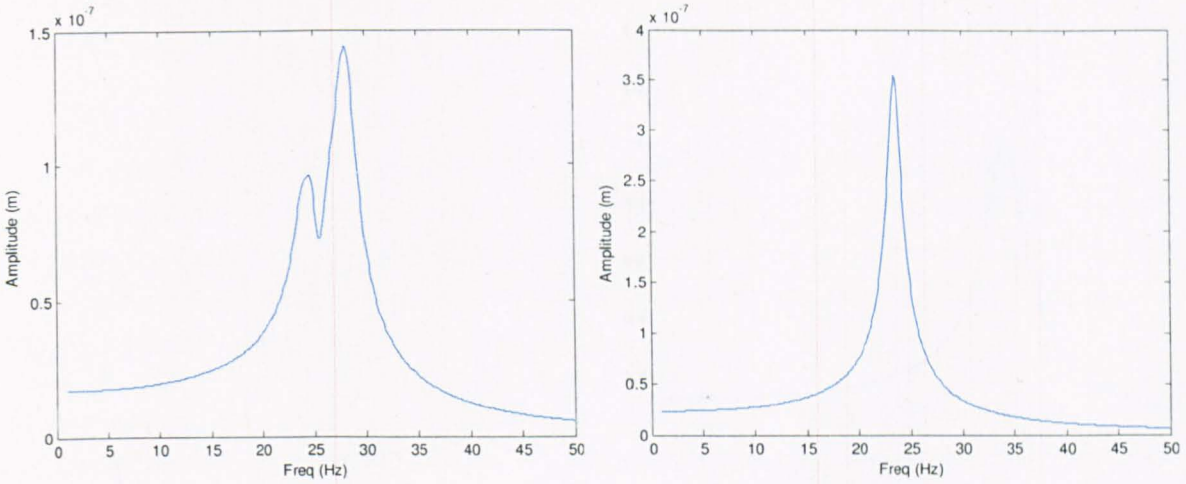

Figure 136 - Displacement spectra comparing the 11 bay structure (left) with the 1 bay structure (right), with no semi-infinite elements

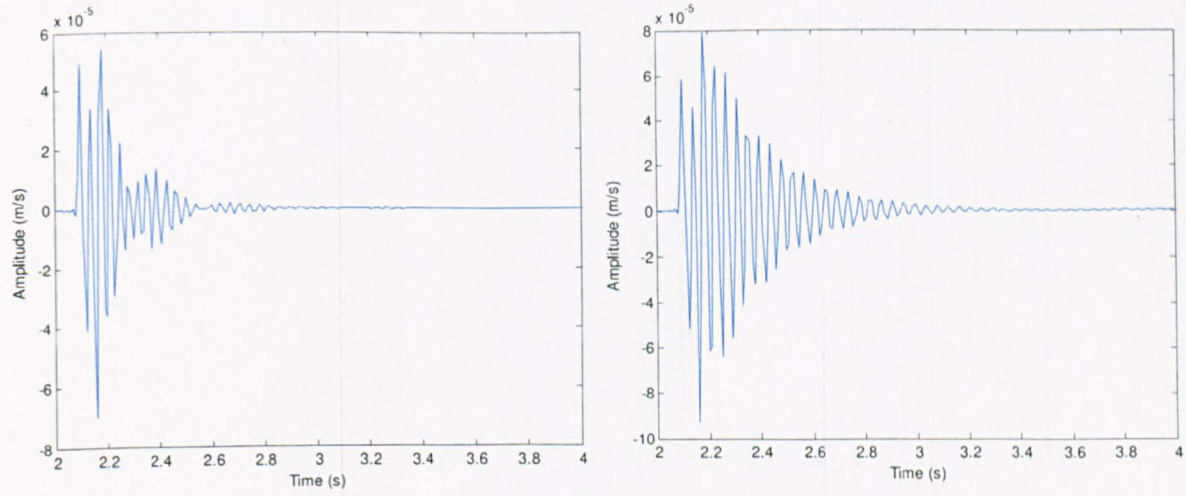

Figure 137 - Velocity time history response comparing the 11 bay structure (left) with the 1 bay structure (right), with no semi-infinite elements

Figure 138 and Figure 139 show the response of the 1 bay structure after semi-infinite beams were added to each end. Considering the velocity time history, the response has reduced and the rate of decay has also reduced. However, the amplitude is now lower than for the 11 bay structure and the response decays quicker. Although no extra viscous damping has been added to the structure, energy is now being dissipated spatially through the semi-infinite beams. Considering the displacement spectra, the peak amplitude has now reduced, although too much, and the frequency has now increased, again too much. The width of the peak has also notably widened, indicating an increased level of damping (spatial dissipation)

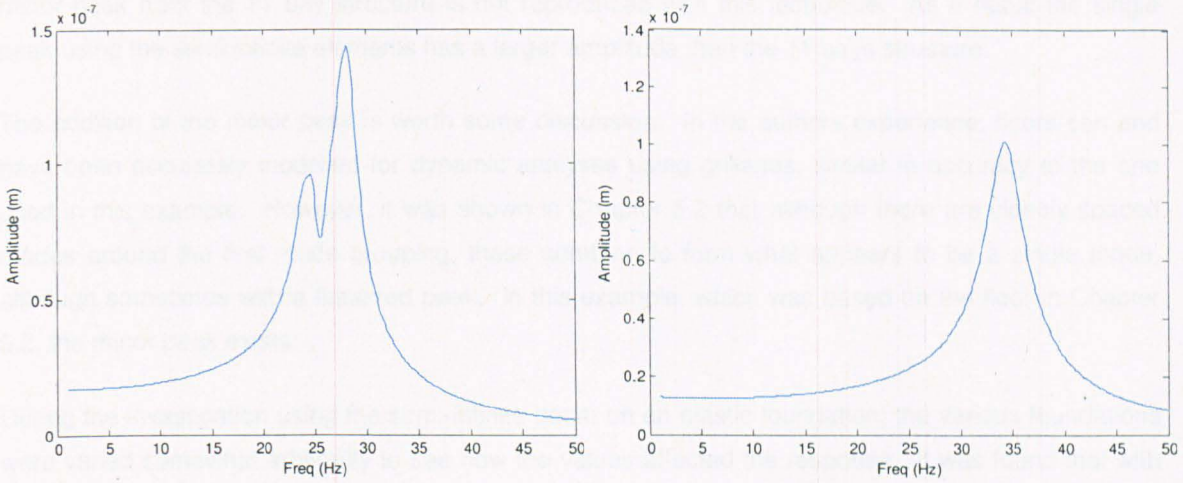

Figure 138 - Displacement spectra comparing the 11 bay structure (left) with the 1 bay structure (right), with semi-infinite elements

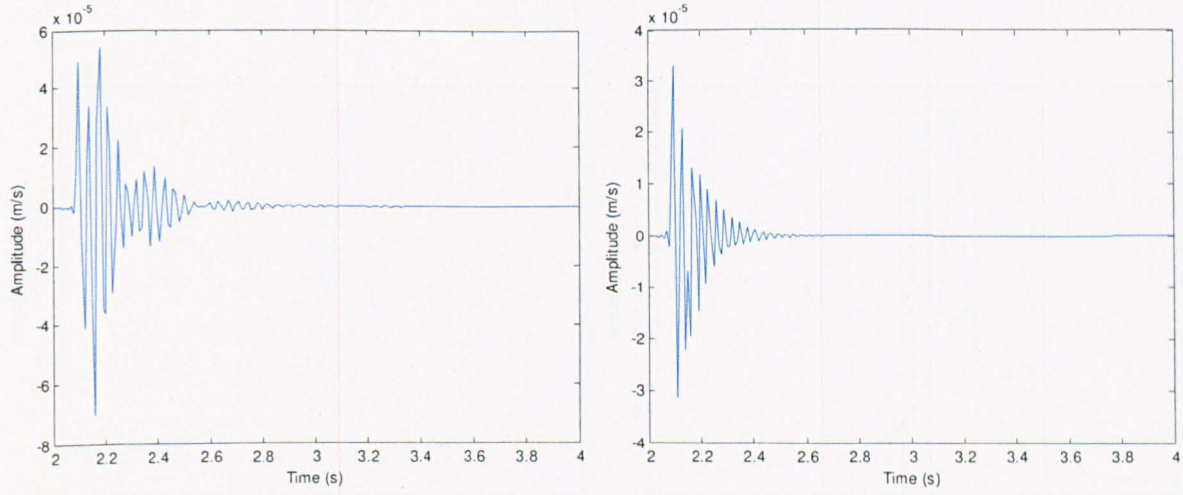

Figure 139 - Velocity time history response comparing the 11 bay structure (left) with the 1 bay structure (right), with semi-infinite elements

As just a single bay over-estimates the response and underestimates the frequency and damping, and using a standard semi-infinite element underestimates the response and over estimates the frequency and damping, something in between is required. The beam was altered to a semi-infinite beam on an elastic foundation. In this example, the procedure was a little more complex then the example shown previously in the chapter in that each beam has a unique stiffness estimated for it using static deflections.

Figure 140 and Figure 141 show the responses. Considering the velocity time histories, the amplitude of response is now comparable with the 11 bay structure, although the response takes longer to decay. Also, in the 11 bay structure there is a beating characteristic due to the interaction of two close modes in the time domain. When considering the displacement response spectra it is clear that the

minor peak from the 11 bay structure is not reproduced with this technique. As a result the single peak using the semi infinite elements has a larger amplitude then the 11 bays structure.

The addition of the minor peak is worth some discussion. In the authors experience, floors can and have been accurately modelled for dynamic analyses using grillages, similar in accuracy to the one used in this example. However, it was shown in Chapter 5.2 that although there are closely spaced modes around the first mode grouping, these combine to form what appears to be a single mode, although sometimes with a flattened peak. In this example, which was based on the floor in Chapter 5.2, the minor peak exists.

During the investigation using the semi-infinite beam on an elastic foundation, the various foundations were varied somewhat arbitrarily to see how the values affected the response. It was found that with various combinations the displacement spectrum could be varied to have almost any amplitude and frequency. The spectrum could also have its peak widened, and the top of the peak could also be flattened to a certain extent. The velocity time domain response could also have almost any amplitude and decay rate, also a response could be obtained the exhibited a beating characteristic.

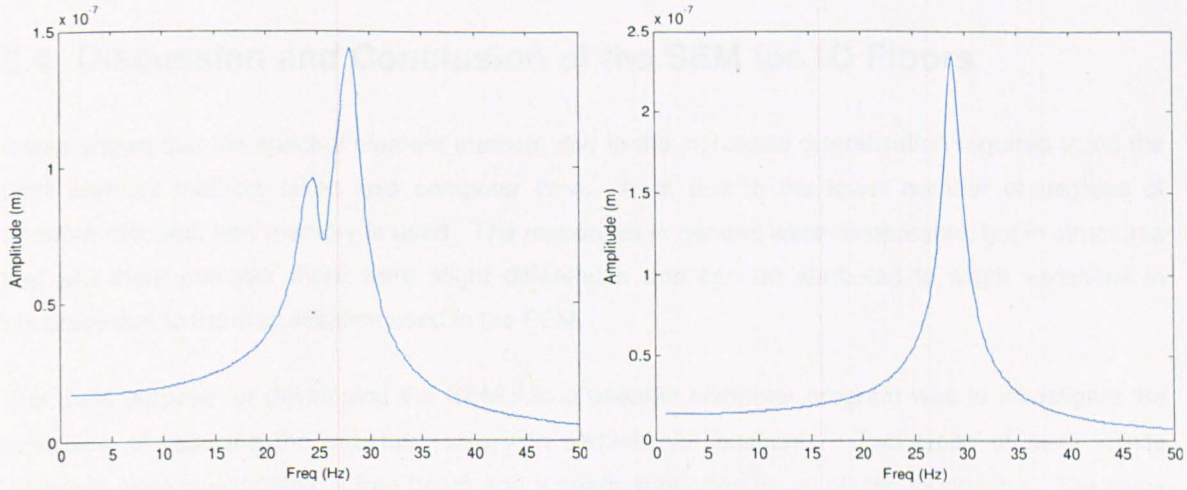

Figure 140 - Displacement spectra comparing the 11 bay structure (left) with the 1 bay structure (right), with semi-infinite elements on an elastic foundation

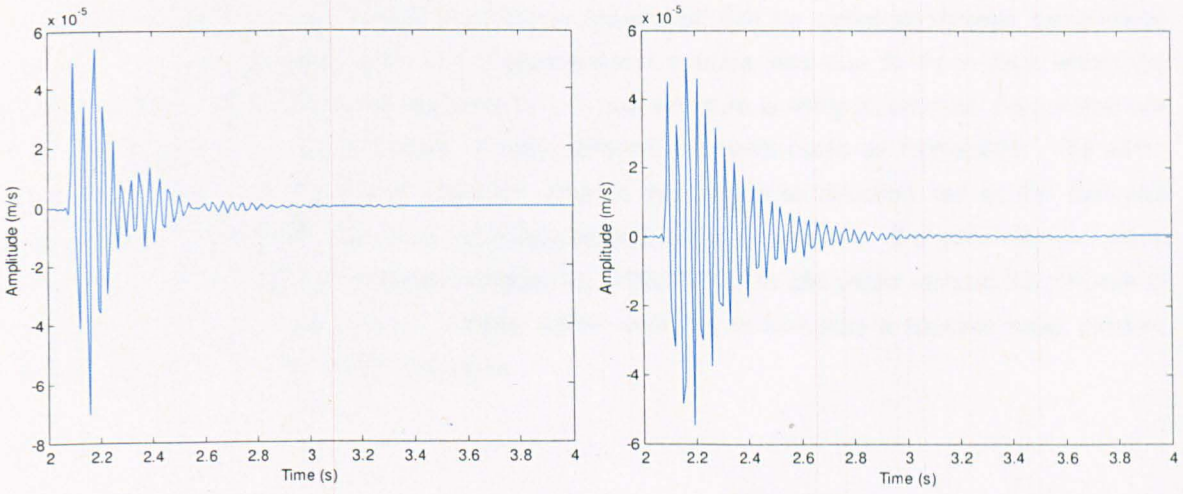

Figure 141 - Velocity time history response comparing the 11 bay structure (left) with the 1 bay structure (right), with semi-infinite elements on an elastic foundation

6.4 Discussion and Conclusion of the SEM for 1D Floors

It was shown that the spectral element method, due to the increased discretisation required using the finite element method, takes less computer time. Also, due to the lower number of degrees of freedom required, less memory is used. The responses in general were comparable, but in structures that are more complex there were slight differences and can be attributed to slight variations in accuracy due to the discretisation used in the FEM.

The main purpose for developing the SEM into a useable computer program was to investigate the possibility of reducing the structural size with semi-infinite elements. Two types of semi infinite elements were investigated: a free beam and a beam supported by an elastic foundation. The semi-infinite elements were evaluated by comparing to an 11 bay structure, which can be considered to respond in a similar manner to a structure of infinite length. When considering a large multi-bay floor from a wave propagation perspective, the main difference between a small and large floor is the area in which spatial dissipation can occur. Although the use of semi-infinite elements did allow for the spatial damping, the response was different from increasing the number of bays.

The semi-infinite free beam considerably increases the natural frequencies of the floor and overestimated the spatial dissipation. It was hoped that the semi-infinite beam on the elastic foundation would solve this problem. However, with the foundation stiffnesses calculated, the frequency estimate and time history amplitudes were accurate, but the spatial dissipation was underestimated.

Although the response of a large floor was not successfully simulated with semi-infinite elements, the study still has merit. It was shown that spatial dissipation can be achieved through semi-infinite elements. As the additional peak in the displacement spectra was due to more bays within the structure, adding the semi-infinite elements to a 3 bay structure is likely to produce results that are more accurate than a 1 bay structure. Finally, different elements could be formulated. The semi-infinite beams were not connected with each other in the transverse direction, but as the floor was modelled as a grillage they should be and it may be possible to include this. If a plate element, along with its semi-infinite counterpart were developed for *SPECTRAL*, its use would remove the problem of connecting the semi-infinite beams. Another option could be to formulate a spectral super element [129] to model the floor bay more accurately.

7 Review of Generic Vibration Criteria

Up to this point, the analysis has been concerned with accurately quantifying the level of vibration. However, until an acceptable level of vibration is known, there is little benefit in conducting the analysis. Vibration criteria have developed over the years, and are described in more detail in Chapter 2.4.2.2. BBN's VC curves [7] are the most popular criteria, and the most widely cited in the literature, however, a number of issues have been brought up regarding their application. A more recent style of guidance, using velocity spectra, has been outlined in ISO/TS 10811-1 [93]. The velocity spectra (VS) method is supposed to address a number of issues that have been brought up about the VC curves. This chapter focuses on the validity of BBN's VC curves and compares with the VS method.

When developing machine specific criteria, whether it is used to design to, or to identify where the machine sits on the VC curves, a number of points must be considered. The problem is increased further in the choice of methods when analysing the floor's response. In testing the equipment, the most simple approach is to see at what amplitude a sinusoidal wave causes failure (failure, in this case, is defined as when the machine cannot perform adequately, not when it falls apart), this method can then be used to develop a spectrum. The problem with this approach is that it does not accurately assess the machine's performance with broadband excitation, or multi-tonal excitation. The problem also goes the other way, if criteria are developed using broadband excitation, it is not relevant for a pure tone excitation. The next problem in developing criteria is the use of RMS response. Firstly, in criteria that already exist, the averaging time is often not stated, and it should be obvious to any analyst that the average time can influence the magnitude of response. Secondly, RMS averaging will remove sharp transients from the signal. If these transients would cause the machine to fail, then RMS averaging should not be used. When considering analysing the response of the floor, a number of methods exist: Fourier amplitudes, power spectra, 1/3 octave spectra, peak to peak, RMS etc. Each has its own advantage with certain signal types and certain types of machinery, as such, one method does not always better another. If, after the criteria for a machine has been characterised, the criteria needs to be generalised and reported using a generic vibration criteria, further issues arise. Appendix A shows a collection of specific criteria. These show that the criteria do not follow any specific trend, and even machines of a certain type do not follow a specific trend (although there is less variation when considering one type of machine only). Characterising any of the specific criteria shown with a generic equivalent would cause large inefficiencies through requiring design to a class at all frequencies.

As discussed in Chapter 2.4.2.1 a number of issues have been brought up concerning the VC curves, the most popular being: why RMS velocity? why 1/3 octave bandwidths? why constant velocity criteria? When the criteria were first developed, they were basically an extension of the velocity human tolerance criteria [10, 11] but extended below the level of human perceptibility. The use of 1/3

octave bandwidth is described in one of the early publications [10, 11], where it explained the analogue analysers that could easily be used in experimental conditions (i.e. while testing a floor) were then not capable of FFT analysis, but 1/3 octave analysers were common. As such, it appears that the criteria were just an extension of what already existed using the technology available at the time, and not specifically developed with sensitive machinery in mind. Since the creation of the VC curves, and after various criticisms, there have been publications defending the method and justifying the approach [8, 137], but they all seem retrospective.

The response spectra method, developed by Ahlin [138] was developed in the hope of eliminating the problems associated with the VC curves. The approach consists of shaking the machine, with pure tone sinusoids, increasing the amplitude until failure of the machine. This is repeated at many frequencies to obtain a failure spectrum. A filter is then designed to be applied to a response time history of the support of the machinery. The filter is applied in such a way that the peak velocity value returned from the filtered time history is applied as a sine wave to excite the machinery, then the response of the machinery would be the same as if excited by the original signal. As such, the magnitude of this equivalent sine wave can be compared with the criteria developed with the sine excitation used to create the criteria, eliminating problems due to RMS, bandwidths, etc.

This chapter begins by discussing the relevance of generic criteria versus tool specific criteria in detail. The chapter then continues to assess the performance of the VC curves for a number of simulated machines and signal types and compares with results from the VS method. And finally, the chapter finishes by discussing the results and how an introduction of variable force models, which give a distribution of response rather than a fixed value, might affect vibration criteria in the future.

7.1 Relevance of Generic Vibration Criteria

The most common generic vibration criteria are the VC curves. Although it is likely that the curves are just an extension of the human criteria, and not developed specifically with sensitive machinery in mind, they still might be relevant. It is shown in Appendix C that specific criteria do not exhibit much of a common trend. As such, any attempt at generic criteria would be difficult to relate to machine specific criteria. Due to this, even if the generic criteria were defined arbitrarily, they would likely have as much relevance as a more rigorous approach.

When considering human vibration criteria, a generic approach is essential. A standard office floor, or a public building, would have many hundreds or thousands of individual human users. As such, when characterising the floor as acceptable, it must be acceptable for many different people and the criteria must echo this. It would be inefficient to ascertain the tolerance of one individual, and design the floor specifically for them, as another user would have a different level of tolerance and the floor could then be unsuitable for them.

The question is: can this rationale be applied to sensitive machinery? To begin with, in a life time of the floor, the floor will not be subject to hundreds or thousands individual machines, the number is likely to be in the order of tens or less. Using the same rationale, four situations have been identified:

1. General high tech industrial floor
    - During the design phase, the occupancy of the floor is unknown and it may, or may not, be vibration sensitive. In addition, it is likely that the occupancy will change many times throughout the structures life. Generic criteria are required.
2. Floor with known machine type, but not the exact model
    - The machine specific criteria is not known, but due to the machine type being known the required vibration limits could be characterised. Generic criteria are required, however, generic criteria for the machine type would lead to a more efficient design.
3. Floor with a known machine
    - If the manufacturer has developed accurate vibration criteria for the specific machine, design to those criteria would be more efficient then to general criteria, athough this would complicate the design process. Generic or machine specific criteria are required.
4. Situation 2 or 3, but with a short machine life span.
    - If the life span of the machine is known to be short, the floor could be host to many different sensitive machines in its life span. As such, some generalisation of the floors performance is required. Generic criteria are required.

Therefore, generic criteria is essential for a number of situations, but designing to machine specific criteria could result in a more efficient design.

A more efficient method to characterise a floor would be with generic criteria but also with the known floor specific criteria, this would have benefits in a number of situations. For example, if a client owns a floor space characterised as VC-B they will have a basic idea of what types of machinery could operate. However, if the client wants to install a piece of VC-C equipment, the floor would be unsuitable. However, if the response spectra for the floor is available and the machine specific criteria is available these can be compared. As shown in Appendix A, the machine specific criteria vary a significantly throughout the frequency range and it would often be the case that the part of the spectrum that caused the machine to be classified as VC-C, would be different to the part of the floor spectrum that classifies it as VC-B.

A further point is how to classify a whole floor area. Figure 142 shows a floor which has been analysed using the VC curves. The largest response is in the centre of the floor bays, which worse than VC-A, and the floor would be classified as such. However, if the sensitive machine was placed away from this area, better floor performance can be achieved, even up to VC-B or VC-C.

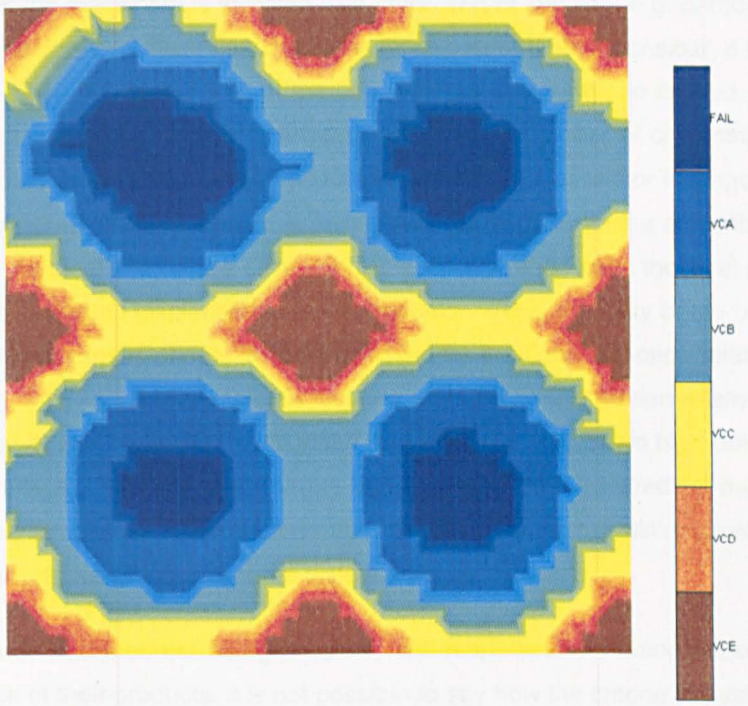

Figure 142 - VC response of a floor to walking; the floor is split up in to 4 bays with a 2 bay x 2 bay configuration, the colour representing 'fail' means worse the VC-A, the VC-E responses represent column locations

It has been shown that in certain circumstances generic criteria are essential. However, the current generic criteria, and the way a whole floor is characterised may not be the most efficient procedure. It remains to examine whether the current analysis methodologies accurately represent the vibrations when comparing to the criteria. The next section presents a small analytical investigation of the vibration analysis methods.

7.2 Assessment of the VC and VS Methods

Unfortunately, it is difficult to actually test a real piece of machinery to determine it vibration sensitivity. As such, it is difficult to assess accurately any criteria that may exist and the corresponding analysis methods. Due to this, an analytical study was conducted on hypothetical machines.

The hypothetical machines consist of SDOF oscillators subject to base excitation. Three machines were considered, each with a different frequency but constant mass. The damping of the oscillator is easily changed and two values were considered: a lightly damped 1% and a heavily damped 15%. When considering how the machines would fail, a number of approaches were used and are worth some discussion.

It is often stated that velocity is a good metric for vibration criteria due to the nature of the sensitive machinery. Much of the machinery is involved with some sort of imaging, e.g. photo-lithography, MRI scanners, microscopes etc.. In these cases there is an exposure time to consider, if the subject of the image displaces to much during the time of the exposure the image will be blurred. This equates to distance divided by time, hence velocity. However, there are a number of circumstances where this rationale is not valid. This example is only valid if the period of the oscillator is longer than the period of exposure. If the period of the oscillator is lower than the exposure time a number of oscillations would occur during the exposure, in this case the displacement (and hence the level of blurring) would be described by the maximum displacement of the oscillator. Also, the fixity of the target needs to be considered. If, in the examples above, the target is rigid on the floor, a motion relative to the floor is required. However, if the target is completely isolated from the floor a motion relative to a fixed point in space is required. This is better illustrated when considering a long-beam high-precision laser. The target, after being reflected through many mirrors and prisms, can be hundreds of meters away and in a different part of the structure. In this case a maximum displacement is still required during the firing time of the laser, but relative to a target some distance away.

Due to testing of real machines not being possible, and manufacturers being rather secretive about the internal workings of their products, it is not possible to say how the criteria should be assessed. In this study, the VS and VC methods are used to assess the vibration, comparing with basic Fourier amplitudes. For each hypothetical oscillator a sinusoidal floor vibration of 1 m/s at the oscillators natural frequency is considered to be the operational limit. The oscillator is then analysed with this excitation and the corresponding total acceleration, velocity and displacement of the oscillator are recorded, along with their counterpart relative to the floor. For clarity, these are shown in Figure 143, where u_g is the ground displacement, u_o is the oscillator displacement, relative displacement can be defined as $u_{rel} = u_o - u_g$, and m, k and c are the mass, stiffness and damping of the oscillator respectively. The ordinates used in the criteria will either be u_o or u_{rel} and their velocity and acceleration counterparts.

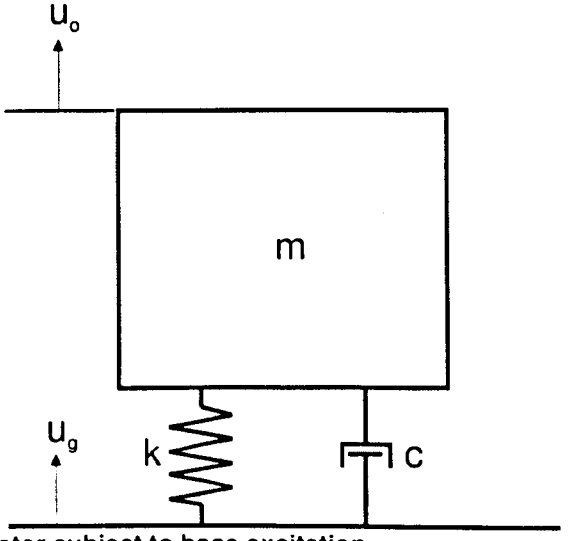

Figure 143 - SDOF oscillator subject to base excitation

7.2.1 Vibration Criteria Generation

Three hypothetical machines (tools) were investigated and are outlined in Table 14 along with their rationale. For each tool, the criteria developed are shown in Figure 144, Figure 145 and Figure 146 for displacement, velocity and acceleration limits respectively. The criteria were developed by applying a sine wave of fixed frequency and increasing the amplitude until the tool 'failed', the frequency was then changed and the procedure repeated to build a failure spectrum.

Tool 1	2 Hz oscillator	A low frequency, close to a natural pace rate.
Tool 2	12.2 Hz oscillator	Frequency matches the frequency of the floor where the walking time history was simulated.
Tool 3	20 Hz oscillator	A high frequency, to assess whether the constant velocity assumption is valid.

Table 14 - Tool frequencies and rationale

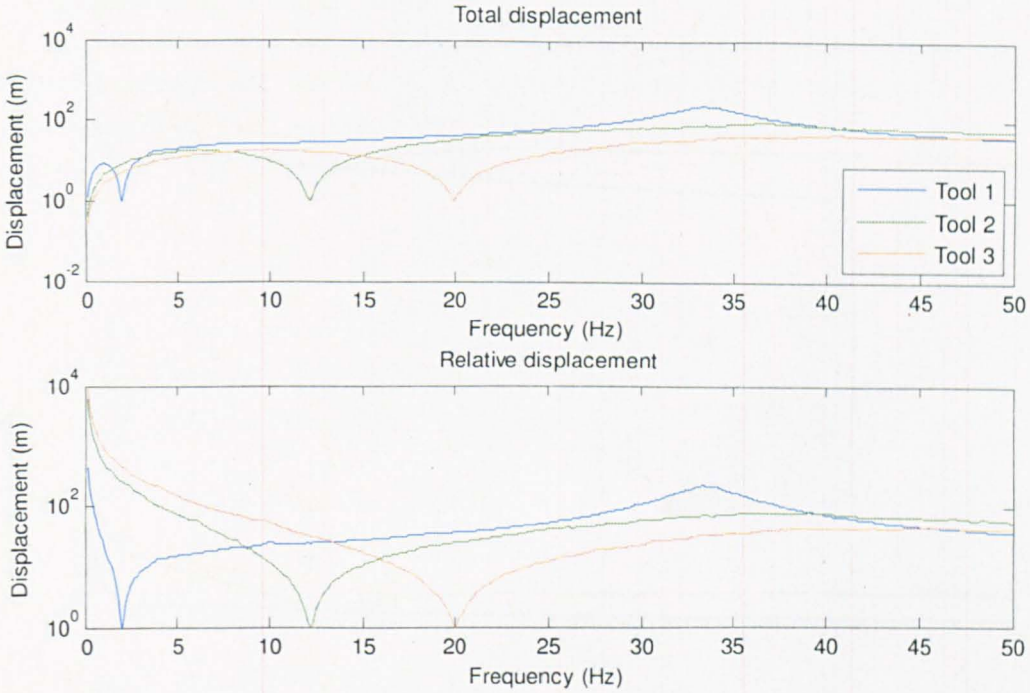

Figure 144 - Displacement failure criteria for hypothetical tools 1, 2 and 3 with 1% damping; total displacement *(top)* and relative displacement *(bottom)*

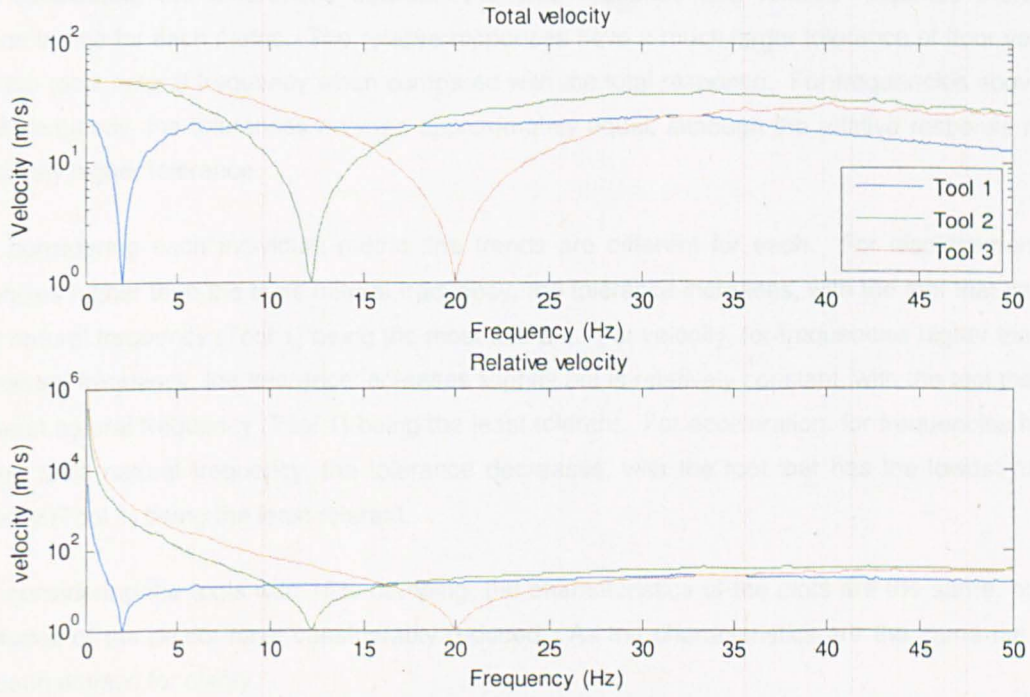

Figure 145 - Velocity failure criteria for hypothetical tools 1, 2 and 3 with 1% damping; total velocity *(top)* and relative velocity *(bottom)*

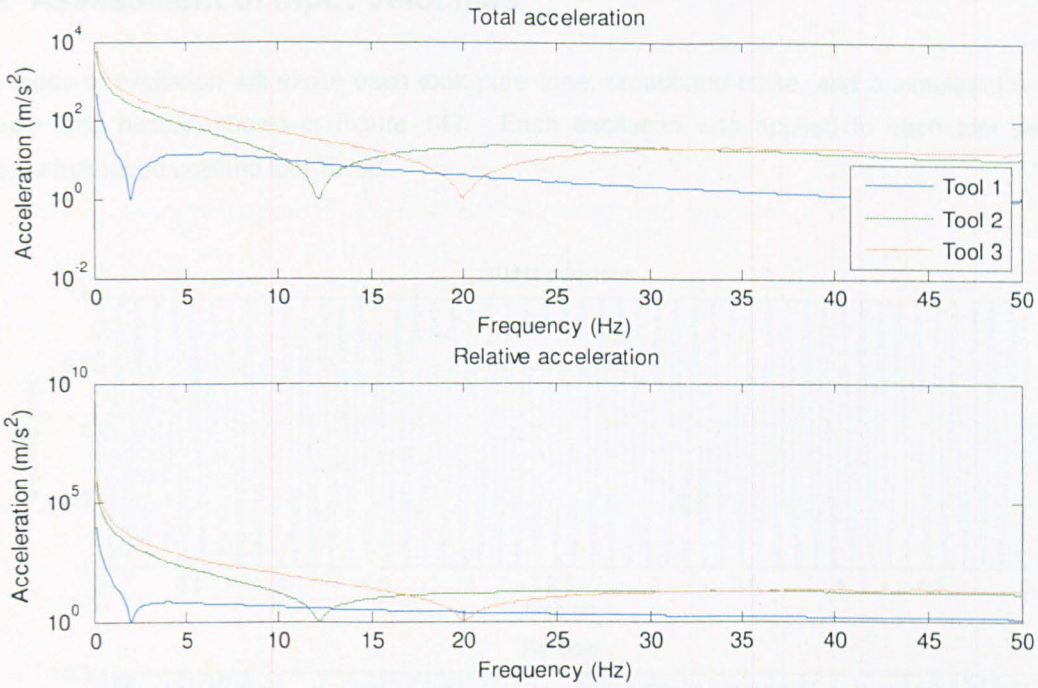

Figure 146 - Acceleration failure criteria for hypothetical tools 1, 2 and 3 with 1% damping; total acceleration *(top)* and relative acceleration *(bottom)*

When considering the differences between the total response and relative response there are common trends for each metric. The relative responses have a much larger tolerance of floor velocity below the tools natural frequency when compared with the total response. For frequencies above the natural frequency, the tolerances become approximately equal, although the relative response has a very slightly higher tolerance.

When considering each individual metric, the trends are different for each. For displacement, for frequencies higher than the tools natural frequency, the tolerance increases, with the tool that has the lowest natural frequency (Tool 1) being the most tolerant. For velocity, for frequencies higher than the tools natural frequency, the tolerance increases slightly but is relatively constant, with the tool that has the lowest natural frequency (Tool 1) being the least tolerant. For acceleration, for frequencies higher than the tools natural frequency, the tolerance decreases, with the tool that has the lowest natural frequency (Tool 1) being the least tolerant.

When considering the tools with 15% damping, the characteristics of the plots are the same, but the magnitudes of the peaks have considerably reduced. As the characteristics are the same the plots have been omitted for clarity.

7.2.2 Assessment of Input Velocities

Three types of excitation will excite each tool: pure tone, broadband noise, and a simulated walking response time history, shown in Figure 147. Each excitation was applied to each tool with its amplitude increased until the tool 'failed'.

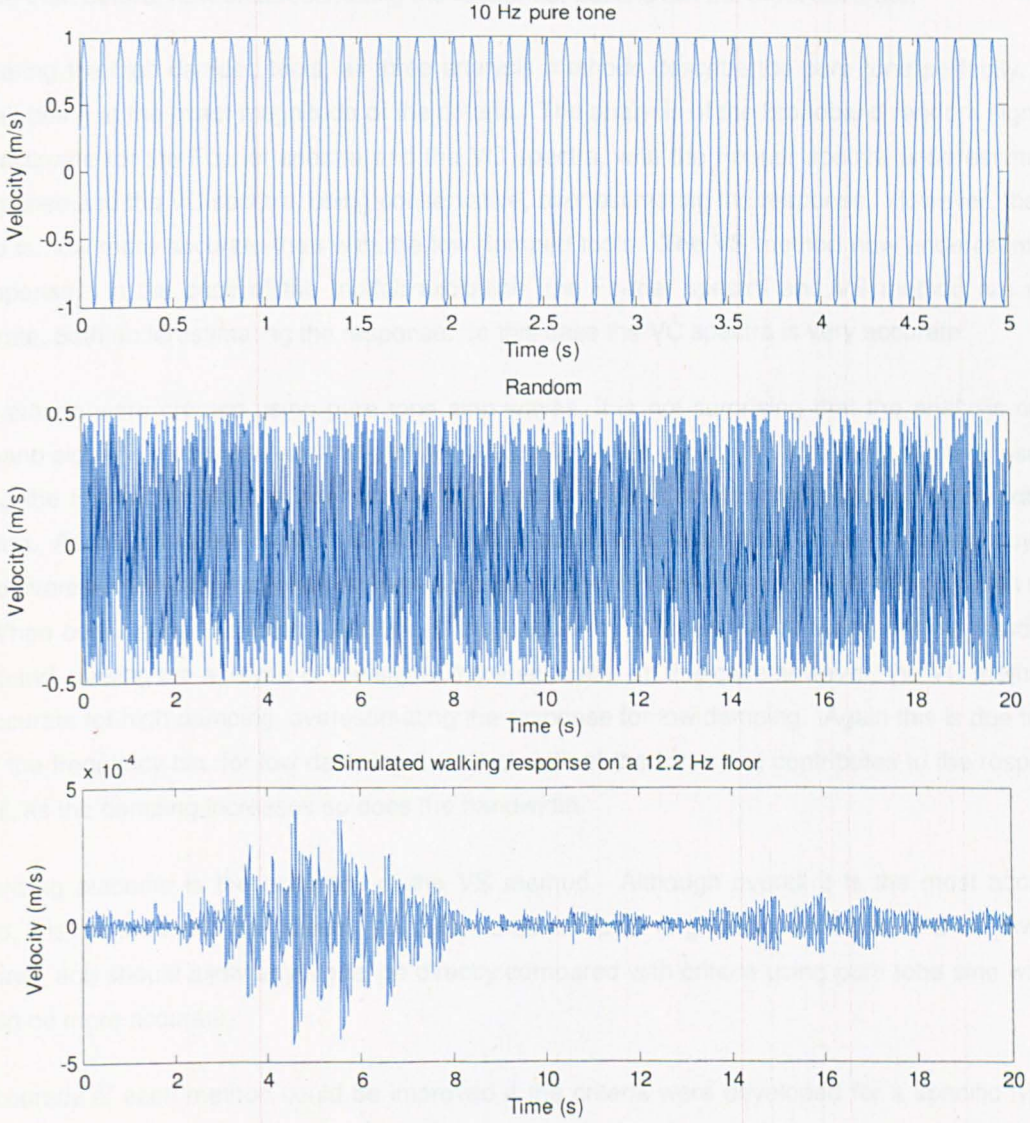

Figure 147 - Velocity base excitation of the hypothetical tools.

The responses that caused the tool to fail were then analysed using three methods: Fourier amplitudes, 1/3 octave bandwidths (VC curves) and the VS method. For clarity, only tool 2 and 3 will be considered with the total velocity response. Figure 148 and Figure 149 show the analysed response against the criteria for tools 2 and 3 respectively with 1% damping. Figure 150 and Figure 151 show the analysed response against the criteria for tools 2 and 3 respectively with 15% damping.

Considering the low damped tools, all three analyses methods describe the pure tone perfectly, with the peak being at the exact magnitude of the criteria. The analysis of the broadband random signal is very inaccurate for the Fourier spectra and the VC spectra, with the Fourier spectra underestimating the response and the VC spectra, being conservative, over estimating the response. The VS method, again is accurate. In the case of the footfall excitation, the Fourier spectra and VC spectra are most inaccurate, underestimating and overestimating the response respectively. The VS method is less accurate than before, now underestimating the response, but it is still the most accurate.

Considering the high damped tools, all three analysis methods describe the pure tone perfectly, with the peak being at the exact magnitude of the criteria. The analysis of the broadband random signal is very inaccurate for the Fourier spectra and the VC spectra, with the Fourier spectra underestimating the response and the VC spectra, being conservative, over estimating the response. However, the VC method is now more accurate then with the low damped tools. The VS method now underestimates the response. In the case of the footfall excitation, the Fourier spectra and VS method are most inaccurate, both underestimating the response. In this case the VC spectra is very accurate.

As the criteria were created using pure tone sine waves, it is not surprising that the analysis of the broadband signal is inaccurate and the pure tone is perfect in all cases. As the frequency bins used in creating the Fourier amplitudes are narrow, the method underestimates the response to broadband excitation. As the frequency bins of the 3rd octave spectra increase on a log scale with frequency, the method overestimates the response as the frequency becomes higher due to more energy within each bin. When considering the footfall excitation, the bandwidth of energy is between narrow band and broad band, making the analysis of the signal more accurate. In this case however, the VC method is only accurate for high damping, overestimating the response for low damping. Again this is due to the size of the frequency bin, for low damping the bandwidth of the force that contributes to the response is small, as the damping increases so does the bandwidth.

A surprising outcome is the accuracy of the VS method. Although overall it is the most accurate method, it is not the best in all cases. As the method is meant to give the amplitude of an equivalent sine wave, and should allow any signal be directly compared with criteria using pure tone sine waves, it should be more accurate.

The accuracy of each method could be improved if the criteria were developed for a specific type of excitation. However, then multiple criteria would be required for each type of excitation and further problems are introduced, e.g. how to classify an excitation for a 1/3 octave band.

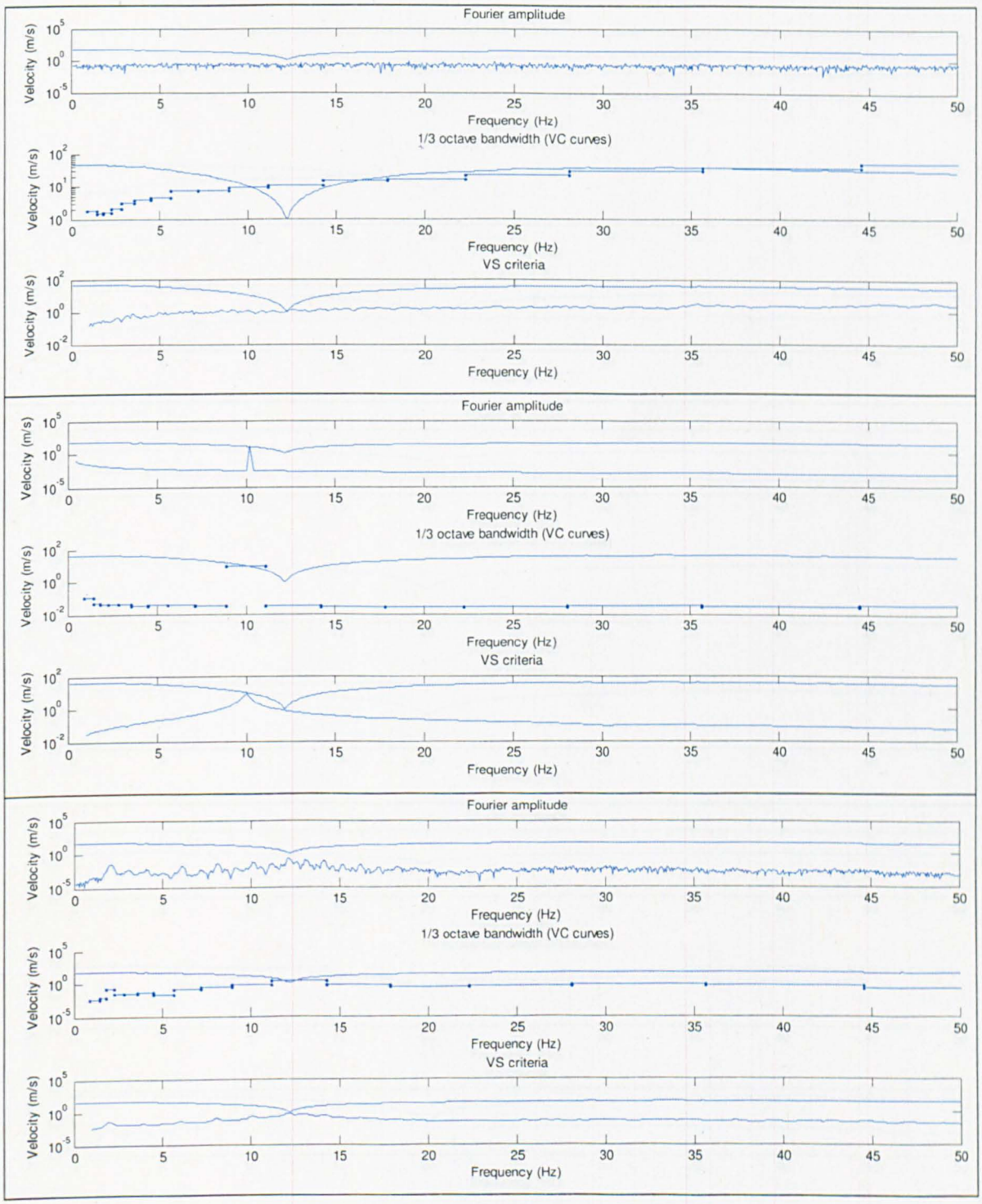

Figure 148 - Response of the floor compared with the criteria of Tool 2 with 1% damping; top box represents broadband excitation, middle box represents 10 Hz pure tone excitation, bottom box represents footfall response excitation; within each box top is Fourier amplitude, middle is VC spectra and bottom is vs. criteria

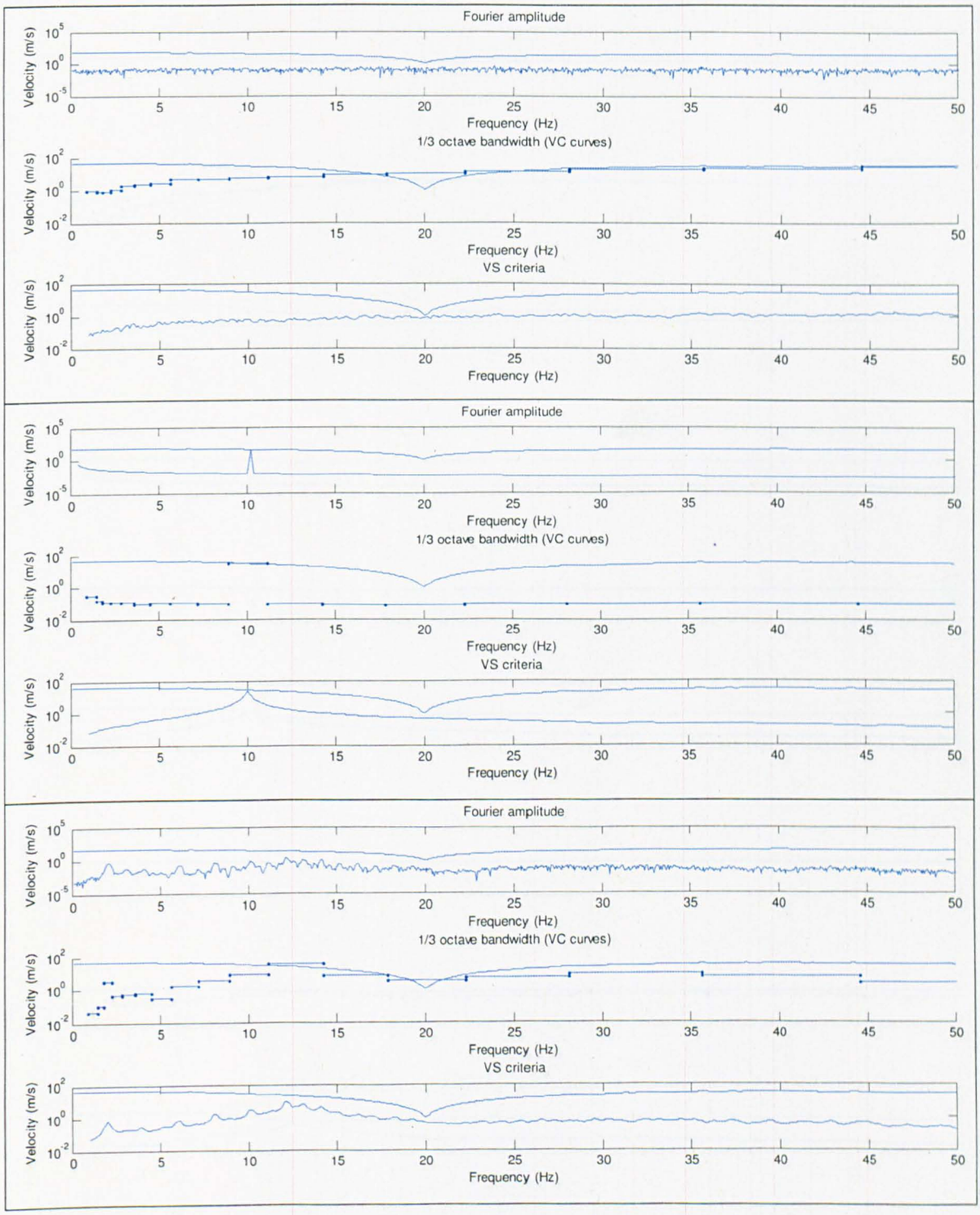

Figure 149 - Response of the floor compared with the criteria of Tool 3 with 1% damping; top box represents broadband excitation, middle box represents 10 Hz pure tone excitation, bottom box represents footfall response excitation; within each box top is Fourier amplitude, middle is VC spectra and bottom is vs. criteria

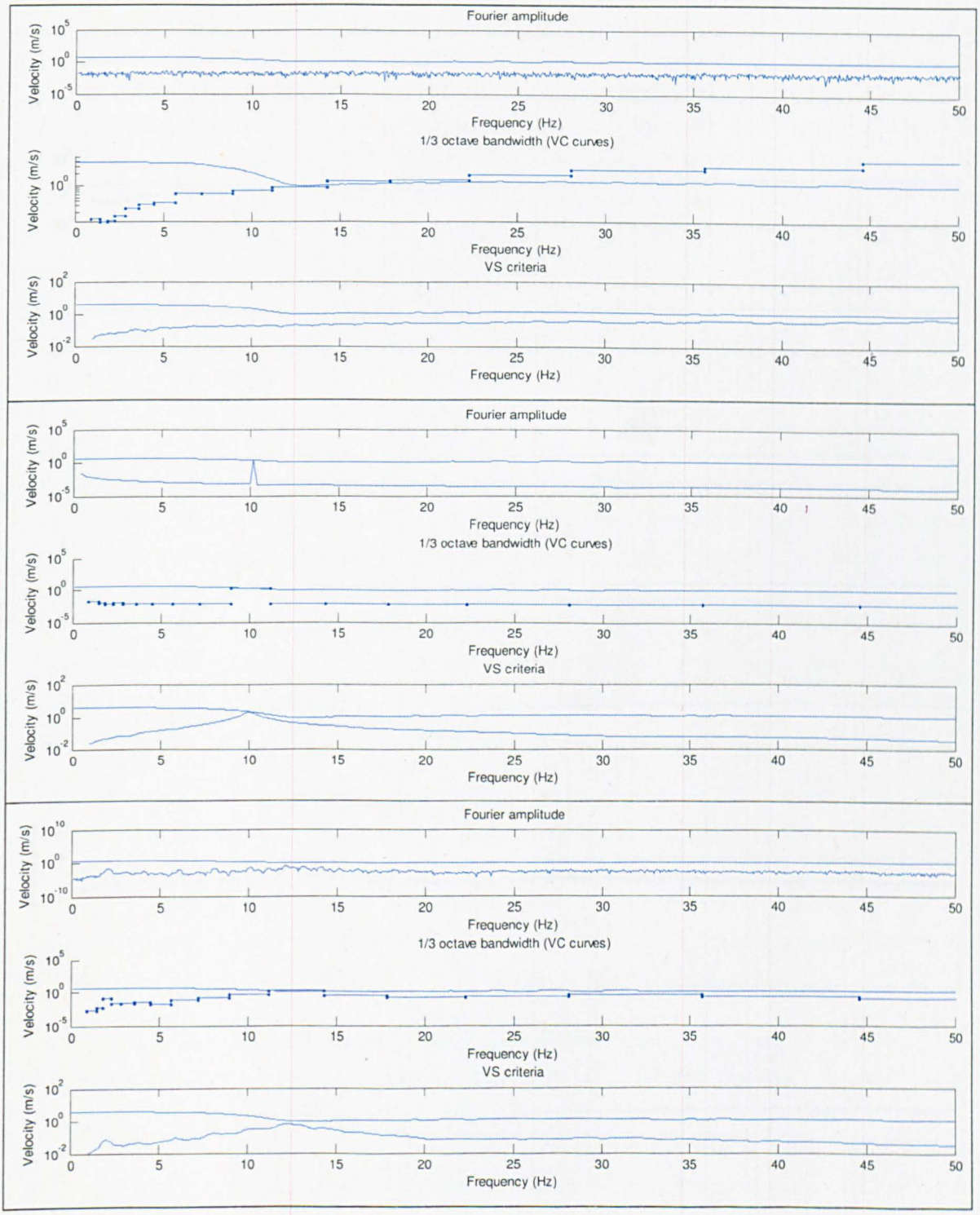

Figure 150 - Response of the floor compared with the criteria of Tool 1 with 15% damping; top box represents broadband excitation, middle box represents 10 Hz pure tone excitation, bottom box represents footfall response excitation; within each box top is Fourier amplitude, middle is VC spectra and bottom is vs. criteria

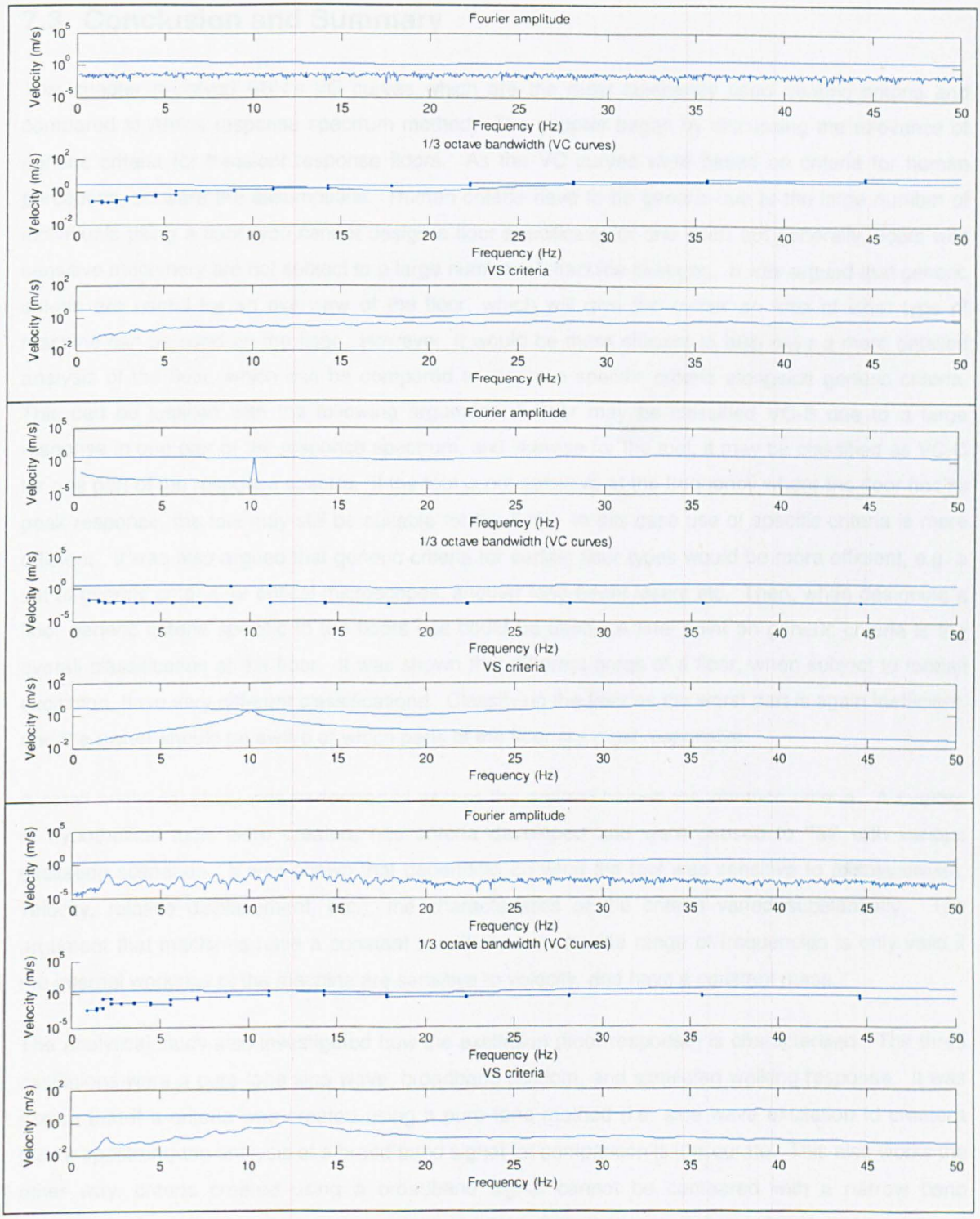

Figure 151 - Response of the floor compared with the criteria of Tool 2 with 1% damping; top box represents broadband excitation, middle box represents 10 Hz pure tone excitation, bottom box represents footfall response excitation; within each box top is Fourier amplitude, middle is VC spectra and bottom is vs. criteria

7.3 Conclusion and Summary

This chapter reviewed BBN's VC curves which are the most commonly used generic criteria and compared to Ahlins response spectrum method. The chapter began by discussing the relevance of generic criteria for transient response floors. As the VC curves were based on criteria for human perception, so were the assumptions. Human criteria have to be generic due to the large number of individuals using a floor (you cannot design a floor specifically for one user) but generally, floors with sensitive machinery are not subject to a large number of machine changes. It was argued that generic criteria are useful for an overview of the floor, which will give the owner an idea of what type of machine can be used on the floor. However, it would be more efficient to also have a more detailed analysis of the floor, which can be compared to machine specific criteria alongside generic criteria. This can be justified with the following argument: A floor may be classified VC-B due to a large response in one part of the response spectrum, and likewise for the tool, it may be classified as VC-C for one part of the response spectra. If the tool is not sensitive at the frequency where the floor has its peak response, the tool may still be suitable for the floor. In this case use of specific criteria is more efficient. It was also argued that generic criteria for certain floor types would be more efficient, e.g. a set of generic criteria for optical microscopes, another long-beam lasers etc. Then, when designing a floor generic criteria specific to the floors use could be used. A final point on generic criteria is the overall classification of the floor. It was shown that different areas of a floor, when subject to footfall excitation, have very different classifications. Classifying the floor as the worst part is again inefficient, and the owner should be aware of which parts of the floor are most responsive.

A small analytical study was performed to assess the method behind the vibration criteria. A number of hypothetical tools were created, had criteria developed and were caused to 'fail' with various excitation scenarios. It was shown that depending on what the tool was sensitive to (displacement, velocity, relative displacement, etc.), the characteristics of the criteria varied substantially. The argument that machines have a constant sensitivity over a wide range of frequencies is only valid if the internal workings of the machine are sensitive to velocity, and have a constant mass.

The analytical study also investigated how the excitation (floor response) is characterised. The three excitations were a pure tone sine wave, broadband random, and simulated walking response. It was shown that if a criteria was created using a pure tone method (i.e. sine wave excitation to create a failure spectrum) the analysis of a broad band signal for comparison is inaccurate. This also works the other way, criteria created using a broadband signal cannot be compared with a narrow band excitation. As a floors response to walking is somewhere between a narrowband and broadband response, it is difficult to assess accurately. To clarify, it is inaccurate to compare VC spectra obtained from ground borne excitation (generally broadband), machine induced vibration (generally narrowband) and footfall excitation (between narrowband and broadband) using the same criteria, specific criteria developed for each type of excitation is required. However, it was shown that if the criteria are developed using pure tone sine waves, the VC method was conservative, where as all other methods investigated underestimate the response.

It is desirable to obtain a failure spectrum using pure tone sinusoidal excitation, as it is simple, and be able to compare any excitation signal to it, removing the issue of RMS averaging, broad/narrowband criteria etc. Ahlins response spectrum method was developed with this in mind, however, it was shown that in this case it did not work. It was more accurate the VC spectra or Fourier amplitudes using different types of signal, but it sometime underestimated the magnitude of the spectra. This would potentially show a level of vibration was acceptable when it is not.

A final point is to be made on the use of variable force models, such as the spline force. Using variable models, the response is not a discrete value, but a probability distribution, which can be expressed as a percent chance of exceedance. But how should this variation be expressed as a vibration criteria, which traditionally has a discrete value? The analyst could estimate how much time that the level of vibration would exceed the machines tolerance. This time could then be equated to cost in terms of lost production. This cost could then be directly compared with the cost of improving the vibration performance of the structure. However, it is likely that in all cases it would be more cost effective to increase building cost then to lose production.

Research into vibration criteria is sparse and it is difficult to perform studies on the sensitive machinery. Manufacturers are reluctant to participate in sensitivity studies on their machinery; which seems counter-intuitive as a better understanding of the machines sensitivity would also benefit the manufacturer. Unless improved co-operation is established between researchers and machine manufacturers progress will be slow in this area.

8 Summary and Recommendations for Future Work

This thesis covered all aspects of response estimation for transient response floors (TRFs, originally termed high frequency floors). The thesis was set out in a classic source-path-receiver layout, each topic being investigated in order. This chapter summarises the main findings and conclusions of the study and suggests future work.

8.1 Evaluation of Footfall Force Models

Firstly, the boundary between the so called high frequency and low frequency floors was investigated. The study then continued to investigate all the footfall force models currently used in the design of TRFs for vibration performance were investigated and reviewed. Each of the footfall models investigated were shown to have a number of positive and negative aspects. After the assessment of the footfall models, a number of characteristics were outlined that an improved footfall model should have.

8.1.1 Evaluation of the High / Low frequency Boundary

The boundary can be defined at which point they harmonics from the footfall force can no longer cause a resonant response of the floor. As such, the magnitude, and the number of significant harmonics of the footfall force governs this boundary. The characteristics of the harmonics are directly related to the variation in pace rate: if there is no variation a large number of harmonics, with steep sides peaks are evident. To investigate the significant harmonics, variations in pace rate must be determined.

An experiment was designed to measure the variation in pace rate of individuals walking at prompted pace rates varying from 1.5 Hz - 2.5 Hz. It was shown that the variation between people varied considerably, with the people who often performed such walking tests exhibiting less variation, especially at faster pace rates. This suggests that an individual can be trained to walk with less variation, especially when prompted. It was also shown that the variation and mean pace rate is not constant throughout a wide frequency range. For uncomfortable pace rates (comfortable pace rates can be assumed to be approximately 1.8 Hz - 2.2 Hz, although this varies between people), the variation was larger. Also, for this structure, the mean pace rate when walking at an uncomfortable pace rate did not match the prompted pace rate, it was biased towards a comfortable pace rate.

The measured variation was used to construct a walking time history by superimposing a single measured footfall force for 100 paces. This variable force was then compared with the same force superimposed with no variation, i.e. a perfect force. Observing the Fourier spectra of the two forces there are clear differences. The spectrum for the perfect force had discrete harmonics, ranging into the high frequency range, with little energy between the harmonics. The spectrum for the variable force only had four visible harmonics (by eye) which confirms the 10 Hz boundary.

A number of points can be identified which can show that using the fourth harmonic (and the 10 Hz boundary) is likely to be conservative. Firstly, the measured variation was measured while the walker was prompted with a metronome, in reality a walker is unlikely to be prompted and their variation would increase. Secondly, half of the participants were used to performing these walking tests, it is likely they will have a certain degree of 'training' and their variation would be lower than the population average, and therefore biasing the results. Finally, the force variation test was conducting using a 2 Hz pace rate, which exhibits a low variation. The 10 Hz boundary is defined using walking at 2.5 Hz, as such, the variation would increase, and it is possible that only the third harmonic would be required for analysis.

In conclusion, the number of significant harmonics is likely to change considerably between different people and different circumstances. The solution to the problem would be a force model that appropriately included the variation, and thus removing the need to classify the floor.

8.2 Evaluation of Current Force Models

The force model investigated were the 'kf method', Arup's 'effective impulse' [31, 98], and the 'EC polynomial method' [45]. A critical review was presented to identify exactly where, and what, errors were introduced during the creation of the models.

8.2.1 The kf Method [46]

The kf method simplifies a footfall force using versed pulse, estimating velocity with an amplification of static displacement. In other research it has been shown that the kf method has a strange relationship with mass [51], where increasing the mass of the floor increases the velocity response. As a single footfall force, and the simplified pulse, is an impulsive type of excitation, the laws of physics state that increasing mass reduces the response. Simply put, the response calculation for the effective impulse is wrong.

It was shown that this error is due to a mistake in the expression given for the amplification factor. If a modified, correct, amplification factor is used the floor responds with the correct characteristics.

However, on further investigation of the pulse simplification it was shown that the model is generally inaccurate. Assuming a footfall force as a pulse is only accurate for very low (1.5 Hz) pace rates, and for a floor frequency range of 10 Hz - 20 Hz. As such, in any normal situation the response estimate will be inaccurate. This method should not be used to estimate floor response.

8.2.2 Arup's Effective Impulse [31, 98]

The effective impulse if created by applying a footfall force to a SDOF oscillator with unit mass and frequency, *f*. If an impulse is applied to an SDOF oscillator of unit mass, the corresponding velocity is equal to the magnitude of the impulse. As such the corresponding velocity of the oscillator to the footfall force can be considered an 'effective impulse' for the explicit frequency, *f*.

The effective impulse is currently the most accurate method published in the design guides for estimating transient response of floors. However, a number of improvements are possible. Firstly, the effective impulse was created with only 600 individual footfalls. If a pace rate range is 1.5 Hz - 2.5 Hz (i.e. ten steps), with an average of ten steps at each, to equate 600 footfalls would only take 6 people, which is not representative. The approach has been applied to a database of over 10,000 individual footfalls and very different values of the impulse were obtained [44]. This illustrates that even if the method is an accurate simplification of a footfall force, the published values still require discussion.

A larger error is introduced due to a process of curve fitting. When an individual pulse is generated for a certain pace rate, it is shown to be very accurate. However, these values are curve fitted to obtain a simple equation, suitable for design. The curve fitting was shown to considerably increase the error in the method.

A final point about the effective impulse can be made about it application. As a different impulse must be calculated for each floor frequency, the method is only suitable for modal superposition. Although this is currently the most common method to estimate floor response, it does limit the method.

8.2.3 EC Polynomial Method

The EC polynomial method [45] is based on fitting an 8th order polynomial equation to a footfall force. The method is not recommended for use in any of the current design guides, but due to its uniqueness, it is worth investigating. On visual inspection of the fit, it was shown that for the most part the polynomial represents the force well, but not the characteristic heel strike. The method can be shown to be inaccurate for RRFs and TRFs, however, it is the best all round performer, for both floor types.

8.2.4 Desirable Characteristics of a New Force Model

On evaluation of the force models, a number of characteristics were defined. If a new force model achieved all of the characteristics, it should be a universal force model, for all floor types, removing the complication of floor classification.

8.3 Creation of a Universal Footfall Model

Using the characteristic identified, a new force model was developed based on a cubic spline. A number of points were identified on a footfall force that was required for an accurate spline fit. All the points were found to be correlated in time and force to the contact time of the force. It was also found that the contact time is directly is also correlated with the pace rate. All the correlations were quantified and their variances measured. The correlations were then used to generate statistically defined, random point to fit the cubic spline, resulting in a randomly generated force. To generate a chain of walking forces with many paces, a random force was generated for each individual pace and superimposed using the variations measured in the pace rate variation experiment.

8.3.1 Comparison of the Spline Fit with the Corresponding Real Force

The simulated spline force was compared with the force used to fit the spline (without variation), to validate the accuracy of the spline fit. It was shown that there was little difference in the time domain, and in the frequency domain. The spline fit proved to be more accurate than any other method.

8.3.2 Comparison of the Randomly Generated Spline Force with Real Force

As the spline force is random in force and pace timings, the comparison method used for the other force models is not possible. The assessment procedure consisted of applying 100 different simulated spline force time histories, each containing many paces, to the system being investigated. A maximum and minimum hold was applied to the corresponding response spectra to form a response envelope. If the response spectrum measured force applied to the same system fitted within the envelope, it was considered that the force is accurate.

The systems analysed were a SDOF oscillator with varying frequency, a resonant response slab strip, and a transient response massive industrial floor. It all cases the response window accurately estimated the response.

The spline force model was shown to be more accurate than the other force models assessed, accurately representing the variation in force, pace timings and response estimations. The spline force is a universal force suitable for all floor types.

8.4 Modelling of Transient Response Floors

It was shown that there were key differences in accurately estimating the response of TRFs when compared to RRFs. When considering a RRF, a single mode generally governs the response. However, for a TRF many modes can contribute to the response, especially for large multi-bay structures. Although these differences exist in correct response estimation, it is not presented in the current design guidance. The current simplified guidance was analysed, and a large parametric study was conducted to investigate the unique properties of multi-bay floors, how to accurately model them for a transient response and offer improvements to current methods.

8.4.1 Evaluation of the Simplified Guidance

The two most recent guides for response estimation of TRFs is the Concrete Centre guide [5] and the SCI P354 guide [6], as such, only these guides were investigated. It was shown that both guides give similar estimated of fundamental natural frequency, both of reasonable accuracy. However, it is shown that for an accurate estimation of a transient response to a footfall many modes are required in the response estimation. Only the Concrete Centre guidance offers a method which can estimate modal properties of higher modes, as such, the SCI method is not suitable for analysis of TRFs.

The modal mass estimates using both guides were again similar. However, the modal mass estimates were very inaccurate estimating the modal mass at approximately 25% of the total floor mass. FEA estimating the modal mass at 44% of the total floor mass. This difference in modal mass estimates can be attributed to one key assumption: the floor mode is represented as a bending mode of a simply supported plate; this is not the case. The modal mass of the floor is related to the mode shape and will vary significantly depending on the floor construction, with its unique mass and stiffness distributions. Due to this, if empirical alterations of modal mass were applied, they would only be accurate for a floor specific case, i.e. guidance in this case is floor specific, accurate generic guidance is not possible. It was also shown that modal mass is a key parameter for an accurate response estimation for TRFs. As such, an accurate estimation of modal mass is essential.

As the Concrete Centre method can estimate higher modes of vibration it was assessed in more detail, comparing it with FEA. Initial comparisons with FEA showed that the Concrete Centre method did not estimate as many modes as the FEA. Investigating further, it was shown that as more bays are added to a structure, more modes appear within the fixed bandwidth. The extra modes appear in a form of mode groupings, focused around the modes of a single bay. The number of modes within a group is equal to the number of bays in the structure. It was shown that the Concrete Centre guide could accurately estimate modes of the first mode group, but not the others.

8.4.2 Results of the Parametric Studies

It was shown that multi-bay floors had a complex relationship with the modal properties. It was also shown that modal mass calculation is very poor, in a part due to column stiffness. To address these issues, and in an attempt to identify trends and characteristics of multi-bay floors two types of parametric studies were conducted: the first varying the number of bays in the structure, for two different floor bay dimensions; the second varying column properties and slab depths to assess the influence on modal mass. In total, the analysis too approximately 6 weeks of computer time and generated a large amount of data. The main findings are listed below:

1. The number of modes within a fixed frequency bandwidth has a linear relationship with the number of bays within the structure.
2. Mode groupings appear around the modes of a single bay floor as more bays are added to the structure.
3. The number of modes within the mode groups is equal to the number of bays within the structure.
4. The average modal mass of the modes within a fixed frequency bandwidth has a linear relationship with the number of bays within the structure.
5. The modal mass of an individual mode has a linear relationship to the average modal mass of the modes within a fixed frequency bandwidth.
6. The modal mass of the modes within a first mode group is relatively constant.
7. As more bays are added, the response at the excitation point reduces. The reduction is asymptotic, and for both floors the limit was approximately 10 bays. The limit was the number of bays, not the total structural size.
8. As 10 bays are required before there is no benefit in adding more bays; to model a large floor accurately, 10 bays would need to be modelled.
9. The reduction in response at the excitation point with increasing bays was small when compared with the reduction is response when the adjacent bay was considered.
10. The velocity FRF at the excitation point did not change in appearance or characteristics much with increasing bays. Up to a point, increasing the number of bays reduced the magnitude of the peaks and a small number of the new modes were evident. However, considering for

some of the floors examined had approximately 100 modes within each mode group, the extra modes were generally not noticeable.

11. The first mode group, not the first mode, governed the response.
12. The mode groups for 2D floors overlap, making characterising the floors much more complex.
13. Both column flexure and axial deformation affected modal mass; a reduction in stiffness increased the modal mass in both cases.
14. Axial deformation of columns had a greater influence on modal mass than flexural deformation.

The floor used in the parametric study was the simplest floor possible to analyse: a flat slab supported by columns with regular bays. As such, it is not possible to characterise all floors with this study. Floors with regular bays will exhibit most of the characteristics, however complications will arise when considering irregular bays.

The bays of an irregular floor can be categorised by their stiffness, i.e. a long span bay will be comparatively soft compared to a short span bay. So long as the stiffness difference is large enough each bay will have its own local modes that to not extend to the whole floor area. When more bays are added to the structure, characteristics described above still occur, but in a much more complex manner. Consider the mode groupings: they still occur. However, the mode groupings are now local to the floor bays local modes. As such, many more mode groupings will exist in the structure, over lapping in such a manner it would be almost impossible to distinguish them.

This causes problems with limits on the number of modes to be included in modal superposition analysis. The common guideline is to include modes up to twice the fundamental modal frequency. From the parametric study, it suggests that all modes within the first mode group should be considered. These guidelines may be adequate for regular floors, with uniform stiffness and regular bay spacings. However, it is dangerous to apply them to irregular structures. The local mode of one of the bays, because it is only engaging one bay will have a low modal mass, and a reasonably high modal frequency. If the floor as a whole has a global mode, the frequency will be considerable lower, and with a considerably higher modal mass. It is very possible that the local mode will be more than twice the fundamental mode, and will not be part of the first mode grouping. Neglecting this mode would be an error, as due to its low mass, its response could categorise the floor.

The problem with irregular bay floors is, by their very nature, their irregularity and the large number of combinations of bay sizes, etc. to consider. As such, it is not possible to characterise them in the same manner as the parametric study did with the regular bay floor, as they are too complex. The characteristics of the regular floor studied in this thesis should be applied to irregular floors with a lot of engineering judgement. The characteristics may help understand why certain things happen in irregular floors, but it would be impossible to predict them with simplified methods. As such, the only method widely available for analysis of irregular floors is FEA.

8.4.3 Investigation of Modelling Detail

Analysts working in industry desire simplified methods to design structure when it is not efficient to develop a detailed FE model. As it is shown that simplified methods are not accurate, and could only be accurate for floor specific scenarios; simplified modelling was investigated. The rationale behind simplified modelling is to develop a small area of interest in detail, then to model the rest of the structure very crudely. This type of modelling could be performed quickly, and should yield more accurate results than the simplified guidance.

It was shown that this type of modelling gives accurate response estimates, in the time domain and frequency domain. The mode shapes obtained using the crude model was not the same as the mode shapes obtained using the detailed model. If simplification of modelling is to be used, this characteristic of the analysis must be appreciated. This will affect tasks such as model updating, comparing with experimental results, etc. The important point is that the summation of the modes yields the same response.

8.4.4 Modal Participation of Multi-Bay floors

Due to the large number of modes obtained using a detail FEA or a crude FEA, it is desirable to evaluate which modes are of importance (i.e. contribute most to the response). An approach first published by NAFEMS [126] was backwards engineered and used to evaluate the modal participations. The modal participations obtained could be directly related to displacement, velocity and acceleration of the modes. The problem with the method is that it required the inverse mass matrix, which can be difficult to obtain from commercial FE packages.

The participation factor was modified to be used within a desired frequency bandwidth. When applied it was easy to see which modes contributed to the response in a discrete and cumulative manner. It was shown that the number of modes required in the analysis is considerably less than the number of modes within each mode grouping. Modal participation can be used to make the analysis process more efficient and to help correlate modes in model updating.

8.4.5 Wave Propagation Analysis of Floors

It was shown that a transient response from a footfall for a large floor can be visualised as a wave propagation problem. The spectral element method (SEM) was used to analyse a number of 3D grillage representations of multi-bay floors and was directly compared with FEA. It was shown that for a like-for-like comparison, the SEM was more accurate and more efficient.

The SEM allows for semi-infinite elements, which are not possible with conventional FEA. The semi-infinite elements were used in attempt to modal a large structure. Although they could be used to remove energy from the floor, and responses could be obtained similar to that of the fully modelled structure, the responses were not accurate.

However, the semi-infinite elements used were not complex. The most complex element formulated was a beam on an elastic foundation. It is likely that the distributed stiffness from the foundation was a poor representation of the floor. There was also no interconnection between the beams that tended to infinity, to accurately model a floor this would have to be addressed. If a more complex element was formulated, it may be possible to model a floor in this manner. Also, if an accurate semi-infinite element could be formed, it may be possible to use it to develop an improved simplified guidance based on wave propagation.

8.5 Investigation of Vibration Criteria

A discussion was presented on BBN's VC curves and their analysis method [126]. The VC curves are the most common method of classifying floors with low levels of vibration. It was argued that generic criteria and floor classification are valid, but an approach that combines generic and machine specific criteria would be more efficient. Also, a total classification of a floor for machinery is inefficient. It was shown hat different areas for a floor have different criteria when excited by walking. As such, classification using the worst part of the floor is inefficient.

The analysis used in the VC curves was also compared with Ahlin's response spectrum method [93] [92] and analysis using Fourier Amplitudes. It was shown that if a failure spectrum of a machine was developed using pure-tone sinusoids, then analysis of broad band signals would be inaccurate, and vice-versa. As creating a failure spectrum using pure-tone sinusoids is a logical method, it is desirable method to develop a method of analysing the floor response of any signal, and compare directly to a criterion based on pure-tone sinusoid. Ahlin's response spectrum method is supposed to do this, but it was shown not to work.

A lot more research is required in this area, but unfortunately, manufactures are secretive about their machines and seem unwilling to participate in research, which hinders progress in this area.

8.6 Recommendations for Future Work

1. Further investigations into pace rate variations.

a. Pace rate variations have so far been studied using measurements from treadmill data, and prompted walking with a metronome. Neither method allows a natural manner of walking. Measurements of pedestrian walking for long walking periods, without promting, to obtain a natural variation should be obtained. Measurements could be taken in different environments, e.g. inside an office building, walking in the street etc. Often, walking to a prompted beat is justified due to a person might be prompted by sounds in their environment (e.g. listening to music). Pace rate measurements could also be obtained while the participant is listen to a portable music device. The beat of the music could be set to match certain pace rates to ascertain any correlation.

b. Currently distributions and correlations in pace rates are very simple, often simplified to a normal distribution. It was found in this study that during uncomfortable walking paces the distribution is log-normal. Also, assuming only random variables from the distribution may cause inaccuracies. It is possible that an uncharacteristic slow pace could follow and uncharacteristic fast pace. This is unlikely to happen in reality as it would cause a limp.

2. Improvements of the spline force.
   a. The spline force is generated with fixed points. It was shown that the heel strike is modelled better at some walking speed then at others. If the spline points that model the spike were allowed to vary the position with relation to the pace rate, this could further increase the accuracy.
   b. Another method to improve the accuracy of modelling the heel strike would be to separate it from the main force. If a spline is fitted to a footfall force, but omitting the heel strike, and then the spline is subtracted from the force, the remainder would be the heel strike. It would then be simpler to model the heel strike separately. When reconstructing the force, the heel strike could be superimposed over the main force.
   c. The modelling technique needs to be applied to more people to assess how constant the identified correlations are between individuals.
3. Future of dynamic response estimation from human excitation
   a. The final goal in response estimation to human excitation would be a rigorous analysis and would likely only be available in software. The procedure in estimating the response could be as follows:
      i. Estimate the human traffic on the floor.
      ii. Create a relevant number of individuals who will walk on the floor. It is likely that each individual will have slightly different walking characteristics (e.g. some will walk faster than others, some will be heavier, etc.)
      iii. Create a variable force time history for each individual and apply to the structure in accordance with i.
      iv. Obtain a response envelope, or a distribution of response to compare with the relevant criteria.

4. Experimental verification of the mode groupings identified
    a. In conducting EMA, the Author has seen large numbers of closely spaced modes in large multi-bay structures. However, the modes have not been identified in exactly the same manner as the FEA predicts. As shown by the modal participation, it is possible that not all the modes would have been excited during the analysis. A large, simple, multi-bay structure is required with uniform bay spacings. A detailed modal analysis will be required to assess whether all the predicted modes exist and compared with FEA of the same structure.
5. Modelling detail
    a. How to model a structure in the least detail if the required response point is in a different bay to the excitation point.
    b. How to model an irregular structure with the least amount of detail.
6. Wave propagation analysis of floors
    a. Formulation of a plate element to replace grillage analysis. This will significantly reduce the computer time required for analysis. A semi infinite slab will also remove the problem of connectivity of semi-infinite beam when conducting grillage analysis.
    b. Formulation of a spectral super element. It is possible to formulate a spectral super-element from a number of standard finite elements. It may be then possible to create a semi-infinite version of the super-element. If this is possible, it may then be able to assess the response at any point along an infinite or finite beam, increasing the accuracy of the response. If, in the formulation of the super-element it is possible to algebraically retain physical properties of the floor it may be possible to create a simplified guidance based on wave propagation techniques.
    c. Formulation of a power flow analysis technique. As spatial dissipation governs the decay of a transient signal, it is desirable to quantify this. Power flow analysis could be implemented to quantify the total power distribution in the structure at any point in time, along with its direction of flow. This could be graphically implemented into a computer program and animated. This would allow for a detailed knowledge of how the vibration energy if flowing through the structure and identify sources and sinks of energy (e.g. columns). This data can then be used to used to modify the vibration performance of the strcuture.
7. Vibration Criteria
    a. Research into a method of classifying and type of vibration for accurate comparison to criteria generated with pure-tone sinusoidal excitation. Ideally, this method would remove the need for RMS averaging, and different methods for different signal types.
    b. Development of a database of criteria of different machine types.

References

[1] S.Zivanovic, A.Pavic, P.Reynolds, Vibration serviceability of footbridges under human-induced excitation: a literature review. *Journal of Sound and Vibration* 279 (2005) 1-74.

[2] H.Bachmann, Case studies of structures with man-induced vibrations. *ASCE Journal of Structural Engineering* 118 (1992) 631-647.

[3] T.A.Wyatt chris, *Design guide on the vibration of floors*, The Steel Construction Institute, Construction Industry Research and Information Association , London, 1989.

[4] Allen, D.E., Murray, T.M., Design criterion for vibrations due to walking. *Engineering Journal AISC* 30 (1993) 117-129.

[5] M.Willford, P.Young chris, *A design guide for footfall induced vibrations of structures*, The Concrete Centre , Slough, 2006.

[6] A.L.Smith, S.J.Hicks, P.J.Devine chris, *Design of floors for vibration: A new approach (SCI P354)*, SCI , Ascot, Berkshire, 2007.

[7] C.G.Gordon, Generic criteria for vibration-sensitive equipment, *International Society for Optical Engineering (SPIE)*, Proceedings of the SPIE, 1991, pp. 71-85.

[8] C.G.Gordon, Generic vibration criteria for vibration-sensitive equipment, 1999, pp. 302-305.

[9] A.Pavic, P.Reynolds, Vibration serviceability of long-span concrete building floors. Part 1: Review of background information. *Shock and Vibration Digest* 34 (2002) 191-211.

[10] Guide to evaluation of human exposure to vibration in buildings (1 Hz to 80 Hz). *BS 6472: 1992* British Standards Institution (1992).

[11] Guide to evaluation of human exposure to vibration in buildings (1 Hz to 80 Hz). *ISO 2631-2: 1989* Internation Standards Organisation (1992).

[12] H.Amick, S.Hardash, P.Gillett, R.J.Reaveley, Design of stiff, low-vibration floor structures, *San Jose, CA*, Proceedings of International Society for Optical Engineering (SPIE), November 1991, pp. 180-191.

[13] T.P.Andriacchi, J.A.Ogle, J.O.Galante, Walking Speed as a Basis for Normal and Abnormal Gait Measurements. *Journal of Biomechanics* 10 (1977) 261-268.

[14] F.W.Galbraith, M.V.Barton, Ground loading from footsteps. *Journal of Acoustic Society of America* 48 (1970) 1288-1292.

[15] T.A.Wyatt, A.F.Dier, Building in steel, the way ahead, International Symposium: Building in Steel, The way ahead.

[16] S.J.Hicks, P.J.Devine, Design Guide on the Vibration of Floor in Hospitals. The Steel Construction Institute (2004).

[17] SCI, AD 253: Design considerations for the vibration of floors - Part 1, SCI Advisory Desk, 2001.

[18] SCI, AD 254: Design considerations for the vibration of floors - Part 2, SCI Advisory Desk, 2002.

[19] T.M.Murray, D.E.Allen, E.E.Ungar, Floor vibrations due to human activity, AISC American Institute of Steel Construction, 1997.

[20] Canadian Standards Association, Guide for floor vibrations. *CSA Standard CAN 3-S16.1-M 89.Steel Structures for Buildings-Limit State Design, Appendix G* Canadian Standards Association (1989) 127-134.

[21] A.Pavic, M.R.Willford, Appendix G: Vibration serviceability of post-tensioned concrete floors, *Post-tensioned concrete floors design handbook*, Concrete Society, Slough, UK, 2005, pp. 99-107.

[22] R.M.Lawson, H.Bode, J.W.P.M.Brekelmans, P.J.Wright, D.L.Mullett, 'Slimflor' and 'Slimdek' construction: European developments. *The Structural Engineer* 77 (1999).

[23] Corrospondance, The Structural Engineer, 19-11-2002, 19.

[24] Corrospondance, The Structural Engineer, 16-5-2006, 36-37.

[25] Masters, J., New guide's subdued response factor, New Steel Construction, 2005, 18-19.

[26] P.Young, M.Willford, Comparing footfall induced floor vibrations on different types of floor structure. *The Structural Engineer* 84 (2006) 19-20.

[27] ARUP, Hospitals and Footfall Induced Vibration. *Concrete Structures* November (2004) 4.

[28] Amick, H., Bayat, A., Dynamics of Stiff Floors for Advanced Technology Facilities, *12th ASCE Engineering Mechanics Conference*, 1998, pp. 318-321.

[29] J.M.W.Brownjohn, T.Botfield, A folded pendulum isolator for evaluating accelerometer performance. *Experimental Techniques* In press (2008).

[30] A.L.Smith, S.J.Hicks, P.J.Devine chris, *Design of Floors for Vibration: A New Approach (SCI P354)*, SCI , Ascot, Berkshire, 2007.

[31] M.Willford, P.Young, C.Field, Predicting footfall-induced vibration: Part 2. *Structures & Buildings* 160 (2007) 73-79.

[32] P.E.Eriksson, Low-frequency forces caused by people: Design force models, *Structural Serviceability of Buildings*, Theme 3: Service Loads and Load Models, 1993, pp. 149-156.

[33] F.C.Harper, The forces applied to the floor by the foot in walking, in: W.J.Warlow, B.L.Clarke (Eds.), Department of Scientific and Industrial Research (DSIR), HMSO, 1961.

[34] F.C.Harper, The mechanics of walking. *Research Applied in Industry* 5 (or15-see Notes) (1962) 23-38.

[35] Y.Matsumoto, T.Nishioka, H.Shiojiri, K.Matsuzaki, Dynamic design of footbridges. *IABSE Proceedings* (1978) 1-15.

[36] J.H.Rainer, G.Pernica, D.E.Allen, Dynamic loading and response of footbridges. *Canadian Journal of Civil Engineering* 15 (1988) 66-71.

[37] J.E.Wheeler, Prediction and control of pedestrian induced vibration in footbridges. *Journal of the Structural Division ASCE* 108 (1982) 2045-2065.

[38] D.R.Leonard, Human tolerance levels for bridge vibrations, Road Research Laboratory, 1966.

[39] J.W.Smith, The vibration of highway bridges and the effects on human comfort, University of Bristol, 1969.

[40] A.Pavic, M.R.Willford, Appendix G: Vibration Serviceability of Post-Tensioned Concrete Floors, *Post-Tensioned Concrete Floors Design Handbook*, Concrete Society, Slough, UK, 2005, pp. 99-107.

[41] B.R.Ellis, On the response of long-span floors to walking loads generated by individuals and crowds. *The Structural Engineer* 10 (2000) 17-25.

[42] S.C.Kerr, Human induced loading on staircases, PhD Thesis. University College London, Mechanical Engineering Department, London, UK, 1998.

[43] P.Young, Improved floor vibration prediction methodologies, *Proceedings of Arup Vibration Seminar on Engineering for Structural Vibration – Current Developments in Research and Practice*, Proceedings of Arup Vibration Seminar on Engineering for Structural Vibration - Current Developments in Research and Practice, 2001.

[44] J.M.W.Brownjohn, C.J.Middleton, Procedures for vibration serviceability assessment of high-frequency floors. *Engineering Structures* 30 (2008) 1548-1559.

[45] G.Sedlacek, C.Heinemeyer, C.Butz, B.Volling, P.H.Waarts, F.Van Duin, S.Hicks, P.J.Devine, T.Demarco, Generalisation of criteria for floor vibrations for industrial, office, residential and public building and gymnasium halls, European Commission, 2006.

[46] E.E.Ungar, R.W.White, Footfall-induced vibrations of floors supporting sensitive equipment. *Sound and Vibration* (1979) 10-13.

[47] M.Willford, C.Field, P.Young, Improved Methodologies for the Prediction of Footfall-Induced Vibration, *Architectural Engineering National Conference*, 2006.

[48] Eurocode. Basis of structural design. *BS EN 1990:2002* British Standards Institution (2002).

[49] S.V.Ohlsson, Ten years of floor vibration research, 1988, pp. 435-450.

[50] S.V.Ohlsson, A design approach for footstep-induced floor vibration, 1988, pp. 722-729.

[51] J.M.W.Brownjohn, Dynamic performance of high frequency floors, Proceedings, IMACXXIV, 2006.

[52] A.Pavic, P.Reynolds, S.Prichard, M.Lovell, Evaluation of Mathematical Models for Predicting Walking-Induced Vibrations of High-Frequency Floors. *International Journal of Structural Stability and Dynamics* 3 (2003) 107-130.

[53] R.D.Blevins chris, *Formulas for natural frequency and mode shape*, Robert E Kreigher Publishing Company , Malabar, Florida, USA, 1995.

[54] A.Zaman, L.F.Boswell, Frequency estimation of long-span floors, 1996, pp. 129-139.

[55] S.S.Rao chris, *Mechanical vibrations*, Addison-Wesley , 1995.

[56] R.J.Bainbridge, C.J.Mettem, Simplified natural frequency prediction for timber floors. *Structures and Buildings, Proceedings of the Institute of Civil Engineers* (1998) 317-322.

[57] F.Ljunggren, Floor Vibration - Dynamic Properties and Subjective Perception, Lulea University of Technology, 2006.

[58] J.Chadha, D.L.Allen, Natural frequency determination of long-span floor slabs. *Transactions of the ASME Journal of Engineering for Industry* 94 (1972).

[59] M.Petyt, Vibration of column-supported floor slabs. *Journal of Sound and Vibration* 21 (1972) 355-364.

[60] S.J.Hicks, P.J.Devine chris, *Design guide on the vibration of floors in hospitalsss*, The Steel Construction Institute , Ascot, Berkshire, UK, 2004.

[61] C.J.Middleton, J.M.W.Brownjohn, Response of high frequency floors to a footfall, *IMACXXVI*, Proceedings, IMACXXVI, Orlando, Florida.

[62] M.Willford, P.Young, C.Field, Predicting footfall-induced vibration: Part 1. *Structures & Buildings* 160 (2007) 65-72.

[63] T.A.Wyatt, Mechanisms of damping, Symposium on Dynamic Behaviour of Bridges, 1977, pp. 10-21.

[64] A.P.Jeary, Damping in tall buildings, *Conference on Tall Buildings*, 1985.

[65] M.T.Boudjelal, On the investigation of material damping parameter identification based on laboratory test results using neural network, Proceedings, EURODYN 1999, 1999, pp. 525-530.

[66] S.H.Chowdhury, Y.C.Loo, S.Fragomeni, Damping Formulae for Reinforced and Partially Prestressed Concrete Beams. *Advances in Structural Engineering* 3 (2000) 327-335.

[67] K.Shye, M.Richardson, Mass, stiffness and damping matrix estimates from structural measurements, *IMAC5 Vol. 1*, Proceedings, IMAC5 Vol.1, 1987.

[68] J.Penzien, Damping characteristics of prestressed concrete. *Journal of the American Concrete Institute* 61 (1964) 1125-1148.

[69] D.L.Allen, Vibrational behaviour of long-span floor slabs. *Canadian Journal of Civil Engineering* 1 (1974) 108-115.

[70] J.Mazars, Material dissipation and boundary conditions in seismic behaviour of reinforced concrete structures, EURO-C Conference on Computational Modelling of Concrete Structures, 1998, pp. 579-592.

[71] S.Falati, The contribution of non-structural components to the overall dynamic behaviour of concrete floor slabs, University of Oxford, 1999.

[72] R.T.Severn, J.M.W.Brownjohn, A.A.Dumanoglu, C.A.Taylor, A review of dynamic testing methods for civil engineering structures (Keynote paper 1), 1988, pp. 1-23.

[73] *A finite element primer*, National Agency for Finite Element Methods & Standards (NAFEMS) , Glasgow, UK, 1992.

[74] D.El, T.Ji, Modelling of the dynamic behaviour of profiled composite floors. *Engineering Structures* 28 (2006) 567-579.

[75] C.P.Heins, Dynamic response of a building floor system. *Building Science* 10 (1975) 143-153.

[76] P.Reynolds, the effects of raised access flooring on the vibrational preformance of long-span concrete floors, University of Sheffield, 2000.

[77] A.Pavic, P.Reynolds, Modal Testing and Dynamic FE Model Correlation and Updating of a Prototype High-Strength Concrete Floor. *Cement & Concrete Composites* 25 (2003) 787-799.

[78] R.J.Guyan, Reduction of stiffness and mass matrices. *AIAA Journal* Vol. 3 No. 2 (1965).

[79] H.Reiher, F.J.Meister, The Effect of Vibration on People, Berlin, 1931.

[80] D.E.Goldman, A review of subjective responses to vibratory motion of the human body in the frequency range 1 to 70 cycles per second, Naval Medical Research Institute, National Naval Medical Center, Bethesda, Maryland, 1948, p. 17.

[81] D.T.Wright, R.Green, Human sensitivity to vibration, Queen's University, Kingston, Ontario, Canada, 1959, p. 23.

[82] A.W.Irwin, Human response to dynamic motion of structures. *The Structural Engineer* 56A (1978) 237-244.

[83] Guide to the evaluation of human exposure to whole-body vibration. *AMERICAN NATIONAL STANDARD* (1979).

[84] T.Kobori, Ergonomic evaluation methods for bridge vibrations. *Transaction of JSCE* 6 (1974) 40-41.

[85] J.Blanchard, Design criteria and analysis for dynamic loading of footbridges, Symposium on Dynamic Behaviour of Bridges, 1977, pp. 90-106.

[86] C.G.Gordon, Generic Criteria for Vibration-Sensitive Equipment, *International Society for Optical Engineering (SPIE)*, 1991, pp. 71-85.

[87] A.Bayat, C.G.Gordon, A Discussion of Vibration and Noise Issues in a Cleanroom Design: Past, Present and Future, Proceedings of the ICCCS 14th International Symposium on Contamination Control, Institute of Environmental Sciences and Technology, April 1998-May 1998, pp. 139-143.

[88] Leung, K. W. and Papadimos, C. A., Micro-Vibration Criteria for 300mm and Beyond, Semiconductor Fabtech, 1999, 167-170.

[89] H.Amick, On generic vibration criteria for advanced technology facilities. *Journal of The Institute of Environmental Sciences* XL (1997) 35-44.

[90] J.M.W.Brownjohn, A.Pavic, Vibration control of ultra-sensitive facilities. *ICE Proceedings: Structures and Buildings* 159 (2006) 295-306.

[91] H.Amick, M.Gendreau, T.Busch, C.G.Gordon, Evolving criteria for research facilities: I - Vibration, Proceedings of SPIE Conference 5933: Buildings for Nanoscale Research and Beyond, San Diego.

[92] Ahlin, K., Response Equivalent Peak Velocity: A New Method for Description of Vibration Environment for Sensitive Equipment in Buildings, *Annual Meeting of SPEI - Conference on Current Developments in Vibration Control for Optomechanical Systems*, 1999.

[93] Mechanical vibration and shock -- Vibration and shock in buildings with sensitive equipment -- Part 1:Measurement and evaluation. *ISO/TS 10811-1:2000* (2000).

[94] H.Amick, Bayat, A., Meeting The Vibration Challenges Of Next-Generation Photolithography Tools, *ESTECH 2001, 47 th Annual Technical Meeting, IEST*, 2001, pp. 1-10.

[95] K.Pratt, Floor vibration requirements for laboratories and micro-electronics facilities, *Engineering for Structural Vibration, Current Developments in Reaearch and Practice*, IMechE, London.

[96] K.Medearis, Rational Vibration and Structural Dynamics Evaluations for Advanced Technology Facilities. *Journal of the Institute of Environmental Sciences and Technology* (1995) 35-44.

[97] *ASHRAE Applications Handbook (SI)*, ASHRAE , 2003.

[98] M.R.Willford, P.Young, Improved methodologies for the prediction of footfall-induced vibration, Proceedings of the Sixth European Conference on Structural Dynamics EURODYN 2005, Paris, France.

[99] A.Pavic, P.Reynolds, S.Prichard, M.Lovell, Evaluation of mathematical models for predicting walking-induced vibrations of high-frequency floors. *International Journal of Structural Stability and Dynamics* 3 (2003) 107-130.

[100] E.E.Ungar, J.A.Zapfe, J.D.Kemp, Predicting footfall-induced vibrations of floors. *Journal of Sound and Vibration* (2004).

[101] C.M.Harris chris, *Shock and vibration handbook*, McGraw-Hill Book Company , New York, 1996.

[102] C.Runger, Über empirische Funktionen und die Interpolation zwischen äquidistanten Ordinaten. *Zeitschrift für Mathematik und Physik* 46 (1901) 224-243.

[103] C.DeBoor chris, *A Practical Guide to Splines*, Springer , 1978.

[104] D.J.Ewins chris, *Modal testing: Theory and practice*, Research Studies Press Ltd. & John Wiley and Sons Inc. Taunton, Somerset, England, 1995.

[105] S.Zivanovic, I.M.Diaz, Pavic A, Influence of walking and standing crowds on structural dynamoc performance, *27th International Modal Analysis Conference (IMACXXVII)*, 27th International Modal Analysis Conference (IMACXXVII).

[106] SCI, AD 256: Design considerations for the vibration of floors - Part 3, SCI Advisory Desk, 2002.

[107] R.J.M.Bainbridge, Serviceability performance of timber floors. *The Structural Engineer* 75 (1997) 269-274.

[108] F.O.Berkoh, Occupant-induced vibration in wood floors: A serviceability approach, Carleton University, 1997.

[109] J.M.W.Brownjohn, A.Pavic, P.Reynolds, Assessing and Managing Vibration Serviceability of Footbridges, *First International Conference on Advances in Bridge Engineering*, 2006.

[110] J.M.W.Brownjohn, A.Pavic, Human induced vibrations on footbridges, *IABMAS06*, 2006.

[111] J.M.W.Brownjohn, P.Fok, M.Roche, P.Moyo, Long Span Steel Pedestrian Bridge at Singapore Changi Airport - part 1: Prediction of Vibration Serviceability Problems. *The Structural Engineer* 82 (2004) 21-27.

[112] A.Ebrahimpour, R.L.Sack, A review of vibration serviceability criteria for floor structures. *Computers and Structures* 83 (2005) 2488-2494.

[113] B.Ellingwood, Structural serviceability: Floor vibrations. *Journal of Structural Engineering ASCE* 110 (1984) 401-418.

[114] M.Kasperski, Vibration serviceability for pedestrian bridges. *Structures & Buildings* 159 (2006) 273-282.

[115] D.E.Allen, Vibration criteria for long-span floors. *Canadian Journal of Civil Engineering* 3 (1976) 165-173.

[116] A.Pachi, T.Ji, Frequency and velocity of people walking. *The Structural Engineer* 83 (2005) 36-40.

[117] A.Z.Khan, Frequency estimation of pre-stessed and composite floors, City University, 1996.

[118] K.H.Lenzen, Vibration of steel joist-concrete slab floor systems, The University of Kansas Center for Research in Engineering Sciences, Lawrence, USA, 1962.

[119] S.Ohlsson, Springiness and human induced floor vibrations, Swedish Council for building Research, 1988, p. 85.

[120] K.Y.S.Lim, A literature survey of design methods for floors subjected to occupant-induced vibrations, Building Research Association of New Zealand (BRANZ), 1991.

[121] K.Y.S.Lim, Dynamic characteristics of New Zealand heavy floors, Building Research Association of New Zealand (BRANZ), 1991.

[122] G.J.Beattie, The vibration performance of timber floors, Building Research Association of New Zealand (BRANZ), 1988.

[123] R.Szilard chris, *Theory and Applications of Plate Analysis: Classical, Numerical and Engineering Methods*, John Wiley & Sons, Inc. New Jersey, 2004.

[124] J.M.W.Brownjohn, A.Pavic, Experimental methods for estimating modal mass in footbridges using human-induced dynamic excitation. *Engineering Structures* 29 (2007) 2833-2843.

[125] R.W.Clough, J.Penzien chris, *Dynamics of structures*, Mcgraw-Hill International Book Company .

[126] NAFEMS chris, *A finite element dynamics primer*, National Agency for Finite Element Methods and Standards , Glasgow, UK, 1992.

[127] A.Pavic, M.Willford, Vibration serviceability of post-tensioned concrete floors. *Appendix G in Post-Tensioned Concrete Floors Design Handbook - Technical Report 43.* Concrete Society (2005) 99-107.

[128] M.Willford, C.Field, P.Young, Improved methodologies for the prediction of footfall-induced vibration, *Architectural Engineering National Conference*, 2006.

[129] J.F.Doyle chris, *Wave propagation in structures: Spectral analysis using fast fourier transforms*, Springer , 1997.

[130] J.F.Doyle, T.N.Farris, A spectrally formulated finite element for wave propagation. *International Journal of Analytical and Experimental Modal Analysis* 5 (1990) 223-237.

[131] T.Black, Spectral element analysis of bars, beams and levy plates, Virginia Polytechnic and State University, 2005.

[132] U.Lee, J.Kim, A.Y.T.Leung, The spectral element method in structural dynamics. *The Shock and Vibration Digest* 32 (2000) 452-465.

[133] P.H.kulla, High precision finite elements. *Finite Element in Analysis and Design* 26 (1997) 97-114.

[134] A.Nishida, Y.Hangai, A study about wave propagation behaviour of spatial structures (in Japanese). *Journal of Structural Construction Engineering* (1995) 117-126.

[135] A.Nishida, Wave propagation properties of frame structures - formulation for three dimensional frame structures. *Japan society of mechanical engineers* 49 (2006).

[136] M.Krawczuk, A.Zak, W.Ostachowicz, M.P.Cartmell, Propagation of elastic waves in beams - including damping effects. *Modern Practice in Stress and Vibration Analysis* 440-441 (2003) 179-186.

[137] C.H.Amick, M.Gendreau, T.Busch, C.G.Gordon, Evolving criteria for research facilities: I – Vibration, *SPIE Conference 5933: Buildings for Nanoscale Research and Beyond*, July 2005.

[138] K.Ahlin, Response equivalent peak velocity: A new method for description of vibration environment for sensitive equipment in buildings, *Annual Meeting of SPEI - Conference on Current Developments in Vibration Control for Optomechanical Systems*, 1999.

[139] A.Belli, P.Bui, A.Berger, A.Geyssant, J.R.Lacour, A treadmill ergometer for three-dimensional ground reaction forces measurement during walking. *Journal of Biomechanics* 34 (2001) 105-112.

[140] C.G.Gordon, T.L.Dresner, Methods of Developing Vibration and Acoustic Noise Specifications for Microelectronics Process Tools, Vibration Monitoring and Control SPIE Proceedings, pp. 1-11.

[141] E.E.Ungar, Vibration Criteria for Healthcare Facility Floors. *Sound and Vibration* (2007).

[142] Leung, K. W. and Papadimos, C. A., Micro-vibration criteria for 300mm and beyond, Semiconductor Fabtech, 1999, 167-170.

[143] Rivin, E.I., Vibration Isolation of Precision Equipment. *Precision Engineering* 17 (1995) 41-56.

Appendix A - Footfall Force Data Acquisition

Chapter 3 and Chapter 4 used measured footfall forces in various analyses. This appendix describes how the forces were acquired and the equipment used.

The forces were measured in a laboratory at the University of Sheffield. An instrumented treadmill was used to acquire the forces. The treadmill is an ADAL3D-F design (shown in Figure 152), consisting of two rotating belts, one for each foot. Each belt has a force transducer at each end to capture the position and force applied to the belt by the foot. The dual belt design allows for an accurate separation of the forces applied by each foot. The treadmill can accurately measure triaxial force components [139]. The treadmill software automatically separates each individual footfall force and outputs a text file containing both separated and complete force time histories. An example of the separated forces from the software is shown in Figure 153. The treadmill has an operating velocity of 0.1 - 10 km/h and is suitable for slow to fast walking and slow jogging. All data were collected using a 16 bit A/D convertor sampling at 200 Hz. For a detailed description of a similar treadmill, please refer to [139].

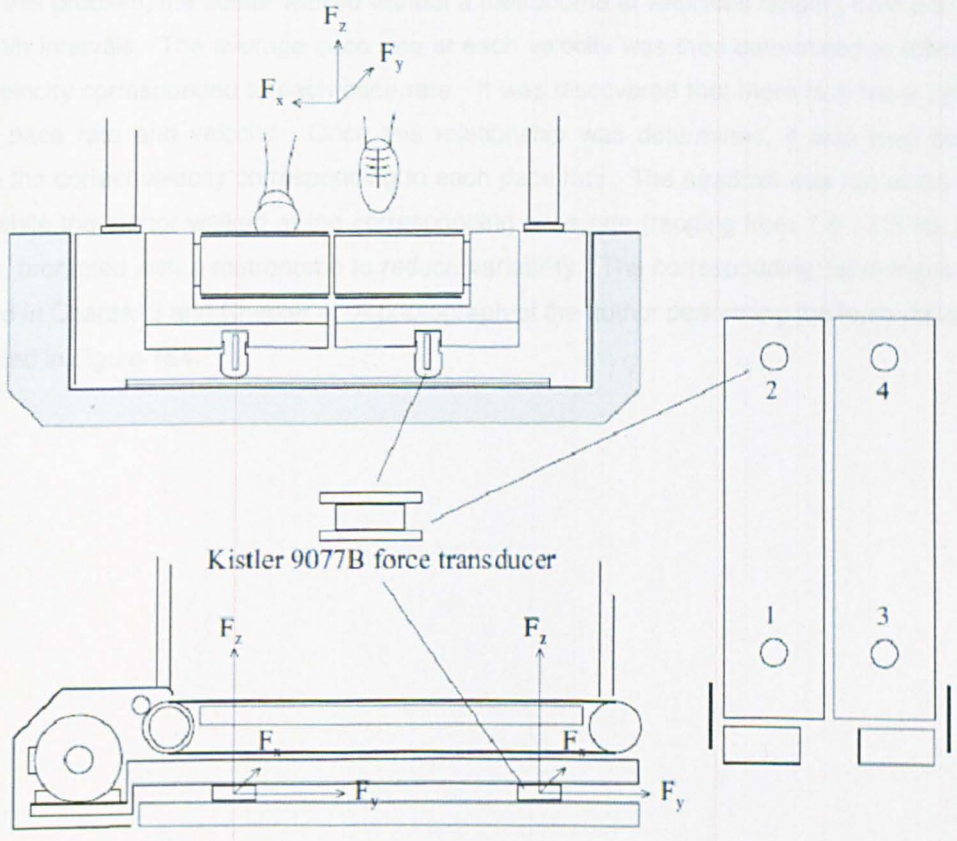

Figure 152 - ADAL3D-F instrumented treadmill

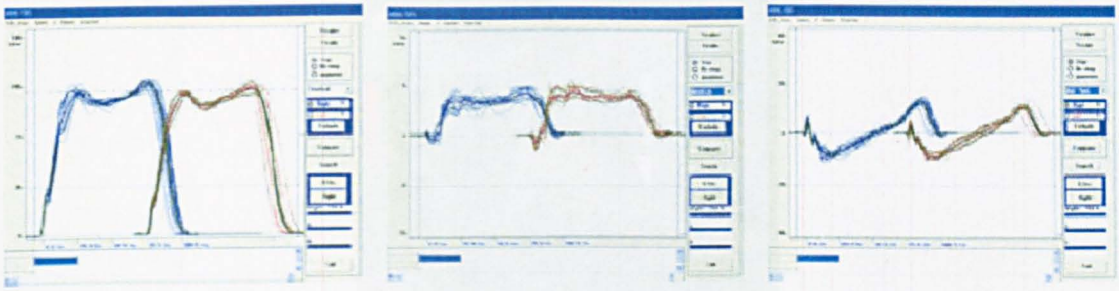

Figure 153 - ADAL3D-F instrumented treadmill software force separation: vertical (left), lateral (middle) and longitudinal (right); red represents the left foot and blue represents the right foot

The force data required Chapter 3 and Chapter 4 was vertical only, at a fixed pace rate. The author performed a number of walking tests on the treadmill prompted by a metronome. However, it was soon discovered that the author could easily walk at a wide variety of pace rates at a single treadmill velocity by varying his step length. Data collected in this manner would not be representative of the authors natural walking due to unnatural step lengths.

To solve this problem, the author walked without a metronome at velocities ranging from 0.5 - 10 km/h at 0.5 km/h intervals. The average pace rate at each velocity was then determined to discover what natural velocity corresponded to each pace rate. It was discovered that there is a linear relationship between pace rate and velocity. Once this relationship was determined, it was then possible to ascertain the correct velocity corresponding to each pace rate. The treadmill was run at the specified velocity while the author walked at the corresponding pace rate (ranging from 1.5 - 2.5 Hz at 0.1 Hz intervals), prompted with a metronome to reduce variability. The corresponding force measurements were used in Chapter 3 and Chapter 4. A photograph of the author performing the force measurement is presented in Figure 154.

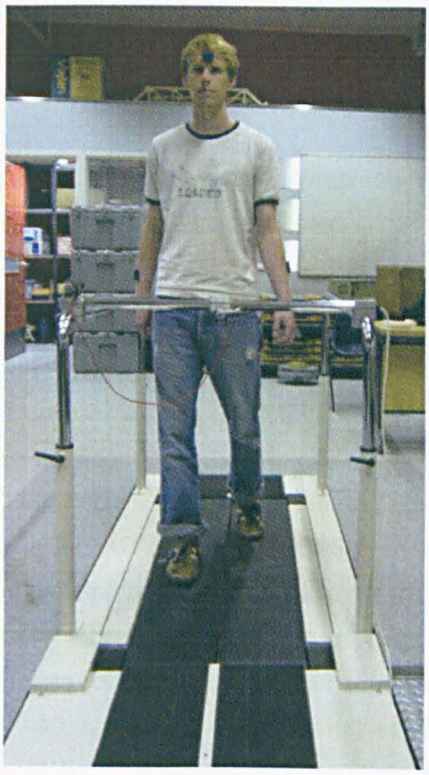

Figure 154 - Measuring the author's footfall forces

Appendix B - Modal Analysis of Singapore TRF

Chapter 4 used measured modal properties from a floor to estimate velocity response due to walking. This appendix describes how the modal testing was conducted.

The floor tested was currently being occupied as a warehouse containing pallets of boxes containing injection mouldings. A typical pallet had a mass of approximately 500 kg. The floor consists of precast hollow core slabs spanning approximately 7.5m.

Hammer testing was performed on the floor using the test grid shown in Figure 155. Acceleration was measured using three endevco 7754-1000 IEPE accelerometers. The data was acquired using a 24 bit NI-USB9233 data acquisition unit (DAQ), sampling at 250 Hz, using a custom LabView virtual instrument. The DAQ had four channels, three were used to aquire acceleration and the fourth was used for the instrumented hammer. Accelerometers were used as references and were placed at points 4, 6 and 11. The hammer was roving, with three hits supplied at each test point. During the testing, there was work being carried out in adjacent industrial units which would introduce immeasurable noise.

An overlay of the measured FRFs is shown in Figure 156. Modal parameter estimation was conducted using GRFP within MODAL, an in-house custom piece of software written in Matlab. The frequencies and modal masses of the first three modes are shown in Table 15.

Mode	Frequency (Hz)	Mass (kg)
1	10.49	119,000
2	19.26	145,000
3	37.1	35,000

Table 15 - First three modal parameters from hammer testing

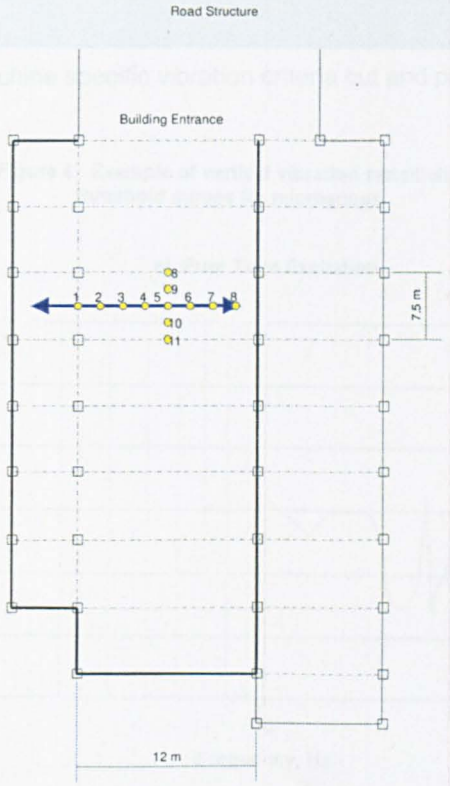

Figure 155 – Test points used for modal analysis; the thick black line represents the walls of the structure, the thin black lines the structures edge, the dotted lines represent beam lines (there are also beams along the other lines), the squares represent columns, the blue arrow represents the walking path and the yellow dots represent test points.

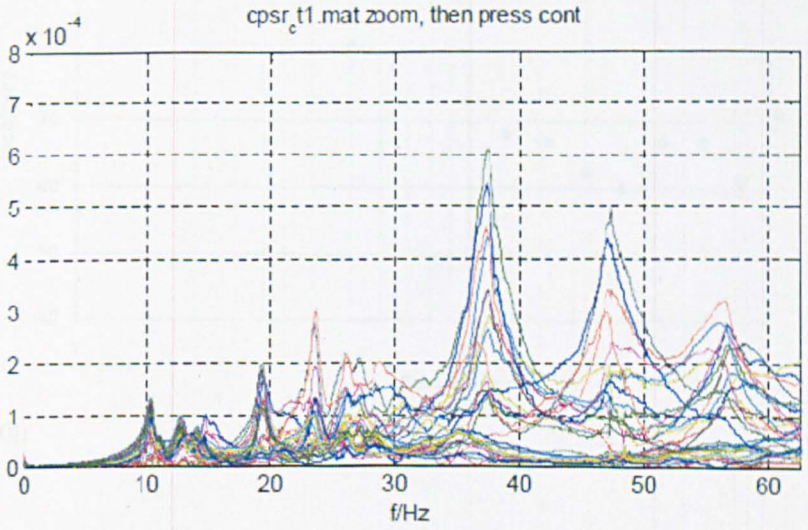

Figure 156 - Overlaid FRFs from hammer testing

Appendix C - Machine Specific Vibration Criteria

Presented are a selection of machine specific vibration criteria cut and paste from the literature.

Figure 4: Example of vertical vibration sensitivity threshold curves for microscope

a) Pure Tone Excitation

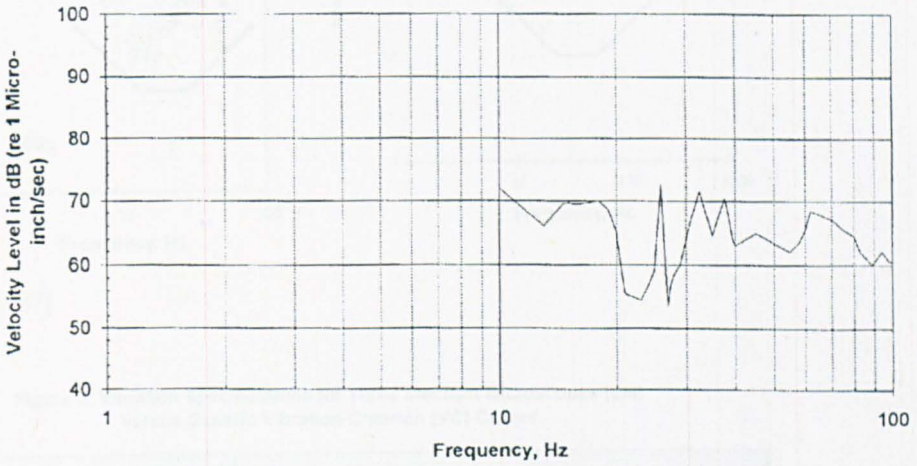

b) One-Third Octave Band Excitation

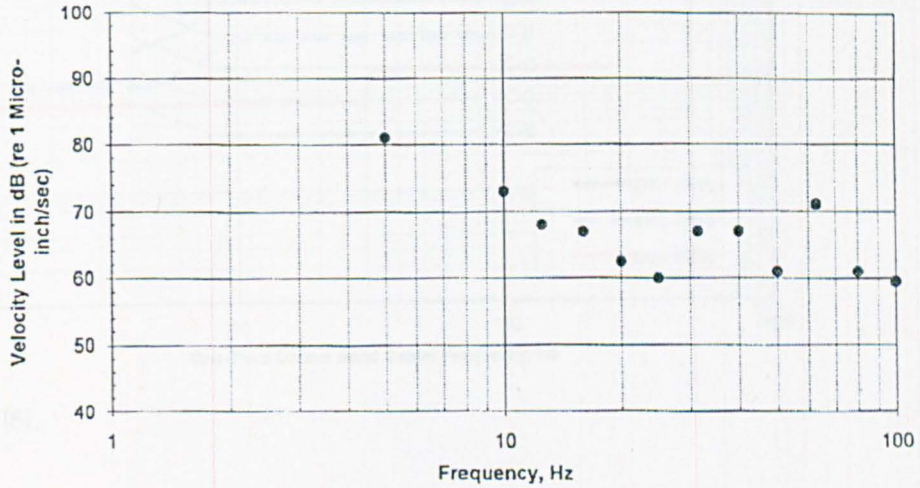

Reference [140]

Microscope

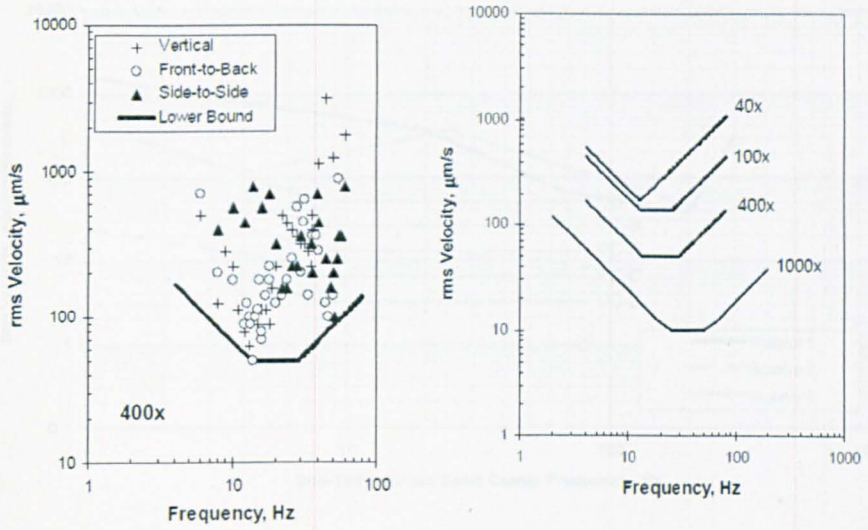

Reference [137]

Figure 2: Vibration Specifications for Three Electron Microscopes (EM) versus Generic Vibration Criterion (VC) Curves

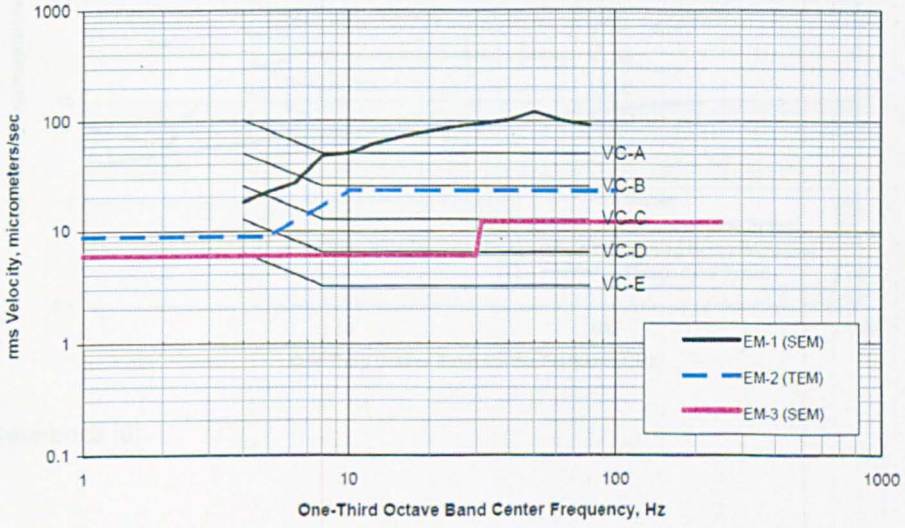

Reference [8]

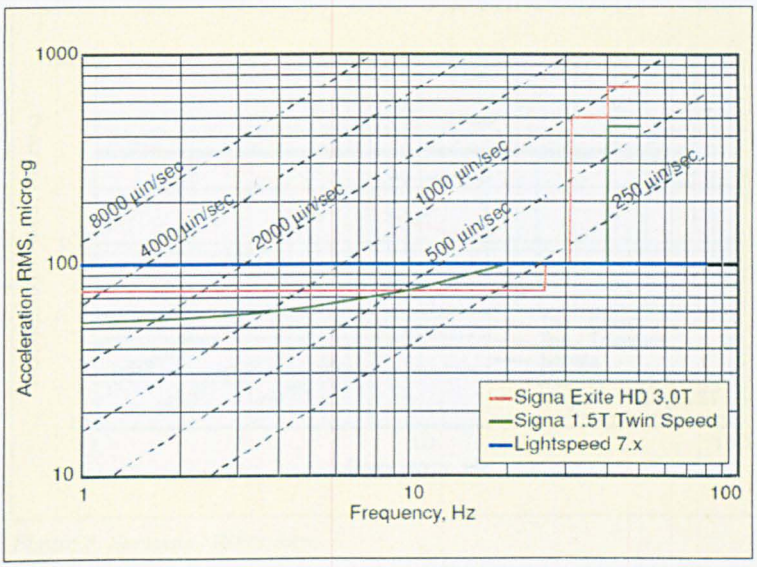

Figure 2. General Electric MRI criteria.

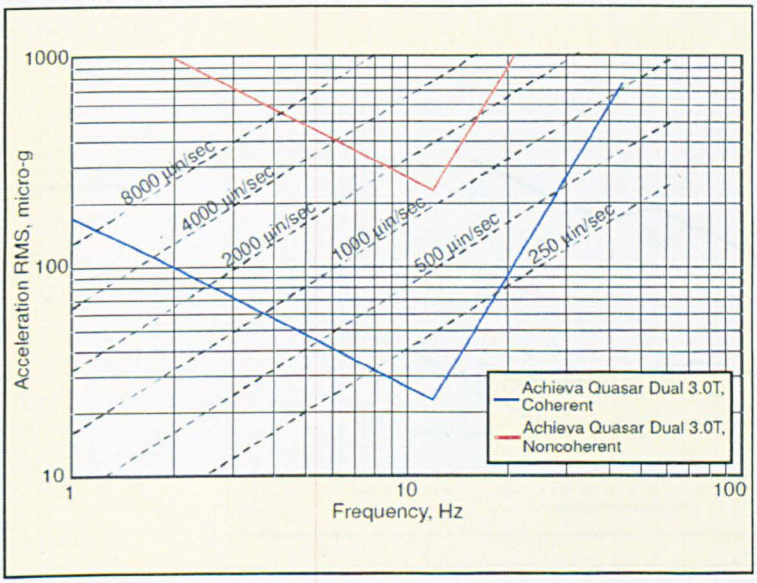

Figure 4. Philips MRI criteria.

Reference [141]

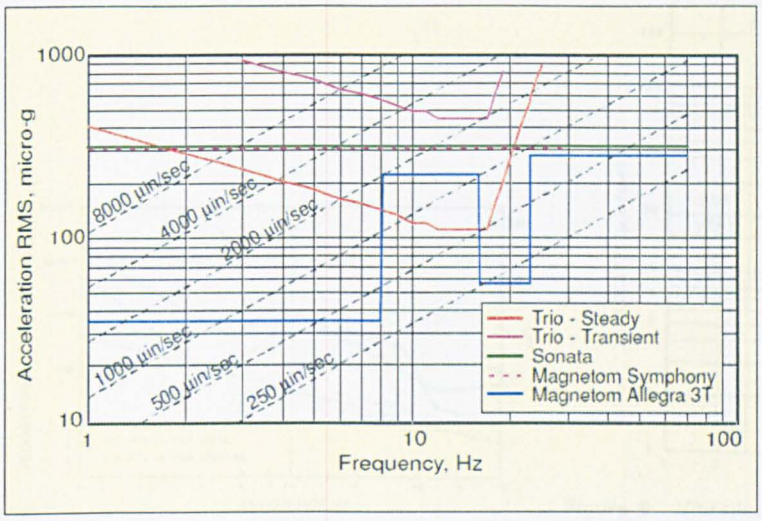

Figure 3. Siemens MRI criteria.

Reference [141]

Figure 2
Vibration criteria for steppers and scanners

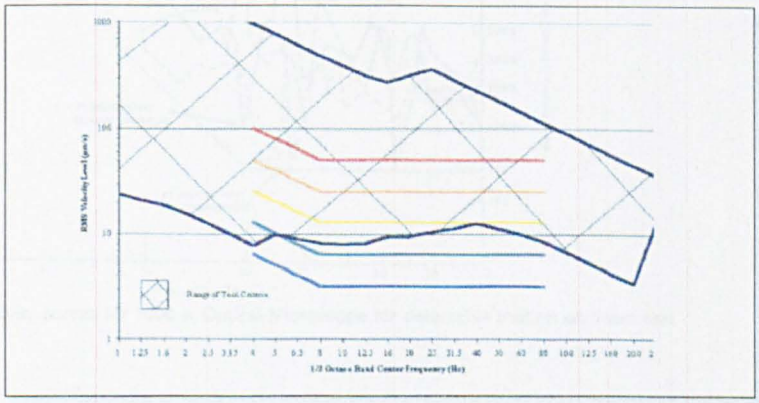

Figure 3
Vibration criteria for metrology tools

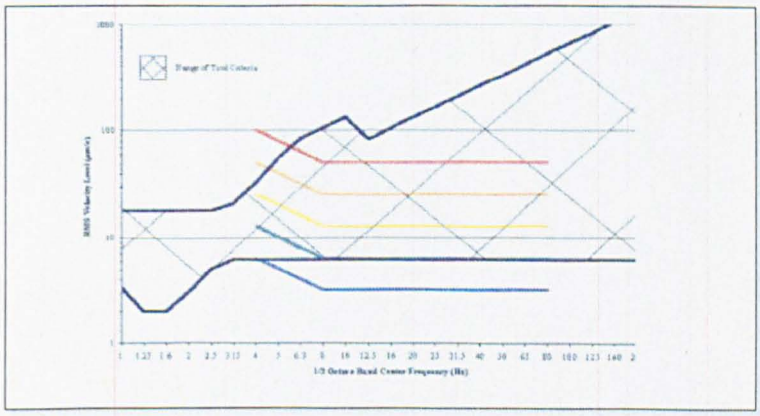

Reference [142]

Figure 3: Vibration Specifications for Three Photolithography Scanners versus Generic Vibration Criterion (VC) Curves

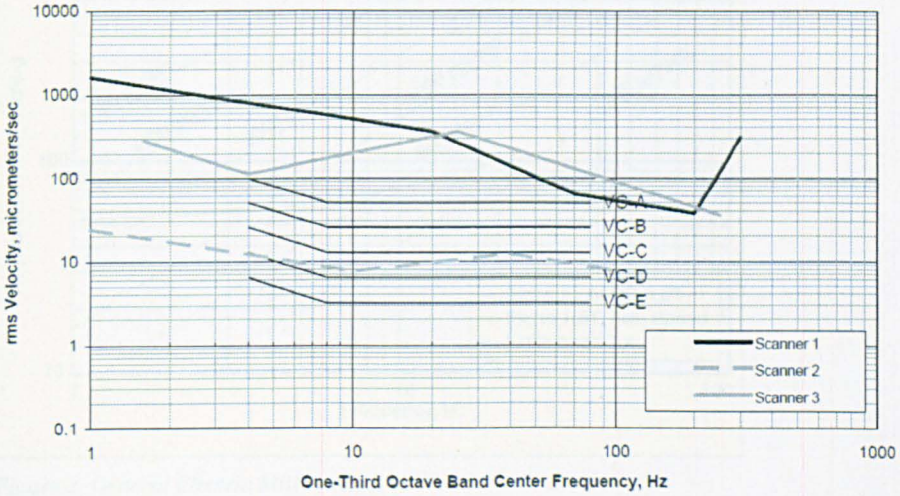

Figure 4: Examples of Vendor Specifications for a Typical Tool Set Used in 0.25 to 0.7 micron Fabrication

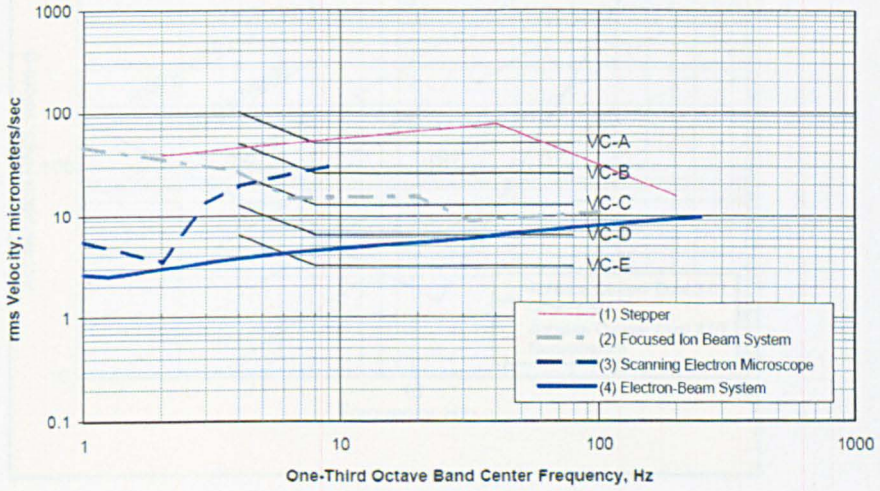

Reference [8]

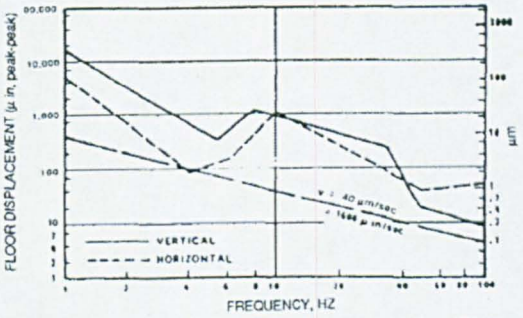

Figure 5 Vibration sensitivity curves for Mann Wafer Stepper 4800 DSW[7]

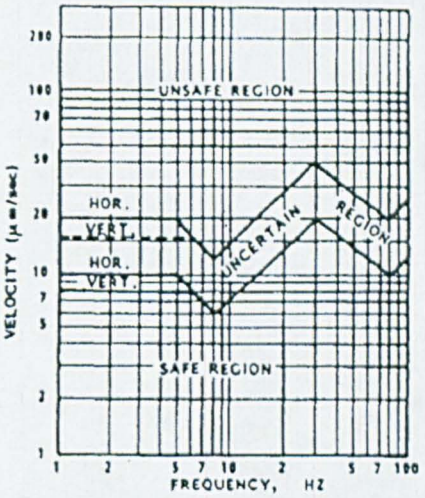

Figure 6 Vibration sensitivity curves for Phil Electron Beam Pattern Generator Beamwri EBPG-4[7]

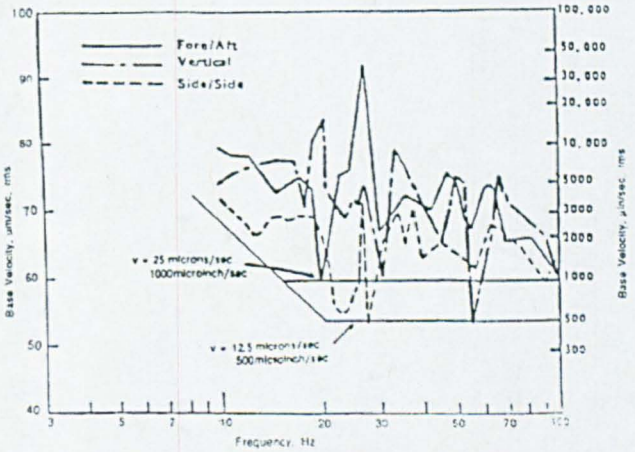

Figure 7 Vibration sensitivity curves for 1000 × Optical Microscope for detectable motion on 1-μm test line[12]

Reference [143]